Aston University

Some pages of this thesis may have been removed for copyright restrictions.

If you have discovered material in Aston Research Explorer which is unlawful e.g. breaches copyright, (either yours or that of a third party) or any other law, including but not limited to those relating to patent, trademark, confidentiality, data protection, obscenity, defamation, libel, then please read our Takedown policy and contact the service immediately (openaccess@aston.ac.uk)

A NOVEL PYROFORMER SYSTEM FOR BIOMASS INTERMEDIATE PYROLYSIS WITH IN-SITU CHAR-PROMOTED REFORMING (BY CHAR RE-CIRCULATION) OF PYROLYSIS VAPOURS AND POTENTIAL INTEGRATION OF PYROFORMER WITH A COMMERCIAL SCALE FLUIDISED BED GASIFIER TO ENABLE PYROGASIFICATION

MUHAMMAD SAGHIR

Doctor of Philosophy

ASTON UNIVERSITY

June 2017

© Muhammad Saghir, 2017

Muhammad Saghir asserts his moral right to be identified as the author of this thesis

This copy of the thesis has been supplied on condition that anyone who consults it is understood to recognise that its copyright belongs to its author and that no quotation from the thesis and no information derived from it may be published without appropriate permission or acknowledgement.

Executive Summary

Strong scientific evidence shows that anthropogenic greenhouse gas emissions from usage of fossil fuels are responsible for global warming and climate change. Biomass is a sustainable and reliable resource for replacing fossil fuels to produce energy and chemicals through pyrolysis and gasification routes. Pyrolysis of biomass leads to three products i.e. bio-oil, non-condensable gas and char. Gasification of biomass leads to a syngas which consists of hydrogen, carbon monoxide, carbon dioxide, ,methane, nitrogen water vapour and some C_1-C_4 gases.

The objectives of this thesis included: to conduct tests on a twin-screw pyrolysis reactor (Pyroformer); to evaluate the effects of char recirculation on products; to characterise the bio-oil and char produced and characterise an in-situ blend of biodiesel/bio-oil; and to review the design of the Pyroformer and its coupling with a bubbling fluidised bed gasifier, thus enabling a novel concept of Pyrogasification.

To observe the biomass and char flow characteristics, and to calculate the residence time and char to biomass ratio (C/B), cold flow tests were performed in a transparent model of 20 kg/h Pyroformer. Biomass throughput limitations were identified at different feeding rates and C/B.

Pyrolysis tests were conducted in a Pyroformer with up to 10 kg/h feeding rates. It was observed that, during pyrolysis of dry digestate pellets, gas yield increased and liquid yield decreased at optimum C/B of 3.1 at 5 kg/h. The organic phase of bio-oil for MSW had an HHV of 30.3 MJ/Kg and a very low total acid number of 0.2 mgKOH/g.

ENPlus certified wood pellets and miscanthus pellets were pyrolysed in a 100 kg/h Pyroformer with in-situ blending of bio-oil with biodiesel. Product yield of 21, 32 and 47 wt% for liquid, char and gas fractions were observed for wood pellets; and 31, 32 and 37 wt% with miscanthus. Bio-oil content in the blend was 19.75 and 11.28 wt% for wood and miscanthus derived feedstocks. The heavy metal content in biochars met voluntary biochar standards for soil remediation. A gasifier commissioning test was done with hydrogen, CO, methane and CO_2 yields of 13.3, 17.3, 4 and 17 vol% at 818 ˚C.

Keywords: 2 stage pyrogasifier, char to biomass ratio, total acid number, bio-oil biodiesel blend, pyrogasification

In the name of Allah,

The most Beneficent,

The most Merciful.

O my Lord! Advance me in Knowledge

(Al-Quran; 20:114)

Dedicated to my family and my parents. I would not be here without your help, courage, prayers, the sacrifices you made for me and support you provided me throughout my life and especially during my PhD.

O our Lord; bless us all with the best in this world and The Hereafter and protect us from the torment of The Hellfire.

Ameen!

Acknowledgement

Contributions from European Commission, Seventh Framework Programme Industry-Academia Partnerships and Pathways (IAPP, Pyrogas Project) Grant agreement number 286244 and from European Union's INTERREG IVB programme, BioenNW project are gratefully acknowledged for enabling the research presented in this report.

Author would like to thank Professor Andreas Hornung, Dr Philip Davies and Professor Tony Bridgwater for their support and guidance during this research project. Dr Andreas Apfelbacher for his guidance, unlimited support, encouragement and help. Dr John Brammer, Dr Jude Onwudili, Dr Yassir Makkawi as my associate supervisors for their guidance and support. I would also like to thank Dr Clara Serrano, Abdelnasir Omran, Sana Siddiqui, and Ms Amparo, Wehrle Werk Team (Christoph and Christian), WSE team, and colleagues at EBRI for their expertise, practical knowledge, guidance, support and explanation of complex terminologies. You made my research bearable and your help made a huge difference to me.

Table of Contents

Executive Summary 1
Acknowledgement 3
List of Abbreviations 8
List of Tables 10
List of Figures 12
Chapter 1- Introduction 14
1.1 Biomass resources and their availability 15
1.2 Biomass to energy conversion routes 16
1.3 Thermochemical methods of biomass conversion 20
1.4 Pyrogasification 22
1.5 Origin of the Thesis 23
1.6 Structure of Thesis 24
1.7 Summary of the chapter 26
Chapter 2- Literature review 28
2.1 Pyrolysis 28
2.1.1 General principles of pyrolysis 29
2.1.2 Products of Pyrolysis 31
2.2 Types of pyrolysis and pyrolysis reactors 33
2.2.1 Slow Pyrolysis 33
2.2.2 Fast Pyrolysis 33
2.2.3 Intermediate pyrolysis 34
2.2.4 Other types of Pyrolysis 35
2.3 Factors influencing pyrolysis products 35
2.3.1. Biomass type and composition 35
2.3.2 Influence of operating conditions during pyrolysis 41
2.4 Methods of enhancing bio-oil quality during pyrolysis 43
2.4.1 Tar cracking with char 44
2.4.2 Thermal tar cracking 45
2.4.3 Catalytic tar cracking 45
2.5 Types of intermediate pyrolysis reactors 46
2.6 Critical review of Pyroformer studies 56
2.7 Lessons from the Pyroformer studies 62
2.8 Gasification 63

2.8.1 Fixed bed gasifiers 67
2.8.2 Fluidised bed gasifiers 70
2.8.3 Plasma gasification 71
2.9 Tars 72
2.10 State of the art, combination of pyrolysis and gasification processes 73
2.11 Summary of the Literature review 78
Chapter 3 – PhD project aims, objectives and methodology 80
3.1 Knowledge gap 80
3.2 Project aim 81
3.3 Project Objectives 81
3.4 Methodology 82
3.5 Limitations of the project 84
Chapter 4- Cold flow modelling in a 20 kg/h transparent Pyroformer 86
4.1 Equipment and materials 87
4.2 Residence time 91
4.2.1 Procedure for residence time determination 92
4.2.3 Residence time calibration data 94
4.2.4 Inferences from residence time calibration 95
4.3 Steady state operations 97
4.4 Char to biomass ratio (C/B) determination 100
4.4.1 Procedure for char to biomass ratio determination 101
4.4.2 Char to biomass ratio data 102
4.4.3 Inferences from C/B data 105
4.5 Summary of the chapter 109
Chapter 5 - Experimental studies in hot Pyroformer 20 kg/h 111
5.1 Parametric study 111
5.1.1 Feedstock characterisation 111
5.2 Experimental method 112
5.3 Results and discussion 116
5.3.1 Effect of char recirculation on pyrolysis products 120
5.3.2 Comparison of quality of organic phase of pyrolysis liquids 131
5.3.3 Effects of feed rate on product yields in 20kg/h Pyroformer 136
5.4 Comparative study 137
5.4.1 Raw materials for comparative study 137

5.4.2 Comparison of product yields 141
5.4.3 Comparison of quality of organic phase of liquids 143
5.5 Chapter Summary 144
Chapter 6 – Pyrolysis experiments in 100 kg/h Pyroformer system 145
6.1 Equipment and materials 146
6.1.1 Process layout 146
6.1.2 Feedstocks 149
6.1.3 In-situ quenching of pyrolysis vapours with biodiesel 150
6.2 Experimental procedure 150
6.3 Results and discussion 155
6.3.1 Mass balance 155
6.3.2 Bio-oil and biodiesel blend sampling and characterisation 156
6.4 Biochar emissions reductions 159
6.5 Summary of the Chapter 173
Chapter 7– Pyroformer engineering design review of critical components 176
7.1 Feeding valve issues 177
7.1.1 Define the problem 179
7.1.2 Gather information 179
7.1.3 Generate multiple solutions 180
7.1.4 Analyse and select a solution 180
7.1.5 Test and implementation of final design solution 183
7.2 Char collection system 185
7.2.1 Define the problem with char collection system 185
7.2.2 Gather information 186
7.2.3 Generate multiple solutions 186
7.2.4 Analyse and select a solution 187
7.2.5 Test and implement the solution 187
7.3 Biodiesel quenching system 189
Chapter 8 - Pyrogasification – Combining of Pyroformer and Gasifier 192
8.1 BFB Gasifier process commissioning test layout 193
8.1.1 Feedstock analysis 197
8.1.2 BFB gasifier working principles 197
8.1.3 Gasifier fuel gas data sampling and results 202
8.1.4 Discussion 205

8.2 Integration of Pyroformer and gasifier by means of a self-cleaning twin screw system 208
8.3 Operational principles of the Pyroformer and gasifier as a combined system 214
8.3.1 General Preparations and working procedure 215
8.3.2 Heating up the gasifier to bring it to working temperature 215
8.3.3 Pyroformer heating up phase 216
8.3.4 General operation of Pyroformer-gasifier coupled mode (Pyrogasification mode) 217
8.3.5 Decoupling the Pyrogasification mode to end the test 218
8.3.6 Shut down of both processes 218
8.3.7 End of test and complete shutdown of ancillary systems 219
8.4 Summary of the chapter 219
Chapter 9 – Conclusion and recommendations 223
9.1 Conclusions 223
9.2 Recommendations 226
List of References 229
List of Publications 246
Conference papers 246
Book chapters 246
Appendices 248
Appendix 1 - 3D Layout of Pyroformer 100 kg ----------249
Appendix 2 - Harper Adams Pyroformer Daily Operations Checklist ----------250
Appendix 3 - Plant layout of BFB Gasifier and Pyroformer processes ----------252
Appendix 4 - Dimensions of the Gasifier ----------273
Appendix 5 - Characterization of the products from Intermediate pyrolysis of miscanthus and wood pellets – internal combustion engine application-------275
Appendix 6 - Characterisation and potential applications of char from Intermediate pyrolysis of different biomass feedstocks----------278

List of Abbreviations

BBF British Biochar Foundation

BFB - Bubbling fluidized bed

C – Carbon (element)

C/B – Char to biomass ratio

CDM – Clean Development Mechanism

CEC – Cat-ion exchange capacity

CFB - Circulating fluidized Bed

CH_4 – Methane

CHP - Combined Heat & Power

CO – Carbon monoxide

CO_2 – Carbon dioxide

C_{org} – Organic carbon

DAC – Digestate from arable crops (corn and green rye)

DCL – Digestate from chicken litter

EC – Electrical conductivity

ER - Equivalence ratio

FR - feeding rate, in kg/h

FR_{IN} - Feeding rate input

FR_{OUT} – Feeding rate output

H- Hydrogen (element)

HHV - Higher Heating Value

IBI International Biochar Initiative

IS - inner screw

K – Potassium (element)

M_c – Recirculated material

Mg - magnesium (element)

m_i - mass of component, i

MSW – Municipal solid waste

N- Nitrogen (element)

OS - outer screw

P - Phosphorus (element)

PG – Pyrolysis gas

rpm - revolutions per minute

RT - residence time, in seconds

SS – Steady state

UNFCCC – United Nations Framework Convention on Climate Change

Wt % - weight percentage

ρ_{char} - density of char kg/m^3

ρ_{plas} - density of particles used in this study, 607 kg/m^3

List of Tables

Table 1 - Major benefits of biofuels compared to fossil fuels – adapted from [39] 19
Table 2 - Lignin, cellulose and hemicellulose content of selected biomass types [18, 25, 77, 85 & 150] 37
Table 3 - Various configurations of pyrolysis screw/auger reactors types..... 48
Table 4 - Proximate, ultimate analysis and heating values of the de-inking sludges. Adapted from [114] 57
Table 5- Wood and barley feedstock and products analysis (dry basis) in the Pyroformer - adapted from Yang et al [110] 58
Table 6 - De-inking sludge bio-oils ultimate analysis and heating values [114] 59
Table 7 - De-inking sludge bio-oil metals analysis [114] 60
Table 8 - De-inking sludge bio-oil fuel properties [114]..... 61
Table 9 - De-inking sludge gas phase analysis [114] 62
Table 10 - De-inking sludge char ultimate and HHV analysis [114] 62
Table 11 - List of reactions in gasification process [122, 123] 65
Table 12 - Types of gasifiers, fuel and oxidant flow configuration [79, 129]..... 67
Table 13 - Pyroformer IS & OS screw dimensions..... 90
Table 14 - Relationship between frequencies (Hz) and rpm of the inverters and motors of inner and outer screw in cold transparent 20 kg/h Pyroformer..... 94
Table 15 - Effect of the inner screw speed on the minimum residence time 95
Table 16 - Material distribution in the cold Pyroformer with counter flows in screws showing accumulation and steady state..... 99
Table 17 – Cold Pyroformer experimental results as shown for various C/B ratio, IS, OS rpm and residence time (RT)..... 103
Table 18 - Corn and green rye digestate feedstock analysis..... 112
Table 19 - Experimental conditions for 3, 5 and 10 kg/h tests in 20 kg/h Pyroformer..... 118
Table 20 – Experimental mass balance results for 3, 5 and 10 kilograms per hour test runs in 20 kg/h Pyroformer 119
Table 21- Fuel properties of organic phase of pyrolysis liquid from dry digestate in 20 kg/h Pyroformer tests..... 132
Table 22 - Effect of C/B ratio on char composition 135
Table 23 - Comparison of feedstocks used in the comparative study..... 138
Table 24 – Experimental settings of digestate, MSW and Chicken litter at 5 kg/h 139
Table 25 – Overall mass balance of digestate, MSW and Chicken litter at 5 kg/h 140
Table 26 - Char analysis of DAC, MSW and DCL at 5 kg/h feeding rate 142
Table 27- Organic phase fuel properties analysis for DAC, MSW and DCL 143
Table 28- Feedstock analysis of wood and Miscanthus pellets 149
Table 29- Mass yields (wt. %) of pyrolysis products from different biomass feedstocks..... 156

Table 30- Elemental analysis and Characterisation of Intermediate Pyrolysis oil & ASTM standard for Biodiesel 157
Table 31 – Comparison of wood and miscanthus derived biochar (from 100 kg/h Pyroformer test in Table 30) showing toxic metal contents comparison with IBI and BBF biochar standards 167
Table 32- Emissions reductions expressed as kg CO_2 Mg^{-1} C^{-1} contained in woody biomass for systems changes –adapted from [154 & 155]..... 169
Table 33- Emissions reductions expressed as tonnes of CO_2 per annum contained in naturally decaying waste wood for systems changes and fossil fuel substitution via pyrogasification 172
Table 34 – A list of valves suited for the feeder valve application 182
Table 35 - EBRI Plant integrated control system with interlocks 196

List of Figures

Figure 1 - Biomass conversion processes [38] 18
Figure 2 - Biomass thermal degradation curve showing various heating stages of biomass from initial heating leading to pyrolysis – adapted from [216] 30
Figure 3 - Typical products from the breakdown of basic components of biomass during pyrolysis [15] 39
Figure 4 - Pyrolysis curves of hemicellulose, cellulose and lignin in TGA [85] 40
Figure 5 - Scheme of Haloclean rotary kiln [106] 49
Figure 6 - Schematic diagram of the parallel counter rotating twin screw pyrolysis apparatus [105] 51
Figure 7 - Schematic diagram of auger reactor [112] 53
Figure 8 - Schematic diagram of the Pyroformer reactor system [20] 55
Figure 9 - Schematic of an updraft gasifier [127] 69
Figure 10 - Schematic of a downdraft gasifier [127] 69
Figure 11 - Schematic of bubbling and circulating fluidised bed gasifiers [130] 71
Figure 12 - Schematic of Plasma gasifier reactor showing the positioning of plasma torch [134] 72
Figure 13a - Viking Gasifier arrangement showing the integrated screw pyrolysis and gasification processes [59] 75
Figure 13b - Progressive decrease in tar levels as measured in various stages of Viking gasifier process [144] 77

Figure 14 - Pyroformer research methodology diagram 83
Figure 15 - Image of cold Pyroformer system, 1. Mains power, 2. Inner screw rpm controller, 3. Outer screw rpm controller, 4. Emergency stop, 5. Feed inlet, 6. Outlet, 7. Inner screw motor, 8. Outer screw motor, 9. Pyroformer transparent body and screws 88
Figure 16– Dimensions of outer screw (OS) of 20 kg/h Pyroformer 89
Figure 17 – Dimensions of the inner screw (IS) of 20 kg/h Pyroformer 89
Figure 18 - Cross section of Pyroformer showing IS & OS integrated setup (A–Feed inlet, B-Inner screw, C-Gas outlet, D- Outer screw, E-char outlet 90
Figure 19 - Material flows in the Pyroformer during various stage 93
Figure 20 - Relationship between Frequency (Hz) of inverters and rpm of motors .. 95
Figure 21 - Relationship between theoretical and experimental inner screw speeds to the residence time of biomass in inner screw 96
Figure 22 - Graphical representation of relationships between IS and OS rpm to C/B (mass basis as grey highlighted in Table 17) 104
Figure 23 - Pyroformer process (20 kg/h) layout - adapted from [110] 114
Figure 24 - Effect of C/B ratio on product yields during 3 kg/h feed rate 122
Figure 25 - Effect of C/B ratio on aqueous and organic phase yields during 3 kg/h feed rate 123
Figure 26 - Effect of C/B ratio on product yields during 5 kg/h feed rate 126
Figure 27 - Effect of C/B ratio on aqueous and organic phase yields during 5 kg/h feed rate 127
Figure 28a –Reliability of the results to evaluate the effect of C/B ratio on product yields at 10 kg/h feeding rate ..... .128

Figure 28b –Reliability of the results to evaluate the effect of C/B ratio on aqueous and organic phase yields at 10 kg/h feeding rate 130
Figure 29 - 100 kg/h Pyroformer process layout 147
Figure 30 - Pyroformer 100 kg/h Reactor dimensions approximately 3m long and 0.4m external shell diameter 148
Figure 31 - P&ID of 100 kg/h Pyroformer (as taken from Pyroformer HazOp study of EBRI Pyroformer archive)..... 154
Figure 32 - 100 kg/h Pyroformer installation at Harper Adams University College (Photo by Louise Ciaravella) 155
Figure 33 - Simple carbon cycle on left and biochar from pyrolysis (with energy recovery) based carbon cycle on right - adapted from [5]..... 160
Figure 34 – Showing 5 steps of engineering design process (Adapted from Khandani [2]) 177
Figure 35 - Feeder valve assembly 178
Figure 36 – Selected knife gate feeder valve for Pyroformer 100kg/h as taken from Stafsjo Valves of Sweden [214] 184
Figure 37 - Char container (shown hanging) of the 100 kg/h Pyroformer (Photo by Louise Ciaravella) 185
Figure 38 - Water cooled screw conveyor for gasifier ash as installed at European Bioenergy Research Institute (Photo by Louise Ciaravella) 188
Figure 39 – A screw conveyor showing water cooling jacket proposed for char collection system of the Pyroformer [1]..... 189
Figure 40 - Biodiesel/bio-oil quench system redesign (adapted from EBRI Pyroformer archives) 191
Figure 41 – Gasifier process layout showing process items for commissioning test – CHP engine not used in the test 195
Figure 42 - Pyroformer and gasifier shown next to each other in white arrows – Photo taken from EBRI archive 198
Figure 43 - BFB gasifier showing biomass feed inlet N1, dolomite inlet N10, pyrolysis gas coupling N8 and fuelgas outlet N11 (Adapted from EBRI gasifier archive)..... 199
Figure 44 - Gasifier fuel gas online composition, flowrate, gasification temperature, sampling time and handheld gas measurement for CO and oxygen (shown in a cross and circle) 206
Figure 45 – Dimensions of twin screw coupling part to fit between Pyroformer and gasifier (electric drive motor not shown) – taken from EBRI gasifier archive..... 211
Figure 46a - Isometric view of twin screw coupling showing extended screw ends - taken from EBRI gasifier archive.....212

Figure 46b - Front view of twin screw coupling showing two holes for twin screw of diameter 61 mm - taken from EBRI gasifier archive 212
Figure 47 - Pyrogasification process flow diagram showing gasifier and Pyroformer 213

Chapter 1- Introduction

This chapter explores the global energy scenario and the important role biomass can play to meet global energy needs. Energy demand is increasing worldwide with population and economic development. Hitherto they have been met mostly by conventional fossil derived energy resources which are now becoming depleted. Such conventional energy resources are unsustainable and contribute to greenhouse gas emissions. Energy from biomass is an attractive alternative due to its low carbon footprint, sustainability, abundance, energy security, local availability and production. In Europe, interest in bioenergy is driven by various factors such as EU's commitment to reduce landfill and concerns about energy security. The EU renewable energy directive spurs on research into biomass and bioenergy.

Energy security is of fundamental importance considering growing energy demands and the urge to maintain and improve living standards. Various energy resources may be utilised to meet these demands including: fossil derived fuels such as coal, oil, natural gas; nuclear energy; and renewable energy such as wind, solar, geothermal, hydroelectric, and biomass. Energy from biomass or bioenergy is gaining increasing global interest because of perceived environmental benefits, local bio-economy development and its wide availability. Biomass reduces net carbon dioxide emissions into the atmosphere by absorbing atmospheric carbon dioxide when it is grown. Biomass to bioenergy production also helps to reduce the greenhouse gas emissions from decaying biomass, complementing food production while using crop wastes. Economically, local biomass production leads to local jobs creation and prosperity. Bioenergy production increases biomass resource efficiency by adding value to low-grade wastes and by eliminating the tax bill from imported fossil fuels. Politically, local bioenergy production favours energy security by avoiding fossil fuel imports from politically unstable regions, reducing the dependence on depleting fossil fuel resources and interlinking the national energy policy with local biomass resources [6, 7].

Due to the above benefits, energy from biomass is considered more sustainable compared to many other resources to meet the energy demands of

increasing populations with aspirations of better living standards [8]. Other factors influencing bioenergy uptake are: greenhouse gas emissions, fluctuations in global fuel prices, increasing municipal solid waste (MSW) production (predicted to reach 2.7 billion tonnes/yr globally by 2050 [9]), increasing landfill costs of waste materials and increasing awareness of greenhouse gases from fossil fuels [10]. Organic wastes of various kinds such as agricultural, forestry, industrial residues and municipal solid wastes are useful materials to be used in energy production. Amongst the various existing conventional waste management technologies such as incineration [11], combustion [12] and anaerobic digestion [13], there are other suitable technologies such as biomass gasification [14] and pyrolysis [15] which can turn biomass materials of varying quality into useful products.

1.1 Biomass resources and their availability

Biomass resources include various natural and derived materials such as forestry and wood wastes [16-19] food processing wastes [20, 21], agricultural and industrial wastes [22, 23]. Other potential biomass feedstocks include waste paper, biogenic municipal solid waste, sewage sludge, digestate solids, sawdust, bio-solids, grass, waste from food processing, animal wastes, aquatic plants and algae, etc. [24, 25]. Biomass feedstocks are attractive due to the absence of contaminants which could be present otherwise in municipal wastes. Bioenergy can satisfy existing energy needs in the form of electrical and heat energy, fuel for transport sector and feedstock for chemicals [26]. Also, biomass is in principle CO_2 neutral; there need be no net carbon emissions to the atmosphere [27] as bioenergy production uses the carbon absorbed by plants during photosynthesis during the growth of biomass [28]. Solid and dry biomass can be used as a coal replacement in conventional combustion energy systems due to its similar properties [29]. Biomass is available in most parts of the world, and is a significant part of the global energy supply contributing about 13% of primary energy and 75% of the global renewable energy mix. Biomass is envisaged to contribute 25-33% of global energy supply by 2050 [30, 31]. The increase in biomass usage as an energy resource is anticipated by the World Energy Council to continue for some decades into the future. Biomass can be used more sustainably, efficiently and by complementing the production of food and fibres when resulting waste crop residues during food production are used for energy production [31].

Although it is considered a sustainable energy resource, there are challenges with the use of biomass which need to be addressed for any biomass energy project to succeed. Biomass has low energy density, potential competition with food and feed production, high moisture content, higher harvesting, collection, transportation and storage costs, seasonal and scattered availability [32].

Biomass, as the name suggests, is formed from living or recently dead microorganisms, plants and animals [33]. Such biomass can generally be defined as any carbonaceous material consisting mainly of carbon, hydrogen, oxygen and nitrogen. Sulphur is also present in low proportion. Some biomass types also carry significant proportions of inorganic species, which constitute ash and chlorine [24, 33, 34]. The concentration of the ash arising from these inorganics ranges from less than 1% in softwoods to 15% in herbaceous biomass and agricultural residues [24]. So-called biogenic municipal solid wastes can contain up to 40 wt% of ash [35]. Normally biomass samples have significant moisture content which, if not dried to acceptable levels (generally <10%), makes the energy conversion process very cumbersome and inefficient. Biomass is generally made up of 3 biopolymer constituents such as lignin, cellulose and hemicellulose. The influence of these biopolymer is evident in the end products of conversion via pyrolysis e.g. variability in bio-oil, pyrolysis gas and char fractions for different materials.

1.2 Biomass to energy conversion routes

Although biomass has been used as fuel for fire since the Stone Age, there are various other pathways (as shown in Figure 1) available for the conversion of biomass to energy to meet current human needs. These include physical, thermo-chemical, chemical and bio-chemical conversion methods as shown in Figure 1. Physical methods involve densification of biomass after drying in the form of pellets or briquettes to be used as a biofuel. Thermochemical conversion methods for energy production include combustion, incineration, gasification and pyrolysis. Chemical conversion includes trans-esterification of plant oils to biodiesel. Biochemical methods include fermentation for bioethanol and biobutanol [36] aerobic fermentation and anaerobic digestion of biomass to produce biomethane [37].

Biofuels exist in many different forms such as bioethanol, biobutanol, vegetable oils, biodiesel, biogas, biomethane, biosynthetic gas (biosyngas), biohydrogen,

bio-oil (from pyrolysis), biochar, biobriquettes and Fischer-Tropsch liquids etc. [19, 37, 39]. Given in Table 1 are some of the benefits associated with biofuels.

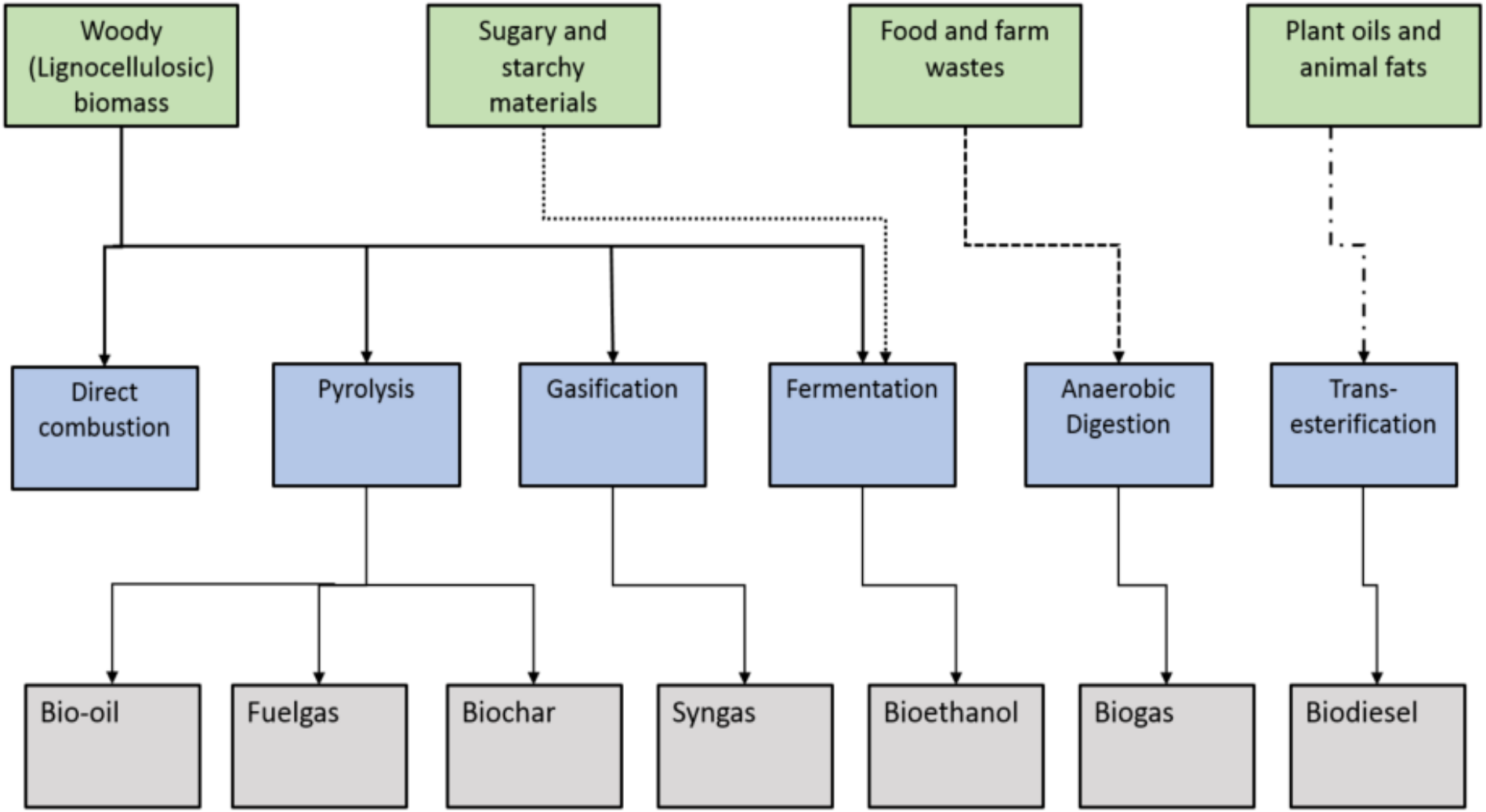

Figure 1 - Biomass conversion processes [38]

Table 1 - Major benefits of biofuels compared to fossil fuels – adapted from [39]

Economic benefits	Sustainability
	Fuel diversity
	More jobs for rural areas
	Increased income taxes
	Increased investment in plant and equipment
	Agricultural development
	International competitiveness
	Reduced dependency on imported fuel
Environmental benefits	Greenhouse gas reductions
	Reduction in air pollution
	Lower biodegradability
	Higher combustion efficiency
	Improved land and water use
	Carbon sequestration
Energy security	Achievement of domestic targets
	Supply reliability
	Reduction in use of fossil fuels
	Readily available
	Domestic distribution
	Renewability

Amongst many, one of the important issues with first generation biofuels is their competition with land available for production of food increasingly in demand [40]. Biofuel production has been linked to many issues such as deforestation [41, 42] of rainforests to grow palm trees, displacement of land available for growing food, and hikes in food prices [43]. Thus first generation biofuels [42] have been proven to be very un-sustainable and efforts are now diverted to second generation biofuel resources such lignocellulosic biomass residues [44], and third generation based on high yield algae production by using wastewater and carbon dioxide to produce biodiesel. Some energy crops (e.g. Jatropha) can be cultivated on marginal and non-agricultural lands to reduce food versus fuel competition with comparatively higher oil yields per hectare potential. Normally, biogas production through AD systems has low [42] energy conversion efficiency of lignocellulosic materials. There are also digestate storage issues over couple of months and disposal later. These issues require alternative processing ways for such materials into energy conversion where more complex waste and non-waste derived feedstock materials can be used [42].

Bio-alcohols such as bioethanol and biobutanol production via fermentation are well established for use in transportation as a biofuel. This pathway is important for reducing the fossil fuels usage and enhancing sustainability factors [39]. Bioethanol production is mostly associated with sugars and starch from biomass, whereas use of lignocellulosic fractions of biomass for bioethanol production has not been widely developed as such. Also, the usage of bio-alcohols is mostly limited to gasoline engines which limits their usage potential.

1.3 Thermochemical methods of biomass conversion

Pyrolysis and gasification are two important thermochemical pathways to divert organic solid mixed waste materials from landfill for energy recovery and also convert agricultural [22, 23] and forestry residues [16-19] efficiently into energy [12, 45]. Gasification leads to a syngas product which can be used in many ways including energy recovery and chemical synthesis. Pyrolysis has the distinct advantage of versatility where feedstock with low calorific value, high ash and moisture contents and diversely mixed materials can be used [46]. These processes are further discussed below.

Although biomass combustion processes have been used by humans since ancient times, they are associated with limited efficiency in producing heat and power and require costly infrastructure for storage, transport and utilisation of the energy away from the point of combustion. For biomass to be a sustainable energy resource it is vital for biomass to conform to existing energy storage, transportation and consumption patterns according to existing applications. Biomass can supply existing energy needs in the form of electrical and heat energy, fuel for transport sector and feedstock for chemicals [26]. Biomass combustion processes are not economically viable to provide transportation fuels and chemicals. On the other hand, gasification and pyrolysis provide flexible end products which can be used in many ways, for example syngas gasifier can be used for energy conversion or in chemical synthesis and bio-oil from pyrolysis provides the ease of storage and transportation.

Gasification is a thermochemical energy conversion process where small proportion of oxygen, air or steam are introduced into a gasifier reactor to convert organic materials under high temperature conditions (>800˚C) into syngas fuel [47, 48]. In other words, gasification is partial oxidation (combustion) of coal, biomass and or other hydrocarbons providing useful gaseous products which have various designations (e.g. syngas or fuel gas) depending on the gas composition and type of oxidant used. These gases are mainly composed of carbon monoxide, carbon dioxide, water vapour, hydrogen, nitrogen, C_1 – C_4 hydrocarbon gases in varying concentrations [31]. Syngas (CO & H_2) is a precursor for the production of liquid fuel through the Fischer-Tropsch (FT) synthesis process [49]. The gaseous product from gasification can be used in many different ways such as in heating applications (furnaces, boilers), power applications (gas engines, IGCC) or in chemical synthesis through catalysts for producing ammonia, hydrogen, FT hydrocarbons and methanol [50].

Pyrolysis is a thermochemical process which does not involve any oxidant and is performed under in-oxidant conditions [51] at temperatures above 350˚C [47, 52]. Pyrolysis in general can lead to three products which are solid (char), liquids (bio-oil) and uncondensable gas. Bio-oil yield is influenced by many factors such as feedstock type, pyrolysis temperature, heating rate, residence time and reactor type [37]. Pyrolysis is further categorised as: (a) fast pyrolysis where feedstock material resides in the reactor for seconds and temperature is >500˚C;

(b) intermediate pyrolysis where residence time is in the range of few minutes and temperatures from 450-550°C [31]; and (c) slow pyrolysis where residence time ranges from tens of minutes to hours and temperature is <400°C [47, 52, 53]. Pyrolysis of biomass and other organic wastes is advantageous due to the possibility of using higher moisture-containing materials and lack of further preparation processes.

Bio-oil from pyrolysis of biomass is of interest due to its higher energy density compared to initial biomass per unit mass [54] and hence can be easily stored and transported. It is a complex mixture of water and oxygen-containing hydrocarbons and is normally unstable. It is red-brown in appearance with high acidity or low pH, high viscosity and lower calorific value compared to crude oil. It is a mixture of organic compounds such as carboxylic acids, alcohols, aldehydes, esters, ketones, sugars, phenols, guaiacols, syringols, furans, terpenes and other minor compounds [31, 55]. Bio-oil can be used as a fuel in diesel engines with some modifications or as a fuel in furnaces, oil-fired boilers and turbines. Due to the complex characteristics of bio-oil, such as high oxygen and water content leading to high acidity and low calorific value compared to diesel, some improvements such as bio-oil upgradation or blending with conventional fuels are necessary to enable its usage as a liquid fuel [3, 31, 54, 56].

1.4 Pyrogasification

Pyrogasification is a technique which has been developed to combine the benefits of pyrolysis and gasification to resolve various issues preventing the uptake of these two conversion routes. There are needs to optimise the biomass to energy conversion process, resolve the end product utilisation issues in existing technologies, and invent new or shorter routes for biomass-to-energy conversion. This thesis focuses on intermediate pyrolysis, as further explained in Chapter 2, and its potential coupling with a bubbling fluidised bed gasifier to enable a relatively new energy conversion route to produce low tar containing syngas. Pyrogasification is the term used for advanced thermochemical energy conversion where pyrolysis and gasification are linked in two separate process steps to produce a syngas. This technique is also termed as 'integrated (or staged) pyrolysis and gasification', and is of particular interest to researchers due to the possibility to produce low-tar containing syngas from mixed wastes and biomass materials of varying quality. Many examples of processes based on this technique

exist, such as the flexible three-stage thermochemical conversion process by Sea Marconi Technologies [57], the NOTAR novel two-stage downdraft gasifier from Xylowatt for industrial applications [58], and a two stage Viking gasifier [59] system. NOTAR is a registered trademark used by Xylowatt to distinguish its gasifier process. All these systems have unique differences and novel ways to combine the pyrolysis and gasification stages but with a view to enhance the syngas quality with reduced tar levels.

1.5 Origin of the Thesis

This PhD project was carried out in the context of various funded projects as mentioned in the "Acknowledgments" section. The INTERREG Bioenergy NW project supported the research to support companies, organisations and local authorities to deliver local bioenergy in parts of the UK, France, Germany, Belgium, and the Netherlands. The Pyrogas IAPP project supported the novel coupling between the Pyroformer (100 kg/h) and BFB gasifier to enable the usage of complex feedstocks to be converted to syngas. This meant that lab resources were shared between different projects and tests had to be done under strict time schedules to deliver results to those projects as well as to contribute towards this PhD thesis. Tests were done in an intermediate pyrolysis screw reactor called the "Pyroformer" as patented by Dr Andreas Hornung and Dr Andreas Apfelbacher [60] in laboratories at Aston University. This reactor encompasses a combination of "pyrolysis" and "reforming by char re-circulation" and hence the name "Pyroformer". Pyroformer (20 kg/h) equipment was shared among different groups and projects, and hence there were some availability which needed to be adhered to when sharing the equipment.

This work was done to support the European Union's constant drive to increase the renewable energy share into the energy mix by looking for better ways to convert waste biomass resource into energy and chemicals. For example, hot pyrolysis tests in the 20 kg/h were done in the context of the Bioenergy NW Interreg and IAPP Pyrogas projects. Pyrogas IAPP project was supported by European Commission Seventh Framework programme, Industry-Academia Partnerships and Pathways (IAPP), weblink http://www.aston.ac.uk/eas/research/groups/ebri/projects/pyrogas-project/ . Cold flow tests were done in parallel to an MSc design project where active

supervision was provided in parallel to MSc students. Hot tests in 100 kg/h Pyroformer were conducted in Harper Adams University labs under Bioenergy NW Interreg project. This project can be found under this weblink http://bioenergy-nw.eu/project-objectives/.

For cold flow tests, plastic beads and wood pellets were used due to their ease of availability as a common feedstock. In the hot 20 kg/h Pyroformer two types of experiments are performed; the first being a parametric study based on the effect of char-to-biomass ratio on pyrolysis products arising from corn and green rye digestate feedstock sourced from mainland Europe under Bioenergy NW Interreg project as explained in the "Acknowledgements" section; whereas the second set of tests involved comparative study of various feedstock materials such as municipal solid waste pellets, chicken litter pellets and corn and green rye pellets. No other materials were tested at 20 kg/h scale.

1.6 Structure of Thesis

This thesis is based on the research on intermediate pyrolysis technique and particularly around the Pyroformer reactor situated in EBRI laboratories at Aston University.

Chapter 1 provides a broad overview of the global energy situation with an increasing trend towards utilizing waste resources and biomass for energy conversion. This chapter provides an outline of thermochemical conversion technologies and the benefits of using biomass for biofuels production. The following chapters of this thesis address the objectives based around intermediate pyrolysis and its potential integration with bubbling fluidised bed gasification (pyrogasification) and explain how these objectives have been met.

Chapter 2: In this chapter a detailed review of the literature on pyrolysis and gasification technologies is presented. Various technological aspects of pyrolysis and gasification techniques are assessed from the literature, with emphasis on the intermediate pyrolysis or screw pyrolysis. A critical review of the Pyroformer reactor (based on intermediate pyrolysis) is presented, highlighting areas for improvement as well as potential integration of the Pyroformer in gasification. Potential applications of the end products of pyrolysis such as bio-oil, biochar and syngas are highlighted in this chapter.

Chapter 3: In this chapter details of the PhD project are formulated following on from the literature review and the gaps identified. The aim and objectives of the thesis are highlighted as well as the scope, limitations and structure of the thesis.

Chapter 4: In this chapter the importance of the cold-flow modelling of a transparent 20 kg/h Pyroformer reactor is highlighted. The experimental method, materials and results are presented. The results of residence time and char to biomass ratio from this chapter pave the way for further research in hot Pyroformer experiments which as covered in subsequent chapters.

Chapter 5: The effects of char-to-biomass ratio on pyrolysis products are presented in this chapter. This constitutes an important original contribution to knowledge of the thesis. The relationship between char to biomass ratio and its effect on bio-oil fuel properties and biochar is presented in detail. The analysis of biochar with regard to its properties suitable for land application are presented. Results of biochar analysis are compared with existing biochar standards to highlight whether biochar field application can be justified based on its micro and macronutrient benefits.

Chapter 6: Experimental results from a 100 kg/h Pyroformer process (scale up model of 20 kg/h Pyroformer) are presented here. Wood pellets and Miscanthus biomass materials are studied for intermediate pyrolysis and an analysis of end products is presented in this chapter. In this experiment, biodiesel is used as a quench and in-situ blending medium to upgrade the pyrolysis bio-oil.

Chapter 7: In this chapter the design of critical components of a Pyroformer are reviewed and potential alternatives are highlighted to resolve the operational issues of the Pyroformer. The operational experience of the Pyroformer is presented to highlight the issues and potential remedies to ensure a near problem free Pyroformer system.

Chapter 8: To enable the integration of Pyroformer with a bubbling fluidised bed gasifier, a design of the coupling parts between both systems is presented in this chapter. This paves the way for so-called "Pyrogasification" where pyrolysis and gasification can be performed in coupled mode in two separate steps. Also, syngas composition data is presented from BFB gasifier commissioning test.

Chapter 9: This chapter reviews the research outcomes of the thesis and the extent to which the objectives are met. It summarises the conclusions of the research thesis and highlights the resulting recommendations.

Contributions to knowledge based around thermochemical processing of biomass are presented together with potential for future work.

1.7 Summary of the chapter

Various biological materials fall under the term *biomass* and can be used for energy generation. Biomass is mainly composed of three biopolymers: lignin, cellulose and hemicellulose. There are many benefits associated with biomass-to-energy conversion, but critics also note significant drawbacks such as competition with food and high costs.

This chapter has explored various biomass-to-energy and chemical technologies and provided an insight into their advantages and disadvantages. The literature reveals a shift towards advanced thermochemical conversion technologies for biomass conversion, due to their flexibility with regard to choice of feedstock, the decoupling of the biomass production to energy conversion, and the diversity of products which can be used in many ways as opposed to combustion systems which provide heat or electricity only. Gasification and pyrolysis are attracting growing interest from the research community, due to the benefits highlighted above. A wide range of energy needs can be met by using these advanced thermochemical conversion technologies to provide electricity, heat, cooling (via absorption or electric chillers), transport fuels and basic chemicals for further synthesis.

Gasification of biomass has the potential to provide syngas (a mixture of carbon monoxide and hydrogen principally) for onsite energy generation, or to synthesise chemicals. Pyrolysis has the advantage of providing bio-oil which can be stored, transported and consumed offsite thus decoupling the low-density rural biomass production and enabling its usage as needed in modern applications. Also, pyrolysis processing can be energy self-sustaining by use of the gaseous product as a combustion fuel for process heat, thus reducing the need for other supporting energy carriers. The solid fraction of pyrolysis called "char" has attracted attention of the global scientific community for use as a carbon sequestration medium to supplement soil organic matter in the form of solid carbon which has been absorbed by the biomass during its growth; this absorbed carbon is then put back into soil to increase the productivity of farmlands.

Combining pyrolysis and gasification leads to Pyrogasification. Pyrogasification can be useful in providing the flexibility of raw material usage through auger pyrolysis and then followed by gasification to reduce the tar component in the syngas. The vapour phase generated from complex raw materials during pyrolysis leads to better conversion into syngas at the gasification step and hence overall tar content in syngas can be reduced to avoid tar-related issues. This thesis will present an investigation of intermediate pyrolysis and the engineering design of combining intermediate pyrolysis with gasification.

Chapter 2- Literature review

Pyrolysis and gasification of biomass and wastes are of particular interest in this study for energy conversion. Separating pyrolysis and gasification into two process stages has shown many benefits as highlighted by various researchers [59, 61-64] and exemplified by Viking and Xylowatt NOTAR™ gasifiers. "NOTAR" is a trademark used by Xylowatt to represent very low tar content in the syngas. It is important to understand the background research into thermochemical conversion route to be well informed of the benefits and the optimum pathways to convert biomass and waste feedstock into energy. Conversion of lignocellulosic material to syngas through gasification has been performed since the Second World War and various patents have emerged since then. Biomass pyrolysis for charcoal production has been done for centuries, but its usage for liquid fuels has become popular only during the last few decades. Now researchers are focusing on more novel techniques which can use feedstocks of varying quality and size to produce syngas, which can be used as fuel gas in engines or chemical synthesis.

This chapter contains a literature review of pyrolysis and gasification technologies. Various pyrolysis reactor types are presented and a section on notable differences between the screw type pyrolysis systems is presented to inform the reader of the variations of design in screw pyrolysis. The influence of various operating conditions such as temperature, biomass composition and tar cracking with char is also explained in this chapter. Various gasifier types are also explained with the advantages and disadvantages of each type highlighted. The benefits of integrated pyrolysis and gasification techniques are highlighted towards the end of this chapter, which introduces the reasons to investigate and design the coupling of the pyrogasification system based on intermediate screw pyrolysis and bubbling fluidised bed gasification systems.

2.1 Pyrolysis

Pyrolysis is a thermochemical conversion process, performed in the absence of any oxidizing environment, to convert carbonaceous material into volatile vapour, gas and char. Volatile vapours can be further condensed to form a liquid called bio-oil leaving non-condensable gases. Pyrolysis can be further divided into three main types as fast pyrolysis, intermediate and slow pyrolysis [47, 52, 53].

2.1.1 General principles of pyrolysis

When biomass is subject to pyrolysis, it goes through both primary and secondary reactions which are based on mass and heat transfer mechanisms. Decomposition of biomass constituents such as cellulose, hemicellulose and lignin are classed as primary reactions which give rise to primary pyrolysis products and some intermediate radicals. These intermediate radicals are transformed through secondary reactions if not condensed rapidly. Operating parameters play major role in determining the composition of final products of biomass pyrolysis [56]. It is reported by [56] that due to biomass having low thermal conductivity (0.1 W $m^{-1}K^{-1}$ along the grain, ca 0.05 W $m^{-1}K^{-1}$ cross grain) the ability to rely on gas-solid heat transfer is limited and requires very fine biomass particle size for efficient heat transfer for fast pyrolysis reasons. For efficient heat transfer, it is imperative to rely on conduction heat transfer (solid-solid) rather than convection (gas-solid) and to carefully select a reactor type between a fluidized bed or packed bed reactors.

When an organic material is subjected to pyrolysis, complex reactions take place both in parallel and series. During pyrolysis, thermal decomposition of material takes place where long chains of carbon, hydrogen and oxygen are broken down into shorter chain hydrocarbons in the form of gases, char and condensable vapours such as tars and bio-oil [65]. Two types of reactions take place; primary reactions which are initial decomposition reactions of biomass and secondary reactions between the products of primary reaction species which can be both homogenous and heterogeneous nature. The probability and severity of these reactions depend on various factors such as type of feedstock, ash content, temperature, mixing between different species, heating rate, pressure and presence of any other catalyst [65].

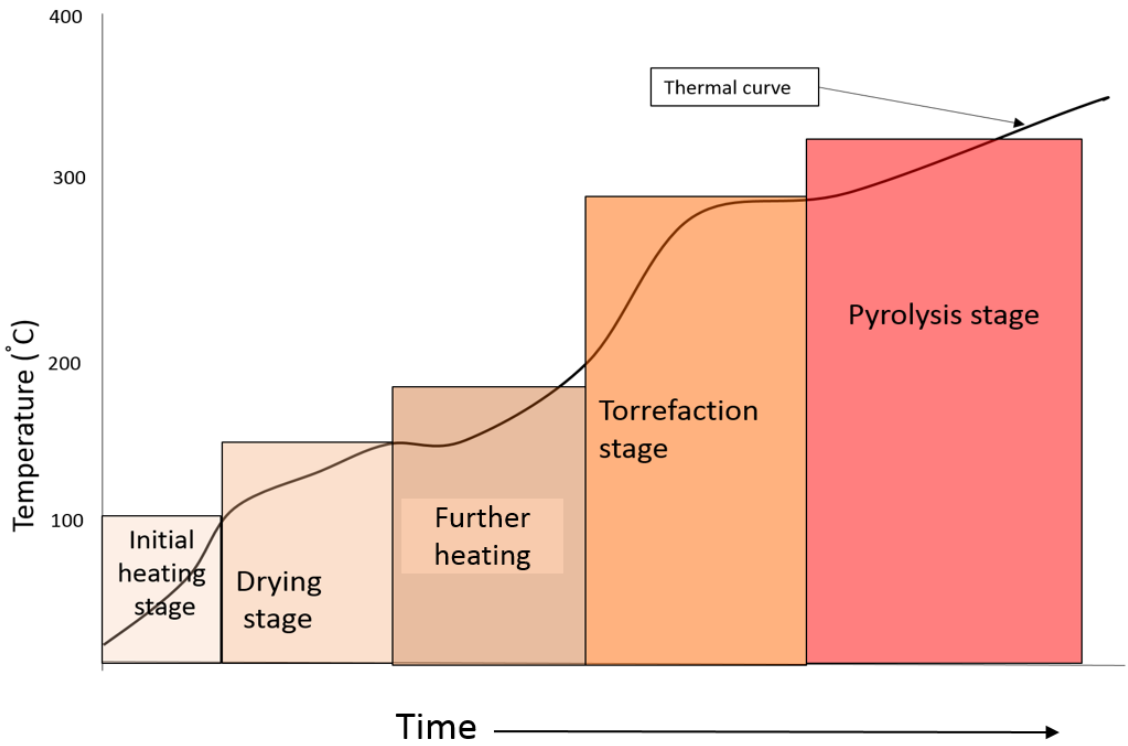

Figure 2 - Biomass thermal degradation curve showing various heating stages of biomass from initial heating leading to pyrolysis – adapted from [216]

When biomass containing some moisture is subjected to pyrolysis it goes through various stages of heating as shown in Figure 2. In the initial heating stage, the biomass starts to warm up gradually, biomass dries up and loses moisture slowly at the end of this stage. The temperature curve is shown steadily increasing with time. At the drying stage the major portion of free water (moisture) from biomass evaporates out and the curve (in the 2nd box from left in Figure 2) starts to flatten out (rate of water evaporation increases) as the temperature stays somewhat constant until nearly all the moisture is driven off the biomass. The rate of water evaporation starts to decrease by the end of this stage. In the further heating stage, the temperature of the biomass increases to 200˚C and during this stage all physically bound water is released and some low boiling point volatiles (e.g. terpenes) are also released. Between 200-320˚C, torrefaction takes place which leads to biomass being partially charred and brittle as most of the moisture is driven out and biomass fuel properties are improved. In the pyrolysis stage, which occurs above 300˚C, most of the volatiles are lost from the biomass and the solid residue remains in the form of char. Pyrolysis temperature can be as high as

800˚C, but the literature suggests most of the mass loss from biomass occurs between 400˚C and 500˚C temperature range [66]; thus further heating is not very beneficial and requires special grade of steel (Inconel, Hastelloy and stainless steel 316Ti) as material construction. The volatiles evolved from biomass can then be condensed into bio-oil and some un-condensable gases remain. Char or solid residue is also formed as a by-product.

2.1.2 Products of Pyrolysis

Pyrolysis of biomass leads to the formation of bio-oil, gas and char fractions. Mass distribution of these products is influenced by many parameters as well as the type of pyrolysis and type of feedstock. Generally fast pyrolysis is aimed at producing higher yields of bio-oil with low char yield and slow pyrolysis is used for charcoal formation with low volumes of liquids being produced. Also, it is well understood from literature [3, 48] that higher the pyrolysis temperature the lower the char fraction and higher the vapours are produced. These products are further explained below.

2.1.2.1 Bio-oil

During pyrolysis, the breakage of bonds between the biopolymers (lignin, cellulose and hemi-cellulose) lead to volatile vapours being produced. The vapours are condensed to form a liquid called bio-oil. Fast pyrolysis leads to higher bio-oil yields and slow pyrolysis to lower yields. Bridgewater [3] and Duman [23] describe the bio-oil as a complex mixture of different organic compounds which requires blending with conventional fuels or hydro-deoxygenation to make it useable as a liquid fuel. Bio-oil is a complex mixture of around 300 different compounds as stated by Zhang [55]. Various researchers [67-69] have described the weighted percentage of compounds present in bio-oil to include water (10-30%), aldehydes (1-17%), acids (3-10%), carbohydrates (3-34%), phenolics (2-15%), alcohols (<4%), ketones (2-11%) and other unclassified compounds between (5-58%). Calorific value, pH and viscosity of bio-oil are shown by Zhang [55] to vary between 16-30 MJ/kg, 2.5-3.4 and 40-100 (cP) which make it an inferior fuel compared to diesel.

2.1.2.2 Char

As stated above, the solid fraction from the pyrolysis process is char which can make up a considerable percentage (10-50 wt. % of starting feedstock) depending

on ash content and pyrolysis temperature used. Char contains ash and hydrocarbons and its percentage yield is dependent on pyrolysis temperature, residence time and feedstock composition. Ash content in char has been reported as high as 83 wt. % by Dominguez [70]. Char yield varies due to the type of pyrolysis, the pyrolysis residence time of solids in the reactor and the type of feedstock being used. For example, char yield varies between 10 wt. % from wood through fast pyrolysis to more than 50 wt. % for digestate and sewage sludge through slow pyrolysis. Sharma [71] reported that the composition of char varies with feedstock composition, but mostly includes carbon up to 70 wt. %, hydrogen and oxygen and some inorganic species such as metal oxides, sulphates, nitrates, halogens and others. The presence of inorganic species in the char is well known to have some catalytic effect on pyrolysis reactions. Calorific values of char vary between low-grade char from sewage sludge (CV of 5 MJ/kg) to higher grade char comparable to lignite coal (CV of 23 MJ/kg) and are mostly dependent on amount of ash present in char [70].

When char is used for soil amendment it is typically referred to as biochar. Char however is a solid residue produced from biomass through pyrolysis where biomass is heated up in no oxygen environment [72]. The application of biochar for soil improvement and carbon sequestration has gained momentum due to the discovery of utilisation of charcoal in fertile soils of Amazon basin. Biochar exhibits high surface area, high density of negative surface charges, characteristic pores and surface functional groups [73]. Various studies highlighted the addition of char to soil increased soil organic matter and subsequently improved soil fertility by enhancing nutrients retention in soil [74-76] leading to enhanced plant growth.

2.1.2.3 Non-condensable gas

The non-condensable gas fraction arising from biomass pyrolysis is a mixture of carbon monoxide, carbon dioxide, water vapour, hydrogen, nitrogen, C_1 – C_4 hydrocarbon gases in varying concentrations [31]. Generally, with increasing pyrolysis temperature (>500°C), the yield of gas fraction increases and char yield decreases [77]. Calorific values for the pyrolysis gas fraction are somewhat comparable to gasifier fuel gas arising from air blown gasifier systems to be around 4-10 MJ/m^3 [78].

2.2 Types of pyrolysis and pyrolysis reactors

Various types of pyrolysis have been reported in the literature to include fast pyrolysis [3, 23], slow pyrolysis [48] and intermediate pyrolysis [15, 20]. However there are other types of pyrolysis such as ablative pyrolysis, microwave, flash pyrolysis, plasma pyrolysis and vacuum pyrolysis which are also used by other researchers [31, 79]. In all these pyrolysis systems, the objective is to pyrolyse biomass to produce bio-oil, except in slow pyrolysis system where charcoal is the desired product.

2.2.1 Slow Pyrolysis

Slow pyrolysis has been used for centuries in the past to produce charcoal. Slow pyrolysis involves slow heating rates for relatively long duration of hours or even days of residence time of biomass material in the reactor. In slow pyrolysis the product is charcoal and there is little interest in vapours. Temperature in this kind of pyrolysis is kept low (<400˚C) and at atmospheric pressure to maximize the charcoal yields. Slow pyrolysis can work with large particle size up to few inches in diameter and hence needs longer residence times (days) to release the volatiles [48]. For example, large chunks of wood logs with diameters up to 10 inches and lengths up to one meter are very normal to pyrolyse and convert to charcoal in sub Saharan Africa where charcoal is used as a fuel source. Charcoal making through slow pyrolysis is a batch process and is normally performed in earth, brick or steel drum kilns with charcoal outputs ranging up to 5 tons per batch [80].

2.2.2 Fast Pyrolysis

Fast pyrolysis involves high heating rates, short residence time of fine ground biomass in the reactor and biomass to bio-oil yield up to 75 %wt. by rapid quenching [3, 23]. The main objective of fast pyrolysis is to maximize the production of bio-oil. Bio-oil product from fast pyrolysis tends to have a heating value about half that of conventional fuel oil [3]. Fast pyrolysis is better done with moisture content below 10 %wt. and biomass particle size less than 3 mm for high heat transfer to produce volatiles which are rapidly quenched to avoid secondary reactions and to maximise bio-oil product [3, 48]. It is well understood that during secondary reactions some high molecular weight hydrocarbons re-polymerize to produce char. Hence to avoid secondary reactions, fast pyrolysis produces

comparatively higher amount of bio-oil by rapid quenching (and low char yield) which are very complex and requires further upgrading for usage. Fast pyrolysis employs bubbling fluidised bed (BFB) and circulating fluidised bed (CFB) reactors for high heat transfer, good temperature control and good conversion efficiencies [3, 23].

Fast pyrolysis is distinguished by the following factors, as described by Bridgwater [3]:

- Very high heating rates and heat transfer rates are required for biomass of 3 mm or smaller particle size due to low thermal conductivity.
- Pyrolysis temperature to be 500˚C or higher to maximize liquid yield.
- Vapour residence time is kept as low as possible, typically less than 2 seconds to reduce the possibility of secondary reactions taking place.
- Rapid removal of char product, to reduce the cracking of vapours.
- Rapid quenching of pyrolysis vapours to get bio-oil to minimize the secondary reactions.

2.2.3 Intermediate pyrolysis

Intermediate pyrolysis involves moderate heating rates with solid residence time of a few minutes in the reactor. It [31] involves considerably shorter solid phase residence time (in the order of minutes) in the reactor compared to slow pyrolysis. In slow pyrolysis the objective is mostly to produce charcoal or char and not liquids from evolving vapours, whereas intermediate pyrolysis focuses on producing liquids at moderate temperatures (450-550˚C) which can phase separate into an aqueous phase and organic phase [31]. This technique is claimed to have improved the HHV of bio-oil [20], whereas the product yields remain somewhat similar in all three phases i.e. one third in each bio-oil, char and gases. Intermediate pyrolysis involves screw or an auger driven system where biomass is introduced in the pelletized or chipped form and reaction occurs at moderate temperatures around 500˚C. The use of a mechanical transport mechanism such as a screw or an auger supports slightly bigger biomass particles than needed for fast pyrolysis. Hence intermediate pyrolysis is more flexible with size and type of biomass as well as tolerance to higher moisture content than fast pyrolysis due to liquid fraction easily separable into an organic oily phase and aqueous phase. Intermediate pyrolysis was shown to be working satisfactorily without the need of hot gas filtration as the solids content in the hot vapours is very low [15, 20].

2.2.4 Other types of Pyrolysis

Flash pyrolysis involves very high heating rates >1000°C/s and very short residence time of materials through the reactor. Operating temperature can be as high as 800-1000°C. The biomass particle size needs to be in few microns to ensure very high heating rates in the bubbling fluidised bed (BFB) or circulating fluidised bed (CFB) reactor configurations [31, 81].

Other less common types of pyrolysis as reported by Hossain and Bridgwater [31, 79] include rotating cone, ablative, microwave, plasma and vacuum pyrolysis. These differ from fast and slow pyrolysis mostly in the way biomass is introduced (ablative pyrolysis) in the reactor or the way reaction is conducted (vacuum, plasma and microwave pyrolysis). In microwave pyrolysis, the biomass is heated from within the particle by microwaves rather than external heat transfer to particle. In a plasma reactor electrical arc is used to generate plasma heat for the process. Plasma pyrolysis reactors are made up of a cylindrical quartz tube which is surrounded by two electrodes to generate plasma arc to meet pyrolysis process heat requirements. A screw system is used to transport the feedstock through the tube and an inert gas is used as a working gas both to displace the pyrolysis vapours as well as to produce the plasma [82]. In another type of pyrolysis called hydropyrolysis, hydrogen is added during the pyrolysis at high pressures to reduce the oxygen content in resulting bio-oil. The product yields from these pyrolysis types are somewhat like fast and intermediate pyrolysis as discussed previously.

2.3 Factors influencing pyrolysis products

Biomass pyrolysis products can be affected mainly by the type and composition of biomass, particle size and reaction conditions including pyrolysis temperature, residence time, feeding rates and pressure. Some of these factors can be controlled or optimized during the pyrolysis such as temperature, residence time and pressure. The factors related to the type of biomass and its biopolymer composition are inherent features of biomass and can only be controlled before the biomass is grown. Normally these factors are hard to manage and demand a massive change in the whole supply chain of the biomass acquisition.

2.3.1. Biomass type and composition

Bio-oil produced from pyrolysis of biomass is directly affected by the type of biomass and the biopolymer composition (lignin, cellulose and hemicellulose) of the biomass feedstock. For example wood derived bio-oils are very acidic with a

total acid number (TAN) as high as 117 mgKOH/g [83]. Whereas, the digestate derived bio-oils have lower total acid number not exceeding 5 mgKOH/g [61]. Total acid number is a measure of corrosiveness of bio-oil and is measured by using an alkali solution such as KOH to neutralise the bio-oil. The amount of alkali solution used to neutralise the bio-oil corresponds to TAN. Other factors which has some minor influence on bio-oil quality are inorganic content in ash, weather conditions and type of soil or water used to grow that biomass.

2.3.1.1 Effect of biomass composition on pyrolysis products

Biomass is naturally made up of three main biopolymer types namely cellulose, hemicellulose and lignin, which give rise to volatiles upon thermal decomposition when subjected to pyrolysis [150]. As mentioned above, the biopolymer composition of biomass is a natural phenomenon and is an area of intense research. Hemicellulose consists of various saccharides (xylose, mannose, glucose and galactose) in the form of short branches which decompose easily during pyrolysis to form CO, CO_2 and some hydrocarbons [18]. Cellulose exist in the form of long strong branches of glucose which are require higher energy to decompose compared to hemicellulose. Whereas lignin is long aromatic rings which form chemical bonds and decompose over a wide temperature range. The typical wt% compositions of these three biopolymers for various types of biomasses are shown in Table 2.

In general, cellulose and hemicelluloses contribute toward the production of bio-oil, whereas lignin contributes in the char production. Percentage variation of these three basic components in biomass which occur naturally will modify composition and yield of pyrolysis oil. Figure 3 illustrates the chemical structures of cellulose, hemicellulose and lignin and it is evident that there is a big portion of oxygen present which accumulates into bio-oil after pyrolysis and can be up to 30 wt%.

Table 2 - Lignin, cellulose and hemicellulose content of selected biomass types [18, 25, 77, 85 & 150]

Feedstock	**Lignin (%)**	**Cellulose (%)**	**Hemicellulose (%)**
Wood	25-30	35-50	20-30
Wheat straw	15-20	33-40	20-25
Switch grass	5-20	30-50	10-40
Sugarcane bagasse	23-32	19-24	32-48
Miscanthus	17	24	44
Corn stover	16-21	28	35
Hazelnut shell	42.9	28.8	30.4
Olive husk	48.4	24	23.6
Corncob	15	50.0	31
Tea waste	40	30.20	19.9
Walnut shell	52.3	25.6	22.7
Almond shell	20.4	50.7	28.9
Sunflower shell	17	48.4	34.6
Nutshell	30-40	25-30	25-30
Paper	0-15	85-99	0
Stored refuse	20	60	20
Plant Leaves	0	15-20	80-85
Cottonseed hair	0	80-95	5-20
Industrial waste paper	5-10	60-70	10-20
Barley straw	14-15	31-34	24-29
Oat straw	16-19	31-37	24-29
Bamboo	21-31	26-43	15-26
Rye straw	16-19	33-35	27-30
Jute fibre	21-26	45-53	18-21

During pyrolysis, cellulose and hemicellulose breakdown to give organic acids, esters, aldehydes, alcohols, ketones, hydroxyl carbonyls, furans and sugars, whereas lignin contributes towards forming the phenolics and substituted aromatic groups [77, 84]. The end products of these biomass types depend upon the percentage of cellulose, hemicellulose and lignin and are also determined by the operating conditions such as pyrolysis temperature, residence time, heating rate etc. Wood, shells and husks tend to have higher percentage of lignin compared to herbaceous species. In biomass, hemicellulose acts like cement in reinforced concrete whereas cellulose acts as steel rods where strands of microfibrils (cellulose) are supported by hemicellulose. Devolatilisation of these biopolymers under pyrolysis conditions is in the order hemicellulose first, then cellulose and finally lignin [18, 37]. This is illustrated by thermo gravimetric analysis (TGA) curves for cellulose, hemicellulose and lignin and is shown in the Figure 4.

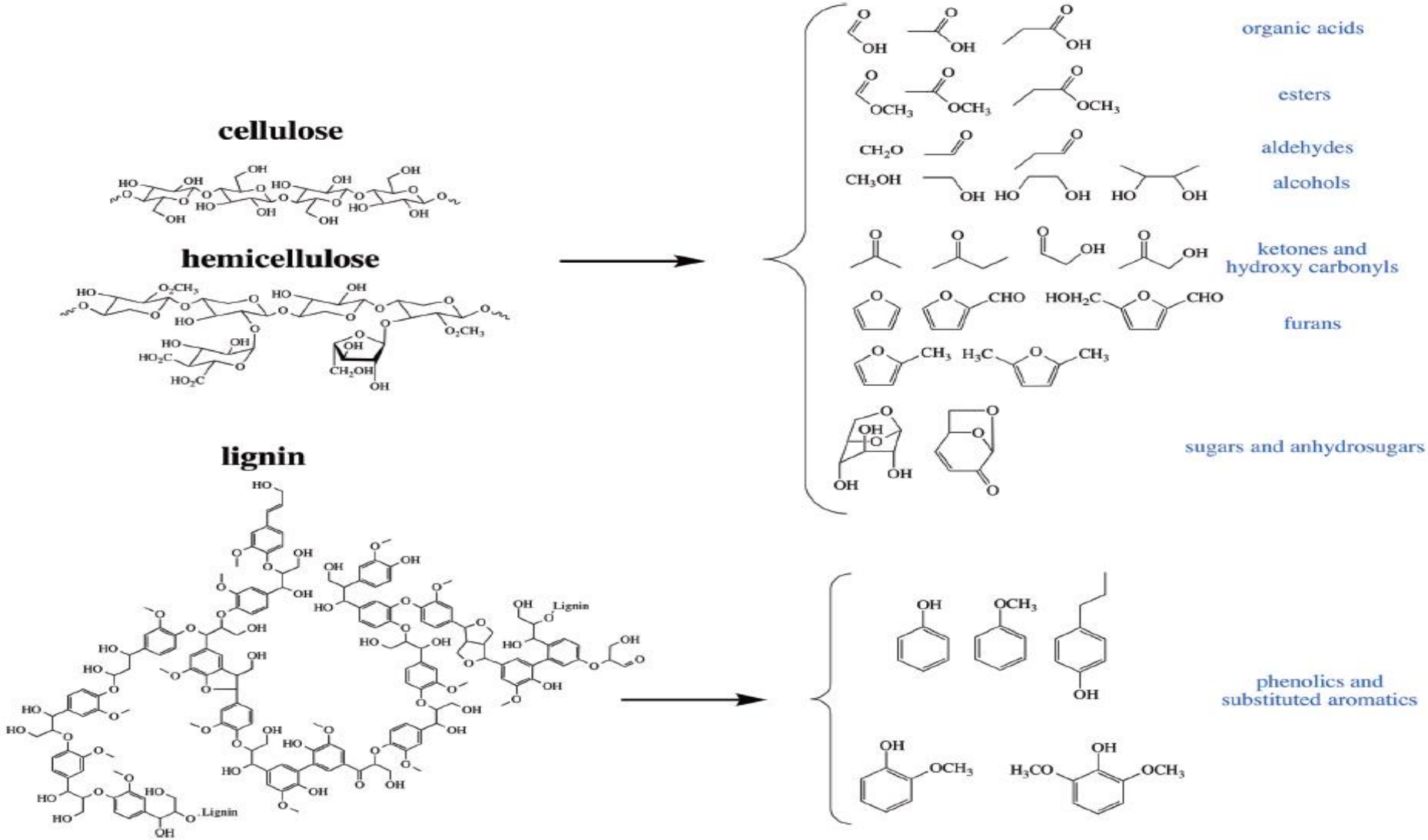

Figure 3 - Typical products from the breakdown of basic components of biomass during pyrolysis [15]

Aston University

Illustration removed for copyright restrictions

Figure 4 - Pyrolysis curves of hemicellulose, cellulose and lignin in TGA [85]

During pyrolysis, hemicellulose decomposes mostly within the temperature range of 220˚C -315˚C whereas cellulose starts decomposing above 300˚C and above 400˚C it's mostly volatilised. Lignin is more resistant to volatilisation and it has a wide temperature range of vaporisation, between a temperature range of 160 - 900˚C [85]. This shows that if the pyrolysis temperature and feedstock residence time in the reactor is low, then lignin devolatilisation is limited and the volatiles are mostly released from cellulose and hemicellulose species. The analysis of resulting bio-oil under these conditions shows the greater portion of organic acids, esters, aldehydes, alcohols, ketones, hydroxyl carbonyls, furans and sugars due to cellulose and hemicellulose breakdown whereas phenolics and aromatics are lower and char percentage is higher due to limited breakdown of lignin [85].

2.3.1.2 Effect of variation in feedstock types

In the literature, various types of feedstock have been reported to produce bio-oils derived from a variety of forestry and agricultural biomass wastes to municipal waste. Mohan et al and Antal et al [45, 86] reported the bio-oil yield in the range of ~60-95 wt.%, depending on the feedstock composition. The woody feedstock during pyrolysis gave rise to bio-oil in the range of 72-80 wt %, which depends upon the relative amount of cellulose by using fast pyrolysis method. The presence of high lignin content, shown to have a tendency to give lower liquid yields (60%-65%) [48, 86]. Volatilization or decomposition of biopolymers contributes to bio-oil, gas and char products. The presence of alkali metals in the char, as reported by Nik-Azar et al [87], has been shown to have a catalytic effect on pyrolysis reactions leading to increased char yields. Sometimes a change in the composition of bio-oil is due to the catalytic effect of alkali metals resulting in an increase in pyrolysis oil and decrease in gas products. The properties of bio-char tend to vary due to the type of feedstock and its biopolymeric composition and presence of other inorganic species in the form of ash [37].

2.3.2 Influence of operating conditions during pyrolysis

The many pyrolysis operating parameters are grouped into two types by Akhtar [88] as : (i) the parameters which are highly influencing (ii) and moderately to low influencing parameters. The temperature and biomass types are considered highly influencing parameters; whereas other factor like vapour residence times, size of feed particles are considered less influencing parameters in the production of bio-oils. The amount of mineral matter and initial moisture

content are negatively influencing parameters for bio-oil yields and energy inputs, respectively. Thermo-chemical decomposition of biomass during pyrolysis depends on various process parameters such as the type of feedstock, operating conditions and physico-chemical properties of biomass – which ultimately affect the biomass conversion time or pyrolysis rate with product distribution and quality. A combination of moderate pyrolysis temperature, rapid biomass heating rates, and short residence times maximizes the yield of liquid.

2.3.2.1 Effect of pyrolysis temperature

Temperature has a significant effect on mass loss of biomass during conversion to pyrolysis products, as shown in Figure 4. It is reported by Xiao et al and Difelice et al [89, 90] that the percentage yield of gases and bio-oils increases with temperature, whereas increases in temperature have an inverse effect on biochar production. The bio-oils or liquid fraction yield reach a maximum at about 500˚C. There are many non-condensable gases such as CO and CO_2 in the decomposition or recombination of unstable oxygenic functional groups. Pyrolysis temperature exerts a great effect on pyrolysis products originating from organic functional groups of biomass [66]. The pyrolysis temperature range is different for the three components of biomass i.e. cellulose, hemicellulose and lignin [91]. The order of pyrolysis of different components of biomass are reported by Wen et al [92] to be, firstly, hemicellulose between 180 and 240 ^{o}C; followed by cellulose and lignin at 230-310 ^{o}C and 300-400°C, respectively. It is also reported by Wen et al [92] that biomass did not pyrolyse and volatiles were not released when the operating temperature was lower than 185°C. Veses et al [54] analysed the distribution of pyrolysis products in terms of their yields. The amount of liquid and gas products were reported to increase with increasing temperature, while char decreased and the yield of liquid shown to be constant (48 wt %) above 450°C pyrolysis temperature.

In another study the mass balance observed by Dufuor et al [97] were 92.1%, 101.8%, 99.4%, and 97.8% for reactor temperatures of 700, 800, 900 and 1000˚C respectively, and the total mass of permanent gases was shown to increase between 700 and 800˚C, then remained almost constant above 800˚C. They also observed the char yield to be decreased from 16.5 wt% at 700˚C down to 13.3 wt% at 1000˚C. The quantified products masses were underestimated at

700˚C in part due to tar, which was not subject to analysis. More than 60 compounds were detected but not quantified. Total amount of the quantified aromatic tar was always lower than 5% mass and reached a maximum at 800˚C. Most of these studies indicate that having a very long residence time leads to an increase in the aqueous phase and that the optimum temperature for screw pyrolysis is around 500˚C

2.3.2.2 Effect of heating rate on pyrolysis products

In another study, Adrados [93] reported that higher pyrolysis temperatures above 750°C and slow heating rates are necessary if the aim is to produce metallurgical grade charcoal, because the liquid products obtained in slow high temperature pyrolysis are low-quality fuels having a large fraction of aqueous phase and some organic phase. The charcoal produced in this way is reported to contain a char product having (80 wt. %) of carbon. They also reported another catalytic step to upgrade the pyrolysis vapours which led to low bio-oil and CO_2 content whereas the gas fraction was increased together with higher hydrogen concentration in the gas product thus enhancing the quality of gas phase. Bridgwater et al [3] also used higher heating rates in fast pyrolysis to produce high percentage of bio-oil (up to 70 %wt) with rapid quenching of vapours to inhibit the impact of secondary reactions.

2.3.2.3 Effect of residence time on pyrolysis products

In another study done by Puy et al [94], forestry waste was pyrolysed in an auger reactor at five different temperatures ranging from 500 to 1000°C at different feeding rates of 3.9, 4.8 and 6.9 kg/h with varying residence times between 1.5 min to 5 min. Different product yields were observed by Puy et al [94] depending on the reaction temperatures and residence times. The liquid yield ranged from 45% to 59% at 500˚C and decreased with temperature due to severe cracking of the primary pyrolysis at higher temperatures. Puy et al [94] also reported the optimum temperature of 500˚C with maximum liquid yield of 58.7 wt%. Increase in gas yield with higher reaction temperatures in auger reactor and similar results were reported by Gilbert et al and Bridgwater et al [95, 96].

2.4 Methods of enhancing bio-oil quality during pyrolysis

The tar content during pyrolysis and gasification can be reduced in many ways such as by thermal tar cracking, catalytic tar cracking and tar cracking with char. Further details about tar will be discussed in section 2.9. Tar cracking is favoured

for various reasons including: improved quality of gas product, better efficiency in conversion of tars into simpler hydrocarbons, and to limit problems related to tar condensation in the downstream processes. In this thesis, the focus is on tar cracking by char as further explained in this section. Other types of thermal and catalytic tar cracking are also presented.

2.4.1 Tar cracking with char

Using char to crack the tars is well established in the literature [95, 98-101]. Char contains carbon together with other organic and inorganic species. Inorganic species which are present in the char such as alkali metal oxides, nitrates and hydrates can catalyse the pyrolysis process. Recycling of char in the Pyroformer by the outer screw to come into direct contact with evolved vapours from pyrolysing biomass in the inner screw is further supported by various authors [98-101] in varying configurations to achieve the similar result. El-Rub et al [99] reported the comparison of biomass derived char from pyrolysis with other inorganic catalysts for the cracking of naphthalene and phenol at a temperature range of 100-900˚C and also found that char as a catalyst was as good as nickel and dolomite. It is reported by Al-rahbi [98] that waste derived pyrolysis chars were effective in minimizing the condensable tars and bio-oil hydrocarbons with waste car tyre derived char with up to 70% reduction in tars compared to no char application in a pyrolysis-gasification experiment. The order of performance of chars by this author for tar removal was highlighted as tyre char>RDF char> date stone char > no char. Al-rahbi [98] used various biomass to char ratios and found that 1:3 ratio of biomass to char by %wt was giving the highest yields of CO, H_2, CO_2, CH_4 and C_nH_m gases which are formed after tar cracking. This tar cracking phenomenon was associated with char catalytic conversion and physical adsorption of tar compounds.

In another study, El-Rub [99] reported that tars can be adsorbed onto active sites of the char thus leading to tar cracking. Tar cracking over the char surface is reported by Hosokai et al [100] to result from various mechanisms such as tar deposition on char surface, dehydrogenation of tar leading to soot formation and gasification of soot. Coke formation and gas formation from char is reported to occur simultaneously, while gaseous products are formed from tars during these processes. Deactivation of char pores due to coke formation is another

phenomenon which limits the usage of char over a prolonged time and necessitates the char regeneration (as reported by Abdullah and Wu [102]) unless char can be replaced by fresh char and spent char can be used as a solid fuel in conventional applications.

2.4.2 Thermal tar cracking

In thermal tar cracking, the tar is reduced to simpler hydrocarbons by means of high temperature treatment. This kind of treatment involves high temperatures with direct heating, or by means of oxygen injection to raise the temperature of the gas containing tars to reduce them, or by means of an electric arc or plasma to elevate the temperature. A study performed by Fagbemi [217] described a kinetic model for thermal cracking of tars in pyrolysis and gasification applications for wood, coconut shell and straw at temperature ranging from 400-900 ˚C. This model showed that a gas residence time of zero to 4 seconds is needed for tar reduction. Thermal tar cracking is effective between the temperature 700-1250 ^{o}C as reported by El-Rub [99] that thermal conversion of phenol occurs at 700–900 ^{o}C. Phenol is stable at a temperature of 700 ^{o}C with only 6.3 wt.% conversion, but loses its stability as temperature increases. The conversion is more than 97 wt.% at 800 ^{o}C and more than 98 wt.% at 900 ^{o}C . In the experiment of Phuphuakrat et al [218], the reduction of the gravimetric tar mass is 78% in the case of the thermal cracking at 800 ^{o}C, whereas it is in the range of 77–92% in the case of steam and air reforming. Similar results were also reported by Chen et al [219].

2.4.3 Catalytic tar cracking

In catalytic tar cracking, a catalyst is used which can be effective at even lower temperatures compared to thermal cracking or combination of both high thermal temperature and catalyst for maximum conversion of tar into gaseous products to achieve better conversion efficiencies. Jude et al [220] used algae species *Chlorella vulgaris*, *Spirulina platensis* and *Saccharina latissimi* under supercritical conditions at 500 ˚C and 36 MPa in a batch reactor for 30 minutes with and without sodium hydroxide and Ni-Al_2O_3 catalyst. They reported tar reduction of 71 wt% with the catalyst. By doing this they were also able to enhance the hydrogen production yield thus achieving the double benefit of tar conversion and hydrogen yield maximisation. In another study Tiejun et al [221] explored the use of Nickel/dolomite catalyst which was prepared by the incipient wetness method over

a dolomite support. They modified the dolomite with Fe_2O_3 powders with natural dolomite powders to increase Fe_2O_3 content for higher activity of tar cracking. They also prepared another four catalysts (natural dolomite, modified dolomite, ICI-46-1, and Z409) and tested and compared them with Ni/dolomite catalyst. The also explored the effects of temperature, steam-to-carbon, and space velocity on tar conversion. They found the Ni/dolomite to be very active and useful for tar removal. A 97% tar removal was obtained at catalyst temperature of 750 °C and space velocities of 12 000/h. A study by Mian et al [222] investigated the tar cracking with nickel catalyst using steam obtained from a char supported nickel catalyst in a lab-scale fixed bed reactor to determine the effects of catalytic cracking temperature, Ni loading and gas residence time on product distribution and gas composition. Their results showed that the optimum catalytic cracking parameters were at 800 °C catalytic cracking temperature, 6 wt% Ni loading and 0.5 s gas residence time.

2.5 Types of intermediate pyrolysis reactors

The reactor is the heart of pyrolysis system and most of the research in pyrolysis has been focused around the reactor development [65]. There are various types of reactors used for pyrolysis such as bubbling fluidised bed, circulating fluidized bed, cone reactor, microwave, screw/auger, cyclonic or vortex, multi-stage, rotary kiln, entrained flow reactors. Screw pyrolysis reactor is essentially a mechanical conveyor mounted inside a tube with the ability to transfer the biomass feedstock along the length of heated reactor tube. The pyrolysis reactor tube can be heated by various means such as electrically [20, 103, 104] or through a mobile hot gas [59] or simply the heat can be supplied through a hot solid such as hot sand [105] or hot steel balls [15].

An auger or screw as used in pyrolysis is simply an Archimedes helical screw driven by mechanical means to transport the solids through the reactor. Various researchers have used auger kilns such as the Haloclean reactor [106-108] and screw pyrolysis systems with interchangeably attribute their systems to fast, slow and intermediate pyrolysis. However, the key principle remains the same in all reactors - the purpose is to convey the biomass through the reactor by some mechanical means [3, 51, 79, 96]. Ingram and co-workers reported [109] the amount of char produced from different feedstock (e.g. wood and barks from pine and oak) in an auger pyrolysis reactor in the range 17.5–19.8%, 17.5–19.9%,

9.7–23.2, 21.3–27.8% and total bio-oil yield in the range 48.7–55.2%, 49.6–56.3%, 42.8–44.2%, 43.8–49.8%, respectively. A screw can be either mounted on a shaft (solid or hollow) within a tube or it can simply be a spring-like structure depending on its design requirements whether it is the strength or flexibility which is required in the screw. Screw-based reactors for pyrolysis have been developed to be either single-screw type [103, 106], parallel twin-screw co-rotating type (for self-cleaning purposes) [105], parallel twin-screw counter-rotating type, or twin-screw counter-rotating type where one screw is mounted inside the other [104, 110]. These variations in screw designs are motivated by some technological advantage, differentiation for patenting, and/or simplicity of design. Given below in Table 3 is a comparison of different screw-based pyrolysis reactors together with information about their operation, design parameters and variations in product yields arising from such a system.

The auger screw mechanism within a pyrolysis reactor gives distinct advantages compared to fluidised bed system. These advantages include the ability of a screw to convey biomass materials which are heterogeneous [3], with varying moisture content, clearing of the internal reactor walls and hence aiding the heat transfer from metal surface of reactor to biomass, prolonged solids residence time, ability to recycle char in twin screw systems, ability to handle a variety of heat-carrying media, ability to control the material flow by rotational speed of screw. The disadvantages of screw pyrolysis include the lack of rapid heat transfer and thermal expansion in the material of construction leading to mechanical problems compared to fluidised bed pyrolysis systems [3]. Once the biomass has passed through the reactor by means of a screw, the resulting vapours are then either passed through a ceramic filter or allowed to condense in a specially designed condensing train. The char or solid residue of pyrolysis products is collected in a char container. The char collection is also aided by the same screw which is transporting the biomass through the pyrolysis reactor.

Table 3 - Various configurations of pyrolysis screw/auger reactors types

Reactor type	**Heating medium**	**Reactor throughput**	**Feedstock used**	**Yields Wt.%**	**Reactor Schematic**
Haloclean[a] auger kiln	Heated circulating steel spheres Temperature: 450˚C	Feed: 2-3 kg/h RT: NA	Brewers spent grains (barley) -as received	Char: 50 Liquid: 51 Gas: 26	Figure 5
Auger[b] reactor Diameter: 7.6 cm Length: 102 cm	Electrical band heaters. Temperature: 450˚C	Feed: 1kg/h RT: 50 s	Pine wood 2-4 mm particle size	Char: 17.5-19.8 Liquid: 48.7-55.2 Gas: NA	NA
Twin Parallel screws[c] counter rotating reactor Each screw diameter: 44 mm Length: 450 mm	Electrically heated Sand as heat carrier @ 2kg/h. Reactor Temperature: 500˚C	Feed: 300g RT: NA	Cassava Rhizome 0.425 – 0.6 mm particle size	Char: 22 Liquid: 40 Gas: 38	Figure 6
Auger reactor [d] Reactor length: 420 mm	Band electrical heaters used. Temperature: 450˚C	Feed: NA RT: NA	Mango wood < 0.425 mm particle size	Char: 22 Liquid: 61 Gas: 17	Figure 7
Two coaxial horizontal screw Pyroformer[e] reactor	Electrical band heaters Temperature: 450˚C	Feed: NA RT: 4 min	Brewers spent grains-6mm pellets	Char: 29 Liquid: 52 Gas: 19	Figure 8

[a] -[106], [b] -[111], [c]-[105], [d]-[112], [e]-[20]
RT-Residence time of solids
NA-not available

Given below in Figures 5, 6, 7 and 8 are schematics of screw-pyrolysis reactors. All systems have a great similarity in the biomass conveying mechanism through the reactor by a screw; however, the differences between these reactors are seen in the way screw is laid out within the reactor, type of heat transfer

medium, number of screws in each reactor, the feeding system and the condensing system.

Screw pyrolysis reactors differ in their ability to transport biomass through the reactor's hot zone according to the different configurations used. For example, a simple screw pyrolysis system [106, 111, 112] can just convey the biomass, provide the mixing and heat transfer from heat media or through reactor wall. Another way to arrange the screw pyrolysis reactor is in the form of a twin screw format which have counter-rotating arrangement in omega shape [105] of the tubes of the reactor. This layout helps in transporting the biomass in a single forward or backward direction. This arrangement provides the additional ability to self-clean the screws and hence can handle sticky materials. Another way to arrange screw pyrolysis reactor is in a twin screw counter rotating system where one screw is installed inside the shaft of other screw which helps to transfer material in same and or opposite directions [20], thus re-circulating the char to enhance the heat transfer in fresh feed and leading to further cracking of evolving vapours by tar.

Aston University

Illustration removed for copyright restrictions

Figure 5 - Scheme of Haloclean rotary kiln [106]

The Haloclean reactor (Figure 5) is different from other pyrolysis reactors in many ways; for example, it has steel balls circulating within the kiln together with biomass thus enhancing the heat transfer between these solids. The reactor body is electrically heated and screw conveyor inside the kiln transfer the fed biomass across the reactor. The advantage of this reactor configuration is rapid heat transfer from steel balls to biomass as well as large particle size irregular shape biomass feed types. The reactor size has a throughput of 1-2 kg/h and a bigger variant of this reactor with a feed throughput of 100 kg/h exists at Karlsruhe Institute of Technology in Germany.

Aston University

Illustration removed for copyright restrictions

Figure 6 - Schematic diagram of the parallel counter rotating twin screw pyrolysis apparatus [105]

Figure 6 shows a laboratory-scale screw pyrolysis reactor with a biomass feed rate of 280-400 g/h with screws driven by DC motors to convey the biomass and hot sand. The system takes 5 times higher sand throughput compared to biomass. Although this system also has efficient direct heat transfer from the hot sand, the disadvantage is mixing of sand with the char. The main twin screws in this pyrolysis reactor are counter rotating and this gives it an advantage over other systems due to its self-cleaning action where both screws are cleaning each other and high protein containing or softened biomass can be conveyed without problems.

In Figure 7, a simple single screw pyrolysis reactor is shown with simple biomass conveying ability. The outside walls of the reactor are heated by means of electrical band heaters to provide necessary heat for pyrolysis. The residence time of the biomass in the reactor is controlled by a motor by varying its rotational speed.

Aston University

Illustration removed for copyright restrictions

Figure 7 - Schematic diagram of auger reactor [112]

In Figure 8, a twin-screw counter rotating pyrolysis screw reactor (Pyroformer) is represented. The main differences between this reactor (Figure 8) and the reactor in Figure 6 are that (i) no sand is used as heat carrier in the Pyroformer and (ii) the material is transferred in series from one screw to another in the Pyroformer. The reactor in Figure 6 has self-cleaning abilities due to its twin screws counter rotating in parallel thus meshing with each other. Other differences between these two reactors are the Pyroformer's ability to recycle char from one screw to other and thus maximising the heat transfer into fresh feed as well as tar cracking by char action as discussed earlier. Both these reactors have their advantages over each other, for example reactor in Figure 6 can handle high protein containing materials and materials which are softened (sticky) during pyrolysis, whereas the Pyroformer (Figure 8) can provide a very long residence time of material, high heat transfer through char and catalytic effect by char recycling.

Aston University

Illustration removed for copyright restrictions

Figure 8 - Schematic diagram of the Pyroformer reactor system [20]

2.6 Critical review of Pyroformer studies

The author has used an intermediate pyrolysis based reactor introduced at Aston University called "Pyroformer" (as shown in Figure 8, item 1). This reactor has been used by various other researchers in their studies such as [15, 20, 110, 113]. The Pyroformer is claimed to have significant advantages in increasing gas yield and quality, low molecular weight bio-oil and its ability to process difficult feedstocks with higher moisture content. Experimental results from various studies [20, 110, 113, 114] showed better bio-oil and permanent gases properties compared to fast pyrolysis bio-oil [46, 48].

Key recent studies to inform the current one include those of Miloud et al [114] and of Yang et al [110] who used a small Pyroformer of 20 kg/h throughput for their experiments. Pelletized biomass materials such as two varieties of de-inking sludges (AN de-inking sludge and KC de-inking sludge) were used by Miloud et al [114], whereas Yang et al [110] used wood pellets and barley pellets for their tests. More details about the sources of these biomass can be found in [114] and [110] which are de-inking paper sludge pellets, wood and barley pellets. The de-inking sludges (as shown in Table 4) exhibit very low carbon, HHV and moisture content and very high ash content [152]. This type of material is generally sent to landfill or combusted in boilers with natural gas to recover some energy; however it is normally deemed inefficient for energy recovery [104].

Yang et al [110] on the other hand has tested more refined materials such as wood and barley pellets. Table 5 shows the feedstock analysis with carbon 47.5% and 44.2% for wood and barley straw pellets with considerably higher oxygen content in both materials. Moisture, HHV and ash content were also shown to be in the average range typical of refined woody biomass.

Table 4 - Proximate, ultimate analysis and heating values of the de-inking sludges. Adapted from [114]

	Aylesford Newsprint (AN) de-inking sludge	**Kimberly-Clark (KC) de-inking sludge**
Moisture content (As received wt %)	35	48
Proximate analysis wt% (dry basis)		
Moisture	1	1.3
Volatiles	46.3	55.1
Fixed carbon	1.1	<0.1
Ash (at 900 °C)	51.6	43.6
Ash (at 575 °C)	74.5	62.9
HHV (MJ/kg)	6.4	7.0
Ultimate analysis wt% (dry basis)		
Carbon	21.1	21.7
Hydrogen	2.3	2.8
Oxygen[a]	24.7	29.8
Nitrogen	0.3	2.1
Sulphur	<0.1	<0.1
Chlorine	<0.1	<0.1

[a] Obtained by difference

It is evident from feedstock analysis that both set of materials de-inking paper sludge pellets [114] and wood and barley pellets [110] exhibit diverse composition properties and were fit for use in Pyroformer. Both researchers have reported the approximate feeding rates of the feedstock. Miloud et al [114] has reported 15 kg/h for both de-inking sludge samples which equates to 4 minutes of residence time if a single pass of material through inner screw is estimated however char recycling through outer screw is the key differentiator step. The rate of char recycling determines the catalytic effect to increase HHV of gas and to crack large molecular weight hydrocarbons in to light fractions. The rate of char recycle within the Pyroformer is determined by relative rotational speeds of inner screw to outer screw rpm. Yang et al [110] has reported the feeding rates of 6kg/h and 5 kg/h of wood and barley straw pellets respectively. Inner and outer screw speeds of 1 and 7 rpm respectively were reported by Yang et al [110] with a residence time of 1.5 minutes.

Table 5- Wood and barley feedstock and products analysis (dry basis) in the Pyroformer - adapted from Yang et al [110]

		Unit	Wood	Barley straw
Feedstocks analysis				
Ultimate analysis	C	wt%	47.5	44.2
	H	wt%	5.3	6.1
	O[a]	wt%	0.4	0.4
	S	wt%	36.4	30.4
	Cl	wt%	<0.1	0.6
Proximate analysis	Moisture	wt%	<0.1	0.4
	Volatiles	wt%	82.1	74.9
	Fixed carbon	wt%	7.0	11.9
	Ash	wt%	7.7	7.2
HHV		MJ/kg	3.2	6.0
Pyrolysis oil analysis				
Elemental analysis	C	wt%	55.69	62.57
	H	wt%	7.93	8.12
	N	wt%	0.36	1.41
	O[a]	wt%	36.02	25.79
Properties	TAN	g/mgKOH	47.5	30.9
	Moisture	wt%	15.4	5.8
	HHV	MJ/kg	24.2	28.9
	Kinematic viscosity @ 40 °C	cSt	14.8	30.5
	Density @ 20 °C	g/ml	1.10	1.15
	Carbon residue	wt%	3.55	6.50
	Ash	wt%	0.18	0.20
Gas analysis				
	H_2	vol%	2.24	1.54
	O_2	vol%	--	0.42
	N_2	vol%	5.54	4.68
	CO	vol%	34.70	21.74
	CH_4	Vol%	7.24	10.48
	CO_2	vol%	50.27	60.13
HHV		MJ/m^3	7.27	6.92
Char analysis				
Elemental analysis	C	wt%	75.60	74.83
	H	wt%	3.38	3.51
	N	wt%	0.22	0.10
	O[a]	wt%	10.20	8.46
Ash		wt%	10.60	13.10
HHV		MJ/kg	30.1	32.9

[a] Obtained by difference

It is better to measure the actual material throughput rather than rely on theoretical calculations which are prone to errors. Faster outer screw speed of 7

rpm should indicate a blockage shortly after start as more and more solids build up in the system rather than leaving the Pyroformer unless the experiment has been performed under unsteady state in which case the experiment must have been completed before reaching the steady state. However, product yields and quality are more interesting for the sake of experiment rather than the screw settings. There is a strong relationship between screw rpm and product yields and quality due to the fact lower the inner screw rpm the longer the solids residence time and higher the char to biomass ratio in the screw thus leading to increased mass loss from feedstock and hence lower the char yield [110 & 114].

The product yields reported by Miloud et al [114] are 9 wt% bio-oil (of which 1 wt% is aqueous phase), 15 wt% pyrolysis gases and 75 wt% is solid phase (char). As expected due to very high ash content in feedstocks up to 75 wt% and 63 wt%, the solid phase after pyrolysis have very high proportional yield compared to liquid and gas. It can be seen that % yields of the products are not well reported, however more attention was given to quality of gases and bio-oil from the materials. Table 6 gives the bio-oil ultimate analysis and heating values.

Table 6 - De-inking sludge bio-oils ultimate analysis and heating values [114]

Aston University

Illustration removed for copyright restrictions

The HHV of these bio-oils are superior to most of the bio-oils produced through pyrolysis with different feedstocks. The heating values are as good as biodiesel. Also, the lower oxygen content is another key factor enabling such high HHV of the bio-oil. The reasons behind having such high HHV can be attributed to solids (char) re-circulation within the Pyroformer as well as high heating rates. During the recirculation of solids, inorganic content (mostly metals such as shown

in Table 7) have played an important role in producing metal oxides and thus lowering the overall oxygen content in bio-oil.

Bio-oil fuel properties as presented in Table 8 show the suitability of the bio-oils as engine fuels with the exception of high total acid number and carbon residues. Carbon residue can be removed by physical methods and total acid number can be improved by blending in high proportion with conventional diesel or biodiesel fuels. The HHVs (37 and 36 MJ/kg) of the bio-oils are much better than fast pyrolysis fuel which have HHVs between 15-18 MJ/kg [48].

Table 7 - De-inking sludge bio-oil metals analysis [114]

Table 8 - De-inking sludge bio-oil fuel properties [114]

Aston University

Illustration removed for copyright restrictions

When comparing the bio-oils from de-inking sludges, wood and barley straw pellets it is evident that HHVs of de-inking sludge oils are much better than those from wood and barley feedstocks. One simple reason for this is comparatively high oxygen content in wood and barley oils of 36% and 26% as opposed to 11% in de-inking sludge. It is also very interesting to see that de-inking sludge pellets have higher throughput compared to wood and barley, which means heating rates for de-inking sludge could be slightly lower but bio-oil properties are still better than wood and barley oils. The quality difference in bio-oils from de-inking sludge to those of wood and barely can be better explained by the presence of metals in ash. The metals (inorganics) must have oxidised by taking the oxygen away from oil into water vapour in gaseous fraction and helped crack the vapours into lighter molecular weight hydrocarbons.

The HHVs for pyrolysis gases are somewhat similar in all cases (Table 5 & 9) with minor differences which hold well with expectations (for char derived tar cracking) due to long chain hydrocarbons cracking into lighter hydrocarbon in the Pyroformer. The gas HHVs of all feedstock are very similar to low quality HHV air blown gasifiers.

Notable differences in the solid phase (char) are evident from Table 10. Ash (60 wt %) and oxygen (24 wt %) contents are very high in de-inking sludge

derived solid phases and carbon content is very low (17.12 wt %). When compared to wood and barley for ash, oxygen and carbon contents are shown in Table 5.

Table 9 - De-inking sludge gas phase analysis [114]

Aston University

Illustration removed for copyright restrictions

Table 10 - De-inking sludge char ultimate and HHV analysis [114]

Aston University

Illustration removed for copyright restrictions

2.7 Lessons from the Pyroformer studies

This review indicated some shortcomings in the way the data are reported by both researchers [110, 114]. The compilation of data shows that more attention was paid towards the analysis of the quality of bio-oils and gases [114] and less towards the optimisation of the pyrolysis parameters. There is a lack of detail into showing the relationship between inner and outer screw speeds, recirculated char to fresh biomass feed ratios and the impact on quality and quantity of the pyrolysis products. Bio-oils from de-inking sludge exhibited better quality but had lower yield compared to barley and wood derived oils [110]. Metals must have played a major role in cracking large molecular weight hydrocarbons or tars into lighter

hydrocarbons. Bio-oils and permanent gases from all feedstock show better qualities than those of fast pyrolysis products [20, 48]. It is evident that more work needs to be done to establish optimum temperatures, char recirculation rate and residence time of test samples in the Pyroformer. The knowledge gained through this review will be extremely useful in making intelligent decisions when testing further samples on Pyroformer. Residence time calculations based on actual runs need to be calculated and a detailed mass and energy balance needs to be carried out for all tests by building upon the experience of [110].

2.8 Gasification

As stated earlier biomass gasification is desirable for fuel production and synthesis of chemicals. Gasification is essentially a lean form of combustion where lower amount of oxygen is supplied than a combustion process to produce a fuel gas (syngas) which can be further used as fuel or for chemical synthesis. Gasification processes have been extensively studied where researchers have tried to optimise the gasification conditions by means of thermal and catalytic treatments to enhance the gas quality by reducing the tar content in the syngas [14, 115], increasing the calorific value, reducing the processing steps to name a few. Furthermore, various studies focused on the effect of gasifier types [116], effect of processing temperatures [117-119], effect of biomass types and its particle size [119], effect of gasifying (oxidant) agent [118, 119], effect of the bed material [120, 121] and combining gasification with other processes to enhance the process economics. During gasification, various complex homogeneous and heterogeneous reactions take place; some of these are shown in Table 11.

Gasification involves four different steps i.e. drying of biomass, pyrolysis, oxidation and reduction [124]. These are further explained below.

Drying - Biomass has varying moisture content which is removed in a drying process at temperatures above 100°C. In this step, no chemical reactions take place and only water vapour is removed from biomass by heat due to the phase change into steam.

Pyrolysis – In this step biomass starts to decompose [51] in the absence of oxidant at elevated temperatures and vapours are released from biomass by means of primary reactions. The proportions of vapours and char produced are influenced by process conditions such as the heating rate and operating temperature. In

addition, the product distribution is also affected by biomass composition (type of free radicals released) and biomass size (heat transfer limitations).

Oxidation – At elevated temperatures and in the partially oxidised environment, heterogeneous reactions take place between oxidant and biomass forming carbon monoxide and water vapour. Oxidation is influenced by chemical composition of biomass, type of oxidant (oxygen, steam, CO_2 or air) and operating conditions. This step is mostly exothermic and results in heat energy being released resulting in energy self-sufficiency to sustain the process.

Reduction – This is a net endothermic step during which high temperature chemical reactions take place in the absence of oxygen. Various reactions between the products of oxidation and char take place to form new hydrocarbons. Ash and some char are the by-products of this reaction step [81, 124, 125].

Table 11 - List of reactions in gasification process [122, 123]

Aston University

Illustration removed for copyright restrictions

–

Gasifier selection involves a detailed understanding of the different types of gasification systems. Selecting a gasifier type between an atmospheric or pressurised type will have cost implications as pressurised systems tend to cost more compared to their atmospheric pressure variants [56]. Selection between a fixed bed and fluidised bed gasifier system will be influenced by the scale of process as well as the upstream and downstream processing requirements such as upstream air preheating for fluidised bed gasifier and downstream heavy air suction requirement for fixed bed gasifiers. Choosing among different oxidant types such as air, oxygen, steam or CO_2 will be influenced by capital costs, syngas

product quality and its application. Using air as an oxidant is a cheaper option with regards to capital investment but it will not give high calorific value syngas due to (inert) nitrogen and hence a compromise needs to be made during selection process [126]. Syngas heating values have huge influence when selecting a gasifier because syngas heating value ranges between 4-40 MJ/kg. The end applications of syngas may necessitate certain heating values e.g. syngas for heating applications can be accepted with a low heating value gas whereas Fischer Tropsch diesel and other chemical synthesis will require the fairly high heating value syngas [127].

There are many types of gasification system configurations which are preferred for various reasons; these are presented in Table 12. Most notably they include fixed-bed downdraft gasification where biomass and syngas flow downward in co-current direction, and updraft gasification where biomass and syngas flow in counter directions with syngas generally flowing upward in the gasifier. Fluidised bed gasification involves a moving (catalytic or non-catalytic) bed material in addition to biomass and oxidant. Fluidised bed gasifiers include bubbling and circulating fluidised beds. In a bubbling fluidised bed gasifier, there is rapid mixing of biomass and bed material by the oxidant which leads to high heating rates and somewhat uniform distribution of temperature within the system [128]. Notable differences between different types of gasifiers arise due to variations in support for biomass material in the gasifier, direction of flow of material and oxidant and the heat supply and control in the gasification process. Table 12 lays out the most common gasifier configurations [79, 129].

Table 12 - Types of gasifiers, fuel and oxidant flow configuration [79, 129]

Aston University

Illustration removed for copyright restrictions

2.8.1 Fixed bed gasifiers

Fixed bed gasifiers are generally suited for small-scale gasification applications under 1 MW. Generally, there is a grate inside the gasifier which supports the biomass while it is consumed during the reaction. The biomass bed normally travels downwards until it is reacted and the char (ash) is then removed from the bottom of the gasifier. The oxidation reaction zone experiences the highest temperature in the process and maintaining this temperature is somewhat difficult giving rise to variations in quality of product gas. Fixed bed gasifiers are further divided in two types; updraft (i.e. counter current) gasifier and downdraft (i.e. co-current) gasifier.

2.8.1.1 Updraft gasifier

This type of gasifier is normally simple, providing a low-cost process with greater flexibility of feedstocks with high moisture and ash containing materials. Ash is the remaining inorganic residue of biomass after complete combustion. Updraft (Figure 9) gasifiers are generally well known for high tar content (up to 20% of tar by weight) which limits the syngas applications unless thoroughly cleaned [117].

2.8.1.2 Downdraft gasifier

This type of gasifier produces a very low tar syngas which can be used in an engine for power production. Tars can be broken down in the hot zone of the gasifier due to presence of oxidant and high temperature. Tars are thermally broken down into permanent gases, thus giving better quality gas with low tar content compared to updraft gasifiers. Another advantage of the down draft gasifier is that it allows turn down in syngas output, thus enabling the system to run at considerably lower syngas output if needed to match with engine syngas demand. Disadvantages of the downdraft gasifier include the problems associated with low-density fibrous feedstocks, and low ash melting point of feedstocks in the oxidation zone causing material flow issues within the gasifier bed. Also, small-scale applications (generally <1 MW) and low moisture content biomass requirements are the other disadvantages of this type of gasifier. A schematic of the down draft gasifier is shown in Figure 10.

Aston University

Illustration removed for copyright restrictions

Figure 9 - Schematic of an updraft gasifier [127]

Aston University

Illustration removed for copyright restrictions

Figure 10 - Schematic of a downdraft gasifier [127]

2.8.2 Fluidised bed gasifiers

Fluidised bed gasifiers have been used extensively for coal gasification for many years. Fluidised bed gasifiers have certain key advantages over fixed bed gasifiers; these include rapid heat transfer, uniform temperature distribution and excellent mixing. Two main types of fluidised bed gasifiers exist [127]:

- Circulating fluidised bed (CFB)
- Bubbling fluidised bed (BFB)

2.8.2.1 Circulating fluidised bed gasifiers

This type of gasifier allows high throughputs of materials as the bed material is circulated between the gasifier and cyclone separator where char can be removed and the bed material and char can be recirculated. These gasifiers can be operated at elevated pressures and can be easily coupled to gas turbines for increased efficiency and economy of scale. Circulating fluidised bed gasifiers exhibit benefits such as rapid heat transfer, uniform temperature distribution, excellent mixing and high conversion rates. Disadvantages of these gasifiers include temperature gradients along the path of solids flow. Heat transfer in circulating fluidised bed gasifiers is poor compared to bubbling fluidised bed gasifiers [79]. Given below (Figure 11) is a schematic of CFB gasifier.

2.8.2.2 Bubbling fluidised bed gasifiers

This type of gasifier (as shown in Figure 11) consists of a vessel with an air distributor nozzle assembly at the bottom of the vessel. Biomass feed enters the bed and finely ground bed material is fluidised by air or oxidizing agent. The temperature of the bed in the gasifier is regulated by the air/biomass ratio within 700-900°C. Biomass is thermally broken down into gaseous compounds and char is produced. The hot char and fluidizing bed material cause further reactions to break long chain hydrocarbons or tars into syngas components. Thus, a syngas product with very low tar content is produced with tar content less than 3 g/Nm^3.

Advantages of BFB gasifiers include uniform syngas product composition, uniform temperature distribution throughout the gasifier, rapid heat transfer between the biomass, bed material and oxidant. It is also possible to achieve high conversion efficiency and low tar content in the syngas. The effectiveness of tar removal can be further enhanced by using catalytic bed materials such as olivine, dolomite and other industrial nickel based catalysts. Disadvantages include

problems with low ash melting point materials and large gas bubbles bypassing the bed [79].

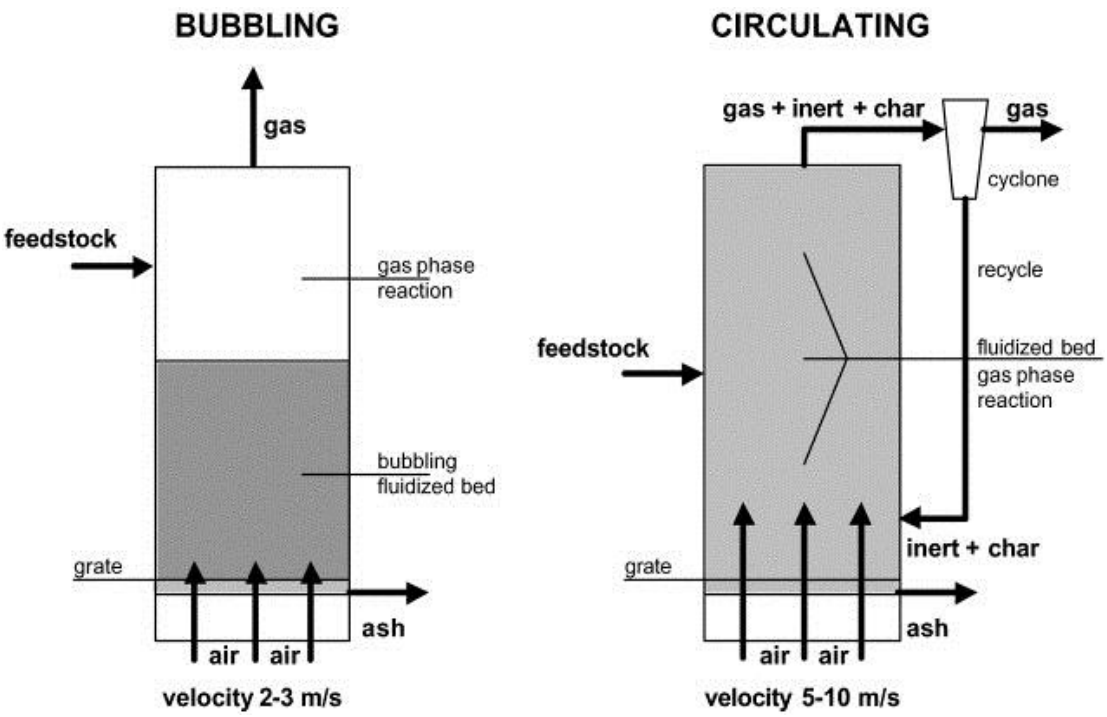

Figure 11 - Schematic of bubbling and circulating fluidised bed gasifiers [130]

2.8.3 Plasma gasification

Plasma gasification is preferred for mixed waste such as MSW or hazardous waste (asbestos and radioactive) where high temperatures are used to produce syngas and a melt arising from inorganic species of feedstock. Distinctive features of the plasma process are higher energy efficiencies and its ability to produce very high temperatures (15000 Kelvin) which are not achievable with conventional gasification and combustion. These high temperatures help to reduce tars and convert all the organic material into syngas. Tar content as reported by [131, 132] is shown to be 1000 times less than that of auto-thermal gasification processes. Thermal plasmas are obtained by arc discharges from DC or AC current or through radio frequency or microwaves. Mostly DC plasma technology is preferred for waste gasification plasma processes. The plasma is formed by high energy from AC or DC sources through the plasma torch close to the bottom of reactor and fuels are gasified through the plasma state. The oxygen demand in this process is small compared to conventional gasification as most of the thermal energy is coming from external energy source rather than through exothermic reactions

between the fuel and oxygen. Oxygen is only used to convert the fuel into syngas [133].

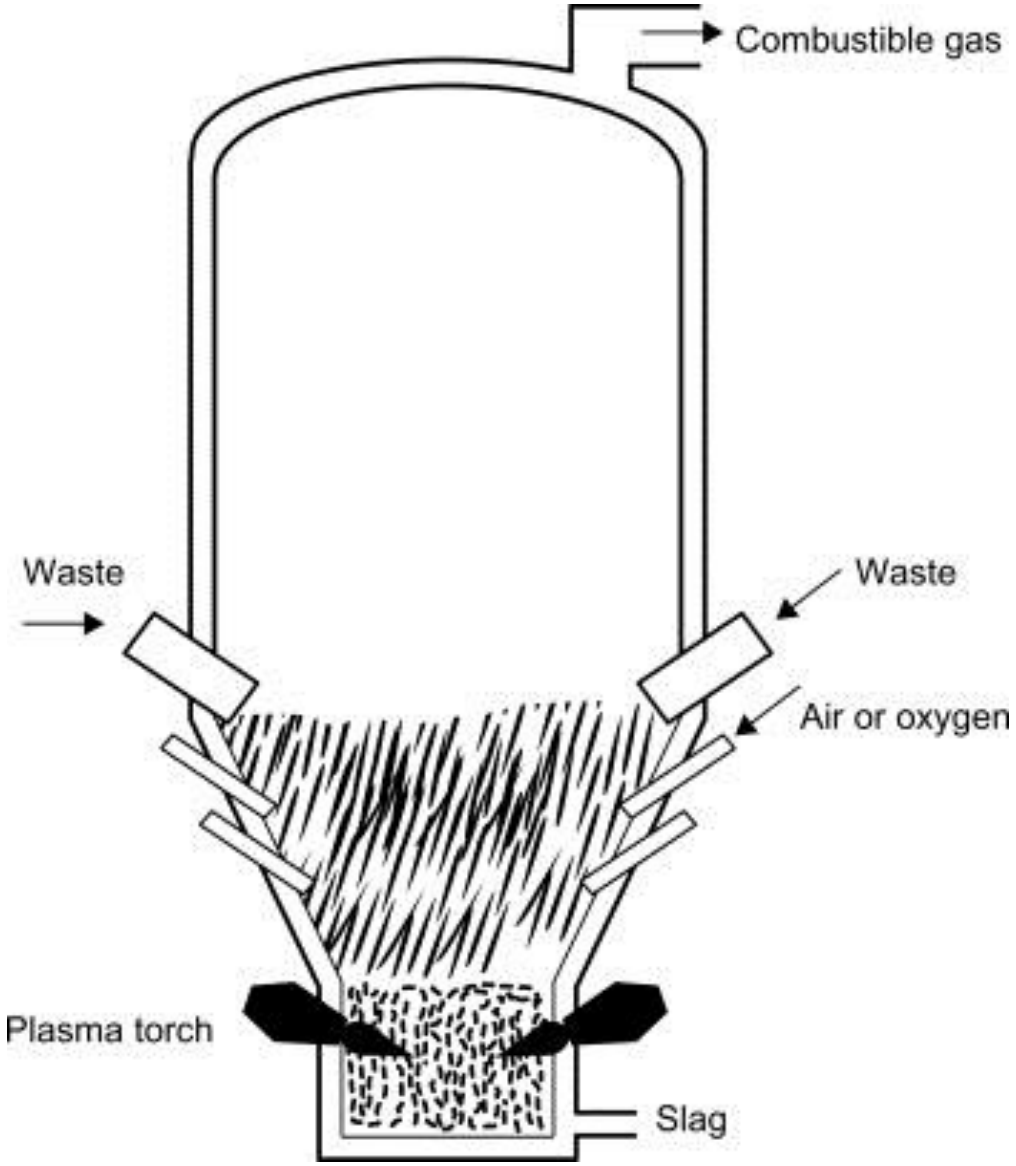

Figure 12 - Schematic of Plasma gasifier reactor showing the positioning of plasma torch [134]

2.9 Tars

Tars are defined by Milne [131] as "the organics produced under thermal or partial-oxidation regimes (gasification) of any organic material are called tars and are generally assumed to be largely aromatic". Other researchers have described tars as a very complex mixture of aromatic and oxygenated hydrocarbons having a molecular weight greater than that of benzene of [135-137]. Benzene and other heavier molecular weight compounds are present in

pyrolysis bio-oil and their presence in syngas tends to cause problems. As previously said in section 2.2.3, intermediate pyrolysis is based around the concept of encouraging secondary reactions between the evolved vapours from biomass and resulting char. Some tars present in the bio-oil can have their molecular weight up to 500 g/mole [138]. The presence of these very high molecular weight tars in bio-oil and syngas lead to incomplete combustion when these fuels are used. High molecular weight tars act as promoters of high viscosity, limit atomization of fuel, cause blockages in fuel pipes and injector lines by condensation [31, 98, 131].

Tar levels as represented by Milne [131], exhibit a wide range in various gasification processes. For example, updraft gasifier tar content in raw syngas is reported between 1-150 g/m^3, in downdraft it is 0.04-6 g/m^3 nominally and in the fluidised bed gasifiers it is 0.1-23 g/m^3. Milne [131] also reported tar tolerance levels in the gas for various applications such as for engines, turbines, fuel cells and compressors. It is imperative to bring down the tar levels in the syngas as low as possible to avoid associated problems in the end use machines.

2.10 State of the art, combination of pyrolysis and gasification processes

Pyrolysis of biomass is possible in various configurations as described in section 2.8 and it leads to the production of bio-oil together with char and gases. During production of bio-oil formation of NO_x and SO_x and other toxic compounds in char, such as dioxins and polycyclic aromatic hydrocarbons (PAH), have been shown to be below the regulatory standards for land application of chars [139, 140] for soil improvement reasons. But the issues of limited economic feasibility of bio-oil usage in conventional energy machines remain due to poor bio-oil fuel properties requiring blending with conventional fuels [3, 31]. Bio-oils are also shown to have solids content up to 3 wt% of solid (char) particle size between 1-200 μm [141]. Tar and solid content in bio-oil leads to incomplete combustion in engines and hence may increase the particulate matter and unburnt hydrocarbon exhaust emissions, thus leading to regulatory compliance issues for emissions monitoring.

Numerous researchers are looking into alternative ways to make use of low-grade biomass by avoiding the need to even produce bio-oils but still pyrolysing and gasifying these materials [57, 59, 61-64, 98, 141- 143]. One such system

is the Viking gasifier as shown in Figure 13a [142] which is a two stage process to thermally crack the tars. This system works by a screw pyrolysis system which produces hot vapours and char at temperature of 500-60 °C at the top of the gasifier to be partially oxidised and tar fractions to be broken down into syngas. The char from the pyrolysis unit is transferred into fixed bed of the gasifier to act as a tar cracking unit where further tar cracking occurs. This system is reported to have a nominal tar content in syngas as low as 15 mg/m^3.

Aston University

Illustration removed for copyright restrictions

Figure 13a - Viking Gasifier arrangement showing the integrated screw pyrolysis and gasification processes [59]

Tar sampling has been performed in various stages of this process in another study [144] which showed a progressive decrease in tar levels starting from the pyrolysis stage to partial oxidation to gasification stages and decreasing to 5 mg/m^3 tar levels as shown in Figure 13b. The syngas from this two-stage process has been shown to work successfully in a gas engine for a couple of hundred hours without major issues. The proposed research on pyrogasification in this thesis is built upon somewhat similar two stage pyrolysis and gasification process with a notable difference of removing the char fraction in the Pyroformer and not taking it into the gasifier. The char fraction is to be used for other applications such as soil amendment or heating. The detail of work is further explained in Chapter 3. It is anticipated that, by separating the pyrolysis stage with in-situ char re-circulation for tar cracking and then taking the tar-reduced hot vapours into a bubbling fluidised bed (BFB) gasifier, a significant tar reduction in the syngas will be achieved. This tar reduction becomes possible, firstly due to char recirculation (tar cracking by char) in Pyroformer and then further tar cracking due to high temperature thermal tar cracking (800-1000 °C) in the gasifier, and finally a dolomite catalytic bed within the BFB gasifier further catalyses the tar reduction.

The Pyrogasifier concept of this thesis differs from Viking gasifier in many ways. These differences include, a BFB gasifier (rapid mass and heat transfer) as opposed to downdraft gasifier in Viking, biomass char and dolomite catalytic bed as opposed to only char bed in Viking, char recirculation in pyroformer to reduce tars as no char recirculation in Viking system. The Viking gasifier has been shown to be reducing the tar content by 100 folds by doing such an arrangement [142]. The notable difference of eliminating char with complex (low melting point) materials will enhance the economic viability of gasification process which is otherwise mostly dependent on wood pellets. Pyrogasification could lead to the minimisation of wood pellets by compensating the input energy from more complex non-woody waste materials in the form of hot vapours. Further similar studies need be conducted, and syngas product quality and tar content in syngas analysis results are to be published in international journals when the experimental work is conducted on this integrated process after the upgrades are done on a pilot plant (Pyroformer and BFB gasifier) based at the European Bioenergy Research Institute, Aston University.

Aston University

Illustration removed for copyright restrictions

Figure 13b - Progressive decrease in tar levels as measured in various stages of Viking gasifier process [144]

2.11 Summary of the Literature review

The literature review strongly suggests that pyrolysis is effective to turn complex feedstocks into useful bio-oils, gaseous fuel and char. The fuel properties and yield of permanent gases and bio-oil show a promising future for energy applications in engines if associated fuel issues can be resolved as indicated by these researchers Hossain [3, 31, 53, 145]. Bio-oil production from biomass is favoured by use of materials containing higher wt% of cellulose and hemi-cellulose whereas materials with higher lignin content tends to have lower bio-oil yield and higher char yield. Bio-oil yields from woody biomass have been reported in the range of 60-95 wt% by Mohan [45, 56, 86]. Bio-oil is a complex mixture of various compounds, containing tars and having low pH, which limit its application as a fuel. When bio-oils containing high molecular weight tars are used as fuel they act as promoters of high viscosity, limiters of atomization of fuel, causing blockages in fuel pipes and injector lines by condensing as reported by these authors [31, 98, 131].

Tar cracking by char is supported by the works of various researchers such as El-Rub [99] who reported comparisons of biomass-derived char from pyrolysis with other inorganic catalysts for the cracking of naphthalene and phenol at a temperature range of 100-900˚C and also found that char as a catalyst was as good as nickel and dolomite. It is also reported by Al-Rahbi et al [98] that waste derived pyrolysis chars were effective in minimizing the condensable tars and bio-oil hydrocarbons. They reported up to 70% reduction in tars when using waste car tyre derived char compared to no use of char catalyst in a pyrolysis-gasification experiment. The order of performance of chars for tar removal was highlighted by this author as tyre-derived char being the best followed by RDF char, date stone char, and no char as the worst. Also of interest in this thesis is to understand the char composition and its usage in soil amendment downstream of the pyrolysis process.

The possibility of coupling the Pyroformer to the BFB gasifier opens new opportunities in avoiding bio-oil production where the aim is to produce onsite heat and power. In this combination, the Pyroformer can act as a complex waste pre-treatment step to process waste materials which cannot directly be used in the gasifier. This is done by pyrolysing the waste and producing the hot vapours

which can be directly fed into gasifier without the need for condensing them and also separating the solid residue (char) which could otherwise be problematic in the gasifier. The benefits are achieved by making use of the augers in the Pyroformer to transport feedstock materials through the reactor and thus produce hot vapours, which would otherwise be hard to feed into a gasifier due to their appearance, composition, size and shape. In this way, depending on the ash content of material, a large fraction of mass (up to 70% to that of feedstock) is supplied to the gasifier via the Pyroformer.

The critical review of the Pyroformer has highlighted, however, that information needed to understand the claimed beneficial effect of char recirculation is lacking. It is necessary to do further research to establish optimum temperatures, char re-circulation rates and residence times of the materials in the Pyroformer. The novelty of char catalytic cracking by solids phase (char) re-circulation in intermediate pyrolysis (through the Pyroformer), and its coupling with a BFB gasifier to produce low-tar containing syngas, needs further research to bring this technology closer to application.

The literature review strongly indicates that further research is needed to evaluate the potential of these technologies by researching into new and optimised conversion routes. Furthermore, it is essential to address the key questions about pyrolysis in general and intermediate (screw) pyrolysis in particular how best to understand the cold flow behaviour of biomass in a cold Pyroformer, improve the product quality by utilising char recirculation, conduct a design review of critical components of a Pyroformer and how best to integrate the Pyroformer and bubbling fluidised bed gasifier to enable pyrogasification.

Chapter 3 – PhD project aims, objectives and methodology

In the literature review commonly known pyrolysis techniques were presented with the focus on the intermediate screw pyrolysis of biomass feedstocks [3, 51, 79, 96]. This PhD thesis builds upon the literature review, Intermediate pyrolysis research on Pyroformer in Aston University, identifying the knowledge gaps and the need to look for applied solutions for biomass feedstocks in thermochemical conversion processes including gasification. From the literature review it is evident that some waste materials including biomass are not easy to process solid fuel resources. These complex feedstocks exhibit high moisture content, high ash, feeding issues, and problems with size reduction and furthermore the end products (especially bio-oil) require further upgrading or blending to enable its usage as a fuel. Also, the literature review highlights [the interest from scientific community [57, 59, 61-64, 98, 141- 143] in using char in pyrolysis and gasification applications to enhance the quality of end products but there are no dedicated studies where the effect of in-situ char re-circulation during pyrolysis has been investigated in detail.

3.1 Knowledge gap

There is little or no information in the literature to study the combined effects of biomass flow behaviour within a screw pyrolysis reactor and to study the char re-circulation ratios to biomass feed and their impact on pyrolysis products. In-situ tar cracking by char recycling studies while char is still hot and in the reactor, are not found anywhere in the literature. It is fair to say there is a knowledge gap in the literature to quantify the benefits of tar cracking by varying the quantity of char to that of biomass in a pyrolysis reactor. The counter rotating twin screws combination, as exhibited in the Pyroformer, offers a state of the art setup to understand and optimise the tar cracking benefits by the recycled char. However, the critical review of the Pyroformer related studies in section 2.6 have shortcomings to address the impact of char to biomass ratio on pyrolysis products, the feeding rate and the residence time. Furthermore, there is a knowledge gap to show an efficient and trouble-free operational pyrolysis process and how best this can be linked to a BFB gasification process if bio-oil route is to be eliminated and syngas is the desired end product.

3.2 Project aim

The work has happened to advance the thermochemical processing of biomass by means of detailed understanding of intermediate pyrolysis and its combination with gasification to derive better end products. The aim of this study is to understand biomass flow behaviour in cold Pyroformer model to calculate char to biomass ratio which is important for hot pyrolysis and then integrate the scale up version of Pyroformer model to a gasifier.

The scope of this thesis is to understand the cold flow behaviour of feedstock in 20 kg/h cold Pyroformer reactor and apply the knowledge to a hot 20 kg/h reactor where feedstock is pyrolysed and then further enhance a scale up model of 100 kg/h Pyroformer which can then be coupled to a BFB gasifier to develop Pyrogasification concept. The work involved the operation of small scale (20 kg/h) Pyroformer, and then experience gained from this unit was used to test the 100 kg/h Pyroformer and its potential coupling with BFB gasifier.

3.3 Project Objectives

The main objectives of the proposed work are to address missing information as explained in critical review of Pyroformer previous studies with regards to Pyroformer operation and its integration in new concept of Pyrogasification.

1. To visualize the cold flow behaviour of biomass in a 20 kg/h transparent Pyroformer model (at ambient temperature), this cold pyroformer unit is similar in size to the hot Pyroformer model. This will help to establish the residence time of material in the inner screw, steady state calculations in the Pyroformer, time taken to reach the steady state and to study the char to biomass mass ratio for char re-circulation within Pyroformer.
2. To test 2 or more types of biomass feedstock materials in small scale hot Pyroformer to understand the effects of material composition on bio-oil product quality and processing ability of the Pyroformer for different feedstocks.
3. Using the different feedstocks, to understand the effects of char re-circulation (by varying inner and outer screw speeds), residence time and pyrolysis temperature variance on products yields and quality within the Pyroformer.

4. To analyse the liquids produced during the test runs for fuel properties and compare the results with the literature.
5. To analyse the biochar properties and compare them with British Biochar Quality Mandate (BBQM) and International Biochar Initiative (IBI) standards for soil amendment and theoretically quantify biochar carbon sequestration potential.
6. To review the design of the Pyroformer reactor and to recommend the modification of key components of the Pyroformer which had technical problems based on operational experiences.
7. To commission the BFB gasifier and get it ready to couple it with Pyroformer and to study the issues of combining 100 kg/h Pyroformer to the BFB gasifier to enable the Pyrogasification. The coupling between the Pyroformer and BFB gasifier is limited to electro-mechanical design and control philosophy of integrated process.

3.4 Methodology

To contribute to the knowledge based on the literature review [98-101], a global research methodology diagram has been created which highlights the areas which need further work with regards to Pyroformer. This is shown in Figure 14. Also, the screw pyrolysis of various complex feedstocks (such as digestates) has seldom been conducted to solve digestate disposal issues, in this thesis attention is focused onto digestate to address this issue. There are various small-scale studies which have been highlighted in the literature but there are a few studies of closer to application scale-up models of pyrolysis systems. In this thesis small scale 20 kg/h and pilot scale 100 kg/h Pyroformer models have been used. These were pre-existing pyrolysis units in the laboratories of European Bioenergy Research Institute (EBRI) at Aston University, and this research has arisen from the numerous technical problems from their operation. The experimental studies presented in this thesis are based on 3 different combinations of a Pyroformer process as given below:

- 20 kg/h Perspex cold model for material flow characteristics (as shown in number 1 in Figure 14)
- 20 kg/h hot Pyroformer for detailed parametric and comparative studies (as shown in number 2 and 3 in Figure 14)

- 100 kg/h hot Pyroformer for large scale comparative study (as shown in number 4 in Figure 14)
- All these 4 steps then provide sufficient knowledge to integrate the Pyroformer with gasifier to achieve best outcomes in the form of tar free syngas

The chronological order of the experimental work (as in the order work was done) was influenced by the equipment and other resources availability as the work was done under various projects as highlighted in Chapter 1. The chronological order of the work is shown in methodology diagram in Figure 14 and is represented by grey arrows in the order 4 – 1 – 2 - 3. The reasoning behind doing the experiments in this order was simply due to the circumstantial dependence on equipment, materials and human resources availability from the Interreg and IAPP projects which provided critical resources for the research.

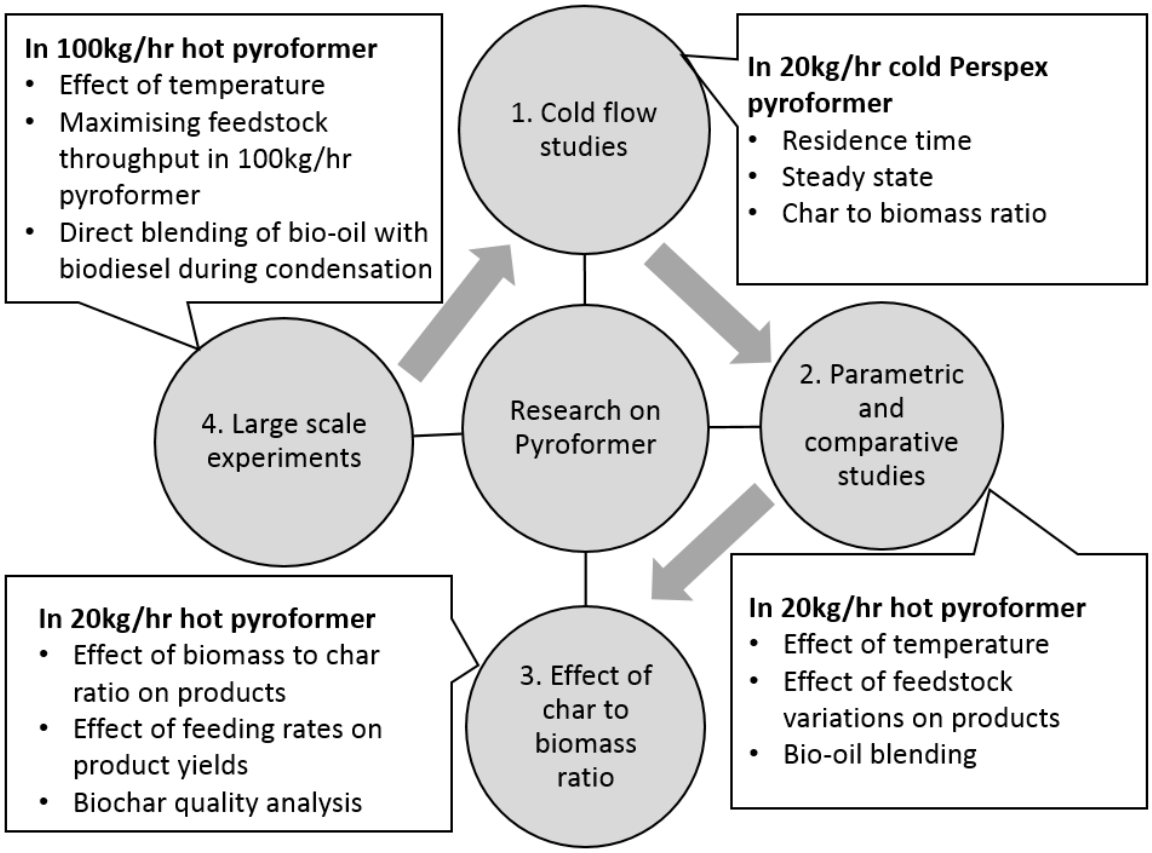

Figure 14 - Pyroformer research methodology diagram

To meet the project objectives three different types of reactors were used in the research experiments. In the first set of experiments a 20 kg/h cold reactor which was a Perspex (transparent) model of 20 kg/h hot Pyroformer was used. This 20

kg/h cold reactor was identical in auger screw dimensions to 20 kg/h hot Pyroformer reactor with notable differences in Perspex transparent body in cold reactor instead of stainless body in hot reactor and also absence of electrical heaters in the cold reactor. The transparent body was considered good for viewing the material flow inside the reactor when both screws are turning. The experimental setup and procedure is explained further in chapter 4.

In the second set of experimental setup there was a 20 kg/h hot Pyroformer reactor involved. This Pyroformer was semi-automated and was able to heat the biomass with precise control and variance of temperatures of electrical heaters and the rotational speeds of the both screws.

In the third experimental setup there was a 100 kg/h Pyroformer involved. This Pyroformer was part of an integrated process where ancillary equipment was used to conduct the experiments. The experimental setup and procedure is explained in Chapter 6.

3.5 Limitations of the project

All the experimental work has been done under various funded projects which are acknowledged in Chapter 1. This means tests were done under tight time schedules to deliver results to these projects as well as to contribute towards this PhD thesis. Hot Pyroformer (20 kg/h) equipment was shared between different groups and hence there were some time limitations which needed to be adhered to.

The analysis of bio-oil and biochar properties was performed in Chapters 5 and 6. The emphasis was more onto bio-oil and biochar quality during pyrolysis tests for their applicability, whereas the gas fraction was not analysed for its composition due to lack of availability of gas sampling and analytical equipment and due to lack of interest as a mainstream pyrolysis product. The gas fraction is hard to store and transport and in reality, can be used as combustion fuel to drive the heating demand of a pyrolysis process. Bio-oil was only characterized for its fuel properties and hence no detailed engine tests are performed to evaluate its fuel combustion characteristics. Also, the biochar study was kept limited to biochar composition analysis and its comparison with newly adapted biochar quality standards from BBF (British Biochar Foundation) and IBI and hence there are no

field trials and lifecycle assessment conducted as this will encompass long duration and effort which is beyond the scope of this thesis.

Large scale pyrolysis tests in 100 kg/h Pyroformer were conducted on a comparative basis between ENPlus standard wood pellets and miscanthus, the results are presented in Chapter 6 section 6.3. It must also be noted here that the nature of the setup of the plant was such that biodiesel was used to directly quench the pyrolysis vapours and a blend of pyrolysis oil and biodiesel was produced which was further analysed for its fuel properties. This was considered beneficial as it will eliminate the need for bio-oil post pyrolysis blending as pyrolysis bio-oil have been proven to be a complex and problematic fuel in pure form.

There are no gasifier tests covered in this thesis as the gasifier plant was still in improvement stages and was lacking certain crucial equipment to merit a detailed scientific study. Commercial scale of gasifier process (as installed at EBRI) operations required significant budget and human resources to merit scientific tests which were not available in time.

The design review recommendations for the 100 kg/h Pyroformer are based on initial operational experience at Harper Adams University before it was relocated to EBRI. This Pyroformer is now relocated in EBRI labs next to 1.2MW BFB gasifier where it is proposed to be integrated. The integration of Pyroformer and gasifier has not fully completed which means there are no combined mode tests between both units. However, a detailed design recommendation of the coupling parts is presented in this study. This is the maximum which can be done in this study to facilitate the Pyrogasification concept. Hence this thesis will not include any combined mode tests between the Pyroformer and the gasifier.

Chapter 4- Cold flow modelling in a 20 kg/h transparent Pyroformer

The literature research [98-101] strongly indicated the positive effect of tar cracking by char, however it is evident that there is a lack of understanding the effect of char to biomass ratio for maximising the tar cracking by char. To fill this gap in scientific literature a detailed experimental study of char to biomass ratio was conducted in an innovative twin screw counter rotating Pyroformer reactor. During this study, the experimental and theoretical residence times of feedstock in the Pyroformer reactor were established so that any change in residence time and its impact on pyrolysis products can be better understood.

To meet the first objective as highlighted in section 3.3 of Chapter 3, cold flow tests were performed in a transparent cold Pyroformer model with capability to see through the transparent body of the reactor as shown in Figure 15. This cold Pyroformer setup enabled to visually observe the material flow for bridging and fill levels in screws through Perspex transparent body of Pyroformer, to establish residence time of material in inner screw of Pyroformer, time taken to reach steady state and char to biomass ratio and fill level characteristics in the reactor. There are no heaters installed on this system and hence there are no hot pyrolysis reactions taking place. The inner and outer screw dimensions were identical to that of 20 kg/h hot Pyroformer where actual pyrolysis reactions take place. It is assumed that material flow characteristics are very similar to that of hot Pyroformer system except hot vapours and material density differences, however the change in material volume was very small compared to density difference. These tests are performed to meet the objectives as stated earlier in section 3.3 which included the following;

- to monitor the material flow inside the reactor, this is essential to establish process limitation in terms of blockages
- to establish the residence time inside the inner screw of the Pyroformer by determining the frequency settings (Hz) on the inverter controllers of Pyroformer screws
- to calibrate the system to understand the steady state limitations of the Pyroformer for various feeding rates while carefully observing the pellet bridging and blockages caused by re-circulated material

- to understand the char to biomass ratio while using the plastic beads (as simulation material) and accounting for any differences in density of biomass pellets and plastic beads as well as the mass loss of wood pellets in evolving vapours.

4.1 Equipment and materials

A cold Perspex see through Pyroformer model was used in this study. The equipment listed below is same as used in the residence time observations, steady state establishment and for char to biomass ratio calculations in cold flow tests. This is because hot Pyroformer is not practical to be used for such tests due to health and safety and operational reasons. A detailed breakdown of Pyroformer screw components is presented in the Figures 16 and 17. The dimension of inner and outer screws are presented in the Table 13. An integrated setup of Pyroformer screw components is shown in the Figure 18. For cold flow modelling to understand the pellet flow behaviour in the Pyroformer following equipment was used as listed below.

- Twin screw transparent Pyroformer mobile assembly
- Motor specifications for both screws: TEC Motor, 0.75 kW, 240 V, model MS802-4 0.7543TECAB3-45DEG
- Low rpm gearbox (coupled to above motor) specification: Goldcrest gearbox, model: M0532, reduction ratio 70:1, 20 rpm
- Single phase 240 V to 3 phase rpm inverter controllers, one for each screw motor (Powtran, type PI8600A1 R75G1, 0.7 5kW 4 A).
- ENPlus standard certified wood pellets of 6 mm diameter acquired from Verdo renewables
- Low density (LDPE) Plastic solid beads of 3.5 – 4 mm diameter (used in C/B tests) manufactured by Sigma Aldrich
- 3 Plastic beakers of 500 ml capacity for biomass weighing and feeding
- Container for collecting the material at Pyroformer outlet
- Ohaus weighing scale, weighing range up to 4000 grams, Model Scout Pro SPU4001, 0.1 gram accuracy
- Stopwatch with 0.1 Sec accuracy

Figure 15 - Image of cold Pyroformer system, 1. Mains power, 2. Inner screw rpm controller, 3. Outer screw rpm controller, 4. Emergency stop, 5. Feed inlet, 6. Outlet, 7. Inner screw motor, 8. Outer screw motor, 9. Pyroformer transparent body and screws

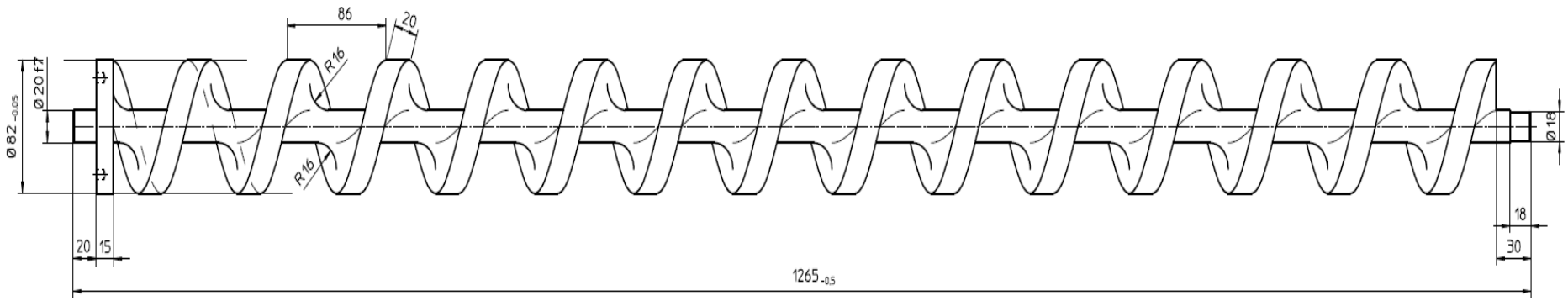

Figure 17 – Dimensions of the inner screw (IS) of 20 kg/h Pyroformer

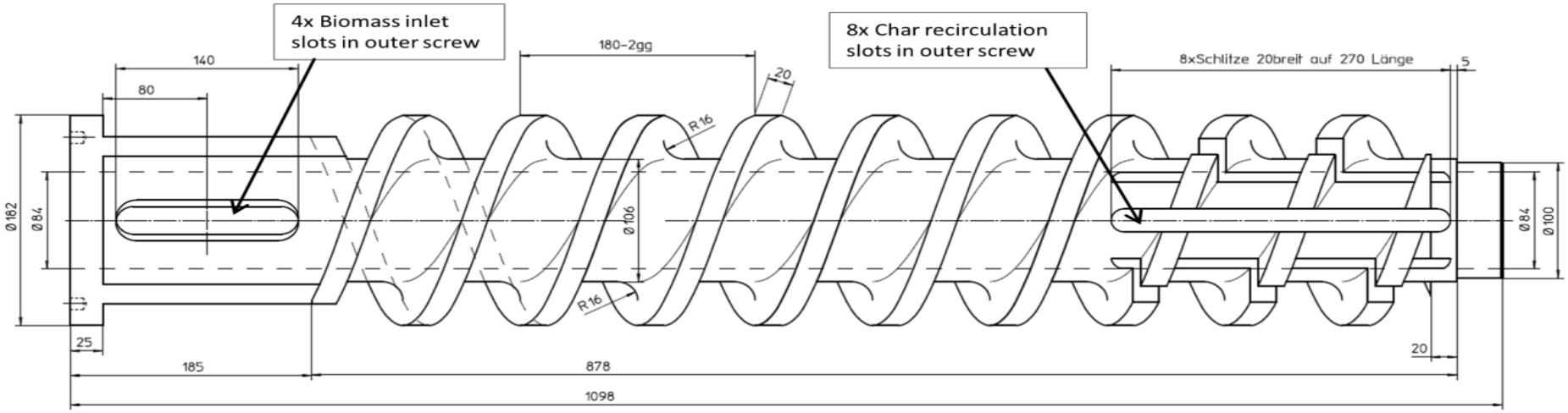

Figure 16– Dimensions of outer screw (OS) of 20 kg/h Pyroformer

Table 13 - Pyroformer IS & OS screw dimensions

	Inner screw (IS) (mm)	**Outer screw (OS) (mm)**	**Reactor length (mm)**	**Number of helixes**		**Helix between spirals**		**Reactor outer diameter (mm)**	**Feed inlet slot in outer screw (mm)**	**Feed inlet slot length (mm)**	**Outlet Diameter (mm)**		**Feed Inlet Diameter (mm)**
				Inner screw	**Outer screw**	**Inner screw**	**Outer screw**				**Top (vapours)**	**Bottom (biochar)**	
20 kg/h Pyroformer	L = 1265 D = 82	L = 1098 D = 182	1317	14	9	86 (single helix)	180 (double helix)	310	4 slots, Width = 35	140	70	115	70

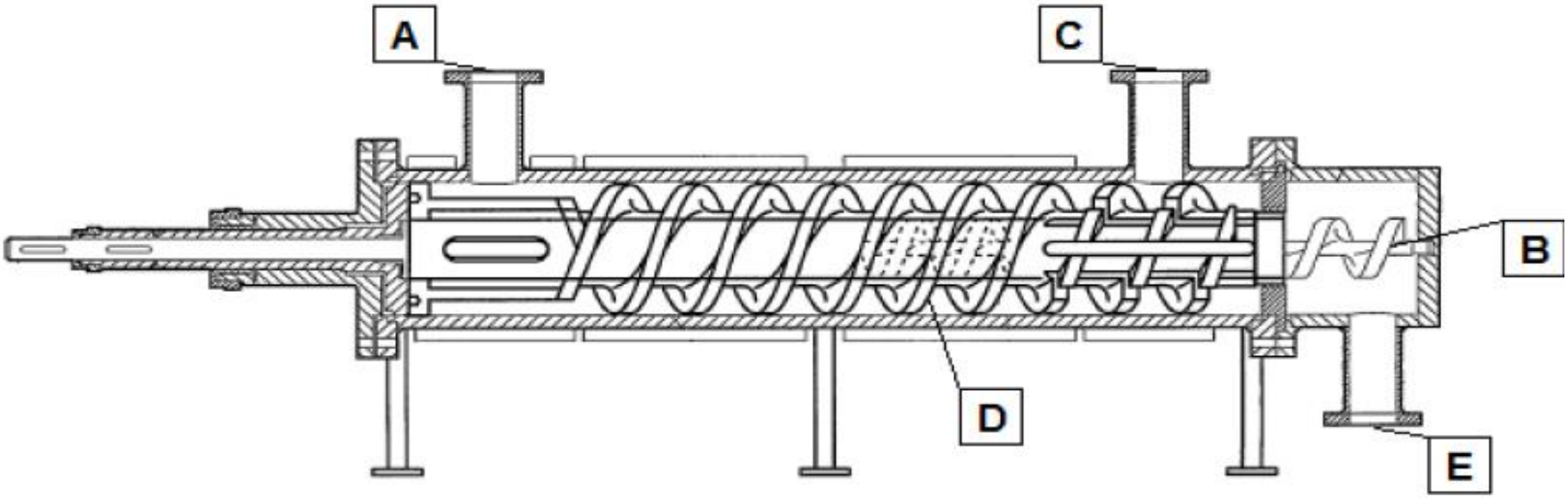

Figure 18 - Cross section of Pyroformer showing IS & OS integrated setup (A–Feed inlet, B-Inner screw, C-Gas outlet, D- Outer screw, E-char outlet

4.2 Residence time

The time biomass feedstock (wood pellets) spent in the reactor when conveyed in the forward direction by the inner screw is called as residence time (RT). This is the pyrolysis time for biomass to give off volatile vapours. RT depends upon the speed of inner screw (IS). The residence time was experimentally determined by feeding the wood pellets in empty transparent Pyroformer and measuring the time taken on stopwatch by wood pellets to travel through the inner screw and to come out at the char outlet. The transparent body of the cold Pyroformer enabled to clearly view the biomass entering and exiting at their respective ports. The mean residence time of the biomass is different for recirculated material and is also dependent on the outer screw speed during C/B calculations.

The residence time can be measured experimentally by observing material entry and exit and measuring the time as well as theoretically by equation 1. Inner screw has 14 helixes as shown in Figure 16. Theoretical residence time *(RT)* can be calculated as the number of sections of the inner screw (*N*=14) divided by the rotational speed of the inner screw (IS):

$$RT\ (\mathrm{min}) = \frac{N}{IS\ (rpm)} \qquad \text{(Equation 1)}$$

For example, taking the first result from Table 15, the theoretical residence time for inner screw is calculated as below

$$RT\ (\mathrm{min}) = \frac{N}{IS\ (rpm)}$$

$$Theoretical\ RT\ (min) = \frac{14}{2.3} = \ 6.1\ \mathrm{min}$$

Where

N=14 number of helixes

And inner screw speed is 2.3 rpm

Whereas the experimental residence time is the actual time taken by the inner screw to convey the pellets from feed point to exit point. This is measured time on the stopwatch after reaching steady state when the pellets are introduced into the Pyroformer at the feed inlet and the time taken by the pellets to appear on the char outlet of Pyroformer at the set speed (rpm) of the inner screw motor.

4.2.1 Procedure for residence time determination

For residence time (RT) determination, both LDPE and wood pellets were used to verify the RT individually for both materials. The residence was verified to be same for both materials. The stopwatch was set to zero then the material was fed into feed inlet (A) which then entered the inner screw (B) through the 4 slots (as shown in Figure 17) in the outer screw (D) and then it gets conveyed away from feeding point. The 4 slots were in feeding end of outer screw and the 8 slots were on the far end from feeding section. Biomass then falls into outer screw through 8 slots in outer screw. When the reactor reaches the solids steady state then feed-in equals the feed-out in cold Pyroformer model.

The normal direction of material flow is from feed inlet (A) to char outlet (E) (as shown in Figure 18) in the inner screw in forward and recirculation of material is by means of outer screw rotating in backward direction compared to inner screw. The residence time of the biomass during pyrolysis must be sufficient to allow for the complete evolution of volatile matter from the biomass. The recirculated biomass from the OS has the longer residence time compared to single pass through inner screw only as it can travel more than one time from within inner screw. Both materials (wood pellets and LDPE beads) show similar RT for a similar feeding rate. Material flows are shown in the Figure 19 during various stages.

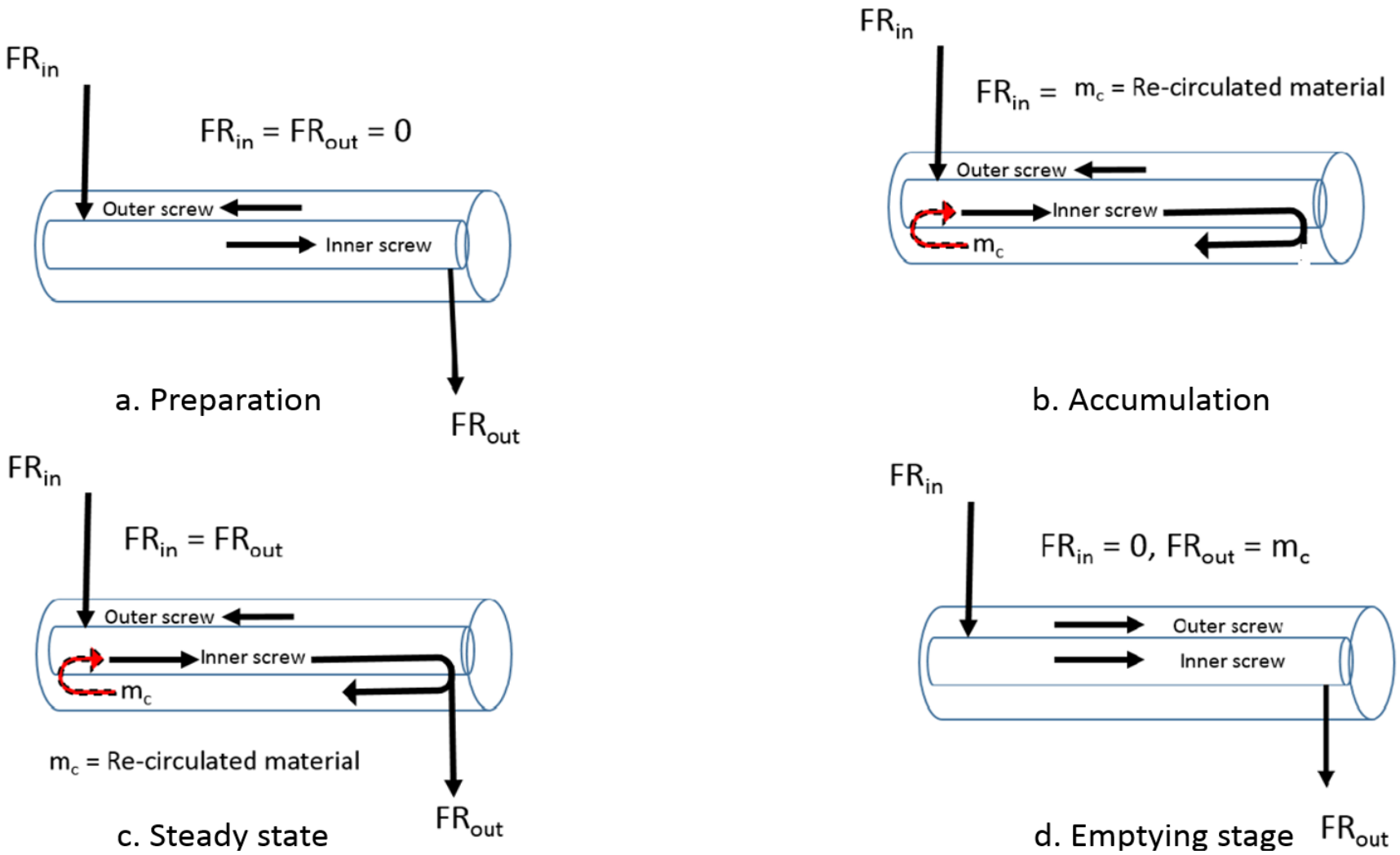

Figure 19 - Material flows in the Pyroformer during various stage

In the initial preparation stage (Figure 19a), before the pellets are introduced in the feed inlet to enter the Pyroformer, both IS and OS are turning in forward and reverse directions respectively and no materials are going in or out. Once the feedstock is introduced, it starts to accumulate (Figure 19b) inside the reactor before both screws are filled, no material comes out of the reactor. After feed introduction into the Pyroformer, it takes between 45-60 minutes to reach the steady state (Figure 19c). In the steady state, material fed in equals the material coming out and OS is re-circulating some of the material (m_C) in backward direction after some material accumulation has taken place as shown in red dashed arrow in Figure 19b. Residence time (RT) is experimentally determined after reaching steady state where FR_{in} equals FR_{out}. In emptying stage both screws are turning in forward direction (Figure 19d) to avoid re-circulation of material and hence all the material is emptying into char container.

4.2.3 Residence time calibration data

The frequency setting in Hertz (Hz) was altered on the Pyroformer screw motors' inverters to get the required rpm of inner or outer screws while precisely monitoring the time for each rpm of screws on the stopwatch. The relationship between frequency in Hz and rpm of the motor was found by calibration. Given below in the Table 14 are corresponding frequencies for required rpm setting which were used on the digital inverter controller of both inner and outer screw motors.

Table 14 - Relationship between frequencies (Hz) and rpm of the inverters and motors of inner and outer screw in cold transparent 20 kg/h Pyroformer

Inner screw	Inner screw	Outer screw	Outer screw
Frequency Hz	rpm	Frequency Hz	rpm
5.21	2	5.15	2
7.80	3	7.65	3
10.25	4	10.30	4
12.50	5	12.66	5
15.00	6	15.00	6
17.65	7	17.65	7
19.55	8	19.55	8
21.30	9	21.40	9
24.00	10	24.00	10

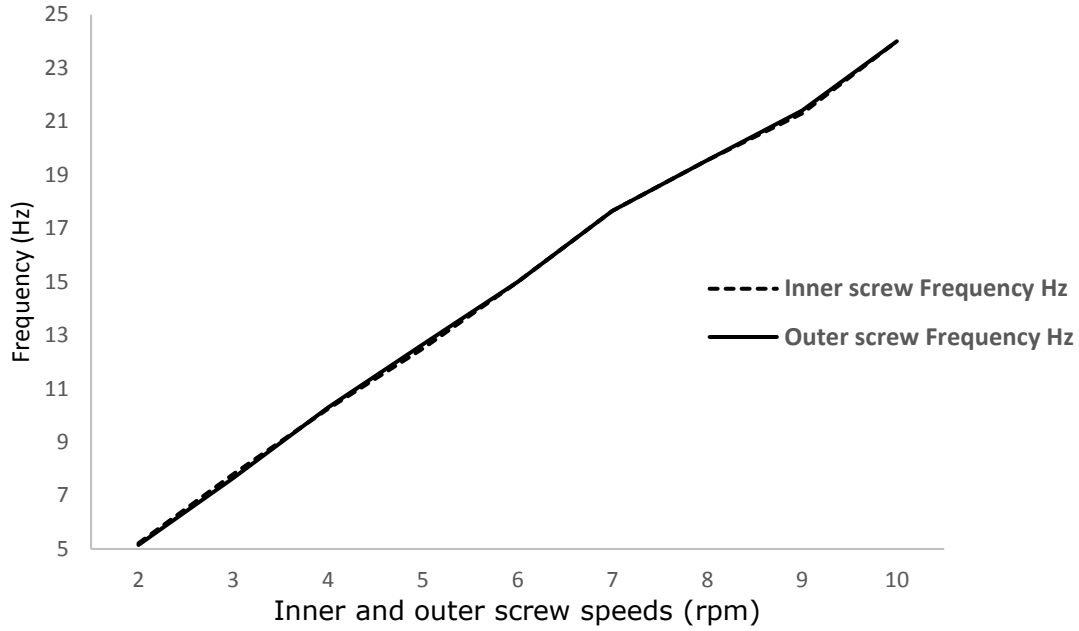

Figure 20 - Relationship between Frequency (Hz) of inverters and rpm of motors

After determining the frequency setting for required rpm then the residence time experiments are performed in the transparent cold Pyroformer. Determining the frequency settings (Hz) is essential to ensure that correct rpm can be set on screw motors. The corresponding frequencies were then used to run the screw motors at desired incremental speed and the results are presented in the Table 15.

Table 15 - Effect of the inner screw speed on the minimum residence time

***IS* (rpm)**	2.3	4	7.1	10	13
***RT* (min)**					
Theoretical RT (min)	6.1	3.5	2.0	1.4	1.1
Experimental RT (min)	5.3	3.3	1.6	1.2	1.0

4.2.4 Inferences from residence time calibration

The relationship between frequency (Hz) setting of the inner or outer screw inverters and the rpm of the respective motor is found to be linear as expected. It is essential to point out that although inner and outer screws have different diameters of spirals or helix and their required frequency settings on inverters are approximately similar to get the same rpm on respective motors due to low rpm reduction gearbox. Even due to the large inertia and diameter of the outer screw relative to that of inner screw outer screw/inverter did not require higher

frequency setting. This relationship between frequency settings of inverters and rpm of the motors is linearly represented in Figure 20.

The difference in theoretical and experimental residence times can be seen in the Table 15 and shown graphically in Figure 21. The shorter experimental residence time is perhaps attributed to the biomass feed point which is above the second helix of the inner screw and when the material enters the inner screw it is conveyed from 2nd or 3rd helix onwards. The conveyance of material from 2nd or 3rd helix of inner screw is due to feed inlet slots in the outer screw which prevent the biomass to start from very beginning of the inner screw upon entry. It is due to the biomass feed joining from second helix which is leading to shorter experimental RT compared to that of theoretical RT.

Figure 21 highlights the relationship between the inner screw speed and residence time. As the rpm of IS increases the RT decreases. However, this relationship is not linear. It is also evident that the theoretical RT is higher than the experimental RT.

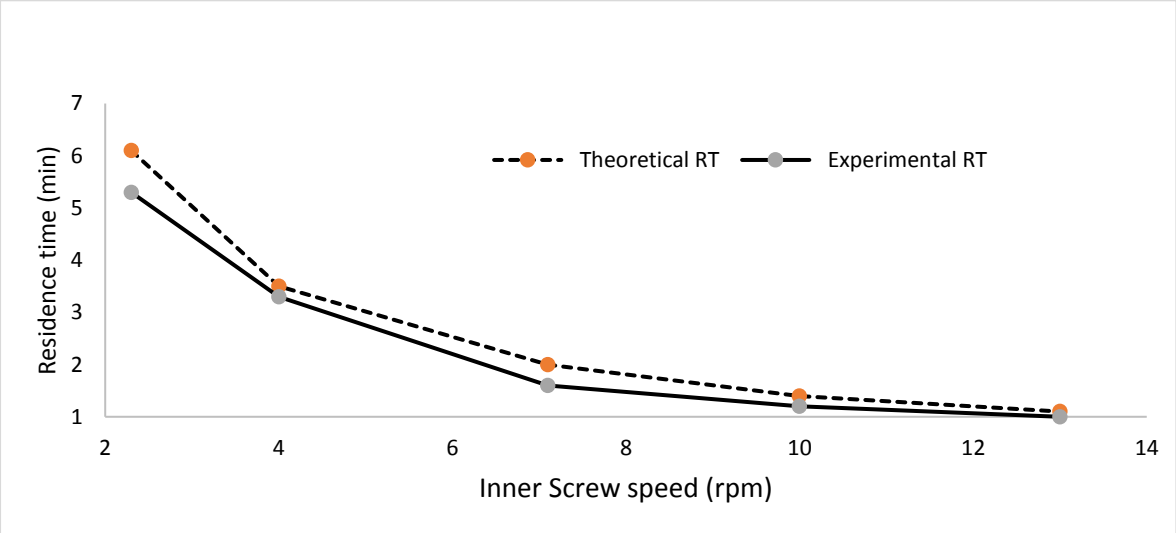

Figure 21 - Relationship between theoretical and experimental inner screw speeds to the residence time of biomass in inner screw

This difference in both values can be attributed to less number of helixes of inner screw used in transporting the material. Such as when biomass pellets enter the inner screw they must pass through the outer screw slot and reach the 2nd or 3rd helix of the inner screw and then they are carried forward. Also, when the pellets are exiting the reactor through the char outlet, here again initial few inches of

inner screw length with spirals/helixes are not used as the char outlet is positioned slightly short of complete length of inner screw or the length of the reactor. This also leads to further questions such as whether the experimental RT should be much shorter and the difference (between both RTs) should be more than seconds as shown in Table 15. The reason behind such small difference between the theoretical and the experimental RTs could be attributed to significantly longer time taken by the pellets in the experimental RT due to the physical resistance to the flow of pellets by the bridging of pellets thus balancing the overall experimental RT of pellets compared to theoretical RT. Which means experimental RT is decreased by less number of helixes of inner screw used and due to the bridging between the pellets causing them to slow down during travel. It is hence fair to say that the experimental RT is balanced by the lower number of IS helix and material bridging to get somewhat similar residence time to that of theoretical RT.

4.3 Steady state operations

When the distribution of the biomass in the reactor is constant after char re-circulation has taken place for significant duration of time this is called steady state. The total volume of the particles in the reactor during steady state do not change but the fresh feed and char materials are replaced provided the feeding rate is constant. During this state the biomass input mass flow rate equals the output mass flow rate at a constant feeding rate as shown in Table 16. During the steady state at a given feed rate same amount of biomass leaves the reactor as the amount of biomass entering the reactor, the material accumulation inside the reactor is controlled by the cut-out slots in the outer screw shaft and the char outlet slots above the char pot. This is true in the cold transparent model whereas it is different in hot Pyroformer where vapours are evolving and hence mass flow rate will different in charpot due to gases leaving in the vapour outlet. The time taken to reach the steady state varies with the feeding rate. In general, steady state is achieved quicker when the feeding rate is higher and vice versa. This means at feeding rates closer to maximum design limit of Pyroformer the steady state can be achieved in 45 minutes whereas the steady state for very low feeding rate of 3 kg/h can be as high as an hour.

In steady state screws are rotating in counter directions with material transport in counter directions as shown in Figure 19b with flow directional arrows. The weight

of the recycled material (m_C) is determined by stopping the OS and emptying the IS in normal forward direction until inner screw is completely empty of all material. This is the material which contains fresh feed as well as the recycled material. At this point stopwatch is started again to run the OS equal to RT while IS also running in forward direction after it was emptied. The material collected is only the recycled material m_C after running both screws as shown in Figure 19b in steady state. To empty the reactor of all the material then both screws are run in forward direction (as shown in Figure 19c) until all material has come out and then the system is ready for next experiments.

The real steady state inside the hot Pyroformer is reached when the evolved pyrolysis gas flow rate is constant at constant feeding rate whereas there will be different material mass flow in and pyrolysed char leaving out into char container due to mass loss into vapours. During the accumulation state, the pyrolysis liquid is having more aqueous phase, while the liquid collected during the steady state contains more organic phase. This phenomenon is further discussed in next chap

Table 16 - Material distribution in the cold Pyroformer with counter flows in screws showing accumulation and steady state

Accumulation	**Steady state**
Material flow direction in OS → During this state the fill rate and material distribution is changing	Material flow direction in OS → During this state, material fill and distribution is constant ***<u>Important!</u>*** It is the feeding rate and screw speeds of both screws which determines the fill volume in the Pyroformer.

In the Pyroformer before the steady state is established the material fed into the reactor is accumulating and both the inner and outer screws are being filled. There could be no or little quantity of material leaving the reactor into the charpot depending upon whether there is excess material build-up at the 8 char recirculation slots in the outer screw. In steady state there is sufficient char recirculation taking place which is dependent on feeding rate and screw speeds. Once steady state is established in cold model the material in equals material out as shown in Figure 19b.

4.4 Char to biomass ratio (C/B) determination

Char to biomass ratio (C/B) as the name states is a simple measure to determine how much recirculated char is present in the inner screw compared to the fresh feed material. Based on literature research where tar cracking by char is highlighted, it is assumed that higher the quantity of recirculated material (char) present within pyrolysis reaction zone, this may lead to higher number of carbon active sites being present for the evolving organic vapours. These active carbon sites (since most of the char is carbon) will promote the re-arrangement of free radicals within pyrolysis vapours to react with long chain hydrocarbons (tars) to further breakdown and lead to improved pyrolysis products. Char to biomass ratio is discussed here on the mass basis. It is linked to the rotational speed of outer screw to the inner screw of the Pyroformer. As both Perspex model and hot 20 kg/h Pyroformer screws and reactor diameter are identical in dimensions, the material flow must be same with the exception of very small volume change and a large density change in the solids and the release of volatiles in the hot Pyroformer system compared to cold Pyroformer model.

For char to biomass ratio (C/B) to be calculated it is important that steady state in the Pyroformer is reached as it is when after this constant char re-circulation occurs and then C/B becomes effective. Figure 19 represents the material flow through the Pyroformer during various stages of tests.

$$C/B = \frac{\dot{m}_C}{\dot{m}_B} \qquad \text{(Equation 2)}$$

The above equation is the baseline equation to represent the C/B. Where, m_C and m_B are mass flowrates of recirculated char and freshly fed biomass. Detailed calculations were performed based on the equation 2 to represent the differences

in densities of plastic beads used in the cold Pyroformer to that of biomass in the hot Pyroformer. To apply the findings from cold tests to hot Pyroformer, adjustments are made for differences in density between plastic material and biomass as well as material lost in the vapours in the hot Pyroformer. This was done by using equation 3. There are variables which need to be adjusted each time a different C/B ratio is concerned, these are inner screw speed in forward direction, outer screw speed in backward direction, feeding rate of material and any variability in feedstock composition.

4.4.1 Procedure for char to biomass ratio determination

The experimental residence time, feeding rate, speeds of inner and outer screws and bulk density of the materials were determined by using a stopwatch, feeding the materials and observing for the flows. Start the screws (with IS forward and OS backward). Set the time to zero and start feeding the reactor continuously at least until the steady state of solid particles (as shown in Figure 19) is reached ($FR_{IN} = FR_{OUT}$). Stop feeding and stop the screws. Reset the time to zero and start only the inner screw. Leave it on during a period equal to *RT*. Then, stop the inner screw and weigh the mass, m_1. Calculate the C/B ratio using the following equation, considering the right units.

$$C/B = \frac{\dot{m}_C}{\dot{m}_B} = \frac{1}{FR} \cdot \left[\frac{m_1}{RT}\frac{3600}{1000} - FR\right]\frac{\rho_C}{\rho_{plas}} \qquad (Equation\ 3)$$

Where

m_1 combined mass of mixture of "freshly fed material in IS" and "recirculated material after going through OS into IS" that enter the inner screw from the outer screw after a period >*RT* in grams, this (m_1) is normally found experimentally in the cold Pyroformer by stopping OS and removing all material from IS after steady state and then weighing the material to determine m_1.

RT residence time, in seconds

FR feeding rate, in kg/h

ρ_{char} density of char 485kg/m3

ρ_{plas} density of LDPE particles with which the test was performed, 607kg/m^3

4.4.2 Char to biomass ratio data

The results from cold tests are presented in Table 17 and graphically represented in Figure 22. These tests are done in cold Pyroformer reactor based on plastic beads as test material. The C/B is in fact ratio of recirculated material to that of freshly fed material. The highlighted column in Table 17 is C/B when the difference in densities of plastic beads to that of char is considered and hence is labelled as char to biomass ratio (C/B). During the determining of C/B ratios experimentally, it was observed that Pyroformer could not take feed rate greater than 10 kg/h at higher than 2 rpm of OS. It was also observed that blockages will occur inside Pyroformer at feed inlet if the feed rate was higher than 10 kg/h and IS rpm was lower than 3 rpm. But at the same time when it was cross checked with the need to have sufficient RT of biomass for pyrolysis reasons (maximum mass loss at RT), it became apparent that Pyroformer system has limitations for liberating volatiles efficiently. The results of various operating parameters leading to C/B are shown in Table 17.

Table 17 – Cold Pyroformer experimental results as shown for various C/B ratio, IS, OS rpm and residence time (RT)

FR_{IN}, kg/h		**IS**	**OS**	**RT**	**OS flow, kg/h**		**IS flow, kg/h**		**C/B**	**C/B**
Plastic	**Char**	**rpm**	**rpm**	**s**	**Plastic**	**Char**	**Plastic**	**Char**	**mass**	**Volumetric**
3	2.40	6	1	151	13.44	10.74	16.44	13.14	3.58	4.48
3	2.40	6	2	151	17.10	13.66	20.10	16.06	4.55	5.70
3	2.40	6	3	151	21.90	17.50	24.90	19.90	5.83	7.30
3	2.40	6	4	151	24.18	19.32	27.18	21.72	6.44	8.06
3	2.40	6	5	151	32.76	26.18	35.76	28.57	8.73	10.92
5	*4.00*	*3*	*1*	*301*	*6.00*	*4.79*	*11.00*	*8.79*	*0.96*	*1.20*
5	*4.00*	*3*	*1.5*	*301*	*6.95*	*5.55*	*11.95*	*9.55*	*1.11*	*1.39*
5	4.00	6	1	151	10.25	8.19	15.25	12.18	1.64	2.05
5	4.00	6	1.5	151	13.00	10.39	18.00	14.38	2.08	2.60
5	4.00	6	2	151	15.25	12.18	20.25	16.18	2.44	3.05
5	4.00	6	3	151	17.65	14.10	22.65	18.10	2.82	3.53
5	4.00	6	4	152	19.79	15.81	24.79	19.81	3.16	3.96
6	4.79	6	8	151	21.51	17.19	27.51	21.98	3.60	3.59
10	*7.99*	*3*	*1*	*301*	*2.00*	*1.60*	*12.00*	*9.59*	*0.16*	*0.20*
10	*7.99*	*3*	*1.5*	*301*	*1.80*	*1.44*	*11.80*	*9.43*	*0.14*	*0.18*
10	7.99	6	1	151	7.00	5.59	17.00	13.58	0.56	0.70
10	7.99	6	1.5	151	7.90	6.31	17.90	14.30	0.63	0.79
10	7.99	6	2	151	8.80	7.03	18.80	15.02	0.70	0.88

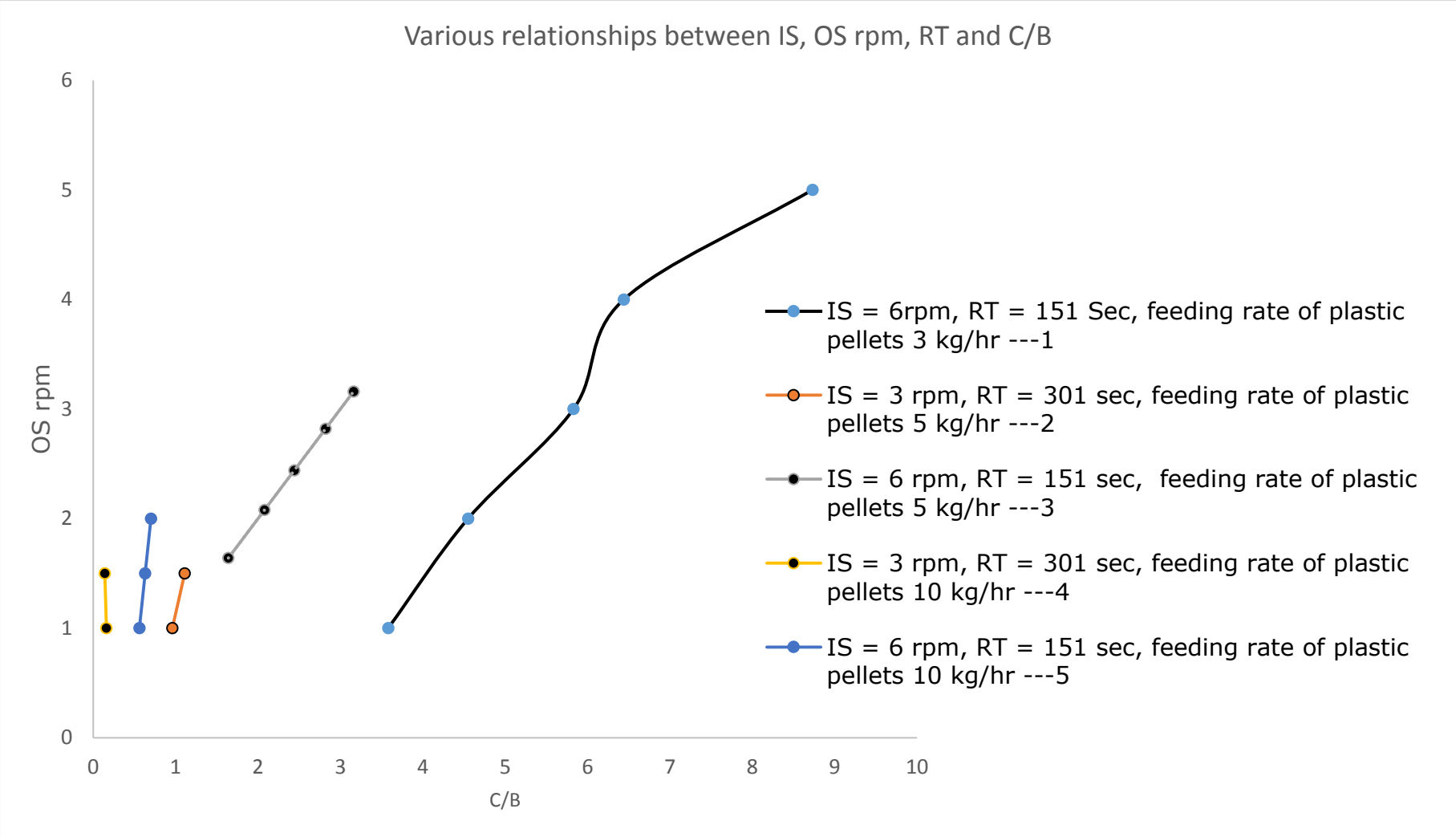

Figure 22 - Graphical representation of relationships between IS and OS rpm to C/B (mass basis as grey highlighted in Table 17)

4.4.3 Inferences from C/B data

Char to biomass ratio (C/B) is calculated from global equations 2 and 3 as described above. In the equation parameter "m_1" was determined by calibrating the cold Pyroformer and removing the combined mass from IS of freshly fed material and recirculated material. This is simply the combined mass of "fresh" and "recirculated" particles within the inner screw after steady state has been reached. Equation 3 is based on the density differences between plastic beads and char as the plastic beads were uniform in size and unbreakable, very close to wood pellets in density and particle size and hence they were used in the study as opposed to wood pellets. As opposed to residence time calculation (where RT was validated to be approximately same in both cold and hot Pyroformer units) C/B could not be validated in hot Pyroformer due to health and safety risks associated with hot Pyroformer if char-pot was to be opened during pyrolysis. The validation was more from an overall perspective where the density of char was known for wood pellets in hot Pyroformer. The results of the tests are presented in the Table 17. C/B of recirculated material when taking into account the density of char is shown if C/B ratio was to be used for hot Pyroformer application. It is observed that the C/B will change with changing feed rate and rpm of both inner and outer screws. This change in C/B must be due to different fill levels due to mass entering per unit time in IS and also the very small difference in the density of pyrolysed recirculated material due to mass loss (only valid in hot Pyroformer case).

It is worth noting here again that cold Pyroformer used in this study has exactly same IS and OS diameter and length to that of 20 kg/h hot Pyroformer used in Chapter 5. This cold system is made up of a Perspex body rather than steel enclosure as in the hot Pyroformer. Also, the 20 kg/h scale of the reactor is only associated with the IS being able to transport all the 20kg of material in one hour without blockages and without any material re-circulation through outer screw. Hence it is fair to say the actual scale of this Pyroformer is drastically reduced when outer screw is rotated (very slowly) in backward direction to recycle the material back towards the feed inlet point. The wood pellets were also tested in the cold Pyroformer to see the pellet breakdown, amount of fine and blockages caused at feeding rates closer to design capacity of 20kg/h. The scale of this Pyroformer is observed to be in the following order depending on which screw is

turning and in which direction. Throughput of the Pyroformer is interlinked in the following order 20 kg/h (IS forward, OS forward or stopped.

During the cold tests when the experimental RT was determined and validated to be same for both wood pellets and plastic beads. Three different feeding rates of 3, 5 and 10 kg/h were tested at two different RTs relative to 3 and 6 rpm of IS. It was noticed through the transparent body of the cold Pyroformer that there was some fine material retained within the system, this was more applicable to wood pellets than the plastic beads which were more robust. This material build-up between the screw shaft and reactor body was due to mechanical forces breaking down some wood pellets during transport through the screws. The other clarification which is important to be highlighted here was that higher feeding rates (>10 kg/h) could lead to blockage at the feeding point. The blockage is caused by too much material entering through the 4 slots in the OS. There were freshly fed material and then recirculated material both joining together from feed entry point in the OS screw slots. The probability of blockage inside the Pyroformer feed inlet was more apparent when the IS rpm was low and feeding rate was higher than 10 kg/h for a constant rpm of OS. For effective material transfer without blockage inside the Pyroformer it was observed that 10 kg/h is the maximum feeding rate which should be used in future with a RT of 3.3 minutes at IS rpm of 4. There was an inversely proportional relationship between RT and rpm of IS. Which means by increasing the IS rpm, the RT will be reduced. This is an important factor for hot pyrolysis where it is necessary for biomass to spend a certain minimum RT inside the reactor to have most of the volatiles released from biomass. A trade off must be made between RT by means of IS rpm and the throughput of the reactor.

The relationship between C/B is explained with the help of Table 17 and Figure 22. It is important to highlight that these tests are done in the cold Pyroformer and without pyrolysis conditions and with plastic beads and the C/B is determined for recirculated material to that of freshly fed material in the IS. However, by ignoring the small volume change during hot pyrolysis and considering the density difference between plastic bead and char materials the same C/B ratios can be applied for hot Pyroformer. Hence, although the observations given below are based on plastic beads experimental study but same is true to great extent for

recirculated char and biomass pellets if a minor change in volume is ignored. The change in volume can be ignored for feeding rates below 10 kg/h as during this time IS was not completely filled so small volume fluctuations do not make any difference as there is ample space available in the screw to account for volume change. Feeding above 10 kg/h meant that IS was near capacity to be full and blockage potential was imminent. Here, C/B is not necessarily char but recirculated plastic beads representing the char when considered with the difference in density.

- Two RTs are tested in the experiments in Perspex cold Pyroformer i.e. with IS of 3 rpm and 6 rpm at different feeding rates, it is important to remember that these RTs are experimental and hence there is a small variance of 10% to those of theoretical RTs.
- With increasing C/B there is higher mass flow rate which is observed in the inner screw. This higher flow rate is caused by initial fresh feed plus any recirculated material coming back from OS to re-join the fresh feed in the IS.
- At constant feed rate and constant IS rpm in forward direction, increasing the OS rpm in reverse direction to convey char towards feed inlet increases the C/B as is evident in curve 1 in Figure 22.
- At low feeding rates and constant IS and OS rpm the C/B is higher compared to higher feeding rates and as the feeding rate increases the C/B decreases as there is more fresh feed compared to recirculated material at the feeding point, this phenomenon is evident from the C/B curve shifting to right with lower feeding rates (e.g. 3, 5 and 10 kg/h) and C/B curve shifting to left at higher feeding rate.
- RT below 151 seconds at IS 6 rpm (curves 1,3 and 5) will possibly lead to a very small mass loss (although not applicable in cold test) during hot tests in Pyroformer and hence any tests faster than 6 rpm of IS were not performed, as this was not going to give any benefit.
- At the same time with increasing feeding rates at 6 rpm of IS, the OS rpm (curves 1-4) can be increased at lower feeding rate (3 and 5 kg/h) to achieve higher C/B but there is a limit to this and blockages are likely at higher feeding rates, if OS rpm was increased beyond 2 rpm (e.g. beyond curve 5).

- To achieve better C/B ratio lower feeding rates and low IS rpm and higher OS rpm is recommended, however Pyroformer system can be sensitive to blockages if very high OS rpm is selected while maintaining reasonable RT for hot pyrolysis reactions in reality.

  When applying the C/B ratio results from cold model to the hot Pyroformer there must be some additional aspects which must be understood, as explained below;

- With regards to C/B from these cold tests and applying it to hot Pyroformer, higher feeding rates lead to lower C/B and thus the catalytic effect of vapour cracking with char (carbon + inorganic ash content) may well be compromised. This can be better explained in next chapter in terms of amount of carbon and inorganic fractions available in the char to that of biomass feed. As more and more carbon (from recycled char) becomes available to evolving gaseous vapours from biomass the vapours are adsorbed onto carbon's catalytic sites and re-organise and or decompose into other hydrocarbons.
- In hot Pyroformer, for the purposes of maximisation of char cracking effect (anticipated to be related to higher C/B) it is better to run the Pyroformer with low feeding rates as it is when more char containing elemental carbon and inorganics are present in the reaction zone with evolving gaseous vapours from fresh biomass feed.
- In hot Pyroformer, experimental RT needs to be sufficient to allow for maximum or effective weight loss due to vapour release i.e. shorter the RT (means higher IS rpm) the less weight loss from biomass pellets will occur and vice versa

4.5 Summary of the chapter

The literature research strongly indicated the positive effect of tar cracking by char, however it is evident that there is a lack of work done in understanding the amount of recirculated material (char) to freshly fed material (biomass) ratio for maximising the tar cracking by char. To fill this gap in scientific literature a detailed experimental study of char to biomass ratio was determined in an innovative twin screw counter rotating Pyroformer reactor. During this study the experimental residence time of feedstock in the reactor was determined and it was compared with the theoretical RT. This study also enhanced the understanding of material flows with the reactor and helped to understand the operational limitations of Pyroformer due to blockages by material bridging.

This study enables to understand the relationship between inverter motor control frequency settings (Hz) and the IS and OS screw speeds. Both IS and OS seemed to be working at similar rpm at approximately similar frequency settings. The residence time (RT) which is a function of rpm of IS was also experimentally observed and theoretically calculated and it showed a small difference between both. This is important aspect of pyrolysis for maximum weight loss from biomass and is interlinked with weight loss curve as done by various researchers in thermo gravimetric analysis (TGA). The RT need to be equal to are greater than the initial maximum weight loss point on TGA curve. It is also well known in pyrolysis field that higher the residence time then the grater is weight loss however excessively unnecessary long RT is not beneficial as it does not bring a lot of benefit and to be sufficient time until weight loss levels on TGA curve.

The ratio between recirculated material and freshly fed material in cold Pyroformer or in hot Pyroformer terms it is char to biomass ratio (C/B) which is another important aspect which is modelled in this study. It enables to understand how much recirculated material was present at any given time if the IS and OS rom and feeding rate of the biomass were known. This C/B ratio also enabled to understand the system limitation which is prone to blockages by excessive OS rpm and hence a trade-off need to be found between the feeding throughput and higher C/B without blockages. The determination of C/b ratio paved the way for better understanding of hot pyrolysis, explained in chapter 5 where the impact of C/B is observed on the quality and quantity of pyrolysis products. Previously it was not known that by changing the IS or OS rpm how much recirculated material was

present relative to freshly fed material. During this study the ratio of recirculated material to fresh feed was determined at various IS and OS rpm, this (C/B) parameter is now quantified and with this information a better understanding of the effect of IS and OS rpm variance on the quality of pyrolysis products can be established. Further work to understand the relationship between C/B ratios was conducted in Chapter 5 to see the impact on quality and quantity of the pyrolysis products.

Chapter 5 - Experimental studies in hot Pyroformer 20 kg/h

In this chapter, the results of two different studies are reported. The first study is parametric study into effects of the ratio of recirculated char to biomass and of variation in the feeding rates of biomass pellets, on quantity and quality of pyrolysis products. In this study only one type of biomass feed stock in the form of corn and green rye digestate pellets is used. In the second comparative study the effect of biomass feedstock variation at similar feeding rate is studied and the results are presented. In this case three different feedstocks are used and the analytical results are presented.

5.1 Parametric study

Three different feed rates of digestate were used to evaluate the effect of feeding rate on the mass yields and quality of pyrolysis products. This meant that the time taken to reach steady state were different. The feed rates used in the study were 3, 5, and 10 $kg.h^{-1}$ of digestate pellets through the Pyroformer reactor. Various screw speeds were used for both screws in both directions to investigate the improvements in the quality and quantity of products.

5.1.1 Feedstock characterisation

The feedstock used in the parametric study was from arable crops (corn and green rye) digestate. This means the feedstock had gone through an anaerobic digestion process where biogas was formed and resulting liquid digestate was then filtered to remove any solids by a mechanical process as is used generally in this industry. The solid fraction of the anaerobic digestate was dried and pelletized by Milson Engineering Ltd of Worcestershire in 6 mm diameter pellets before being used in this Pyroformer. The pellets were chosen over the powder and granules of digestate because of their uniform particle size, uniform heat transfer due to similar size and better flow performance against material bridging. The pellets from this digestate were also suitable to be used in the Pyroformer due to the low fines content, low moisture content and high density. Table 18 gives the results of the feedstock analysis. As shown, the moisture content in the feedstock was 11.5% whereas ash content was 35.7% in weight.

Table 18 - Corn and green rye digestate feedstock analysis

Parameter	Units	Analysis Value
Proximate analysis		
Moisture content	Wt. %	11.5
Ash	Wt. %	35.7*
Volatile matter	Wt. %	54.1*
Gross Calorific Value	MJ/kg	15.02*
Ultimate analysis		
Chlorine	Wt. %	0.87*
Carbon	Wt. %	35.95*
Hydrogen	Wt. %	3.91*
Nitrogen	Wt. %	3.54*
Oxygen[a]	Wt. %	55.73

* Dry basis analysis

[a] Oxygen by difference

The ultimate analysis of the feedstocks was determined using combustion analysis on a Flash EA 1112 Series CHNS analyser. Oxygen was calculated by difference. The density was measured according to the ASTM D-285. The moisture content of the feedstock was determined using a moisture analyser (Sartorius MA35) with a programmed temperature of 105°C. The gross calorific value in HHV (MJ/Kg) of the dried feedstock was determined using a Parr 6100 bomb calorimeter.

5.2 Experimental method

The samples were supplied by Milson Engineering Ltd of Worcestershire in 6 mm diameter pellets, these were fed into the Pyroformer reactor as shown in Figure 23 where a detailed layout of the Pyroformer process is also presented. This Pyroformer setup was used in the parametric and comparative studies. The differences between parametric and comparative studies were the different feed materials and the operating parameters whereas the equipment setup remains

the same. The Pyroformer process layout includes various parts which are integrated together which are explained below and represented in Figure 23:

1. Pyroformer mild steel body
2. Biomass feeding hopper with screw feeder motor (Motor specification; Danfoss Bauer, BS02-34v/d06la4/tf-k305/sp, 230V, 0.73A, 0.12KW, IP65)
3. Sluice valve assembly made up of two ball valves (2-inch Internal diameter) and a hopper, 3a Nitrogen purge line
4. Electrical heaters fitted on outside body of reactor tube across the length (Total 5 band heaters, 2×3kW and 3×2.5kW) to provide the heat for the process
5. Inner auger screw (as shown in Figure 16)
6. Outer auger screw (as shown in Figure 17)
7. Electrical drive motors for inner and out screw with solwertsteller rpm controller (Motor specifications; Sew Eurodrive, Model: R57 DRS71M4/mm/7, Power: 380-500V, 1.90A, 0.75kW)
8. Pyrolysis gas outlet 40mm diameter (with KF40 flange)
9. Metal stand for mounting the Pyroformer
10. Char container of 15 Litres capacity
11. Pyrolysis gas line (insulated) connecting the gas outlet to condenser
12. Counter current bio-oil condenser, 12a & 12b cooling water inlet and outlet
13. Ice bath for tar removal
14. Bio-oil collection vessel (1 Litre glass bottle with screw tight lid)
15. A dual stage fabric filters
16. Gas flare

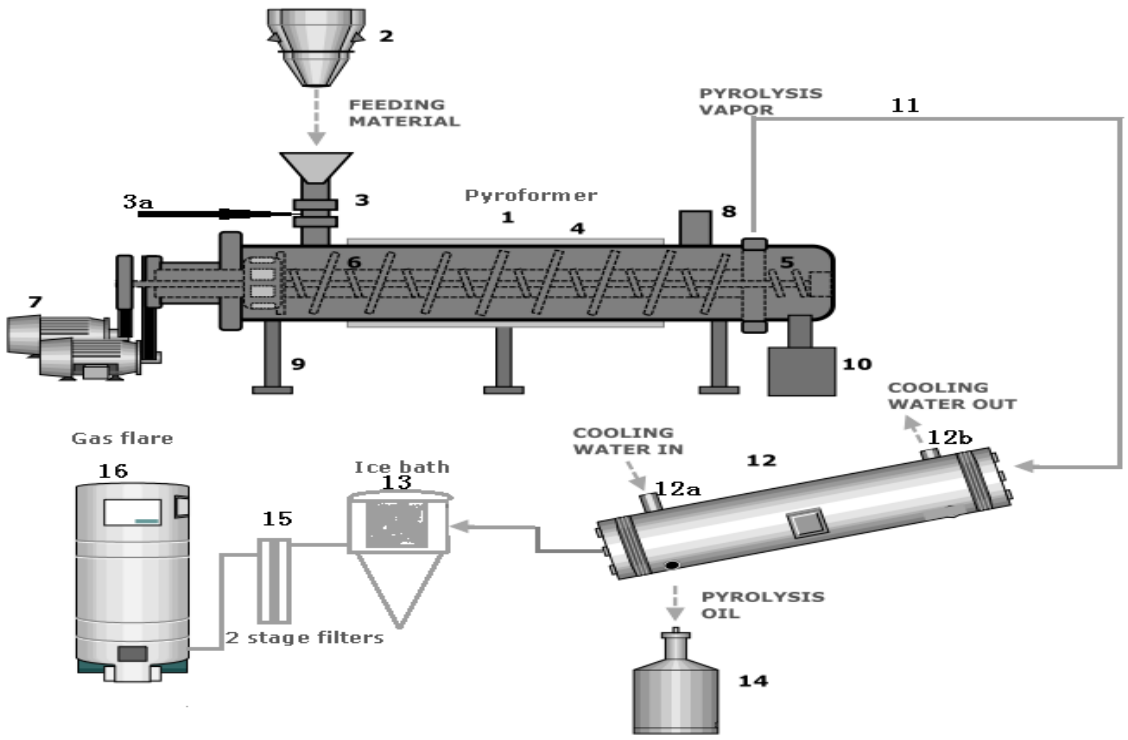

Figure 23 - Pyroformer process (20 kg/h) layout - adapted from [110]

After general preparations, the process of preheating the Pyroformer was performed to reach the set temperature in the Pyroformer reactor. The temperature of the electrical heaters (4) was raised in 50°C increments every 30 minutes to pyrolysis reaction temperature of 500°C for all the tests. This incremental temperature increasing procedure was implemented to ensure the uniform temperature distribution across the Pyroformer body (1) and also to avoid any hot and cold spots. The time taken to reach the set temperature was dependent on initial starting temperature of the Pyroformer. If the reactor was heated a day before then it took shorter time to reheat due to some residual heat present from last time. A nitrogen purge (3a) was introduced at a 20-25 $ml.min^{-1}$ flow rate to ensure vapours evolving from the biomass could be facilitated by nitrogen flow to leave the Pyroformer and to drive off any air from within the Pyroformer during start-up. The rotational screw speeds of both inner (5) and outer (6) screws were selected before the introduction of feed to avoid sagging of screws due to heat. It was also ensured that during the heating process the Pyroformer was empty of any residual biomass and char from previous tests; and a nitrogen purge was introduced to ensure there was no air in the system. The biomass was fed from a hopper (3) by means of a screw motor. The screw motor

rotational speed was calibrated before heating up the reactor to ensure correct feeding rate was maintained during the test. Once the Pyroformer reached the desired temperature of 500°C then feed was introduced. Both feeder sluice valves on the vertical feeding section (3) were actuated to allow the biomass to enter the reactor while maintaining a sluice.

Once the material entered the Pyroformer reactor, it was moved forward by the inner screw motor and just before the char outlet, material dropped into outer screw through special cut-outs. The outer screw moved the material backward towards the feed entry point where pyrolysed biomass (now char) joined the fresh feed and then got conveyed again with freshly entering biomass. It was also possible that some of the materials would be recirculated more than one time. During the material transfer forward by inner screw and backward direction by outer screws, pyrolysis reactions took place by means of the electrical heaters. During pyrolysis in the Pyroformer hot vapours are generated which are taken out from gas outlet (8) whereas the solid residue (char) comes out from char outlet into the container (10).

It was also possible that, while resident in the reactor, some of the biomass underwent no recirculation instead coming straight out in the char container as pyrolysed material. Pyroformer was accumulating the biomass initially to fill the both screws rotating in counter directions to each other until any material came out in the char container. The actual residence time of the material in the Pyroformer was hence based on time taken by the biomass material in the inner screw after entering the reactor to exit into char container without any recirculation through outer screw as only a fraction of the material was recirculated through outer screw. Most of the feed material was exposed to a single pass through inner screw only. Exiting pyrolysis vapours were then condensed in a counter current shell and tube water cooled heat exchanger (condenser) (12) with hot pyrolysis vapours entering one side (to condense) and non-condensable gas coming out on the other side. Bio-oil was collected in the air tight glass bottle (14). The condensation took place with cooling water in counter current direction in a shell and tube heat system. The condensing pyrolysis bio-oil was collected at the exiting bottom end of the condenser in glass bottle fixed at the end.

The remaining non-condensable gases were then passed through an ice-cold bath (13) to recover any further traces of bio-oil. The gases then passed through a two-stage fabric filter (15) and then was burnt in a gas flare (16). The resulting exhaust gases were discharged outside the building. The condensing liquids in the glass bottle was dominated by an aqueous phase. The system was defined to be in steady state when the organic phase became dominant in the liquid collection bottle, as before then there was some likelihood of residual air (until fully consumed) present which lead to combustion and produced mostly the combustion water. When the organic phases started to dominate then glass bottle was changed and the resulting liquid collected after this stage was then taken for further liquid analysis. However overall mass yields of the liquids were based on all the collected liquid. The liquid collected after steady state was sampled and was analysed for its fuel properties. The results of analysis are presented later in this chapter.

5.3 Results and discussion

The experimental results from 3, 5 and 10 kg/h pyrolysis tests are presented in the Tables 19 and 20. Various details of the tests are presented in these tables. During the tests for 3 kg/h feeding rates, it was observed that the time taken to reach steady state was the longest compared to 5 and 10 kg/h. Also, when the char to biomass ratio (C/B) was increased for a fixed feeding rate, the time taken to reach steady state was also increased. This confirmed that by increasing the char to biomass ratio by means of increasing OS rpm, the material was accumulating in the Pyroformer reactor, this accumulation led to longer time taken to reach steady state.

The overall mass balance for the tests is presented in Table 20. There is a clear reduction evident in liquid fraction with increasing char to biomass ratio (C/B), as is evident in tests 7, 14 and 3 at 3 kg/h feeding rate. There was also a good indication that by increasing C/B a significant increase in gas yield was achieved at 19 and 25.7 wt.%, whereas char yield decreased at 3 kg/h feeding rate. Similar results were also obtained for the char and gas yields at 5kg/h feeding rate during tests 9, 10 and 16.

The bio-oil samples produced from these tests were phase separated into an upper layer organic phase and bottom layer aqueous phase (mostly water) were

obtained by gravity settling the bio-oil overnight in a conical separator apparatus. The organic phase of pyrolysis liquid showed mixed results and a conclusive trend is hardly visible to justify the effect on organic phase fuel properties. Perhaps due to lack of data for all analysed properties missing for some samples is one contributing factor to make a balanced conclusion. More is discussed about this in Section 5.3.2. One interesting phenomenon presented in Table 21 in section 5.3.2 was the values of total acid numbers which stood between 0.2 And 0.4 mgKOH/g of oil. These values were found to be lower than fast pyrolysis bio-oil and were in agreement to another study by Neumann [61] who also reported low total acid number value of 4.9 mgKOH/g for a digestate derived bio-oil pyrolysed at 750°C by influenced by tar cracking promoted by char.

Table 19 - Experimental conditions for 3, 5 and 10 kg/h tests in 20 kg/h Pyroformer

Test run no.	Feeding (kg/h)	Input total (g)	Operational Time (min.)	Input SS (g)	SS (min.)	Screws rpm IS	Screws rpm OS	C/B
7.0	3.0	9500.0	190.0	4500.0	90.0	6.0	-1.3a	3.6
14.0	3.0	13990.0	282.0	6986.2	137.0	6.0	-3.0a	5.6
3.0	3.4	8500.0	180.0	2833.0	60.0	6.0	-4.0a	6.4
16.0	5.0	13118.0	155.0	4167.0	50.0	6.0	0.0	0.0
9.0	5.0	14167.8	170.0	5833.8	55.0	6.0	-1.0a	1.6
10.0	5.0	12501.0	155.0	5000.4	65.0	6.0	-4.0a	3.1
11.0	5.0	15834.6	190.0	9584.1	115.0	6.0	-8.0a	3.6
12.0	10.0	17430.0	105.0	9960.0	60.0	6.0	-1.0a	0.6
15.0	10.0	19999.2	120.0	11666.2	70.0	6.0	-1.0a	0.6

"a" - indicates reverse rotation of outer screw to that of inner screw for char recirculation

SS – Steady state

IS - inner screw rpm

OS - outer screw rpm

C/B – Char to biomass ratio

Table 20 – Experimental mass balance results for 3, 5 and 10 kilograms per hour test runs in 20 kg/h Pyroformer

			Overall Mass balance wt %			Steady state wt% distribution of liquid	
Test run no.	**Feeding (kg/h)**	**C/B**	**Liquid**	**Char**	**Gas[b]**	**Organic phase**	**Aqueous phase**
7.0	3.0	3.6	32.2	48.8	19.0	55.0	45.0
14.0	3.0	5.6	28.3	46.0	25.7	46.0	54.0
3.0	3.4	6.4	27.8	49.9	22.3	45.0	55.0
16.0	5.0	0.0	29.7	59.3	11.0	33.0	67.0
9.0	5.0	1.6	32.1	49.6	18.3	59.0	41.0
10.0	5.0	3.1	32.0	43.8	24.2	48.0	52.0
11.0	5.0	3.6	32.9	54.1	13.0	57.0	43.0
12.0	10.0	0.6	34.9	51.3	13.8	42.0	58.0
15.0	10.0	0.6	30.6	55.2	14.2	44.0	56.0

"b" Gas calculation by difference

5.3.1 Effect of char recirculation on pyrolysis products

In addition to varying feed rates of biomass between 3, 5 and 10 kg per hour, the C/B was also varied to evaluate the mass yields of products as well as the quality of products. This was done by varying the relative inner and outer screw speeds in counter rotating directions. It is important to remember that char re-circulation took place only when the inner screw was moving in the forward direction (i.e. it was conveying the fed biomass from feed inlet towards the char outlet) and the outer screw was recirculating some of the pyrolysed char just before the char outlet through the cut-outs in the outer screw towards the feed inlet. The re-circulated char then re-joined the fresh biomass feed and this was where the heat from the electrical heaters and hot recycled char transferred into fresh biomass as well as the catalytic effect due to the formation of active sites in the pores of the char shown to be playing their role in tar cracking. Tars are long chain hydrocarbons which are undesirable due to their impact on increasing bio-oil viscosity and inefficient combustion due to reduced atomisation of fuel.

During the recirculation of char (after steady state) through the outer screw to inner screw most of the pyrolysed biomass experienced a single pass through the inner screw and then fell into char container. It was also possible for some particles of the recirculated char to recirculate multiple times. The recirculation of char was a function of both the inner screw and out screw speeds as well as the biomass feeding rate, i.e. the fill rate of inner screw. When the outer screw rotated in the forward direction same as the inner screw then the C/B ratio was considered zero as the recirculation of biochar could not take place as both screws conveyed the contents towards char container. During this state, the conduction heat transfer from electrical heaters to biomass in inner screw was going to be minimised due to the empty outer screw (only heat convection to IS) and heat transfer mechanism was radiation and convection through gas phase to inner screw. However, some biomass could also be conveyed through the feeding inlet into the outer screw and then to char container in which case some heat conduction could take place. The enhancement of better heat transfer and increasing C/B ratio resulting in increasing char and surface area availability seemingly enhanced the product yields. The effect of C/B is further discussed below. Gas yield was calculated by difference as the accurate gas yield determination was not possible due to some gas escaping from the feeding section into a suction ventilation

system for disposal outside the lab. During this small gas loss, it was likely that some condensable vapours were also lost thus further impacting the mass balance. Solid residue collected in the char container, acquired after pyrolysis is called char. However, the carbon content in this char from digestate pellets was very low compared to char derived from pyrolysis of wood pellets [110].

Gas yield % + liquid yield % + char yield %= Biomass input X 100 %

Gas yield % = 100 – (Liquid yield % + char yield %)

The data collection for mass balance may have suffered some in-accuracies due to the scale of plant being slightly larger in 20 kg/h rather than hundreds of grams per hour in some cases. There were elements of data collection which could have influenced the inaccuracies in the date. These inaccuracies in data collection include; some fine feedstock particles deposited inside the feeding section where some fugitive gas emissions may have condensed, char left inside the Pyroformer screws or in the voids between the screws and reactor body, some vapours condensing inside the feeding section or condensed vapours elsewhere in the condensing train but not recoverable due to large volume and complex pipe joints and the escaping gaseous vapours from feeding section into suction ventilation system for safe disposal outside the lab. These errors in mass balance are not quantified as the gas fraction was not metered to provide a complete mass balance to highlight the percentage error.

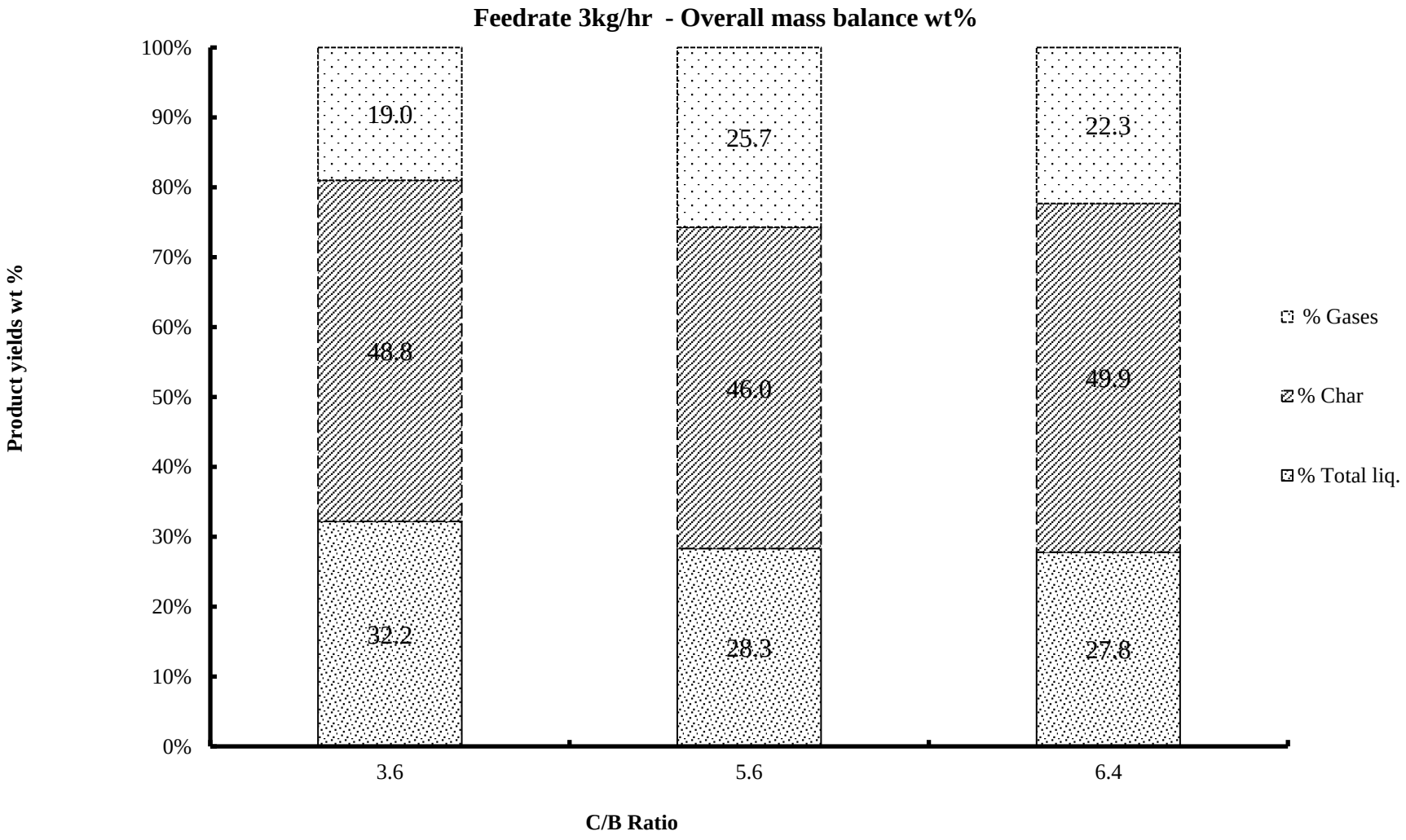

Figure 24 - Effect of C/B ratio on product yields during 3 kg/h feed rate

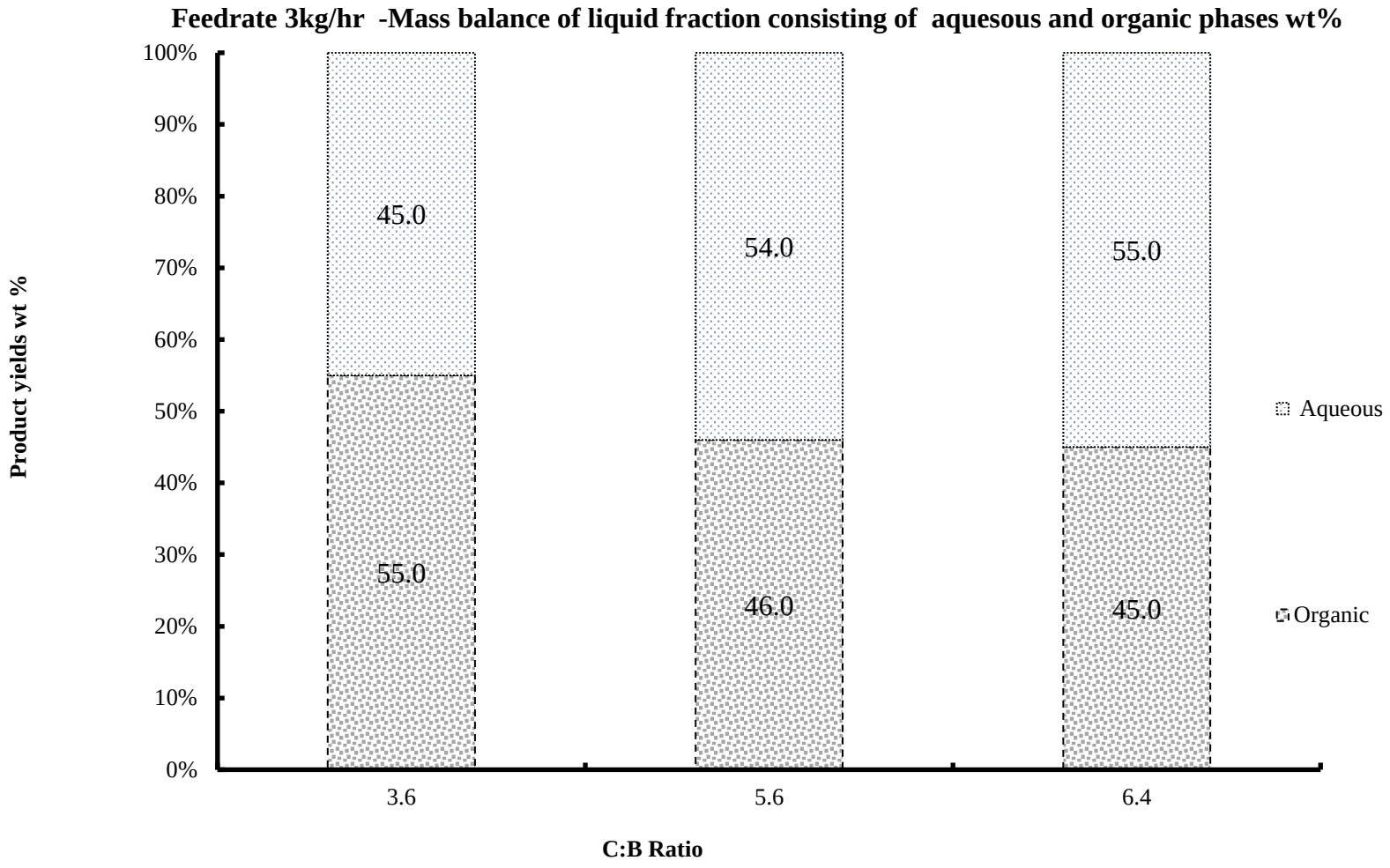

Figure 25 - Effect of C/B ratio on aqueous and organic phase yields during 3 kg/h feed rate

Experimental results are presented in Tables 19 and 20 where various operating conditions and the experimental data are shown. It was observed that there was a significant difference in time to achieve the steady state. The time taken to reach steady state was directly linked to the reaction conditions inside the Pyroformer in terms of thermal conditions, as the delayed steady state indicated poor reaction conditions due to longer drying time of biomass. A large time difference was noted between run 14 and 3 which was more than double for run 14 compared to run 3 at 137 and 60 minutes. A comparison between the product mass yields from Figure 24 indicated that char fraction was considerably higher in all tests at around 3 kg/h. This was an indication that due to the limited volume fill of the Pyroformer there were limited secondary reactions taking place and hence less of the pyrolysis vapours came into contact with char compared to 5 and 10 kg/h.

The total liquid yield seemed to decrease with increasing C/B ratio and also there was an increase in the aqueous phase compared to organic phase of the liquid as presented in Figure 25. However, the differences in are negligible in both organic and aqueous phases. A progressive increase in the aqueous phase as well as the higher char fraction combined with lower organic phase indicated no improvements in the pyrolysis reactions to form better quality liquid. The longer time taken to reach steady state was commensurate with the high char fraction and aqueous phase. There was a minor indication of improved performance at C/B of 5.6 where considerably more permanent gases were produced at considerably longer time of 137 minutes to reach the steady state (SS). This longer SS time could be attributed to a random error in the test run as such longer delay in SS could not be justified when compared with other two tests at same feeding rate.

When comparing the quality of organic phase at 3 kg/h during various C/B ratios at the constant pyrolysis temperature of 500°C, it was evident that after 137 minutes of time delay to reach SS, a better calorific value of organic phase of bio-oil fuel (26.5 MJ/kg) was produced. As there were limited fuel analyses available for other samples at same feeding rate, it is not completely justifiable to state that this fuel is any better than other two samples but based on the information for run 7 it is clear that it has led to a fuel which has even though comparatively higher water content but has higher carbon content and lower oxygen content compared to run 14 and thus can be a better fuel. Hence with further testing and

fuel analysis a C/B ratio of 5.6 could well be a better operating condition for this feedstock at 3 kg/h.

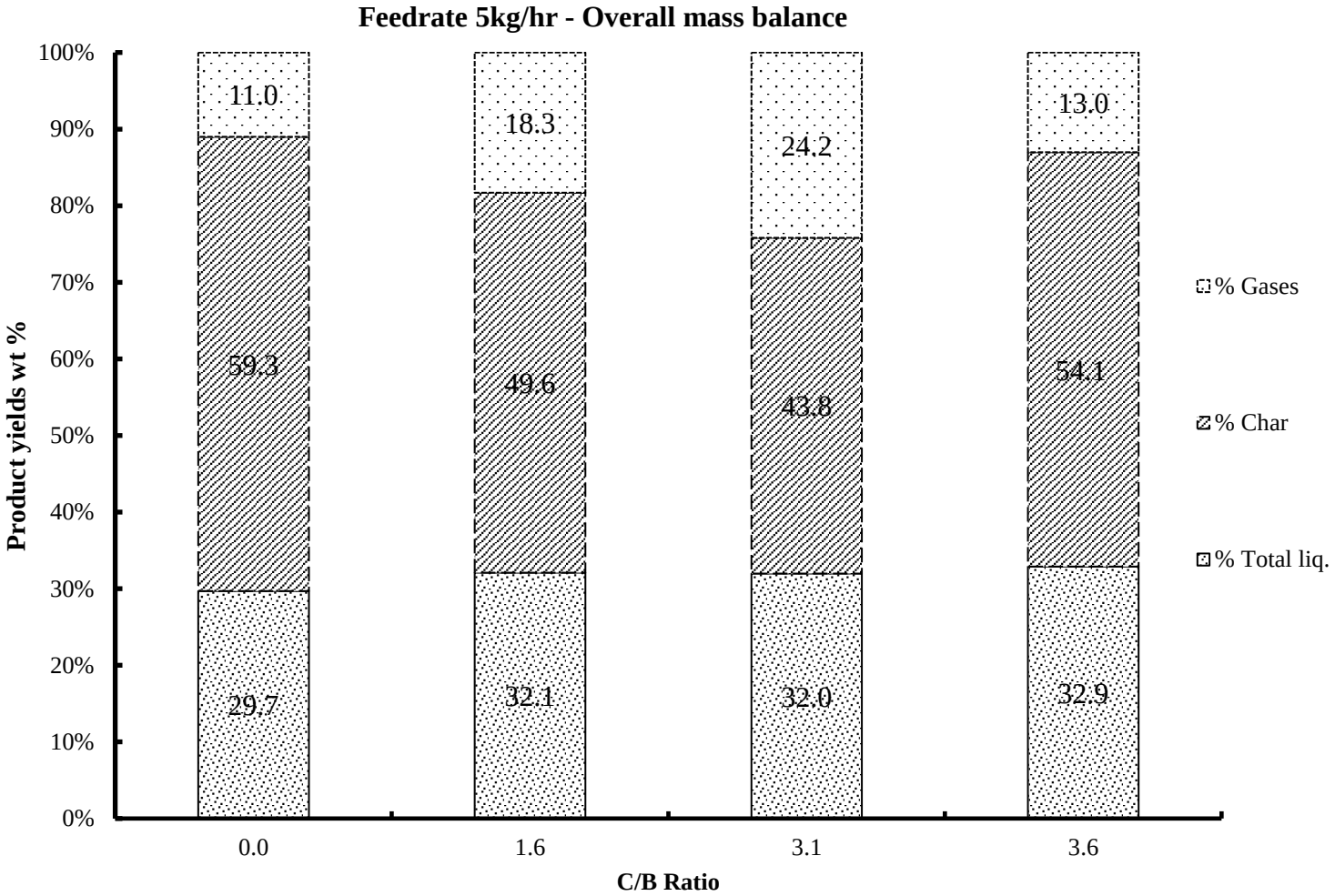

Figure 26 - Effect of C/B ratio on product yields during 5 kg/h feed rate

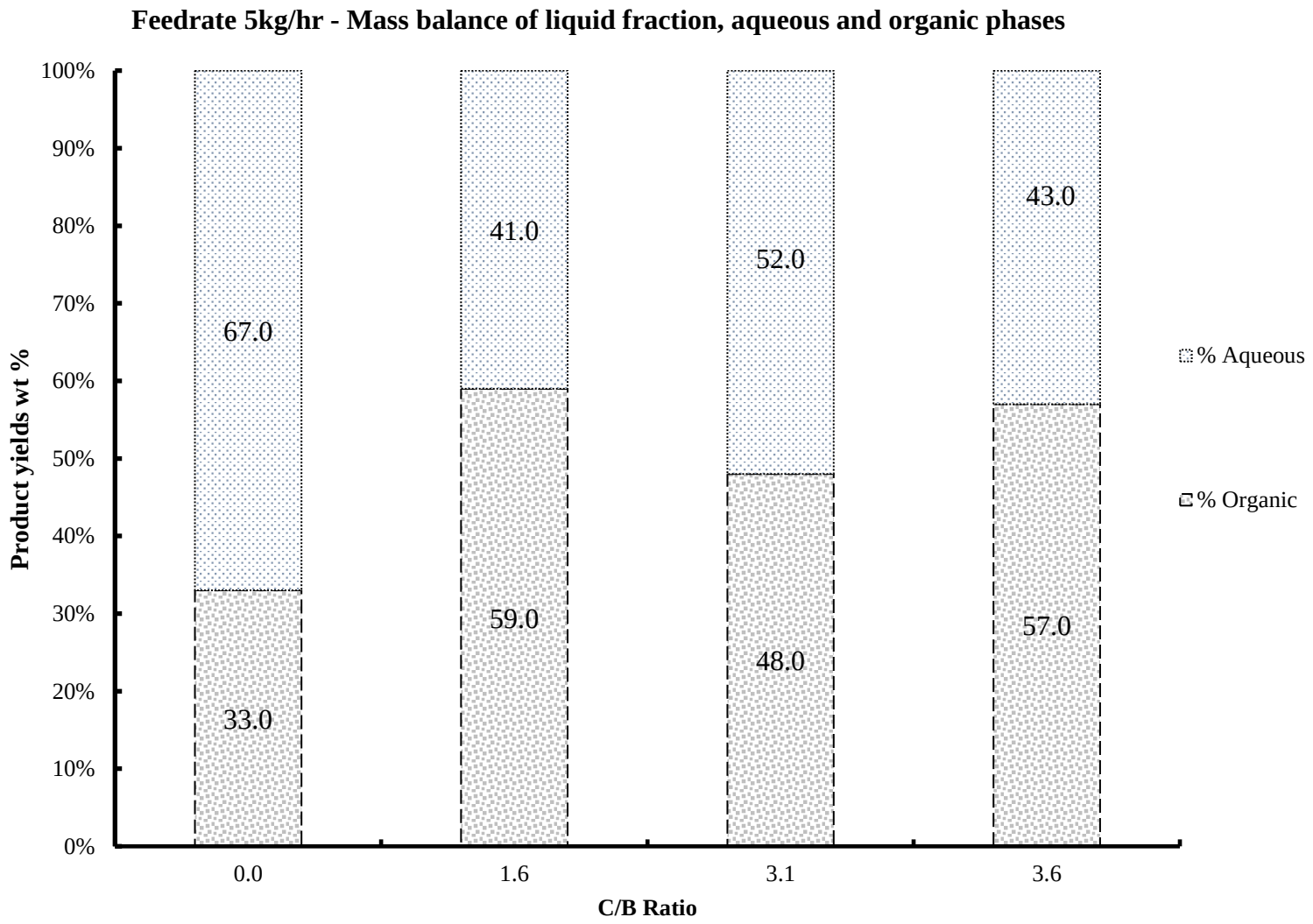

Figure 27 - Effect of C/B ratio on aqueous and organic phase yields during 5 kg/h feed rate

The effect of C/B ratio on product yields is represented in the Figure 26 for a digestate pellets feeding rate of 5 kg per hour. At C/B ratio of zero i.e. no char recirculation, it can be seen that the char yield is 59.3 wt%, which is higher compared to most of the results during char recirculation. It is also evident that with increasing C/B ratio the char yield decreases which is an indication of secondary reactions taking place between the evolving vapours from the fresh feed and pyrolysed char. This is true to some extent until increasing the C/B ratio to 3.6 then the char yield shows an increase. Also, there is an increasing trend for the gas yield which indicates more gas is formed with increasing C/B up to a certain point of C/B. The increase in gas yield is similar to that of Jin et.al [146] where they reported low liquid yield and higher gas yield. Jin et.al [146] reported the char addition in a different manner but the ultimate objective was the same to evaluate the effect of char on product quality and yields.

The gas yield increases with increasing C/B ratio until to a C/B of 3.6 when it decreased compared to char yield. In all cases there seems to be an increasing trend with total liquid yield. The reduction in char yield due to increasing C/B ratio caused the positive effect on liquid yield as the organic phase of the liquids in steady state can be seen increasing from 33.0 to 57 wt %. It is important to remember that the organic phase wt % are only taken from steady state sample whereas the total liquid yield is an overall Figure for all the liquid during both steady and unsteady states which accounts for overall mass balance. The applicability of steady and unsteady state is valid for all tests and for all liquid and organics yields in weight percentages. The gas yield was based on the difference as explained above and it can also be seen that the gas yield was low at 11 wt % during C/B ratio of zero and it increased to 24.2 wt % with increasing C/B ratio of 3.1. It can be concluded that with increasing C/B ratio the increase in gas and liquids yields was evident up to a point of C/B ratio of 3.1 whereas char yield decreased. Also with increasing C/B ratio the organic phase of liquids during steady state also increased as shown in Figure 27. From these results it could be concluded that char recirculation had a positive effect on enhancing the liquid yield whereas gas yield increased to some extent. There is a strong relationship between the secondary reactions, char and evolving vapour with increasing the char recirculation within the Pyroformer. The optimum C/B for 5 kg/h is 1.6 where an organic phase yield of 59 wt % was achieved.

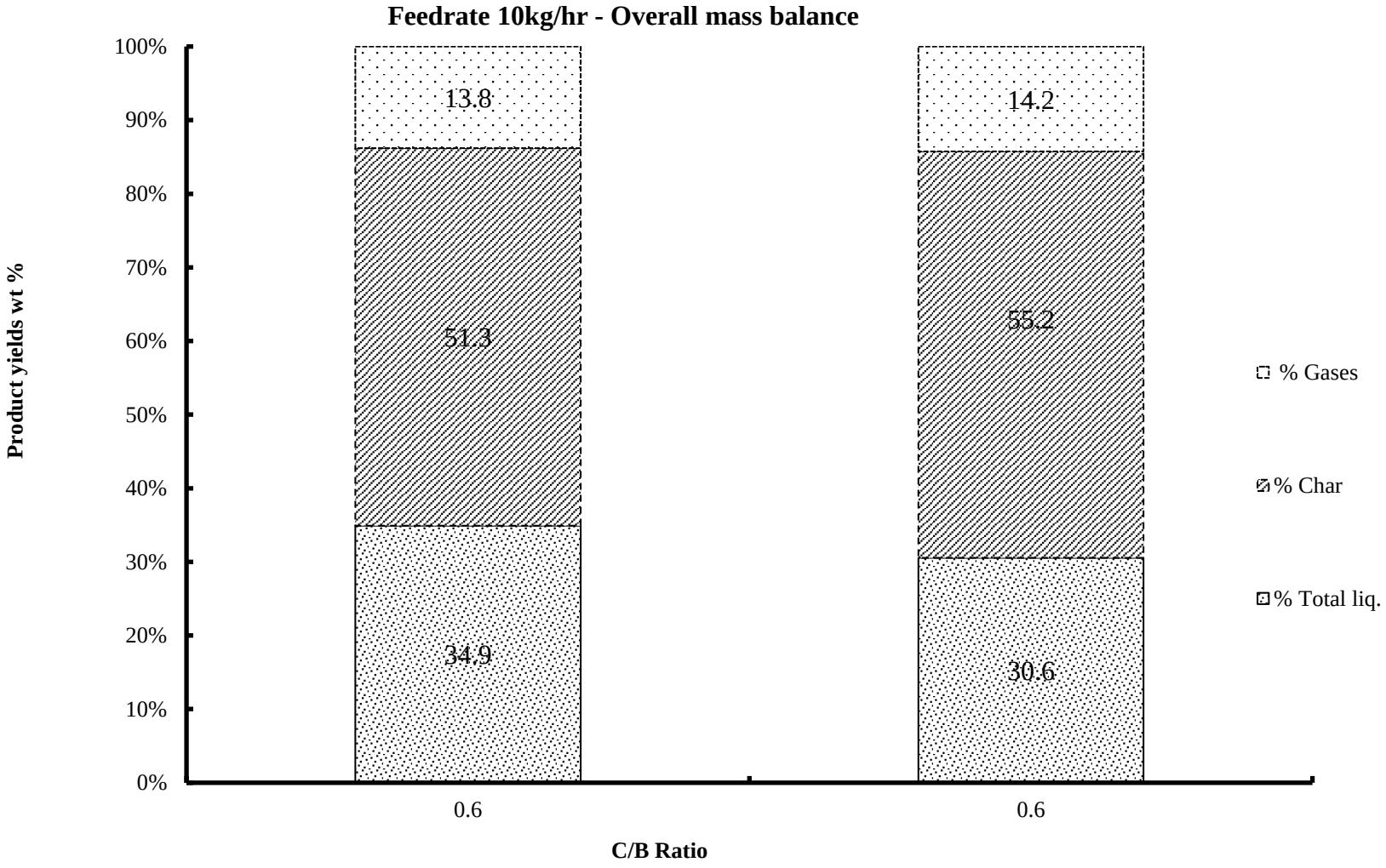

Figure 28a –Reliability of the results to evaluate the effect of C/B ratio on product yields at 10 kg/h feeding rate

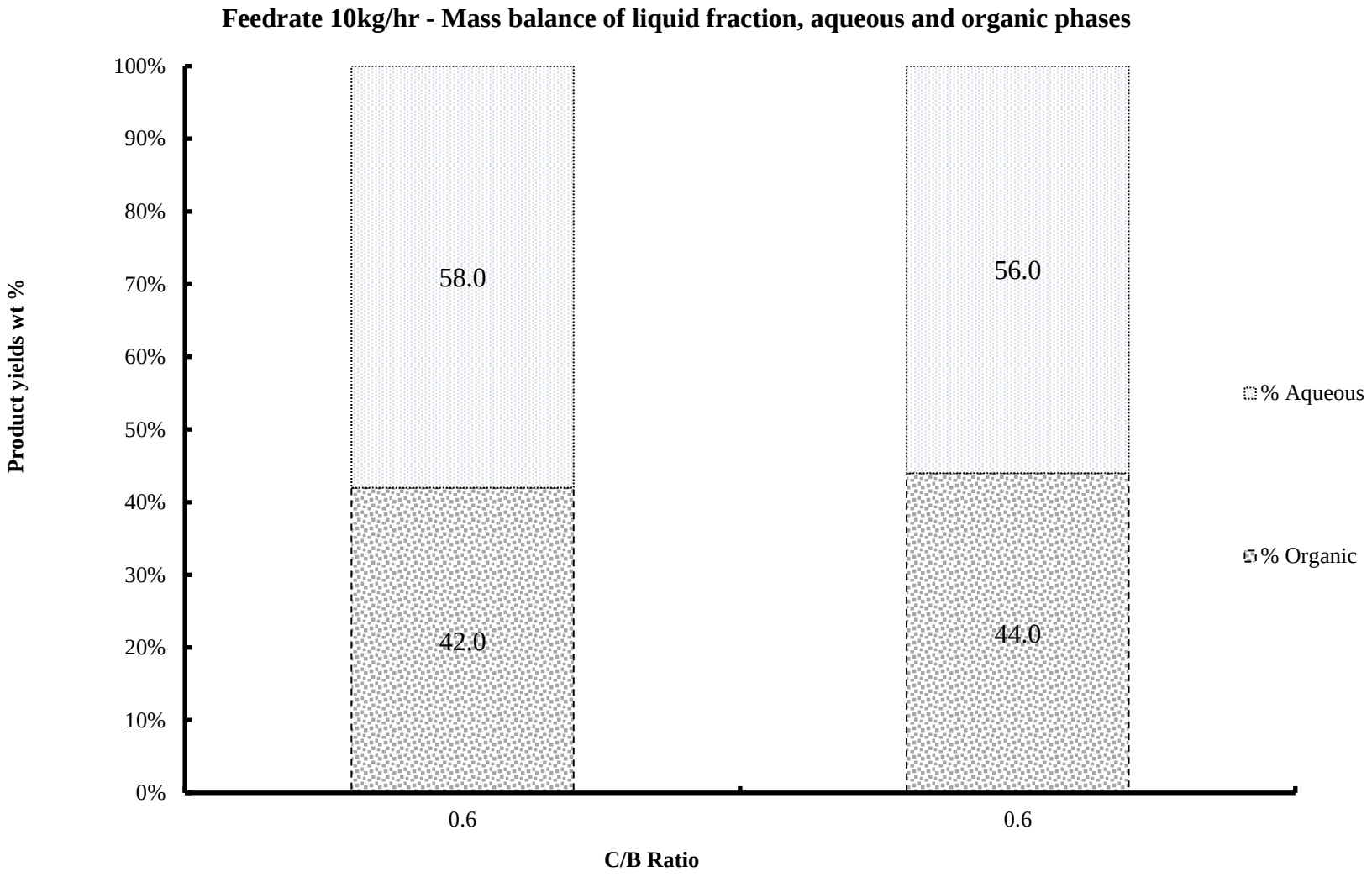

Figure 28b –Reliability of the results to evaluate the effect of C/B ratio on aqueous and organic phase yields at 10 kg/h feeding rate

Two tests were done at the same C/B ratio of 0.6 for a feeding rate of 10 kg/h as shown in Figure 28a however more tests need to be done for other C/B ratios at this rate. In this report only at a C/B ratio of 0.6 the data is presented in Figure 28a. As both tests were conducted at the same feeding rate and C/B, it is good to compare between both tests to see the reliability of data. Small variations in product yields could be noticed as well as the different times taken to reach steady state respectively (60 and 70 minutes) as shown in Table 19. During this C/B ratio, the inner screw was rotating at 6 rpm in forward whereas outer screw rotated at 1 rpm in backward direction, which meant there was very little char recirculation and when compared to 5 kg/h at same rotational speed (which equated to C/B of 1.6), the mass yields of liquid and organic phase are somewhat similar at 34.9, 30.6 and 32.1 as shown in Figure 28a. The variability in the mass yields at similar C/B ratio of 0.6 and extended steady state time in test 15 could be associated with random errors in data collection or influence by ambient conditions and variations in the quality of feedstock. There were minor noticeable differences in the product yields which means the reliability of data was questionable and perhaps the best way will be to average the data based on triplicate results in future. Organic phase yields (as shown in Figure 28b) were found to be 42 and 44 wt % which were significantly lower than other feeding rates at 3 and 5 kg/h as shown in Table 20. This meant that organic phase yield decreased with increasing feeding rate.

5.3.2 Comparison of quality of organic phase of pyrolysis liquids

In this section a comparison between the qualities of organic phase of the liquids is presented. Organic phase is the upper phase of bio-oil liquid when gravity settled, it separates into an upper layer of organic phase oil and bottom layer into an aqueous phase. It is the upper layer organic phase from intermediate pyrolysis liquids which carried most of the energy of the starting feedstocks after pyrolysis. Various feeding rates were used to determine the effect of C/B and feeding rate on the quality of organic phase. Table 21 contains the results of fuel properties of the organic phase during 3, 5 and 10 kg/h at various C/B ratios. Lack of data for the HHV of organic phase for all the tests prohibits the complete analysis of fuel quality. However, the downward trend in HHV with increasing C/B ratio at 3kg/h between the values of 21 and 26.5 indicated there was a very limited effect on the calorific value of the fuel.

Table 21- Fuel properties of organic phase of pyrolysis liquid from dry digestate in 20 kg/h Pyroformer tests

			Organic Phase properties (as received basis)							
Test run no.	**C/B**	**Feeding (kg/h)**	**Water wt%**	**HHV (MJ/Kg)**	**C wt %**	**H wt %**	**N wt %**	**O wt %**	**Acid No. (mgKOH/g)**	**Viscosity (c St)**
7.0	3.6	3.0	3.1	n/a	61.6	7.4	5.1	25.9	n/a	n/a
14.0	5.6	3.0	1.3	26.5	54.8	9.3	6.0	29.9	0.3	3.5
3.0	6.4	3.4	6.4	21.0	55.1	9.2	6.0	29.7	n/a	n/a
16.0	0.0	5.0	1.3	26.1	55.9	10.2	5.8	28.1	0.3	3.1
9.0	1.6	5.0	2.9	n/a	60.4	8.7	6.0	24.9	n/a	n/a
10.0	3.1	5.0	1.9	27.6	59.9	8.6	5.1	26.4	0.4	3.6
11.0	3.6	5.0	2.4	24.3	56.6	8.9	5.5	29.0	0.3	3.1
12.0	0.6	10.0	1.5	26.4	59.0	9.2	5.9	25.9	0.2	3.3
15.0	0.6	10.0	2.0	26.7	53.9	10.3	6.3	29.5	0.2	4.6

"n/a" – not available data due to no analysis was done for this property

Fuel properties of the organic phase during all three feeding rates at various C/B ratios are presented in Table 21.

The total acid number value was very low at around 0.3 mg KOH/g which indicated the digestate to be alkaline and it showed an improvement in quality over other pyrolysis oils as shown by Yang in [113], where the acid values for sewage sludge pyrolysis oil, de-inking sludge pyrolysis oil and biodiesel were 19.90, 33.03 and 0.80. There is a downward trend in the yield of the organic phase with increasing C/B ratio and the opposite is happening to the aqueous phase as can be seen in Figure 28b. There is an upward trend in the hydrogen in the organic phase which can be associated with the inorganic or mineral species in the char playing their part to enhance hydrogen yield, this is in agreement with literature such as [146] and [147]. Most of these properties together indicate poor reaction conditions even with increasing C/B ratio. It is fair to conclude that there was no significant improvement in the organic phase fuel properties whereas there was an undesirable improvement in aqueous phase yield with increasing C/B ratio. The increasing trend for the char yield with increasing C/B ratio indicated there were secondary reactions taking place which favoured the char and aqueous phase which could be due to some combustion reactions and lack of volume occupied by char in the inner screw when biomass was recirculated.

There were no significant trends seen in Figure 27 for the organic phase at 5 kg/h feeding rate. There was an increasing trend for more carbon content in the organic phase up to a C/B ratio of 3.1 and then this trend diminished with further increasing the C/B ratio to 3.6. This indicated the limitation of the positive char effect for carbon transfer in the organic phase up to C/B of 3.1. The similar trend could be seen with HHV of organic phase with increasing C/B ratio up to 3.1. One considerable trend was the increase in gas yield as per Table 21. The reduction in the hydrogen content in the organic phase also indicated more hydrogen was carried over in the gas phase as with increasing C/B ratio of 3.1. There were some inconsistencies in the tests but overall it is fair to say there as a positive effect on yield of the organic phase with increasing C/B ratio. In the Table 21, the results of organic phase properties and the effects of C/B ratio on organic phase properties are presented. Due to the lack of data for increasing C/B ratios, only limited comparisons could be made but one noticeable difference between the 5 kg/h and 10 kg/h was the decrease in the yield of organic. This could be associated with the increase in feeding rate as at higher feeding rate more vapours are released which

do not have enough proportional active carbon sites for reaction available to have better organic phase yield due to low C/B at 10 kg/h.

The results of the properties of the char are presented in Table 22. The analysis for nitrogen (N), phosphorus (P) and potassium (K) were important to evaluate the fertiliser potential of the biochar. C_{org} is the organic carbon content which is linked to amount of carbon which can be sequestered in land for thousands of years. More on these properties will be presented in Chapter 6. The overall char yield had a decreasing trend with increasing the C/B ratio for both 3 and 5 kg/h but it then showed the increasing trend at significantly higher C/B ratios of 6.4 and 3.6 for 3 and 5 kg/h feeding rates. This special phenomenon is evident in Table 22. By looking at the rpm of both IS and OS it was evident that C/B increased significantly which resulted in the increase in char yield. Also, generally the HHV of the organic phase showed a downward trend commensurate with the special phenomenon of carbon carry over in char due to increasing C/B. This led to the conclusion that there was a negative impact on the HHV of the organic phase of liquids when more carbon was carried into char with increased char recirculation. Ideally it is desirable to have as much carbon and hydrogen taken into gas and liquids phases through volatiles so that value addition for fuel from biomass can be maximised. At the same if char was then to be later used as a Carbon sequestration medium then organic carbon content need to be as high as possible. Thus, an optimum value for char recirculation can be drawn to be C/B ratio of 5.6 and 3.1 for 3 and 5 kg/h feeding rates respectively. Unfortunately, not enough information was available to draw a conclusion for 10 kg/h feeding rate.

Table 22 - Effect of C/B ratio on char composition

Test run no.	**C/B**	**Feeding (kg/h)**	**Ash wt%**	**HHV MJ/Kg**	**C wt %**	**C org[a] wt %**	**H wt %**	**N wt %**	**P wt %**	**K wt %**
7.0	3.6	3.0	64.8	10.0	30.5	>25	1.0	1.0	2.7	4.4
14.0	5.6	3.0	66.1	9.7	27.1	21.9	0.9	1.7	2.8	5.9
3.0	6.4	3.4	62.5	11.7	29.5	>25	1.5	1.9	2.7	8.8
16.0	0.0	5.0								
9.0	1.6	5.0	63.4	10.1	27.0	>25	1.1	1.8	2.6	3.9
10.0	3.1	5.0	66.7	9.5	27.8	24.9	1.0	1.8	2.8	5.4
11.0	3.6	5.0	66.3	9.2	26.9	21.5	1.0	1.7	2.8	5.7
12.0	0.6	10.0	63.7	10.3	29.2	21.0	1.4	2.0	2.7	5.5
15.0	0.6	10.0	57.2	10.3	27.9	22.0	1.2	1.9	3.1	6.6

[a] Organic carbon wt. % (considered important for biochar carbon sequestration)

5.3.3 Effects of feed rate on product yields in 20kg/h Pyroformer

Apart from exploring the effects of char re-circulation on intermediate pyrolysis products, the effects of feeding rate variations on intermediate pyrolysis were also analysed. This section discusses the effects of feeding rate variations observed during the experiments. The Pyroformer has a design throughput of 20 kg/h. However, this design throughput was not tested due to recurring (blockage) issues with the Pyroformer at higher throughput, instead 3 different feed rates were used which are 3, 5 and 10 kg/h. These feed rates were chosen with a view to establish the effect of the fill level of the inner and outer screws. When the feeding rate was 3 kilograms per hour there was less biomass available to fill the inner and outer screws per unit time and hence the time taken to fill both screws was longer compared to 5 and 10 kg/h. This meant the inner screw would have more empty space available within the helix as there was the feedstock material available compared to higher feed rates. This also meant that the char container at 3 kg/h feeding rate would see the less and delayed arrival of char compared to higher feed rates as less material is conveyed through the screws.

Comparing the effect of feeding rate can only be done at similar screw speeds for both IS and OS. This means only 1 test run can be compared for each feeding rate. So, a comparison between test runs 7, 9 and 12 was done here from Tables 20 and 21. Runs 7 and 9 (at 3 and 5 kg/h) represented higher gas yields of 19 and 18.3 wt% whereas gas yield for run 12 (10 kg/h) was considerably less at 12 wt%, however liquid yield had an opposing trend to go up for 10kg/h and lower for 3 and 5 kg/h. The organic phase was at maximum at 5 kg/h run 9 followed by run 7 and 12. This shows the pyrolysis reactions were at optimum when feeding rate was low at 5 kg/h. More liquid was produced at 10 kg/h but with high aqueous phase at 58 wt %.

When 3 and 5 kg/h feeding rates were compared at the higher OS and constant IS rpm rather than the C/B ratio, it was evident that run 3 (3.4 kg/h) and run 10 (5 kg/h) had increasing values for organic phase at 45 and 48 wt % with increasing feeding rates. This phenomenon was also true for total liquid yield which was increasing at 27.8 and 32 wt % with increasing feeding rate. This could be justified with regards to the fill rate in the IS as there is more char available leading to more liquid yield. When HHVs of the organic phase are compared it is evident that 5 kg/h has considerably higher value of 27.6 MJ/kg (run 10) compared to any

lower feeding rates of 3 kg/h. It is fair to conclude that by increasing the feeding rate up to 5 kg/h, better reaction conditions were created which led to improvements in the HHV of organic phase, total organic phase yield and gas yields. Due to increased interactions between free radicals from released vapours and char led to higher carbon carry over into organic phase and this increased carbon carry-over increased the HHV of the resulting organic phase. This can be justified based on the following reasons; that more optimum C/B ratios were obtained due to char recirculation within the IS, this resulted in the creation of relatively more active carbon sites with the pores of char and as there was comparatively (compared to 3 kg/h) more volatiles (free radicals) present in the vicinity of the active carbon pores this resulted in long chain hydrocarbons being broken into simpler hydrocarbons and thus more hydrogen and carbon was carried into condensable vapours and ending up in the organic phase.

5.4 Comparative study

This study looked into the effect of differences in feedstock composition on the pyrolysis product quality and quantity. Three different feedstocks were used to evaluate the effect of material composition which they differed significantly due to their origin. The difference in material composition were attributed to high ash and moisture content of 46.9 wt% and 24 wt% for chicken litter digestate, high carbon content in green rye and corn derived digestate after biogas production and very low moisture content of 7.35 wt% in municipal solid waste (MSW) with significantly higher energy content due to plastic content in the material.

5.4.1 Raw materials for comparative study

In Table 23 the analysis of feedstocks is presented as used in the comparative study. Municipal solid waste (MSW) residue was acquired from municipal works and was pelletized to 6 mm pellets. The chicken litter digestate material originated from poultry farms and was pelletized to 6 mm pellets. These feedstocks were pelletized by Milson Engineering Ltd. The digestate material (corn and rye) is same as explained above in section 5.2.1. The ultimate analysis of the feedstocks was determined using combustion analysis on a Flash EA 1112 Series CHNS analyser. The oxygen content in feedstocks was calculated by difference. The density was measured according to the ASTM D-285. The moisture content of the feedstock was determined using a moisture analyser (Sartorius MA35) with a programmed

temperature of 105°C. The gross calorific value in HHV (MJ/Kg) of the dried feedstock was determined using a Parr 6100 bomb calorimeter.

The proximate and ultimate analysis of these feedstocks is presented below in the Table 23

Table 23 - Comparison of feedstocks used in the comparative study

S/O	Parameter	MSW pellets	Chicken Litter digestate pellets	Digestate pellets
1	Moisture content Wt. %	7.35	24.0	11.5
2	*Ash Wt. %	33.6	46.9	35.7
3	*Volatile matter Wt. %	54.1	n/a	54.1
4	*Carbon Wt. %	29.73	27.64	35.95
5	*Hydrogen Wt. %	4.21	2.39	3.91
6	*Nitrogen Wt. %	1.15	2.66	3.54
7	*Oxygen[a] Wt. %	64.91	67.31	56.60
8	Higher Heating Value MJ/kg	16.34	8.55	15.02

* Dry basis

[a] Oxygen by difference

Table 24 – Experimental settings of digestate, MSW and Chicken litter at 5 kg/h

							Screws rpm		
Feedstock	**Test run no.**	**Feeding (kg/h)**	**Input total (g)**	**Time (min.)**	**Input SS (g)**	**SS (min.)**	**IS**	**OS**	**C/B**
DAC	9.0	5.0	14167.8	170.0	5833.8	55.0	6.0	-1.0a	1.6
MSW	18.0	4.8	16861.0	210.0	9430.0	120.0	6.0	-1.0a	1.6
DCL	1.0	5.0	14167.8	170.0	4583.7	55.0	6.0	-1.0a	1.6

"a" - indicates reverse rotation of outer screw to that of inner screw for char recirculation

SS – Steady state

IS - inner screw rpm

OS - outer screw rpm

C/B – char to biomass ratio

DCL – Digestate from chicken litter

Table 25 – Overall mass balance of digestate, MSW and Chicken litter at 5 kg/h

				Overall Mass balance wt %			**Steady state wt% distribution of liquid**	
Feedstock	**Test run no.**	**Feeding (kg/h)**	**Total liquid (g)**	**Liquid**	**Char**	**Gas[b]**	**Organic phase**	**Aqueous phase**
DAC	9.0	5.0	1262.0	32.1	49.6	18.3	59.0	41.0
MSW	18.0	4.8	3927.0	41.6	43.0	15.4	30.3	69.7
DCL	1.0	5.0	1470.0	32.1	49.0	18.9	77.1	22.9

"b" Gas calculation by difference

The results in Table 24 and 25 are for similar feeding rates at around 5 kg/h with IS 6 and OS 1 which gives the C/B ratio of 1.6 calculated as explained above. The results for 5 kg/h feed rate have been chosen for a fair analysis for all feedstocks at similar operating conditions. The Pyrolysis temperature in the Pyroformer was 500°C for all materials and the process was slightly above atmospheric (10-20 mBar) in terms of pressure to get the flow of evolving volatiles. By selecting the similar operating conditions, a good comparison between the quality and quantity of the products from these feedstocks can be made.

5.4.2 Comparison of product yields

Table 25 represents the mass yields of digestate (DAC), MSW and digestate from chicken litter (DCL). MSW gave the highest liquid yield of 41.6 wt% whereas the other two materials gave similar liquid yield of 32.1 wt%. The organic phase yields were higher for DAC and DCL at 59 and 77 wt %. This is interesting as total liquid yield for these two materials were low but organic phase yield during the steady state was considerably high. This could mean that the quality of the DAC and DCL was better to that of MSW whereas the quantity of the total liquids in MSW was higher. Given that similar operating conditions were used, then it was right to assume that material characteristics must be playing their part to show the differences in quality and quantity.

Despite DCL having a very high moisture content of 24%, the yield of organic phase was comparatively higher than DAC at 77.1 wt %, this could be associated with considerably higher inorganic metal content within the char leading to better organic phase production as most of the oxygen was reacted with metals to form oxides and was either in the metal oxide form or in the gaseous state such as water vapour or carbon dioxide. The higher ash content of 46.9 wt % in DCL feedstock is the good indication to link the better quality behaviour of organic phase from DCL. The presence of inorganic species in the form of ash in DCL at 59.1 wt %, such as phosphorus and potassium at 3 and 9.6 wt % in the ash could have a good effect on yield of higher organic phase. There is no data available for MSW to compare against but the similar data from Table 26 for DAC shows that a high ash content of 63.4 wt % in the char has somewhat similar effect to yield an organic phase of 5 wt %.

Table 26 - Char analysis of DAC, MSW and DCL at 5 kg/h feeding rate

Feedstock	**Ash**	**HHV**	**C**	**H**	**N**	**C_{org}**	**P**	**K**
	wt.%	MJ/kg	wt.%	wt.%	wt.%	wt.%	wt.%	wt.%
DAC	63.4	10.1	27.0	25.0	1.1	1.8	2.6	3.9
MSW	n/a	11.02	22.6	2.19	0.61	n/a	n/a	n/a
DCL	59.1	9.7	29.5	1.4	2.0	19.0	3.0	9.6

The effect of potassium (K) on the organic phase of the liquids is similarly reported in the literature. As reported by various authors, it was shown that the presence of K lowers the activation energy and increases the pyrolysis rate [148-151]. Varhegyi et al [150] have also reported the reduction in total liquid yield but better organics and gas calorific values. Higher nitrogen, phosphorus and potassium values together with high ash content indicate that these chars could also be good soil improvers.

5.4.3 Comparison of quality of organic phase of liquids

The fuel properties of the organic phase of the DAC, MSW and DCL are presented below in Table 27. The presence of potassium as stated above seems to have the effect on the total acid number of 0.2 of MSW and DCL. As it was evident that the oxygen content was considerably higher for the DCL at 38.7 wt% and this led to a significantly lower calorific value of 19.3 MJ/kg compared to 30.3 MJ/kg of MSW. MSW has the higher carbon % and hence this led to its higher calorific value. There was a minor difference available for viscosity for both DCL and MSW.

Table 27- Organic phase fuel properties analysis for DAC, MSW and DCL

		Organic Phase (as received basis)							
Feedstock	**Feeding (kg/h)**	**Water wt%**	**HHV (MJ/Kg)**	**C wt %**	**H wt %**	**N wt %**	**O wt %**	**Acid No. (mgKOH/g)**	**Viscosity (c St)**
DAC	5.0	2.9	n/a	60.4	8.7	6.0	24.9	n/a	n/a
MSW	4.8	1.1	30.3	62.1	9.4	3.3	25.2	0.2	3.1
DCL	5.0	1.1	19.3	45.8	10.8	4.7	38.7	0.2	4.1

There were mixed results for these materials both for overall yields and quality. MSW showed the higher total liquid yield but lower organic phase with higher HHV whereas DCL although had higher organic phase yield but exhibited lower HHV. So, where the quantity of organic phase was maximised, the fuel exhibited lower HHV whereas it was opposite for MSW where there was lower organic yield but better HHV. These characteristics could be attributed to mineral content in ash such as Potassium. These findings were somewhat similar to other researchers as reported by Knudsen et.al [148], Varhegyi et.al [150], Pan et.al [149] and Williams and Horne [151].

5.5 Chapter Summary

Novel work has been done for this thesis which looked at the effect of char recirculation on the quality and quantity of pyrolysis products. The study highlighted a lot of mixed results with a notable increase in gas yield and a bio-oil which benefits from two phases separation. The recirculation of char led to higher gas yield and lower liquid yield with increasing C/B ratio at feeding rate of 3 kg/h whereas the HHV of the liquid increased. The effect of char recirculation at 5 kg/h led to the increase in gas yield up to a C/B ratio of 3.1 whereas there was an overall increasing trend with (liquid) organic phase yield at steady state. Lower acid values of around 0.2 mgKOH/g were evident during all tests which indicated that these oils certainly had better fuel properties with low oxygen content of around 30 wt% compared to fast pyrolysis oil where oxygen content can be of mid 40 wt% range. The ease of 2 phase separation of intermediate pyrolysis bio-oil was further proven to be beneficial with better higher heating values. The steady state time was also different for different C/B ratios and this was another factor which demands further tests.

With increasing feeding rate and at same C/B ratios it was found that the gas yield decreased at 10 kg/h. The organic phase was higher at 5 kg/h feeding rate up to a maximum of C/B of 3.1 due to catalytic effect from char recirculation as explained before and then it decreases whereas there was high liquid yield at 10 kg/h but with lower organic phase yield compared to aqueous phase. Overall the total acid number for all the organic phase samples was in modest range around 0.2 mgKOH/g when compared to other intermediate pyrolysis oils [152].

The comparative study showed some interesting results where the DCL and DAC gave higher percentage of the organic phase but overall the liquid yield was low when compared with the MSW results. It was discovered that char had high ash and potassium content for both DCL and DAC char samples. Potassium is known to have some catalytic effect on the organic phase yield whereas it limited the overall liquid yield. Potassium effect on the mass yield was further backed up by other researchers such as Knudsen et.al [148], Varhegyi et.al [150], Pan et.al [149] and Williams & Horne [151]. Higher nitrogen, phosphorus and potassium wt % in char indicated good soil improving characteristics for DCL and DAC materials.

Chapter 6 – Pyrolysis experiments in 100 kg/h Pyroformer system

Large scale experiments were done using wood pellets and miscanthus pellets of 6 mm diameter in a 100 kg/h Pyroformer while it was installed at Harper Adams University College as part of Bioenergy Interreg NW project. The chronological order of these experiments (No. 4) is shown in Figure 3.1 which depicts the methodology of the Pyroformer research.

These tests addressed the objectives 3, 4, 5 and 6 as explained in Chapter 3, Section 3.3. Also, during these tests, there were some operational issues with the key components of the 100 kg/h Pyroformer, these issues and their solutions are explained in detail in Chapter 7. The operational experience gained from these experiments as well as during the commissioning stages of the whole process helped to highlight the key operational limitations and technical issues with this system. These experiences became the basis of engineering design of critical components of the 100 kg/h Pyroformer.

This 100 kg/h Pyroformer (as shown in Figure 30) process was a scale up variant of the 20 kg/h for the reactor type and there were significant variations in the auxiliary units upstream and downstream of the Pyrolysis reactor. The experiments with this system were performed at the much lower throughput (61 kg/h for wood pellets and 70 kg/h for miscanthus pellets) compared to the design throughput of 100 kg/h.

These experiments were conducted to make use of a technique called in-situ blending of pyrolysis vapours during condensation with biodiesel. So, this meant pyrolysis vapours were in direct contact with biodiesel immediately after exiting the reactor. There was a likelihood that some reactions might have occurred between both fluids (re-polymerisation and cracking of pyrolysis vapours) which are not elaborated further in this thesis. This process arrangement was a major difference when compared to the pyrolysis tests in 20 kg/h Pyroformer where the heat transfer medium (cooling water for condenser) did not come into direct contact with pyrolysis vapour. The main reason for doing in-situ blending of pyrolysis vapours with biodiesel was to produce a blended fuel which can be used in a diesel engine with little upgrade, thus reducing the processing steps. However,

this study did not consider detailed combustion analysis of blended fuel in the engine. This was due to resource limitations and was limited to characterisation of blended fuel properties which are presented in the results section of this chapter. Instead, another area of the focus was the characterisation and application of biomass derived char (biochar) for carbon sequestration. This will be discussed in this chapter.

6.1 Equipment and materials

The pyrolysis process was installed in an out-building at Harper Adams University College which was a key partner of Bioenergy Interreg NW Project as explained in section 1.5 of Chapter 1. The process layout is shown in Figure 29 with further 3D layout images in the Appendix 1.

6.1.1 Process layout

Process layout of the Pyroformer 100 kg/h process is shown in Figure 29.

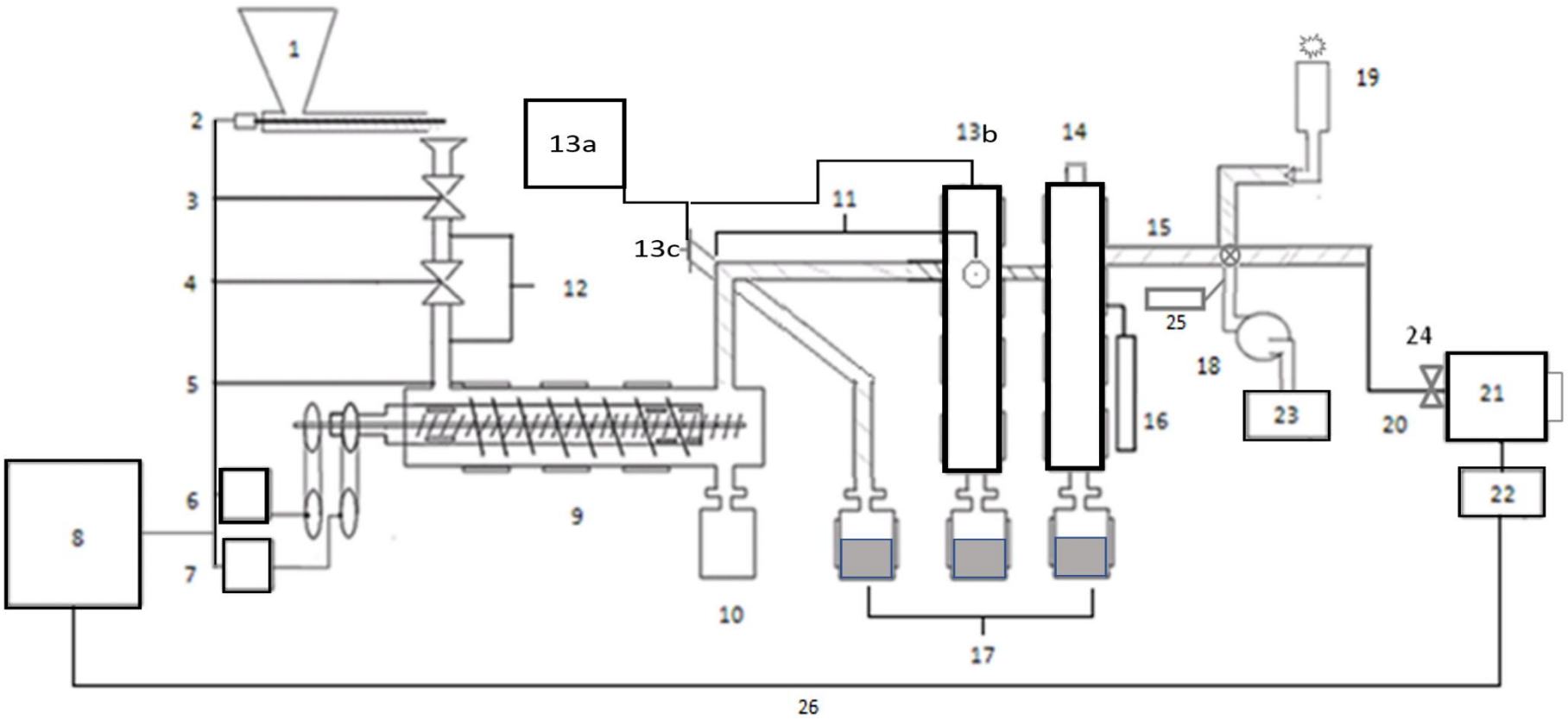

Figure 29 - 100 kg/h Pyroformer process layout

1-Feed Hopper, 2 -Auger, 3&4-Pneumatic Ball Values, 5-Electric Heating Bands, 6 & 7-Electric Motors, 8-Main Control Board, 9-Pyrolysis Reactor, 10-Char Collection Vessel, 11-Wet Scrubber, 12-N2 Purge Line, 13a-Biodiesel supply for quench, 13b-Biodiesel quench stage 2 and air cooled condenser, 13c-Biodiesel quench stage 1 -Air cooled condenser, 14-Electrostatic Precipitator ESP (not turned on), 15-Syngas line 16-ESP Control Board, 17-Pyrolysis Oil Collection Tanks, 18-Gas Suction Pump, 19-Flare, 20-Gas Line to Engine, 21-Dual Fuel Engine, 22-Electrical Generator, 23-Gas Calorimeter, 24-Electronic valve, 25-Oxygen sensor, 26-Electrical connection

Aston University

Illustration removed for copyright restrictions

Figure 30 - Pyroformer 100 kg/h Reactor dimensions approximately 3m long and 0.4m external shell diameter

6.1.2 Feedstocks

Two different feedstocks were tested in these experiments, wood pellets and miscanthus pellets of 6mm diameter each. Wood pellets were supplied by Verdo Renewables Limited of Andover, Hampshire. These pellets were supplied in 10 kg packaged bags which were desirable for ease of handling and storage. These pellets were made to ENPlus A1 standard which is an EU wide quality standard for wood pellets quality and sustainability. Miscanthus (Miscanthus X Gigantueus) pellets were supplied by Agripellets Limited of Alcester, Warwickshire in 6 mm pellet diameter and delivered in 1000 kg bulk bags. These pellets were made to CEN/TS 335 standard which is also an EU wide quality standard for all types of biomass pellets. Biodiesel was sourced from a local supplier and was manufactured from waste cooking oil to EN14214 standard.

The ultimate analysis of the feedstocks was performed using combustion analysis on a Flash EA 1112 Series CHNS analyser. Oxygen was calculated by difference. The density was measured according to the ASTM D-285. The moisture content of the feedstock was determined using a moisture analyser (Sartorius MA35) with a programmed temperature of 105°C. The gross heating value in HHV (MJ/Kg) of the dried feedstock was determined using a Parr 6100 bomb calorimeter whereas the LHV was theoretically calculated using a standard empirical formula. The results are shown in the Table 28 below and are also presented in Appendix 6a in a conference paper from this work.

Table 28- Feedstock analysis of wood and Miscanthus pellets

Feedstock	Unit	Wood pellets	Miscanthus
[a]Ultimate analysis			
Carbon	wt.%	46.2	41.34
Hydrogen	wt.%	5.96	5.27
Oxygen[b]	wt.%	47.6	52.5
Nitrogen	wt.%	<0.01	0.57
Sulphur	wt.%	0.28	0.35
[a]Proximate analysis			
Moisture	wt.%	8.71	10.4
Ash content	wt.%	0.46	2.98
Density @20°C	kg/m^3	688	640
Higher Heating Value (HHV)	MJ/kg	18.3	17.3

[a]Analysis based on pre-treated feedstock, as received basis

[b]Calculated by difference

6.1.3 In-situ quenching of pyrolysis vapours with biodiesel

The process layout of the Pyroformer needed an external quenching solvent to be used as a quench medium for pyrolysis vapours. Bio-oil in its pure form is a very complex mixture to be used as a fuel on its own and often leads to problem with engines [3]. Biodiesel is a renewable fuel derived from plant oils, very safe to handle, high flash point and a good solvent [26 & 100]. It also has heating value, density and viscosity somewhat similar to petroleum derived diesel. Biodiesel was chosen due to these properties as it has the tendency to blend well with pyrolysis oils as opposed to petroleum diesel [153].

The purpose of this work was to create a blend of bio-oil and biodiesel to avoid the downstream oil upgrading to enable its usage as a diesel engine fuel. This selection also fulfilled the direct quenching requirement for the Pyroformer process and it also fulfilled the need for a blending fuel for engine compared to water which may have needed separation and then further blending.

6.2 Experimental procedure

Intermediate pyrolysis of two different biomass fuels (pelletized miscanthus and Wood, 6mm) was performed using a 100 kg/h Pyroformer under the European Union funded project called Bioenergy Interreg NW. The process was patented (Patent number GB 0808739.7 and WO 2009/138757) by researchers based at European Bioenergy Research Institute (EBRI) of Aston University. This process was installed at Harper Adams University in Shropshire during the tests, UK under a project partnership agreement.

Each experiment involved at least 3 personnel including the author. Various duties were assigned to each operator while operating the plant. A detailed checklist of the equipment and its status was performed to ensure the availability and safety of each process item. A detailed content of this checklist is given in Appendix 2 (Harper Adams Pyroformer Daily Operations Checklist). The 3D lay out of the whole process is given in the attached 3D drawings in the Appendix 1.

For simplicity reasons and to keep the operational procedure concise, only the details of the Pyroformer related activities are mentioned here. Although the checklist and 3D drawings show an engine installed in the room next to

Pyroformer main hall. This engine was providing the electrical power to process only and was not part of these experiments. A gas flaring system (with Natural gas supporting flame) was installed outside the Pyroformer building to burn un-condensable gases from the Pyroformer process.

On the day of the experiment after going through the checklist as shown in Appendix 2, the Pyroformer control panel was made live by switching on the main power supply. Then a USB memory stick was inserted into the control panel which was used as an access control device. After this the ancillary units of the Pyroformer such as air compressor, building ventilation system, nitrogen purge system, biodiesel for the pyrolysis vapour quenching, copper grease lubrication system, carbon monoxide detectors and gas flaring system were made live as and when needed. Air compressor was delivering the compressed air to drive the pneumatic valves with an operational air pressure between 6-8 Bar.

The Pyroformer operation was controlled in three different modes and this was programmed in the Pyroformer control system. These three modes were labelled as "Start-up mode", Pyrolysis mode" and Shut down mode". Each of these modes have certain process items inter-linked and controlled to achieve a certain objective. These are further explained below.

The Pyroformer was started after logging in with a USB memory stick. Biomass pellets were weighed and put into the feeder hopper. Then the lubrication copper grease was started with an automated controller by means of a pneumatic piston pump. Then the temperature of the Pyroformer band heaters was set in increments of 100°C to ensure the steady heat distribution across the length of the Pyroformer reactor body. The total installed capacity of electrical band heaters was 70kW and this comprised of 8 band heaters as shown in Figures 29 and 30. Five of these heaters were installed on the main body of the reactor and other three were installed at the feeder inlet, vapour outlet and char outlet. After setting the temperatures, both Pyroformer screws were started to rotate by means of electrical motors of 1 hp each. The motor was linked to a gear drive to lower the rotations of the electric motor. The direction of the screws was interlinked with the start-up mode and both screws

were rotating to empty the reactor with the inner and outer screws turning anti-clockwise to carry material towards the char outlet. Once all the thermocouples (linked to each band heater) were reached at set temperature then the next incremental value was set. This was done to ensure uniform temperature distribution in order to minimise thermal shocks in the reactor body and uniform thermal expansion of steel. When the temperature reached 300°C, nitrogen gas was purged through the reactor to ensure no air was in the system during the pyrolysis mode. A small nitrogen purge was activated for 5 minutes during start-up mode to displace any volatile vapours out of the reactor. Biomass pellets feed was not started until "pyrolysis mode" was selected.

Once the set temperature of 400°C was achieved on all heaters, then the "Pyrolysis mode" was enabled with all the valves and motors parameters sequenced through automation. The gas flare was started with natural gas supporting flame. Then the feeder motor was started to convey the pelletized material by means of an auger to both feeder valves (in vertical section) and then into the Pyroformer. The screw motors of the Pyroformer in the "Pyrolysis mode" were turning in counter directions to each other. The inner screw was turning in the clockwise direction at 6 rpm to convey pelletized biomass material forward from feed inlet and the outer screw in the opposite direction at 3 rpm to recycle the char. The biodiesel quench was started at this point and the biodiesel flow rate was measured on liquid flow meters. Biodiesel was injected at the desired flowrate in 1st stage quench point (K0110) and second stage quench point (K0115) as shown in Figures 29 and 31.

After starting in "Pyrolysis mode" it took around 45 minutes to reach steady state. Steady state in this case was achieved when both screws of the Pyroformer were filled with feedstock and char particles start to drop into the char container. Two feeding rates were used for these tests such as 61 kg/h for wood pellets and 70 kg/h for miscanthus as shown in Table 26. The variation in the feeding rate was done to achieve the gradual increase in feed rate and maximum design throughput in stages. The vapours released during the pyrolysis are directly quenched with biodiesel. Although there was an electrostatic precipitator unit number 14 was installed (as shown in the Figure

29) but it was not used during these tests due to technical problems and short circuiting of the unit. Also, the gas calorimeter number 23 as shown in Figure 29 was not used in the tests.

Any non-condensable gases after the quenching stages were then passed on to the gas flaring system which was installed outside the building. The gases were burnt with a noticeable bright orange flame. The quenched liquids were collected in three separate tanks (number 17 in Figure 29), one tank under each quench stage and then third one at the bottom of Electrostatic precipitator stage which was acting as a cooling unit only. The quench liquids were then blended together into one tank. The mixtures at this point included quenching biodiesel with 80-88 parts and remaining 18-20 parts of pyrolysis bio-oil. The char fraction of the biomass was collected in the char container and the contents were weighed on the next day, after they were naturally cooled sufficiently. A mass balance of the materials was then performed.

It is important to highlight here that it was not possible to measure the total gas flow or gas volume of non-condensable gases as the gases were not free from aerosols and a suitable gas flow meter was not available at the time. Hence the quantity of un-condensable gases was estimated by difference.

Aston University

Illustration removed for copyright restrictions

Figure 31 - P&ID of 100 kg/h Pyroformer (as taken from Pyroformer HazOp study of EBRI Pyroformer archive)

Aston University

Illustration removed for copyright restrictions

Figure 32 - 100 kg/h Pyroformer installation at Harper Adams University College (Photo by Louise Ciaravella)

6.3 Results and discussion

After conducting the experiments, the mass balance of the biomass feed in the Pyroformer was performed. The methodology used for mass balance is given below.

6.3.1 Mass balance

Mass balance was derived based on the biomass consumed in the experiments. Mass balance is represented by equation below.

$$M_{liquid} + M_{gas} + M_{char} - M_{feedstock} = 0$$

Where

M_{liquid} *is the mass of bio − oil*

M_{gas} *is the mass of non − condensable pyrolysis gases*

M_{char} *is the mass of char*

$M_{feedstock}$ *is the mass of feedstock pellets*

The gas yield or mass of non-condensable gas was calculated as below

$$M_{liquid} + M_{char} - M_{feedstock} = M_{gas}$$

Table 29- Mass yields (wt. %) of pyrolysis products from different biomass feedstocks

Feedstock	**Quantity** (kg)	**Feed rate** (kg/h)	**Bio-oil** wt. %	**Biochar** wt. %	**gas*** wt. %
Wood pellets	117	61.0	20.77	32.0	47.23
Miscanthus pellets	105	70.0	30.90	31.62	37.48

*Gas yield was calculated by difference + also considering the uncondensed bio-oil lost from the feeding section as gas

As it is seen in Table 29 a significant quantity of biomass feedstock was consumed in each experiment and a healthy feeding throughput was achieved with wood pellets at 61 kg/h and Miscanthus pellets 70 kg/h. There is a significant difference of 10% more syngas produced for wood pellets compared to Miscanthus derived material. Also, there was significantly less bio-oil produced (20.77 wt %) compared to (30.90 wt %) from miscanthus pellets. Biochar wt % is somewhat similar for both materials.

6.3.2 Bio-oil and biodiesel blend sampling and characterisation

The liquid characterisation was done by Al-control Labs based at Conwy in Wales. The samples were prepared from the blended liquids from all 3 tanks of the Pyroformer and were sent off for analysis within a week after the experiments. Due to budgetary constraints, the liquids were characterised only for important fuel properties. It is important to mention that the blended liquids contained 19.75 wt. % bio-oil from wood pellets and 11.28 wt. % bio-oil from Miscanthus pellets. There was no water separation in the blend. The samples were collected randomly from the 1000 litres plastic IBC tank from the approximate middle of tank with the height adjustable suction port on the pump. The liquid was then put into plastic clear bottles in the required quantity as was specified by the external Lab. The samples were clearly marked for correct identification.

Table 30- Elemental analysis and Characterisation of Intermediate Pyrolysis oil & ASTM standard for Biodiesel

Bio-oil	**Unit**	**Wood pellets Bio-oil/biodiesel blend**	**Miscanthus Bio-oil/biodiesel blend**	**Biodiesel[b]**
Compositional analysis				
Carbon	wt.%	76.34	74.34	77.04
Hydrogen	wt.%	11.13	11.59	11.73
Oxygen[a]	wt.%	12.33	13.87	11.21
Nitrogen	wt.%	<0.10	<0.10	<0.10
Sulphur	wt.%	<0.10	<0.10	<0.10
Higher Heating Value (HHV)	MJ/kg	38.50	38.16	40.11
Lower Heating Value (LHV)	MJ/kg	36.14	37.01	37.47
Ash content	wt.%	<0.01	0.70	<0.01
Density @20°C	kg/m^3	886	885	820
Total acid number	mg KOH/g	17.06	5.33	0.62
Kinematic Viscosity @40°C	cSt	14.0	21.0	6.0
Water Content	wt.%	0.52	0.36	0.12

[a]*Calculated by difference*
[b]*Biodiesel (made from waste cooking oil) obtained from a local supplier*

Fuel characterisation for solid contamination was measured according to IP375, viscosity according to IP71 modified, Water content according ASTM D4928, Total Acid number (TAN) IP177, elemental analysis BS1016;1977, HHV according to BS1016:1992.

Considerably greater char and gas yields are apparent due to intra and extra particle reactions. The lower liquid yield of 20.77 wt% indicates that due to higher lignin content in wood pellets may have contributed to more char formation thus more catalytic activity to produce simpler hydrocarbons in gas rather than liquids as was reported by Yang H. et al [85]. The lower liquid yield from wood pellets could also be attributed to a greater percentage of condensable vapours lost through the feeding section.

There was no water phase separation from the blended liquid which shows the water may well be miscible in the whole blend. The fuel properties of both liquid blends' (presented in Table 30) were very similar to that of biodiesel with considerable difference in the density of biodiesel to be 820 kg/m^3 to that of wood and miscanthus derived liquid blend around 885 and 886 kg/m^3. From Table 30 it was strongly evident that both liquids from wood and miscanthus possessed higher viscosities of 14 and 21 cSt whereas it was 6 cSt for biodiesel. Hence, it's an indication that liquid fuel flow ability will be an issue and may lead to premature failure of the engine's fuel injection system due to increased stress during pumping during use. The water content for both liquids are also higher by 3 times for miscanthus and nearly 4 times for wood derived blend. This was an indication that initial feedstock moisture content and water formation during pyrolysis is present in the ultimate blend and will lead to high oxygen content in the fuel as well as leading to somewhat lower calorific compared to biodiesel. The effect of the water content was evident in the lower heating values for both liquids. An important fuel property, Total Acid Number (TAN) is the key determinant of the corrosion properties of the fuel. In this case TAN value is nearly 8 times greater than biodiesel for miscanthus derived bio-oil/biodiesel blend and nearly 27 times higher for wood derived bio-oil/biodiesel blend. The results suggest that wood derived blend was highly acidic and miscanthus derived blend had higher viscosity. The elemental analysis shows somewhat similar carbon, hydrogen and nitrogen contents but the oxygen content was significantly higher (13.87 wt %) for miscanthus derived blend compared to 12.33 and 11.21 wt. % for wood derived

blend and biodiesel. In theory the higher oxygen content of miscanthus should lead to higher TAN compared to water but this was not evident.

6.4 Biochar emissions reductions

Carbon dioxide (CO_2) is a potent greenhouse gas which is emitted into atmosphere due to natural and anthropogenic activities; it absorbs the sunlight reflected from earth's surface into atmosphere and leads to global warming. The anthropogenic greenhouse gas effect [154] can be minimised by reducing the carbon emissions into the atmosphere. CO_2 is normally absorbed by plants during photosynthesis from the atmosphere. During the photosynthesis, the CO_2, sunlight and water absorbed by plants lead to the formation and accumulation of organic matter in the plant [5, 28]. This accumulated CO_2 in the form of organic matter (biomass) can be locked into soil through biochar application thus making the whole process carbon negative [5, 155].

Greenhouse gas emissions associated with biomass decay can be reduced in two ways. Firstly, by converting the biomass into energy thus displacing the fossil fuels for energy production. Secondly, by sequestering carbon contained in the biochar made by pyrolysis into land for soil remediation. Gaunt and Lehmann [155] conducted a Life Cycle Assessment (LCA) of biochar which showed a carbon savings of 2 to 5 times greater when biochar is applied in agricultural land. Figure 33 highlights only the carbon cycle in biomass and soil and does not show the lifecycle of the methane and other greenhouse gases.

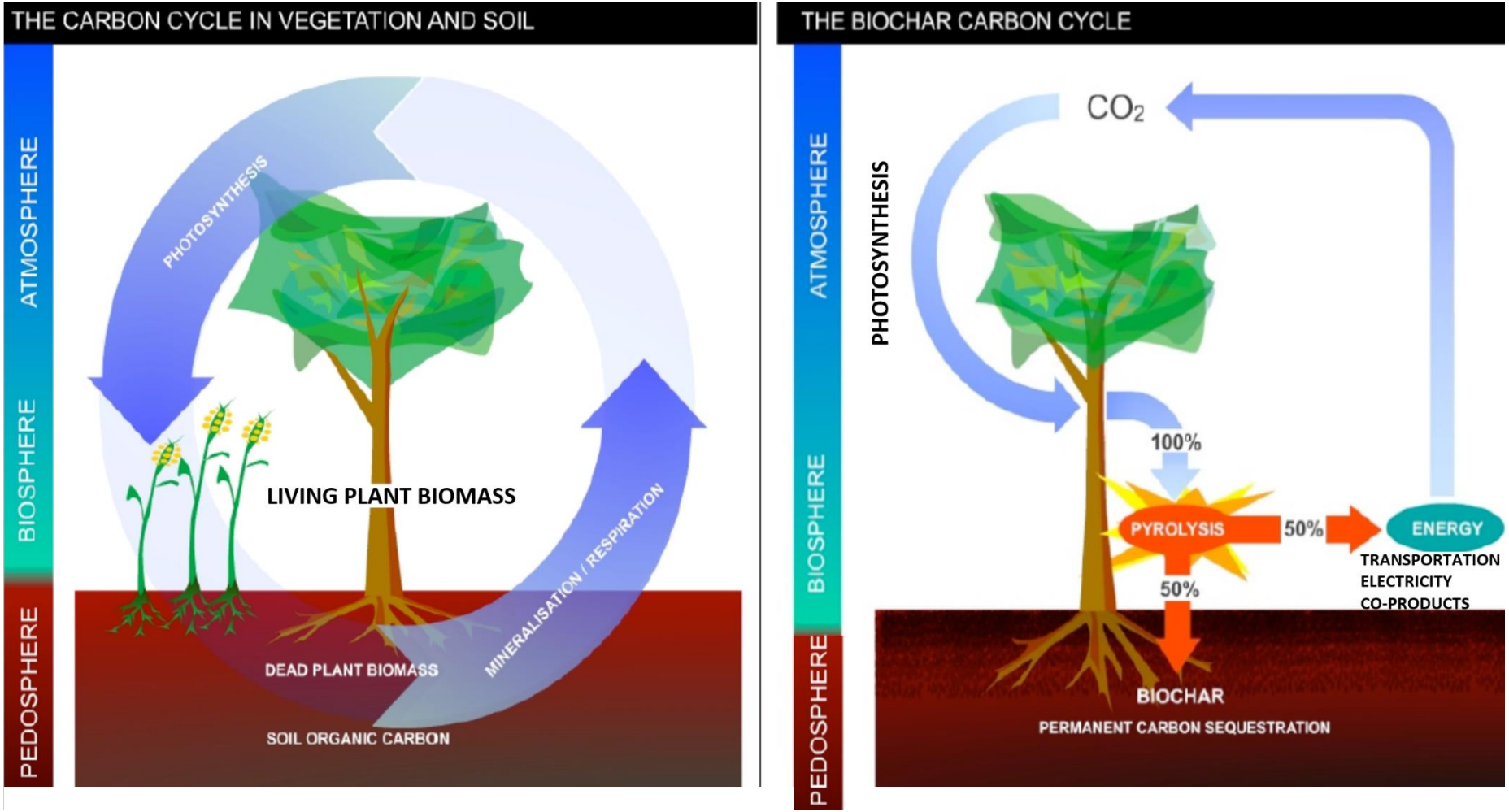

Figure 33 - Simple carbon cycle on left and biochar from pyrolysis (with energy recovery) based carbon cycle on right - adapted from [5]

Shackley et.al. [156] highlighted the potential benefits of biochar application in soil. Biochar balances the acidity of soil to neutral, enhances the cat-ion exchange capacity (CEC) and provides beneficial growth conditions for microbes within the pores of biochar to name a few.

The properties and yield of biochar depend on feedstock type and pyrolysis temperature (400, 500, 600, 700°C). For example, soil cation exchange capacity of manure-based biochars is higher than that of wood (Eucalyptus) biochar [157]. Char produced at low-temperature leads to high char yields but low Carbon content. In contrast, high-temperature pyrolysis produces less char yield but high C content, large surface area, high porosity, high adsorption characteristics and recalcitrant chemical character in woody biochars [158]. Biochar derived from low-temperature pyrolysis is characterized by a high content of volatile matter that contains easily decomposable substrates, which can support plant growth [159, 160]. The addition of woodchip based biochar results into highly saturated hydraulic conductivities compared to manure-based biochar [109]. Similarly, poultry-litter based biochar presents higher specific surface area and porosity than wheat-straw based biochar despite their preparation at same temperature (400°C).

Feedstock type and pyrolysis temperature can influence molecular structure and pores size distributions in biochars, and thus it affects biochar sorption characteristics [161, 162]. Sohi et al [163] reported that different feedstocks resulted in different magnitudes of surface areas, pores and functional groups in biochars, and all these variables affect sorption characteristics of biochars. Sun et al [164] reported that poultry-litter biochar had a larger specific surface area and porosity than wheat-straw biochar, despite the fact that both biochars were produced under the same temperature (400°C). Lei and Zhang [109] have reported the high specific surface area and C/N ratio for the biochars obtained from woodchips compared to that of dairy manure [109]. High pH of poultry manure derived bio-oil has been reported by Novak et al [165] due to the presence of the calcium (Ca) and magnesium (Mg) in the feedstocks, high concentrations of Ca and Mg are desirable for biochar in soil applications.

In general, high pyrolysis temperatures lead to greater specific surface areas and aromaticity of biochars [161]. Chun et al [166] reported that charcoal made from wheat straw residue at 500–700°C is well carbonized and its specific

surface area is relatively high (300 m^2 g^{-1}), whereas chars formed at 300–400°C are partially carbonized and have a lower specific surface area (200 m^2 g^{-1}). This indicates higher pyrolysis temperatures lead to higher specific surface areas of biochar which increase the adsorption of micronutrients and thus prolongs their availability for plant growth functions.

The pH of biochar significantly increases with higher pyrolysis temperatures probably as a consequence of the relative concentration of non-pyrolysed inorganic elements, already present in the original feedstocks [165]. Wu et al and Lehmann et al [72, 167] also reported that the biochars (from rice straw and wood) they produced were alkaline in pH range (8.2 and 10.4) common for pyrolysis produced biochars.

Electrical conductivity (EC) is a measure of soluble salts or ions in a sample [168]. Cantrell et al [169] reported that the biochars produced from swine separated-solids; paved-feedlot manure; dairy manure; poultry litter; and turkey litter exhibited similar EC values. However, the EC values increased significantly with the higher pyrolysis temperature. The increase in EC of biochar with the increase in pyrolysis temperature is sown likely to be due to the loss of volatile materials at high temperatures, which promoted the relative concentrations of salts in the ash fraction [169].

The ash contents of different biochars from wheat straw, corn straw and peanut shell were measured by Cao et al [170] to be between 11 to 18 wt%, which are lower than the original ash content of the feedstock (wheat-straw 28 wt%, corn-straw 31 wt% and peanut-shell 27 wt%). Apparently, ash content increased with a rise in temperature due to increased concentrations of minerals and organic combustion residues. Similarly, the *CEC* of different biochars significantly differ due to the type of feedstock used and pyrolysis temperature. Biochars produced from all feedstocks have shown an increasing trend of CEC with the increase in pyrolysis temperature. Cao et al [170] also discovered that all biochars pyrolysed at 400°C and 500°C had higher CEC than that at 600°C and 700°C. Whereas in other findings by Yuan et al [171], the CEC of biochar prepared from corn at 500°C was higher than that at 300°C and 700°C; and the CEC of biochar prepared from peanut at 700°C was higher than that at 300°C and 500°C.

Specific surface area, pore volume and pore size of the biochars obtained from different feedstocks were significantly affected by biochar feedstock and pyrolysis temperature [172]. This is likely due to the removal of H- and O-carrying functional groups, including aliphatic alkyl-CH_2, ester C_5O, aromatic -CO and phenolic - OH groups, in biochars produced at 600°C, which has greatly enlarged their surface areas [173]. The porosity and surface area represent the most critical physical properties of biochar for the improvement of soil properties such as soil nutrient adsorption capacity and water retention ability [174].

Biochar is widely recognized as an efficient tool for carbon sequestration and soil fertility. The understanding of its chemical and physical properties are strongly related to the type of the initial material used, pyrolysis conditions and process type [5, 154].

Its use as a soil additive has been proposed to simultaneously mitigate anthropogenic climate change and improving agricultural soil fertility. The feedstock selection for producing biochar seemingly plays an important role [175], as does soil fauna and microbiology. Due to its high chemical stability, high carbon content and its potential to reside in soil over decades to millennia, biochar applications have the potential to become a long-term carbon sink [176-180]. Lehmann and Rondon [181] reviewed 24 studies with biochar additions to soil and found 20 to 220 wt% improvement in productivity at application rates of 0.4 to 8 tons carbon per hectare. Steiner et al [182] reported a doubling of maize grain yield using a combination of NPK fertilizer with charcoal compared to use of NPK fertilizer alone. Biochar is also reported to improve nutrient availability [182, 183]. These observations could be attributed to reduced leaching of applied nutrients as well as reduced percolation of water [183-185] and increased fertilizer use efficiency [186].

Biochar additions to sandy acidic soils significantly reduced acidity and improved soil fertility [169]. Although, the BC itself has a low nitrogen content [187], thus a wide C/N ratio does not immobilize nitrogen [188] and may be an important amendment for nitrogen dynamics with the ability to improve the efficiency of mineral nitrogen fertilizer [185]. Biochar helps improve soil health, microbial activity and nutrient availability through a variety of mechanisms [189-192]. It has the potential to alter the microbial biomass and microbial composition

[185, 190, 193, 194]. Soils amended with BC show increased mycorrhizal colonization of plants [192], and increased biological nitrogen fixation [195] . An increase in soil respiratory activity has also been reported [196]. In high organic matter soil, however, biochar was found to reduce CO_2 emissions [196]. Charcoal may contribute to the adsorption of metals [170, 197]. According to [198] charcoal is several orders of magnitude more sorptive than soil organic matter and can thus limit the mobility, toxicity and transport of xenobiotics in contaminated soils. Buss et al [199] reported reduced Cu toxicity in soils amended with 4% BC. The BC helps maintain structural stability of soil through increased porosity, greater cation exchange capacity (CEC) and better micro-/macro-aggregation [183, 188, 197]. Besides, biochar improves soil water permeability and soil water holding capacity [165, 200, 201]. Laird [201] reported significantly increased CEC and extractable plant nutrients in biochar amended soils. [184] Lehmann et al [184] found lower cumulative leaching of mineral nitrogen (24 wt %), potassium (25 wt%), calcium (24 wt%) and magnesium (79 wt%) in unfertilized Amazonian dark earth compared to normal soil in that area; leaching from fertilized samples of the former exceeded that from the latter. This may be attributed to the strong adsorption affinity of BC for ammonium [202], nitrate [203], phosphate [4] and other ions [204]. It has also been suggested that biochar may have the potential to reduce leaching of pollutants from agricultural soils [154].

The above account based on literature review suggests that biochar has the potential for i) mitigation of GHG emissions, ii) C sequestration and iii) improving soil productivity. However, considerable uncertainties remain about its applicability to different soils and crops. The origin of feedstock and pyrolysis conditions are of significant importance. Likewise, BC application may be more beneficial to less fertile and sandy/sandy-clay soils of arid and semi-arid regions [205]. While a beneficial effect of soil-applied biochar on crop yields has been demonstrated for a number of soil/crop combinations, its utility in a wide range of soil/crop types (particularly in arid/semiarid and temperate zones) awaits demonstration. Of interest will also be to introduce the concept of biochar production and use on poor soils (a good proportion of which degraded or marginal in terms of fertility and productivity) to improve soil productivity. The best route

of biomass utilisation seems to be combined with bioenergy production and biochar application for soil amendment for truly sustainable reasons [154 & 155].

The literature review [185, 190, 193, 194] strongly suggests that there are potential benefits when biochar is applied in the soil. Carbon capture and sequestration via pyrolysis is advantageous because carbon evolved into vapours is retained in bio-oil and pyrolysis gas and used as fuel thus offsetting the use of fossil fuels. During pyrolysis, solid fraction containing the carbon is retained in the char which can be easily used for sequestration in the land since soil is the biggest carbon sink. Before biochar is applied in the soil, it must be analysed for its benefits as well as for potential contaminants leading to high toxicity in the form of dioxins, furans, polycyclic aromatic hydrocarbons (PAH) and polychlorinated biphenyls (PCBs). Regarding the potential contaminants in biochar, Shackley et.al [206] reported that "biochar could potentially contain two types of contaminants: a) those present in the feedstock itself (e.g. heavy metals, dioxins, polycyclic aromatic hydrocarbons (PAHs), etc.) and b) those produced during pyrolysis (e.g. PAH). Careful selection of feedstock is necessary to avoid or minimise the first category of contaminants, though some could be separated and removed during biochar production. The formation of PAH can be minimised by appropriate selection of operating conditions, specifically temperature range, and biochar with negligible PAH content should be achievable. Consistent analytical methods for quantifying contaminants such as PAH in the inherently stable matrix presented by pyrolysis char are yet to be defined. Better identification of specific PAHs is required, and targeted according to their toxicity".

There are various voluntary guideline biochar standards established for their application into soil. These include European Biochar Certificate [207] by European Biochar Foundation, International Biochar Initiative's (IBI) Biochar Standards v2.1 [208] and Biochar Quality Mandate (BQM) from British Biochar Foundation(BBF) [209]. These standards set guidelines for biochar manufacture, usage and contamination levels. These standards are derived from various other standards for synthetic and organic fertilisers, pesticides, digestate and other growing media (clay pellets, coconut coir etc) for soil and soilless applications. Hence, they provide a solid guideline to ensure biochar application returns the perceived benefits.

Table 31 contains trace metal analysis of wood and miscanthus derived biochar from pyrolysis tests. Also, a publication based on this work is attached in Appendix 6. It was evident that the trace metal content in both chars is well within the set guidelines from International Biochar Initiative (IBI) and British Biochar Foundation (BBF). Hence it is possible to use these wood and miscanthus derived chars in agriculture and horticulture.

There are set guidelines from UK Environment agency for applying the biochar with a maximum of 1 tonne of biochar per hectare from uncontaminated biomass. These application guidelines are set-out in a regulatory position statement by the Scottish Environment Protection Agency [210] and similar guidelines are set by UK environment Agency. Carbon savings of 50% compared to normal carbon cycle (photosynthesis and then decay) of biomass and soil can be achieved by making biochar and bioenergy (bio-oil and gas). This is done by sequestering 50% of the carbon in the form of biochar in soil from biomass and remaining 50% converted into energy via bio-oil and pyrolysis gas thus offsetting fossil fuel usage [5].

Table 31 – Comparison of wood and miscanthus derived biochar (from 100 kg/h Pyroformer test in Table 30) showing toxic metal contents comparison with IBI and BBF biochar standards

Metals	**Wood biochar (ppm)**	**Miscanthus biochar (ppm)**	**IBI Biochar Standard** [208] **(ppm)**	**BBF BQM Biochar Standard** [209] **(ppm)**
Arsenic	<1	<1	12- 100	10-100
Cadmium	<1	<1	1.4- 39	3-39
Chromium	1	1	64-1200	15-100
Cobalt	<1	<1	40-150	n/a
Copper	184	4	40-1500	40-1500
Lead	3	1	70-500	60-500
Mercury	<1	<1	1-17	1-17
Molybdenum	1	<1	5-20	10-75
Nickel	41	2	47-600	10-600
Zinc	62	317	200-7000	150-2800

In a study by Gaunt and Lehmann [155] which was based on data from Accardi Dey et al [211], they estimated the benefits associated with biochar. They found that making biochar as well producing energy from slow pyrolysis, 2 to 5 times more avoided carbon emissions savings can be made compared to only bioenergy production for off-setting the fossil fuel usage. This means that by using the Pyroformer for purpose grown energy crops and/or for crop waste residues for biochar and bioenergy production, maximum CO_2 savings are achievable. They reported that 41-64% of these avoided emissions resulted from carbon sequestered in the agricultural land where as the remaining percentage is associated to off-setting fossil fuel for energy use and fertilizer savings. These additional (2 to 5 times) CO_2 emissions savings are possible because carbon is sequestered into agricultural land in the form of biochar as opposed to slash and burn system where all the carbon is burnt to make bioenergy; for example, in biomass combustion systems where no element of carbon sequestration is involved.

The emissions reductions from woody biomass are shown in Table 32. It can be seen that by displacing the previously decaying wood waste by converting it into biochar and bioenergy and then applying the biochar in acidic or alkaline agricultural land, maximum carbon emissions savings can be made from woody biomass. These carbon emission reductions range between 1854-1925 kg CO_2 Mg^{-1} C^{-1} for acidic soil and 2356-2427 kg CO_2 Mg^{-1} C^{-1} alkaline soils. It can also be seen that some carbon emissions reductions are still possible even if the existing energy production from wood waste was also to include the biochar production and its application in the agricultural land. In this case carbon emission reductions range between 249-550 kg CO_2 Mg^{-1} C^{-1} for acidic soil and 751-48 kg CO_2 Mg^{-1} C^{-1} for alkaline soil application of biochar while producing the same amount of energy.

Table 32- Emissions reductions expressed as kg CO_2 Mg^{-1} C^{-1} contained in woody biomass for systems changes –adapted from [154 & 155].

Systems	**Systems change**		**Fossil fuel substitution**			
	Emissions	**Emissions reductions**	**Natural gas**	**Coal**	**Emissions reductions**	**Total emissions reductions**
Char systems standalone						
Slash-and-burn	3300[a]				0	
Slash-and-char	1705[b]	1595	0	0	0	1595
Charcoal production system	1705[b]		0	0	0	
Charcoal production system with application of char to soil	1705[b]	0	0	0	0	
Energy production system with pyrolysis to produce energy and biochar						
Wood waste currently applied to soil/allowed to decay	3666[c]		0	0		
Wastes to produce energy and biochar applied to acid soil	1913[d]	1753	101[c]	172[f]	101-172	1854-1925
Wastes to produce energy and biochar applied to alkaline soil	1411[g]	2255	101[c]	172[f]	101-172	2356-2427
Wood waste burnt for disposal	3300[a]			0		
Wastes to produce energy and biochar applied to acid soil	1913[d]	1387	101[c]	172[f]	101-172	1488-1559
Wastes to produce energy and biochar applied to alkaline soil	1411[g]	1889	101[c]	172f	101-172	1990-2061
Wood waste burnt for energy	3300		1239[c, h]	2109[f, h]		
Wastes to produce energy and biochar applied to acid soil	1913[d]	1387	101[c]	172[f]	-113-1937	249-550
Wastes to produce energy and biochar applied to alkaline soil	1411[g]	1889	101[c]	172[f]	-1138-1937	751-48

[a]Assumes 90% C is released as CO_2 (IPCC 1996).
[b]Assumes 46.5% C is released as CO_2 (Lehmann et al 2002).
[c]Assumes 100% released as CO_2 in a 10-year period (IPCC 1996).
[d]Assumes 52% released as CO_2 (Day et al 2005).
[e]Assumes that pyrolysis system produces 1.8 GJMg C^{-1} (Day et al 2005). Burning natural gas produces 57 kgCO_2 GJ^{-1} (http://www.videncenter.dk/gule%20halm%20haefte/Gul Engelsk/halm-UK02.pdf).
[f]Assumes that pyrolysis system produces 1.8 GJMg C^{-1} (Day et al 2005). Burning coal produces 97 kgCO_2 GJ^{-1} (http://www.videncenter.dk/gule%20halm%20haefte/Gul Engelsk/halm-UK02.pdf).
[g]Assumes that 38% released as CO_2 when bio-char is used to scrub CO_2 wastes gas stream (Day et al 2005).
[h]Assumes that 1 Mg C in wood produces 22 GJ energy (calculated from http://www.thecarbontrust.co.uk/carbontrust/low carbon tech/ dlct2 1 6 3.html)

The above account shows that significant carbon emission reductions are possible if using a pyrolysis system. This is because only if a system change in wood waste is introduced to avoid the decaying of wood waste to convert into energy and biochar production, this will at the same time substitute the usage of fossil fuels such as natural gas or coal for energy production.

The carbon sequestration is a recognised Clean Development Mechanism (CDM) under Kyoto protocol was recognised by United Nations Framework Convention on Climate Change (NFCCC) in 1997 but is only limited to carbon sequestration in newly afforested land. Thus the methodology used by Gaunt and Lehmann [155] can be used for afforested land for biochar application for carbon sequestration in agricultural soils. Under the Clean Development Mechanism (CDM), carbon sequestration was shown to be limited only to afforested land due to limited data available for benefits of carbon sequestration in agricultural soils. It also includes the benefits of biochar application such as carbon sequestration in agricultural land, reduction in fertiliser use due to biochar application and off-setting the fossil fuels by energy production through pyrolysis.

A calculation of carbon emission reductions of wood waste by using the 100 kg/h Pyroformer coupled to a BFB gasifier were made based on same methodology as used by Gaunt and Lehmann [155] and Dey et al [211]. The scope and limitations of their methodology are shown in foot notes of Table 32 and in the original publications. For simplicity reasons some assumptions are made to apply this methodology for Pyroformer and BFB gasifier (Pyrogasification) application which include the following:

- It is assumed that naturally decaying wood waste is used as the feedstock for the Pyrogasification process
- Carbon emissions' associated with the transportation, size reduction or pelletisation are not considered in this calculation. Also, methane and nitrogen oxide emissions are not taken into account for this study.
- Only carbon emissions' reduction by systems' change and fossil fuel substitution for energy production and carbon sequestration for biochar application in acidic or alkaline soils is considered in this study.
- Feedstock characterisation data for wood pellets is taken from Table 28.

- Elemental analysis of wood pellets shows a carbon content of 46.2 wt %, which is used for calculating the carbon emissions reductions by using a Pyrogasifier system. This combination is proposed as pyrolysis bio-oil is complex to use in its pure form and fuel gas from pyrogasification is assumed to be only directly useable product in a gas engine
- It is assumed that the gasifier is not consuming any other wood pellets and only dolomite is used as the bed material and the energy contained in the syngas is used to substitute natural gas or coal
- Any other associated issues are not taken into consideration
- It is assumed that the Pyroformer is fed with waste wood pellets by diverting decaying waste wood from fallen trees at a 100 kg/h for 8000 hours per annum operation.

Thus

By taking carbon content of wood pellets of 46.2 wt% from elemental analysis from Table 28

Total carbon consumed in the Pyrogasification process per hour = 46.2 /100x 100 kg/h

= 46.20 kg/h C consumed in the process;

Carbon (C) consumed for bioenergy and biochar per tonne of wood pellets

= 46.2 kg/h x 10 h of Pyroformer at 100kg/h

= 462 kg C consumed for one ton of wood pellets in the Pyroformer

Which is

= 369.6 ton C consumed per year of Pyrogasification of wood pellet feedstock

Also, as 1 Mg (mega gram) = 1 ton

By using Gaunt and Lehmann [155] and Dey et al [211] methodologies, it means,

The emissions reductions for biochar application in <u>acidic soil</u> and offsetting <u>natural gas</u> for energy production from Pyrogasification

= 1.854 ton CO_2/ton C x 369.6 ton C/annum = **685.24 ton CO_2 emission reduction per annum,** which is 685.24 ton of CO_2 emissions are saved from the total carbon used from the feedstock per year

The emissions reductions for biochar application in acidic soil and offsetting coal for energy production from Pyrogasification

= 1.925 ton CO_2 Mg^{-1} C^{-1} x 369.6 ton C /annum = **711.48 ton CO_2 per annum**

The emissions reductions for biochar application in alkaline soil and offsetting natural gas for energy production from Pyrogasification

= 2.356 ton CO_2 Mg^{-1} C^{-1} x 369.6 ton C /annum = **870.78 ton CO_2 per annum**

The emissions reductions for biochar application in alkaline soil and offsetting coal for energy production from Pyrogasification

And for substituting energy production from coal, it is

= 2.427 ton CO_2 Mg^{-1} C^{-1} x 369.6 ton C /annum = **897.02 ton CO_2 per annum**

So, the total carbon emissions reductions from pyrogasification of waste wood displaced from natural decay are given in Table 33.

Table 33- Emissions reductions expressed as tonnes of CO_2 per annum contained in naturally decaying waste wood for systems changes and fossil fuel substitution via pyrogasification

	Biochar in acidic soil	**Biochar in alkaline soil**
Substitution of natural gas for energy production	685.24	711.48
Substitution of coal for energy production	870.78	897.02

The above emission reductions in CO_2 are shown only for using waste wood which is currently left to decay and by using this wood waste into bioenergy and biochar, the Pyrogasification process of 100 kg/h in 8000 hours of plant operation will save. However, this is not the case with wood waste as sometime the wood waste is burnt for disposal rather than left to decay naturally or it is burnt for energy recovery in which case the CO_2 emissions reductions will be significantly low as there is no biochar application. The analogy used in the Tables 32 and 33 can be expanded for other waste wood usage options such as whether the waste wood is going to displaced from current combustion only processes for disposal or for waste wood for energy production. The maximum CO_2 emission reductions are only possible if naturally decaying waste wood is displaced from decaying and then used for energy production to substitute fossil fuel usage and the biochar produced from Pyrogasification process is then sequestered into land. The Table 33 represents the values for such an application where biochar is used for carbon sequestration into acidic or alkaline soils.

The reduction in carbon emissions is maximum with biochar application in alkaline soil and by substituting coal for energy production by using pyrogasification technique. However, as carbon sequestration by biochar into agricultural land is not yet recognised under CDM, still a lot needs to be done to make this route attractive. Because the potential revenue generation by trading the carbon reduction certificates based on biochar application under CDM is not possible under current scenario. As developing and least developed countries may have more potential project implementation sites, they themselves may not be able to fund such projects except otherwise if they can access the revenue generated by trading the emissions certificates with developed nations [154].

6.5 Summary of the Chapter

The hot pyroformer tests are a significant achievement in scaling up the Pyroformer from a small bench scale process 20kg/h) to a Pilot scale of 100 kg/h. A novel way to blend bio-oil with biodiesel was presented in these tests with elemental fuel properties mostly representing the biodiesel qualities with the exception of total acid number, water content, density and viscosity. The results also show that by doing in-situ blending of pyrolysis vapours with biodiesel the

water content in bio-oil also becomes miscible with biodiesel and does not readily separate. This leads to increased oil yields. Since, bio-oil is the least expensive liquid fuel obtainable from lignocellulosic materials compared to biodiesel from plant oils and by doing in-situ blending of bio-oil and biodiesel it is possible to use it without the major upgrade. In this way an engine can be operated with the lower cost bio-oil/biodiesel blend rather than biodiesel alone. Solid content (ash & carbon) in the blended oil shows an increase as compared to biodiesel only and can easily be overcome by adding a simple filtration step from decanting tank after in-situ blending. Density and viscosity are somewhat interlinked and an improvement on this can be made by adding a minor preheating process to slightly increase the temperature of fuel to overcome higher viscosity issues in fuel injection system. This leaves the total acid number which is an inherent feature of most pyrolysis oils and need further investigation to manage it. One possibility is to use fractional condensation to separate the water content while the vapours are hot. This can be done so the hot pyrolysis vapours are condensed above water condensing temperature and only a liquid fuel free from water can be produced. This can eliminate the moisture inherently present in the biomass but any oxygen present with organic molecules may still give rise to increase in total acid number. A strong possibility for this oxygen is to remove the water content in the bio-oil through fractional condensation followed by catalytic cracking by char to react with high concentration hydrogen syngas to form water vapour and carbon dioxide leaving behind better quality liquids with less oxygen content. Consequently, this will also lead to better calorific value of blended bio-oil compared to raw bio-oil. More importantly, the characterisation and potential application of the biochar derived from the pyrolysis process was discussed in much greater detail. The comparison of biochar toxic metal content produced from wood and miscanthus feedstocks with IBI and BBF biochars standards showed that these biochars were beneficial and can be safely applied to land for soil remediation and for carbon sequestration. This shows that the biochar potential for carbon sequestration can lead to a CO_2 negative system as not all the carbon is released into atmosphere after the plants has absorbed it through photosynthesis during the growth of biomass. An emissions reductions calculation based on displacing the woody biomass from natural decay for biochar and bioenergy production has been performed. The results suggest that if the decaying biomass is to be utilised in a pyrogasification system, then a significant reduction in CO_2 emission can be

achieved. The emissions reductions are possible by introducing a system change for currently naturally decaying woody biomass through pyrogasification and by substituting the energy production from fossil fuels and using biochar in land application. Carbon emissions reductions of 685.24 tons of CO_2 per annum from a 100 kg/h system for biochar application in acidic soil; by substituting the natural gas, 711.48 tons of CO_2 per annum for biochar application in alkaline soil; substituting natural gas for energy generation, 870.78 tons of CO_2 per annum for biochar in acidic soil and by substituting natural gas for energy production and 897.02 tons of CO_2 per annum for biochar in alkaline soil and by substituting coal for energy production are achieved by using pyrogasification technique. Currently, pyrogasification is the only possible route which can provide the biochar and a fuel gas which can be directly used energy purposes without further modifications as opposed to complex bio-oil from pyrolysis only.

Chapter 7– Pyroformer engineering design review of critical components

In this chapter an engineering design review of the Pyroformer is presented from the operational experience of the 20 and 100 kg/h systems as described in Chapters 4, 5 and 6. For the success of any pyrolysis process, it is fundamentally important that all units of the process perform as intended without any issues. If any unit malfunctions, then the whole process fails and serious consequences can follow. This engineering design review of critical components was based on 6 years of operational experience gained during the installation, commissioning and operational stages of all three Pyroformer systems as explained before. The key issues associated with the Pyroformer were feeding valve failures, seizing of screws due to inappropriate lubrication, feedstock blockages, lack of char storage in char container leading to shorter test runs and excessive biodiesel demand (more than 80 wt%) for quenching of gases from the 100kg/h Pyroformer, thus compromising the economics of the process.

For a redesign of the critical components, a detailed 5-step process was used as explained by Khandani [2] shown in Figure 34. In the first step, the actual problem with the system or component is defined which includes what is expected of the product and any special features defining the demand. For example, what size of the valve was needed and what type of opening and closing function (gate type, butterfly etc.) of the valve was required. In the second step, the relevant information about the product is gathered which includes functional specifications such as whether the valve needed electric or pneumatic actuation, single or double acting, material of construction etc. In the third step, multiple alternative solutions are analysed for their suitability for the application which can fulfil the basic requirements. In 4th step, the final design solution is agreed based on detailed analysis of the multiple solutions as identified earlier. The selection criteria for analysis involved costs, safety aspects and material compatibility as well as ease of installation. In the final step, the final design solution is tested for its intended purpose and then a solution is implemented to resolve the problem. If the problem persists after these 5 steps, then the redesign process is restarted until a final design solution is found.

In this study, critical components of the Pyroformer were subjected to the same five-step process and a detailed design solution for each one of the problematic components is presented below.

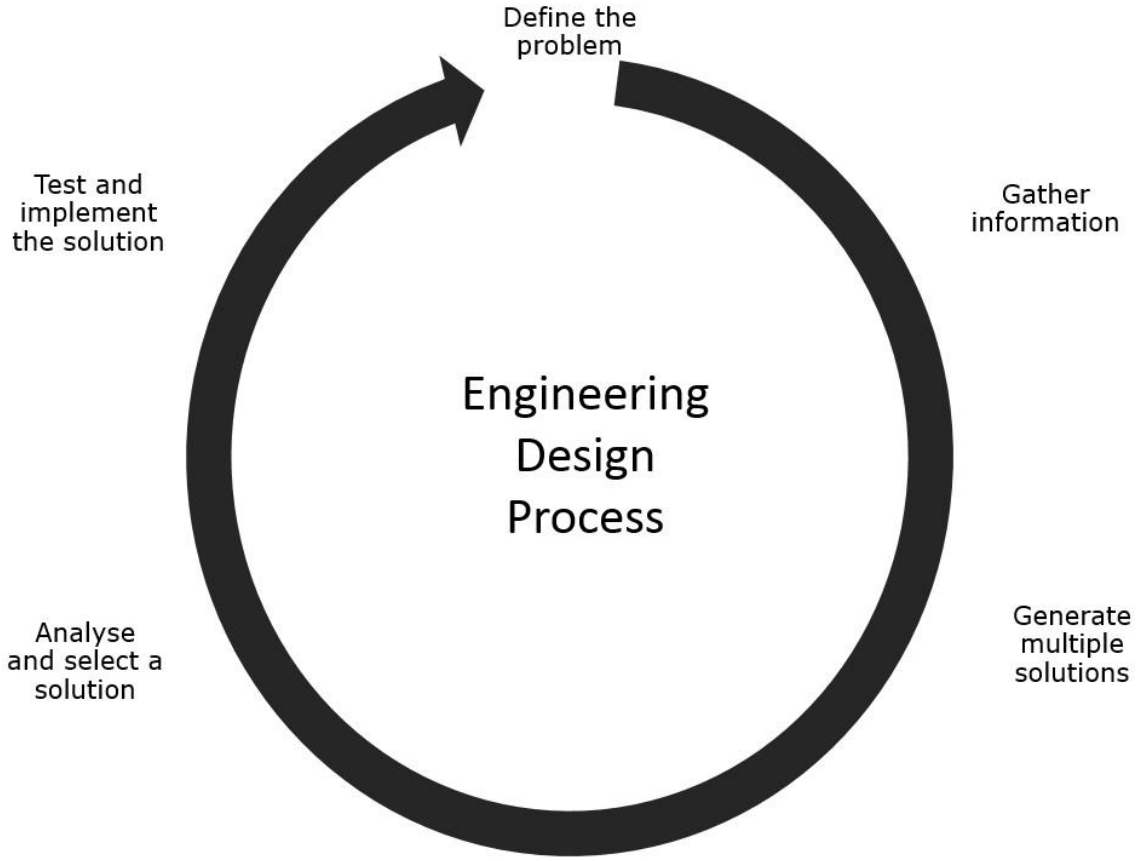

Figure 34 – Showing 5 steps of engineering design process (Adapted from Khandani [2])

7.1 Feeding valve issues

The feeding valve assembly is the key system of the Pyroformer whose function was to deliver the biomass pellets through it, while maintaining an air lock to prevent escape of pyrolysis vapours. Two different types of valve combinations were tried one after the other on 100 kg/h Pyroformer. These included an air pinch valve supplied by AKO Valves GmbH and the other valve was a custom made (provided by Pyrotop GmbH) pneumatically driven piston valve with water cooling jacket. Two pinch valves were connected in series and were driven by compressed air at >4 bar pressure, whereas only one piston valve was used to replace two pinch valves with no avail. When the pinch valve was actuated, a known volume of the compressed air was forced into the sleeve of the valve which expanded (or inflated) under compressed air resulting in the valve being shut. The valve

specifications were model no, VF200.04HTEC.33.30GLA. With the two valves in series, when one valve was opened the other was closed, thus maintaining an air lock. Biomass pellets entered through the top valve when it was opened and rested in between both valves until lower valve was opened and upper was closed. There was a nitrogen gas purge between both valves to ensure no air was entering the system. This valve assembly can be seen in Figure 33 with both valves shown with arrows. This whole assembly can be seen at the top of the Pyroformer feed inlet in Figure 35.

The lower pinch valve was exposed to the highest temperature which was just under set temperature of the Pyroformer in excess of 300°C. This valve failed after few days of operation. The reason for the failure was excessive heat damage to the pinch valve sleeve which was an EPDM fibre reinforced sleeve. Later, upon further investigation it was discovered that the valve was designed for a maximum of 120°C temperature duty. This valve sleeve was replaced a few times with no success before a different valve was proposed by the supplier (WSE Ltd); this was a water-cooled piston valve with pneumatic piston actuator. However, this valve also failed due to exposure to high temperatures - the bottom end of the piston expanded resulting in jamming of the valve. The associated problems with this valve assembly are summarised below:

Figure 35 - Feeder valve assembly

- The layers of EPDM sleeve showed signs of disintegration and softening under pyrolysis temperature
- Pinch valve EPDM sleeve failure after a while resulting in air leakage
- Air leakage lead to temperature hikes in the Pyroformer due to combustion of hot biomass inside the

- Valve sometimes failed to retract, thus leading to biomass pellet blockages
- Valve sleeve failure could lead to formation of explosive atmosphere due to compressed air leakage into Pyroformer

7.1.1 Define the problem

Using the methodology developed by Khandani [2] for engineering design process astep by step breakdown of the process is presented for slecting the appropriate design solution for the Pyroformer related issues. The design requirements and problem of the valves are explained in this stage. The purpose of the feeder valve assembly was to provide an air lock against pyrolysis vapour while allowing the biomass pellets to be fed into the Pyroformer (100 kg/h). The problems with the pinch valves were blockages of biomass materials while it passes through the valve, leakage of compressed air from the pinch sleeve material leading to hazardous consequences in the Pyroformer and non-compatible sleeve material for the process temperature. The replacement piston valve assembly had different problems such as piston being stuck during operation due to expansion of bottom end of piston and when the valve opened it was splashing biomass everywhere due to pressure difference between the Pyroformer process and atmospheric pressure. So, due to the failures of both valve types it was necessary to find a better alternative to resolve the issues with the feeding valves assembly.

7.1.2 Gather information

The valve assembly consisted of two valves connected in series as shown in Figure 35. The valve must be able to withstand temperatures above the feeder inlet flange (50-100°C lower than pyrolysis set temperature) and be not affected by the solid and coarse media such as dust and fibres. As the body of the Pyroformer had a flanged connection of DIN200 (8 inches) then it was essential for the valve to have a flanged connection of DIN200. The valve must not have any air or oxygen which may leak into the Pyroformer thus leading to explosive area (ATEX) formation. The pressure rating of the Pyroformer process was less than 30 mBar, so the valve need to be rated for 1 Bar working pressure at least to allow for safety margin. Due to the high possibility of thermal expansion it was essential that a double acting valve must be selected which means the valve must be able to open and close by means of an external

motive force such as by means of pneumatic actuation or electric drive. Also, the valve must be able to be controlled by programmable logic controller (PLC) and should be interlocked with a position sensor to confirm it's opened or closed position so that the other valve working in series with it must not perform its action until the required action of the first valve had been finished. All the seals and seats of the valve must be able to withstand the temperatures and pressures involved in the process.

7.1.3 Generate multiple solutions

To find the most effective solution for the feeder valve, various types of valves were considered such as ball valves, knife gate valves and rotary valves. When comparing the types of valves which could suit the desired application, the following valves were identified as possible solutions as presented in Table 34.

7.1.4 Analyse and select a solution

Three valves were considered suitable as shown in Table 34 for feeding the biomass to the Pyroformer. All three valves work on completely different principles but they met the basic selection criteria. When explored further and compared against the examples in the industry for solid, abrasive material such as biomass then it was apparent that ball valves are not highly suitable for this kind of application. Other two valves were rotary valve and knife gate valve. The rotary valve provides an airlock with motor speed which can be adjusted to required throughput of 100kg/h, but it is very heavy and costly due to steel body, steel rotary vanes and electric motor and control inverter. The knife gate valve however is much lighter in weight and cheaper due to simple pneumatic air piston, works best with abrasive media. This valve also has explosive area (Atex) classification as well as meets or exceeds the temperature and pressure requirements. Hence it is recommended that the knife gate valve with carbon steel body, stainless steel gate, metal and grafoil seat and graphite packing be used for the Pyroformer. This valve is pneumatically actuated and has limit switches to confirm its open or close position, thus truly providing an air lock when used in series with exactly same kind of valve. Other advantages of this valve when compared to other two were simple design leading to lower cost of the valve enabling in-situ replacement for ease of maintenance of the grafoil seat and graphite packing. The full specification

of the valve for procurement is MV-E-200-MHT-TG-EC-PN10-ILS-SV. Figure 36 provides a detailed design of the knife gate valve.

Table 34 – A list of valves suited for the feeder valve application

S/O	Valve type	Model no.	Material of construction	Manufacturer and reference	Other relevant information, T (°C), P (Bar), ATEX or not
1	Motorised Rotary Valve	S-250 DN200	Cast iron body, special seals for high temperature	J. Englesman AG [212] Germany	ATEX rated, 600°C, 1 bar
2	Hard graphite seated floating ball valve	B-300UTDZ 3H M DN200	Stainless steel body, graphite seated, Ball A276, Type 304	Kitz Corporation, Japan [213]	500°C, double acting Pneumatic actuator, 20Bar, ATEX
3	Knife gate valve MV	MV-E-200-MHT-TG-EC-PN10-ILS-SV DN200	Carbon steel body, stainless 316 gate, metal with grafoil seat, graphite packing	Stafsjo Valves AB, Sweden [214]	425°C, ATEX rated, 10 Bar. Pneumatically actuated

7.1.5 Test and implementation of final design solution

The final selected solution of knife gate valve provides further confidence due to its recommended usage in high temperature and abrasive material applications by the vendor and other end users. These type of valves are used in biomass combustion boiler feeder systems with coarse media in Sweden and are shown to be working satisfactorily [214]. This valve can meet all requirements such as high temperature and material compatibility, ATEX area classification, limit switches to confirm desired operation and pressure rating greater than 1 bar. This valve will need to be interlocked with another similar valve to provide the air lock. A similar combination of two knife gate valves can be used for char outlet to ensure an air tight seal for char leaving the Pyroformer. Both pairs of these knife gate valves will need to be sequenced with each other so that only one valve opens at a time thus reducing the compressed air burden for actuators as well as providing perfect air tight seals on feeder and char outlet assemblies. The diagram and details of knife gate valve components are presented in Figure 36 [214].

Aston University

Illustration removed for copyright restrictions

Figure 36 – Selected knife gate feeder valve for Pyroformer 100kg/h as taken from Stafsjo Valves of Sweden [214]

7.2 Char collection system

The char collection system is another important part of the Pyroformer (100 kg/h) process as the duration of operation of the Pyroformer is directly linked to the char storage capacity in the char container. The char outlet of the Pyroformer also must form an air tight seal to prevent any pyrolysis vapour loss into atmosphere. Also, at the same time the char fraction of pyrolysis must be cooled to ambient temperature while in continuous operation so that it is not a heat hazard in the char container. The original cubical shape metal container of the Pyroformer can be seen in Figures 32 and 37. There is no valve between the Pyroformer and char container, thus exposing it to high pressures and leading to bulging of container if there was a blockage in the Pyroformer gas outlet

Aston University

Illustration removed for copyright restrictions

To resolve the issues associated with char container it was necessary to find a better solution which could enable the Pyroformer (100 kg/h) to be operated on continuous basis as well as make it a safe system. To identify and design a better solution, a five-step design process was followed as shown in Figure 34.

Figure 37 - Char container (shown hanging) of the 100 kg/h Pyroformer (Photo by Louise Ciaravella)

7.2.1 Define the problem with char collection system

For an effective design solution, it was important to highlight the problems associated with the char collection system which are highlighted below.

- Lack of storage capacity (500 litres) thus making the Pyroformer a batch system
- Container was hanging onto Pyroformer thus causing unnecessary stress on Pyroformer body

- No insulation on the body of char container thus a major health and safety hazard due to hot char presence inside the container
- Pyrolysis vapour leaks from the joints on lower rectangular plate

7.2.2 Gather information

Further detailed specifications of the char collection system are summarised as below;

- The char collection system must be leak proof to avoid any gas leaks thus avoiding the formation of explosive area near the Pyroformer
- The system must be able to support the continuous operation of the Pyroformer
- It must not stress the Pyroformer and should be able to hold its own weight
- The char collection system should cool the char down to ambient temperature to avoid any health and safety risks
- It must be able to withstand the pressures up to 3 bar to allow for sufficient safety margin pressure within the Pyroformer
- The material of construction must be able to tolerate thermal expansion due to a large temperature difference between hot Pyroformer and container at ambient temperature
- There must be temperature and pressure indication on the char container to show the char storage conditions

7.2.3 Generate multiple solutions

There were two potential designs identified which could resolve the issues related to char collection system. The first potential solution was a replaceable char collection steel drum (205 Litres capacity) with an expansion bellow and two knife gate valves installed between char drum and char outlet on the Pyroformer (as stated in section 7.1.5). Both knife gate valves can be interlocked in the control system to maintain a gas tight seal to avoid the pyrolysis gas escaping through this route. Between both valves a low flow volume of nitrogen could be introduced which could act as a cooling medium and be a safeguard against air ingression and to dilute the flammability potential of pyrolysis gas. A ventilation pipe could be installed on the welded lid of the drum, venting outside the building to avoid any local fugitive emissions when changing the drum. The lid of the char drum was to be welded

onto the pipework below the lower knife gate valve. The whole area of the char drum could be insulated with a high temperature insulation jacket to mitigate the heat hazards. A temperature and pressure indicator could also be installed on the drum with a local display to show the status of contents inside the drum.

A second solution could be a more robust and continuous char removal system. This system could consist of a pair of knife gate valves as stated earlier with an expansion bellow attached between Pyroformer outlet and upper char outlet valve. This expansion bellow could compensate the thermal stresses between the hot Pyroformer and char collection system. Between both knife gate valves could be a nitrogen gas purge to cool the char as well as to displace any incoming air. After both valves there could be an auger screw with a water-cooled jacket (counter flow heat exchanger) along the length of the auger. The water-cooled jacket would provide cooling of the char. The water could be circulated through a chiller or cooling tower for heat removal. Temperature and pressure monitoring could be easily added on to ensure the char leaving the cooling system has cooled sufficiently and there are no auto-ignition (smouldering) risks.

7.2.4 Analyse and select a solution

Both the solutions discussed above for char collection systems had to be custom made as they were currently available off-the-shelf. When a comparison was made between both systems, it was evident that continuous char removal system based on water cooled auger screw was the preferred choice. This was because it could support the continuous operation of the Pyroformer. It is more robust, requires minimal operator interface and most importantly it appears to be safer than drum based system.

7.2.5 Test and implement the solution

For the design and implementation of such as system the throughput of char was taken as the percentage yield of char from the Pyroformer design capacity i.e. 100 kg/h. This yield could be estimated based on some high ash containing materials for pyrolysis to be around 50 wt%. This meant that the mass flow rate of char through the water-cooled screw was approximately 50 kg/h on the upper limit at steady state. A heat balance could to be made to establish the

water flow rate, cooling surface area requirement for char, screw and water jacket length and the rotation speed (residence time of char in screw) of the screw motor which are important functions for heat transfer from char to cooling water. One such system is shown in the Figures 38 and 39. A somewhat similar system to transport hot ash from the gasifier system is used in European Bioenergy Research Institute at (EBRI) at Aston University as shown with white arrow in Figure 38.

Figure 38 - Water cooled screw conveyor for gasifier ash as installed at European Bioenergy Research Institute (Photo by Louise Ciaravella)

The whole system would need to be backed up by a chiller to cool the water so that there is enough cooling capacity in the water when it is being used as a heat exchange medium in the water-cooled jacket of the screw conveyor. It may also be that the length of water-cooled screw is excessively long compared to Pyroformer and in which case more than one such water-cooled screw could be used, where outlet from the first is fed into the inlet of second water-cooled screw. Once a sufficient temperature below 50°C is achieved then the char can be collected in a bulk bag with a plastic liner and sealed with nitrogen gas to avoid any spontaneous ignition.

Aston University

Illustration removed for copyright restrictions

Figure 39 – A screw conveyor showing water cooling jacket proposed for char collection system of the Pyroformer [1]

7.3 Biodiesel quenching system

Biodiesel is used for direct quenching of the pyrolysis vapours soon after they leave the Pyroformer gas outlet. Biodiesel is used as an in-situ blend medium to form a bio-oil/biodiesel mixture which can be used as a fuel with little or no further upgrading as well as to rapidly quench the pyrolysis vapours. The issue with biodiesel quench in the prescribed manner as described in section 6.1.3 is that it consumes significantly large quantities of biodiesel in single pass due to no re-circulation of biodiesel. If the consumption of biodiesel is reduced to increase the bio-oil blend ratio then it is very likely that some pyrolysis vapour may not condense due to lack of cooling capacity. Hence, to increase the bio-oil content in the liquid blend and to increase the economics of the pyrolysis process it is essential to re-circulate the bio-oil/biodiesel blend through a chiller. The re-circulation of the blended liquid will lead to the increase in bio-oil ratio in the blend as more and more vapours will be condensed.

It is possible to control the blend ratio of bio-oil and biodiesel by introducing known quantity of biodiesel in the quenching system. By controlling the biodiesel quantity in bio-oil/biodiesel will lead to better economics of pyrolysis by reducing the expensive biodiesel in the first place. However, this will lead to higher total acid number as bio-oil content in the blend will increase. There are ways where different types of bio-oils can be blended together to balance the total acid number of the resulting blend. For instance, the pyrolysis bio-oil from digestate feedstocks

show a total acid number around 0.2 mgKOH/g. This also means that bio-oils derived from pyrolysis of digestate materials (as shown in section 5.4.3) having low total acid number (0.2 mgKOH/g) can be used as quench liquid for high acid number producing materials such as wood pellets to neutralise the acidity effect. The resulting blends and/or digestate derived bio-oil having low calorific value (19.3 MJ/kg) can also be used in post quenching blending (not in-situ) with biodiesel to improve the blend calorific thus enabling its usage as could be influenced by process economics.

The author has contributed in redesigning the existing biodiesel quench design which was to pump the re-circulating blended liquid (bio-oil/biodiesel) by means of a diaphragm pump (P0110) driven by nitrogen gas rather than compressed air as shown in Figure 40. Although an electric driven centrifugal pump will be a better choice but since a diaphragm pump already existed for this purpose hence a nitrogen driven diaphragm pump system is proposed for safety reasons. Driving the diaphragm pump with nitrogen is essential in case the diaphragm in the pump ruptures then the hot pyrolysis vapours will start to combust if compressed was used instead of nitrogen.

During the quenching a known quality of the biodiesel is initially introduced and then re-circulated together with freshly collected bio-oil blend through a counter current heat exchanger which is connected to a chiller. In the redesign, there is an electric chiller shown as EC0100 after a counter current heat exchanger as shown in Figure 40. The chiller is there to provide extra cooling capacity to the re-circulating liquid blend. The re-circulating blended liquid after passing through heat exchanger is delivered to existing quench points as was previously designed. The quantity of total liquid can be controlled in the system either by having a tank of large volume or by taking a small volume of blended liquid out by means of another pump from time to time controlled by high and low-level indicators.

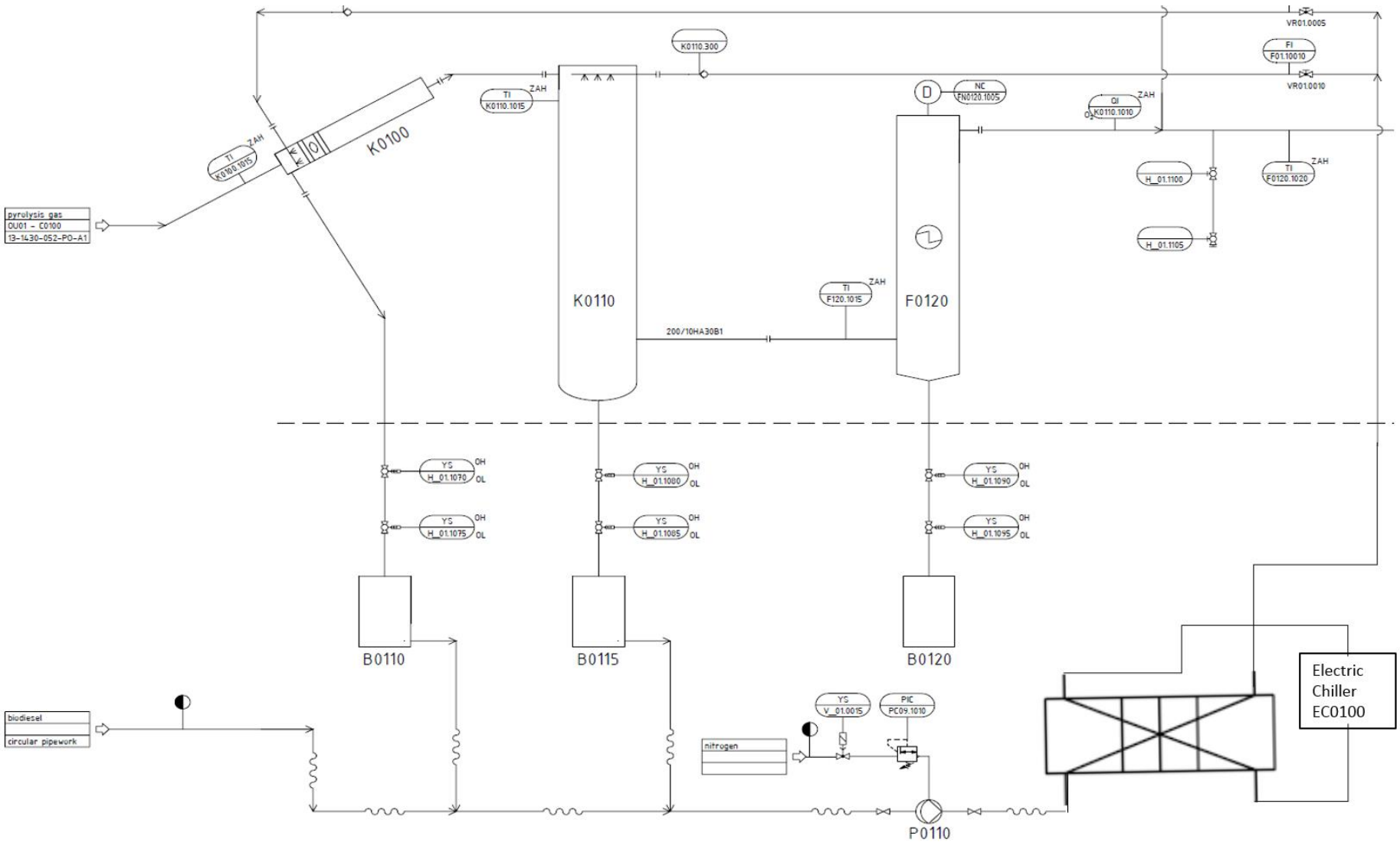

Figure 40 - Biodiesel/bio-oil quench system redesign (adapted from EBRI Pyroformer archives)

Chapter 8 - Pyrogasification – Combining of Pyroformer and Gasifier

Gasification of biomass leads to the production of a gaseous product which is a mixture of carbon monoxide, hydrogen, carbon dioxide, nitrogen, methane and some light alkane and alkene gases in very small quantities. Gasification is attractive due to the production of a uniform quality gas which can be used as a fuel or for chemical synthesis. However, tar content in the gas is highly undesirable as its presence in fuel gas can lead to serious problems with fuel injection system of engines. Pyrogasification involves the thermal treatment of biomass in two dedicated stages. Pyrolysis of biomass in the first stage, followed by takes place followed by gasification in the second stage as demonstrated by other researchers [98, 141, 142]. Pyrogasification is considered beneficial as this leads to significantly lower tar levels in the fuel gas compared to gasification alone. As highlighted in the literature review in section 2.10, pyrogasification provides improved gas quality by tar reduction [98, 141, 142]. Henriksen [59] has measured the tar content in the pyrolysis vapours, then in the char bed of a downdraft gasifier and finally before the use of syngas in the engine to prove that, by separating the pyrolysis of the biomass and then introducing the hot vapours and char into a gasifier with a char bed, tar content is reduced by 100 folds. This phenomenon of tar reduction by pyrogasification is attributed by Gassner [131] for easier breakdown of pyrolysis vapours (within a separate pyrolysis process) in the gasifier compared to gasifier alone application without a separate pyrolysis stage. The pyroformer has shown the potential to treat complex biomass (with high moisture, low ash melting point, high ash content) due to its operation at mild pyrolysis temperature (~500°C) by using the screw system to re-circulate char. Hence, combining the Pyroformer with a gasifier should lead to further tar reduction in the fuel gas in the pyrogasification system, compared to the so called the Viking gasifier developed by Technical University of Denmark as described by Henriksen [59].

The Pyroformer process developed by researchers at the European Bioenergy Research Institute (EBRI) has been introduced in chapters 4, 5 and 6. This system is the key component for the proposed pyrogasification process by combining it

with a bubbling fluidised bed gasifier. There is a significant difference in feeding throughputs of both systems, where the Pyroformer is 100 kg/h and gasifier 300 kg/h of biomass. Originally the pyrogas coupling was going to include two 100kg/h Pyroformers under ERDF funding but one of these was cancelled due to budgetary constraints. The apparent disparity between the throughputs of both systems however can be mitigated by the fact that siginificant amount of solids (wood pellets + char + dolomite) are always present as gasifier bed materials, to maintain a fluidised bed in the gasifier for rapid mixing, mass and heat transfer. A one third proportion of wood pellets feed in the gasifier is compensated by a small fraction of pyrolysis gas. As this coupling is only an experimental demonstration system, the close match between feed intake quantity was not considered important at this stage. Both these systems are installed as standalone processes at the EBRI laboratories as shown in Figure 42. They are spread over 4 floors of a purpose built building to include all the ancillary items such air compressors, ventilation equipment, gas detection equipment for safety, pumps, motors, chillers, heat exchangers, dedicated automation and control systems and a a diesel fueled engine which is adapted to run on gasifier gas together with liquid fuel. A 3D layout of these processes is shown in Appendix 3. The engine is a water cooled MAN diesel engine converted by NEK GmbH of Germany to run on gasifier fuel gas. This engine (Model D2842) is a V12 21.9L displacement coupled to a Leroysomer electric generator of 400kW. This engine was not used in any of the tests as it was not commissioned in time.

8.1 BFB Gasifier process commissioning test layout

For clarification purposes it is worth mentioning that this thesis is limited to only a design study of an integrated pyrogasification system based on a 100 kg/h Pyroformer and a bubbling fluidised bed gasifier of 300 kg/h. There was only one gasifier commissioning test conducted during the plant commissioning and the results presneted to show the working principles and the fuel gas quality obtained during this test. As this test was conducted when some elements of plant or its control were still at the installation stage, hence a full scientific study with detailed data was not possible as not all plant items were available and fully comissioned at the time of tests. Only a comissioning operational test was carried out and the only available data arefuel gas compositions in terms of hydrogen, carbonmonoxide and methane fractions as measured online by an industrial type

Siemens gas analysis equipment (Model numbers, CALOMAT 6E and ULTRAMAT 23E). The fuel gas produced during the test was burnt in an oxidiser flare and the resulting combustion gases were discarded safely into the environment. The CHP engine was not used in this test or in any other tests in this thesis. Hence, apart from a gasifier only commissioning test this thesis proposed a solution about how best to integrate both these systems (Gasifier and Pyroformer) to achieve the benefits of pyrogasification. As stated pyrogasification is desirable to provide feedstock flexibility to the gasifier by acting as upstream treatment unit and also to resolve the complexity of bio-oil fuel issues as it requires upgrading to be used in the engine.For the gasifier commissioning test, only the gasifier process was running with its very basic safety control functions. There were no possibilities to gather sufficient information to merit a sophisticated scientific experiment with all inputs and outputs monitored. Figure 41 shows the gasifier process layout for commissioning test. The whole plant is integrated by means of 6 different control systems which are explained in the Table 35. A small fraction of the fuelgas after the final filtration stage is taken to Siemens industrail gas analyser equipment and the rest is sent to a gasbuffer for temporary storage to manage pressure fluctuations in the process. From gas buffer the fuel gas is either sent to a thermal oxidiser flare for disposal, or could be used in CHP engine in future for heat and power production.

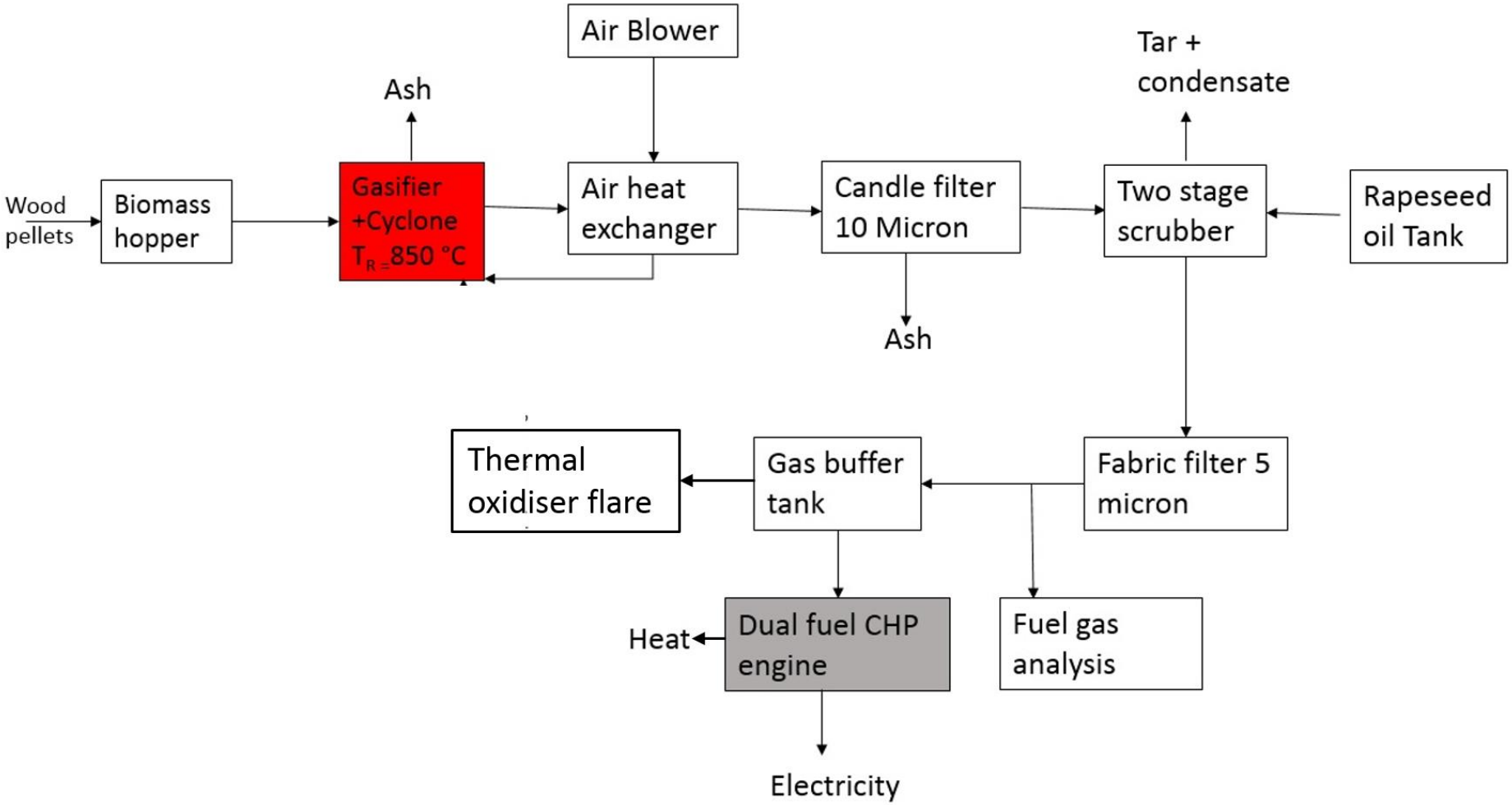

Figure 41 – Gasifier process layout showing process items for commissioning test – CHP engine not used in the test

Table 35 - EBRI Plant integrated control system with interlocks

S/O	Process type	Control system PLC*	Purpose	Interlocks
1	Pyroformer 100kg/h	Wago I/O module with 16 channel - CoDeSys fieldbus PLC	Automation of Pyroformer process	Interlocks with 2 and 6
2	BFB Gasifier 300 kg/h	Siemens Simatic S7 -300 PLC,Profibus protocol	Automation of gasifier process system	Interlocks with 1, 3, 4,5 and 6
3	Man dualfueled engine CHP	ComAp engine PLC with InteliMonitor monitoring controller	Openation and control of MAN engine for power generation	Interlocks with 1, 2, 4,5 and 6
4	Load matching system	Siemens PLC modbus protocol	Automation and control of CHP heat, power and cooling	Interlocks with 1, 2, 3,5 and 6
5	Building management system	Trend IQ3 LAN controller	Management of EBRI building utilities	Interlocks with 1, 2, 3, 4, and 6
6	Gas detection and HVAC system	Trend IQ3 LAN Controller	Fire safety and ventilation system	Interlocks with 1, 2, 4,5 and 6

PLC* - denotes Programmable logic controller

8.1.1 Feedstock analysis

Only standard wood pellets were tested in this commissioning test, with 6 mm diameter. The pellets were supplied by Verdo Renewables Limited of Andover, Hampshire. These pellets were supplied in 1000 kg big bulk bags which were desirable for easy handling and storage by means of a forklift truck and gantry crane. These pellets were made to ENPlus A1 standard which is an EU wide quality standard for wood pellets quality and sustainability. The same pellets were also used in the Pyroformer 100 kg/h system in Chapter 6.

The ultimate analysis of the feedstocks was determined using combustion analysis on a Flash EA 1112 Series CHNS analyser. Oxygen was calculated by difference calculation. The density was measured according to the ASTM D-285. The moisture content of the feedstock was determined using a moisture analyser (Sartorius MA35) with a programmed temperature of 105°C. The gross heating value in HHV (MJ/Kg) of the dried feedstock was determined using a Parr 6100 bomb calorimeter whereas the LHV was theoretically calculated using a standard empirical formula. The results are as shown in the Table 36.

Table 36- Feedstock analysis of wood pellets

Feedstock	**Unit**	**Wood pellets**
[a]Ultimate analysis		
Carbon	wt.%	46.2
Hydrogen	wt.%	5.96
Oxygen[b]	wt.%	47.6
Nitrogen	wt.%	<0.01
Sulphur	wt.%	0.28
[a]Proximate analysis		
Moisture	wt.%	8.71
Ash content	wt.%	0.46
Density @20°C	kg/m^3	688
Higher Heating Value (HHV)	MJ/kg	18.3

[a]Analysis based on dry basis

[b]Calculated by difference

8.1.2 BFB gasifier working principles

The BFB gasifier was developed by a German company called Wehrle Werk AG and was supplied to EBRI under a project funded by European Regional Development Fund (ERDF) to act as a demonstrator test bed to support biomass research in the West Midlands region of the UK. The integration of the Pyroformer and gasifier

was further supported by IAPP Pyrogas project and Bioenergy Interreg NW projects as stated in the acknowledgments section.

For convenience, the bubbling fluidised bed gasifier referred to simply as "the gasifier" from now on. The gasifier is rated as 1.4 MW biomass thermal energy input based on ENPlus A1 standard wood pellets. Note that such standard pellets had to be used as the system was not able to handle any other size, shape, moisture and ash content of feedstock.

Figure 42 - Pyroformer and gasifier shown next to each other in white arrows – Photo taken from EBRI archive

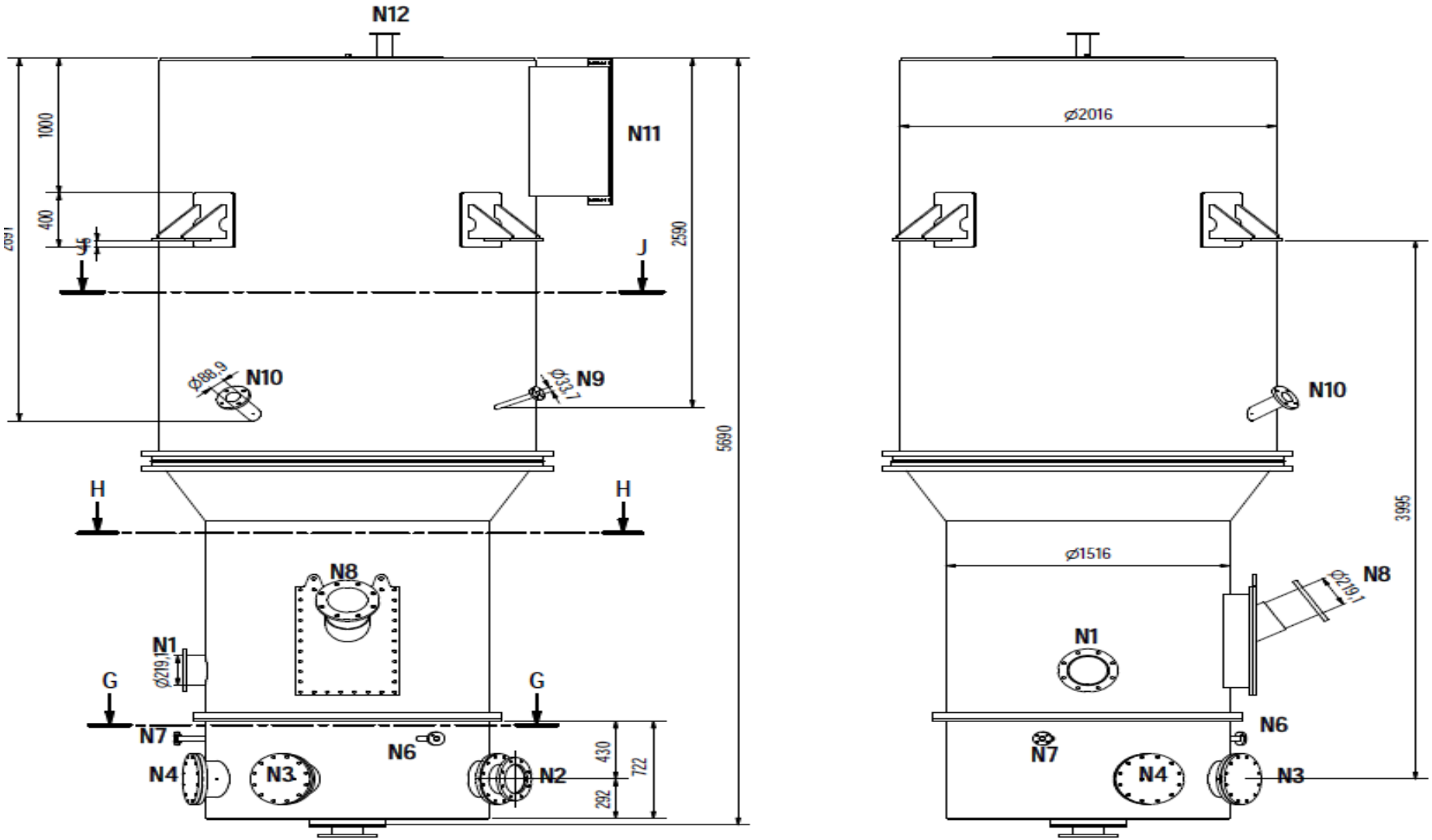

Figure 43 - BFB gasifier showing biomass feed inlet N1, dolomite inlet N10, pyrolysis gas coupling N8 and fuelgas outlet N11 (Adapted from EBRI gasifier archive)

The gasifier produces a low calorific value (4-5 MJ/m^3) gas to feed into an engine in dual fuel mode for electricity generation; however the engine was not tested. Before wood pellets can be fed into the gasifier, the gasifier went through a preheating stage where a solid bed material was maintained in the form of fine ground dolomite particles of less than 2 mm diameter. Dolomite was chosen by the vendor as a catalyst due to its good tar cracking potential and absorption of chlorine and sulphur contents from biomass [215]. The dolomite also acts as catalyst to minimise tar formation from wood pellets during the fluidisation. Preheated air (by an electrical heater) was used as main oxidant media for the gasifier and was supplied by means of an air blower fan. The working pressure at the inlet to the air injector nozzles at the base of the gasifier was maintained around 200 mbar and the gasification temperature was maintained between 800-850 °C. Due to the presence of dolomite and wood pellets as bed materials in the gasifier there was a signification pressure loss which was measured online by a differential pressure gauge system and it was mostly controlled between 95-105 mbar. The differential pressure was measured between the preheated air inlet pressure at the air injector nozzles and the fuelgas exit point on top of the freeboard. Three different temperatures were monitored in the various heights of free board to main process temperature around 800-850 °C. Initially process air was electrically heated to 450 °C by means of an electrical heater of 100 kW and then supplied to the gasifier bed material through air nozzles to maintain fluidisation. After combustion had started, the exiting hot fuel gases preheated the air by means of a heat exchanger.

Once a temperature of 450°C had been reached then wood pellets were introduced into the gasifier and the combustion process was started to elevate the gasifier temperature to its normal working temperature. Wood pellets were fed by means of a feeding system which consisted of a storage silo, screw conveyor, sluice double valve system with nitrogen purge and a final plug screw (N10 in Figure 43) to compress the pellets at the entry point to the gasifier to avoid any hot gas back draught. Dolomite was introduced from its own dedicated feeding system which was somewhat similar to wood pellet system but the main difference is the entry point of dolomite in the gasifier. The entry point of the dolomite is at the start of the freeboard section (N10 in Figure 43), whereas wood pellets were fed just above (N1 in Figure 43) the air inlet nozzles.

Wood pellets reacted with preheated air at 450°C and combustion started resulting in temperature increase and hot syngas was formed which left the gasifier at the top outlet. When a temperature greater than 850°C was reached in the gasifier, a transition from combustion to gasification was enabled (by reducing air flow) which also brought the temperature within the gasification set point temperature. This meant there was a lean oxygen environment and stoichiometric oxygen required for complete combustion (lambda, λ) was maintained between 0.3-0.4. By definition, a lambda value of 1 means complete combustion oxygen condition. Hence for a gasifier a lambda value of 0.33 means there is one third the amount of oxygen supplied (oxygen deficiency) to that of complete combustion of biomass [215]. The supply air fan maintained sufficient air pressure for fluidisation (the suspension of solids in gas under pressure) for intense mixing of dolomite, wood pellets and air. During the gasification stage fuel gas was produced which was mainly a mixture of carbon monoxide, hydrogen, water vapour, nitrogen, carbon dioxide and methane. The fuel gas exited into a cyclone and coarse solid particles are removed in this stage. The solids removed from the cyclone were then taken into a water jacket screw cooler to be transferred into a flexible big bag for storage below 50°C and disposal. The resulting clean gas then entered a counter-flow hot gas-air heat exchanger and its temperatures was further reduced, whereas now the process air was preheated by heat recovered from fuel gas. A thermal oil heat exchanger was used in next step to reduce the fuel gas temperature to below 300°C.

Fuel gas was then filtered down to 10 μm by means of sintered stainless-steel candle filters while still loaded with water vapour before being sent to a rapeseed oil scrubber. The rapeseed oil scrubber was a counter flow two-stage process where the fuel gas was further cooled and cleaned with the rapeseed oil in direct contact. In this stage, water vapour, tars and remaining solids were removed. The rapeseed scrubber oil was supplied from a buffer tank by means of pumps while passing it through heat exchangers to cool it down as shown in in the process flow diagram of Figure 41. Heat from the process was removed by means of the heat exchangers water cooling circuit which was connected to the dry cooler fan unit on the roof of the building (as shown in Appendix 3). Some of the rapeseed oil was sent to a water/oil separator (centrifuge) by means of a different pump at slightly higher temperature to remove combustion water from the process.

The fuel gas was now at almost ambient temperature and left the oil scrubber to pass through a fabric filter where it was filtered down to five μm to ensure it was sufficiently cleaned before it was flared in a thermal oxidiser or sent to the Siemens industrial gas analysers (Model numbers, CALOMAT 6E and ULTRAMAT 23E) for hydrogen, carbon monoxide and methane (H_2, CO and CH_4) content. After this fabric filter, the fuel gas was then temporarily stored in a large flexible PVC gas buffer vessel of 60 m^3. The gas blower fans then delivered the fuel gas to a gas flare for combustion, as long-term fuel gas storage is not possible and the CHP engine was not ready to use it. The fuel gas pressure is maintained at 15 mbar for delivery to the flare or engine (when available). The produced gas quantity was maintained by controlling the wood pellets feed rates and the preheated air temperature from air blower by means of a PID controllers on the respective electrical motors, in response to monitoring of the fuel gas constituents (H_2, CO and CH_4). Fuel gas composition and higher heating values (HHV) are dependent on lambda.

8.1.3 Gasifier fuel gas data sampling and results

During the commissioning test the fuel-gas composition was measured online for H_2, CO and CH_4 with Siemens gas analysers (models; CALOMAT 6E and ULTRAMAT 23E)and the carbon dioxide and oxygen content was measured by a portable biogas analyser (model GFM436) from Gas data analytics UK ltd. The results presented below for gas composition, gasification temperature and fuel gas flowrate were taken on the day of the test once the process was running in gasification mode. There were some fluctuations in the gas composition and flow. These were due to the fact that the process was being commissioned with various other tests on ancillary equipment being carried out in parallel. The output of the gasifier was determined by the amount of combustible gases produced and their energy content in terms of the higher heating value (HHV).

(1) $\dot{Q}_{total} = \sum(\dot{m}_{gas,i} \cdot HHV_i)$ (Thermal energy of the gas)

HHV_i: Higher Heating Value of each gas component (i) in MJ/kg

$\dot{m}_{gas,i}$: Mass flow of the i-th component in kg/s

$\dot{Q}_{total}$: Thermal power in MW

In the gasifier plant, the total flow of syngas was determined by a combined measurement of absolute pressure, differential pressure and temperature. The calculation of the volume flow was conducted according to EN ISO 5167-1 but with the simplification of a constant expansion number and the assumption of ideal gas behaviour.

The volume flow shown and recorded in the process control system was the volume flow based on standard conditions, i.e. T = 25°C and p = 1.013 bar. In order to calculate the mass flow of the i-th component the ideal gas equation was used:

(2) $pV_i = \frac{m_i RT}{\widetilde{M}_i}$ (Ideal gas equation)

(3) $\dot{m}_i = \frac{p}{RT} \dot{V}_i \widetilde{M}_i$

(4) $\dot{V}_i = \widetilde{x}_i \cdot \dot{V}_{total}$

(5)

$\widetilde{M}_i$: Molar mass of each gas component (i) in kg/mol

m_i : Mass of each gas component (i) in kg

p: pressure in Pa ($p_{standard} = 1.013 \cdot 10^5\ Pa$)

R: Gas constant = 8.314 kJ/(kmolK)

T: Temperature in K ($T_{standard}$ = 273.15 K)

V: volume in m³

$\dot{V}_{total}$: Volume flow m³/s under standard conditions (p, T)

$\tilde{x}_i$: Proportion of i-th component in mol/mol

The proportion of the i-th component $\widetilde{x}_i$ was measured for CO, H_2 and CH_4 in the Siemens industrial online measurement system (SIEMENS CALOMAT & ULTRAMAT). These gases were the main components of the combustible part of the gasifier gas, which contributed to the energy content. Depending on the gasification conditions, smaller amounts of alkanes and alkenes as well as aromatic components and oxygenates may contribute to the energy content. These components were not measured and left the system undetected. However, normally these components are very small in vol % and will not influence the

results drastically. For a detailed scientific experiment at later stage these constituents of the fuel gas can be measured to present the conclusive results.

The standard higher heating value which is the heat of combustion for the gas components is given below

CO	Carbon monoxide (g)	283.0 kJ/mol	M = 28 g/mol
H_2	Hydrogen (g)	285.8 kJ/mol	M = 2 g/mol
CH_4	Methane (g)	890.8 kJ/mol	M = 16 g/mol

The average gas composition was measured during gasification for couple of hours as shown in Figure 44 between time 11:24 to 16:48 hrs during the commissioning test. The composition data are presented in Tables 37 and 38.

Table 37 – Gasifier fuel gas composition as measured (on average) for

	Temp. °C	**Flow m³/h**	**H_2 Vol%**	**CO Vol%**	**CH_4 Vol%**	**CO_2* Vol%**	**O_2* Vol%**
Average	818.5	788.3	13.3	17.3	4.0	17	0
Stand. Dev. ±	4.3	13.4	0.6	0.8	0.3	N/A	N/A

Table 38 - Gasifier fuel gas composition, flowrates and higher heating values

	x_i	**M_i**	**m_i**	**HHV_i**	**Q_i**
i	Vol%	kg/mol	kg/s	MJ/kg	MW
CH_4	4.0	0.016	0.006	55.7	0.348
CO	17.3	0.028	0.047	10.1	0.478
CO_2^*	17.0	0.044	0.073	0	0.000
H_2	13.3	0.002	0.003	142.9	0.371
O_2^*	0	0.032	0.000	0	0.000

*data sampled by handheld analyser for a short time only

The following data were also recorded:

Average gasification temperature in freeboard zone = T = 818°C

Total flow of fuel gas = 788.3 m^3/h

Total energy in gas at given flowrate = 1.197 MW

Energy flowrate in fuel gas per cubic meter = 1.52 kWh/m^3

8.1.4 Discussion

As stated earlier, this test was only a commissioning test as such subject to certain limitations. Also, during the test various plant items such as pumps, heat exchangers, gauges, flow meters, heat exchangers and other ancillary process units were brought on and off line to check their working status and to adjust the process. Hence, fluctuations can be seen in the gasifier gas quality as well in the flows and gasification operating temperature. Nonetheless, it is very interesting to note that during its first commissioning test in the EBRI labs, the system was made to work and the fuel gas was produced without major problems. Results and sampling were taken during the gasification period, as during this time the process was somewhat more stable. The data presented were collected over a 5-hour period and the averaged results are presented here. Most of the fluctuations in the flow caused the gas composition to fluctuate. It can be noticed that the gasifier was able to produce fuel gas around its design temperature of 800-850°C with average gasification temperature of 818°C. The process was well within defined parameters, with an averaged fuel gas flowrate of 788 m^3/h and total energy flow in the fuel gas of 1.197 MW.

For stable gasifier operation, it was necessary that the fluctuations in the temperature, pressure, gas flow and fuelgas composition were kept to a minimum. Figure 44 shows the temperature profile of the gasifier during operation. There are couple of temperatures which can be seen with a temperature variance of less than 50°C between higher and lower readings. It is also noticeable that, each time temperature is peaking the gas flowrate is dropping which indicates that this was happening when the biomass in the gasifier bed must have been consumed thus also leading to a sharp drop in CO composition.

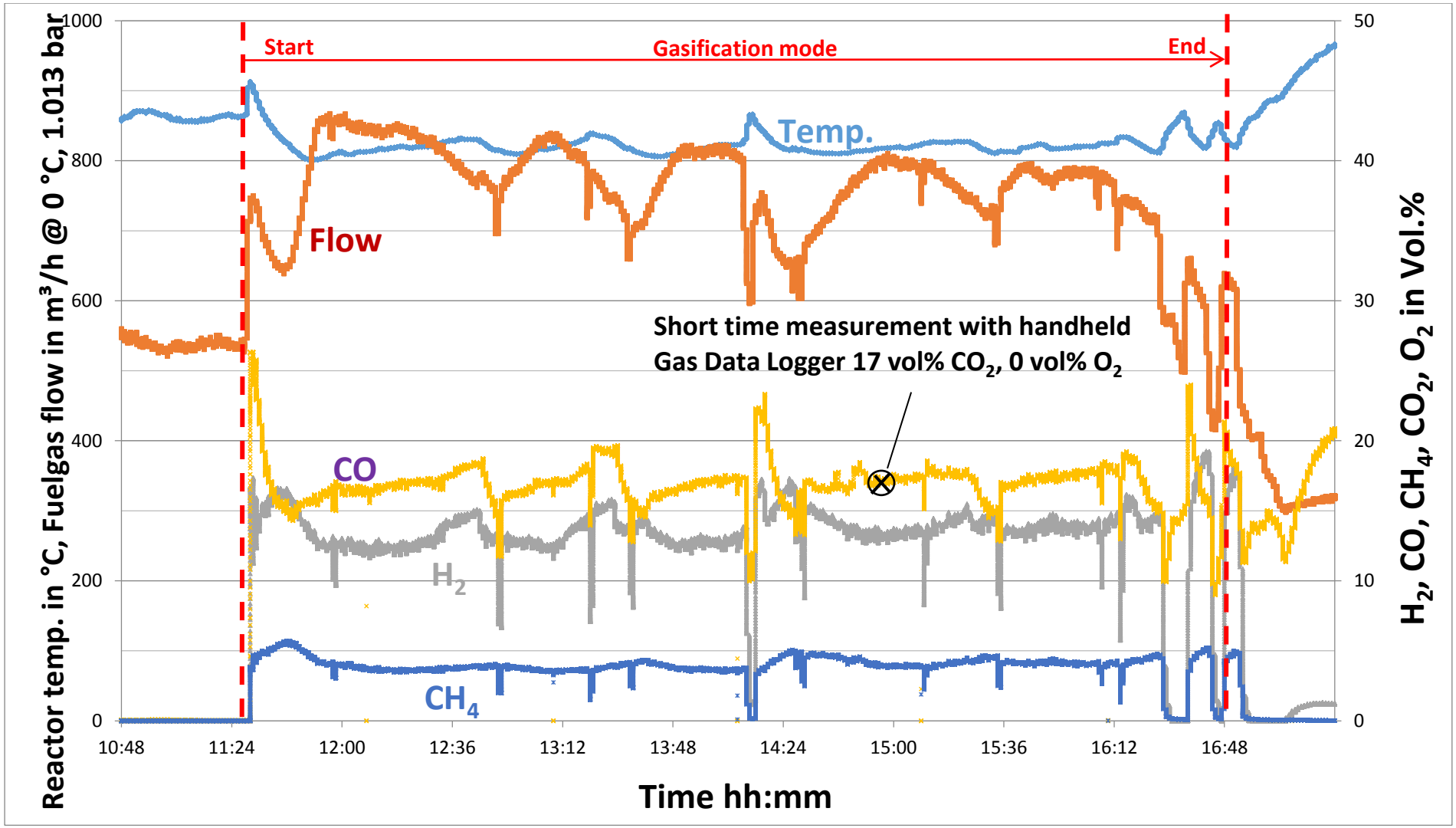

Figure 44 - Gasifier fuel gas online composition, flowrate, gasification temperature, sampling time and handheld gas measurement for CO and oxygen (shown in a cross and circle)

The gas composition in terms of CO, hydrogen and methane can be seen varying even without big changes in gasifier operating temperature. These changes in the fuel gas constituents can be related to gas flowrate as it is evident that there is a strong relationship between air flow and gas composition which proves the basic point for gasification where air flowrate is controlled to optimise the fuel gas composition. The CO composition varied between 10-25 vol %. Similarly, hydrogen and methane also followed the same pattern of composition variation at same peak levels compared to CO profile. The changes in gaseous composition can be linked to changes in overall gas flow, as when the individual gas constituent composition is dropping low the gas flowrate also followed the same profile. As the biomass gets consumed, the amount of biomass reactant is reduced which leads to less reactions between air and biomass hydrocarbons. It is also partially evident from Figure 44 that each time the temperature peaks, the flowrate reduces which is another strong indicator of the process starting to deviate away from gasification into combustion until a batch of biomass feed is introduced in the gasifier and all parameter start to recover to their set points. However as there were no data logged for biomass and dolomite input intervals (or in continuous) this cannot be fully confirmed. The oscillations associated with gas flow can be linked to biomass and dolomite catalyst feed pulsation (these were not fed continuously) as the feedrate of material into the gasifier is automatically controlled to maintain a certain minimum and maximum pressure difference between the air inlet and freeboard. The controller monitors when the lower pressure differential is active, indicating less bed material. Then the automation starts the feed motors to feed in dolomite and wood pellets. This feeding pulsation is also reported by Henriksen [59] and Narvaez et al. [222]. There is some indication that, when the temperature is increasing, there is a small increase in hydrogen and CO production which is a basic feature of gasification as tar cracking reactions are optimised leading to more tar conversion. The increase in hydrogen production with temperature is similarly reported by Narvaez [222] and Li et al. [223]. This commissioning

test was without major problems, but showed some variations in product gas composition which can be further optimised in future test runs. Unfortunately, due to the lack of any other experimental data from this commissioning test, it is not possible to draw further conclusions.

8.2 Integration of Pyroformer and gasifier by means of a self-cleaning twin screw system

Since the biomass tests in the 100 kg/h Pyroformer as reported in Chapter 6 which was based at Harper Adams University College, this Pyroformer was relocated to EBRI laboratories and situated next to a gasifier as shown in Appendix 3. Hence the height of the Pyroformer mounting from its base was changed compared to its height at Harper Adams University as shown in Figures 30 and 32. The Pyroformer is now situated right next to the gasifier unit at ground floor level as shown in Figure 42. This suggests a straight forward connection between both units by means of a stainless steel flanged pipe coupling of diameter 200 mm.

Before the actual design solution is presented it is essential to have a look at the anticipated problems when combining both systems. Given below are a list of anticipated mechanical and flow problems with twin-screw coupling and their solutions as presented in Table 37. The solution is in the form of twin screws which are driven by a single electrical motor. The screws rotate in opposite directions while pulling the solid material from the sides into the centre core. Figures 42, 43 and 44 show the dimensions and layout of the twin screw assembly.

The screws are mounted on separate shafts and they both extend outside the barrels. The reason for this is to keep the twin-screw pipes clear of any gasifier bed media so that pyrolysis vapours can easily find their way into the gasifier bed material. This layout of the twin screw assembly is beneficial to clear any dolomite and char residue which can get into the pyrolysis vapour pipeline as well as to clean any char residue which could be carried over in the pyrolysis vapours. When the Pyroformer is coupled to the gasifier then the flow to the bio-oil collection system is disconnected by means of a high temperature knife gate valve which can be automatically interlocked on both systems. This valve acts as a barrier to prevent any vapour loss. There are two vapour outlets on the Pyroformer: one connected to existing bio-oil quenching system and the other where the twin screw coupling is attached. Both these outlets are of 200 mm diameter and are

perpendicular to each other where bio-oil quench outlet is vertical to that of the horizontal body of the Pyroformer.

Both vapour outlets on the pyroformer have a high temperature knife gate valve such as the one mentioned in section 7.1. Neither of these knife gate valves is shown in the Figures 43 and 44 but one of them is shown in Figure 47. These valves are essential to save time by providing a quick changeover between Pyroformer only and Pyrogasifier operational modes. Another important aspect which is worth mentioning is the pyrolysis vapour temperature which is always lower compared to the heater set temperature. This difference in Pyroformer heaters set temperature and evolving pyrolysis vapours is between 50-130°C due to the fact that heat is absorbed by the steel body of the Pyroformer at heater interfaces and due to poor convection heat transfer into pyrolysis vapours, pyrolysis gas temperature is low. However, a slow progressive increase in pyrolysis gas temperature has been observed over an extended operational time due to the fact that residual heat builds up in the mass of Pyroformer steel body as operation continues leading to vapour temperature increase. But even after hours of operation there was always at least a 50°C less temperature in pyrolysis vapours compared to heaters set temperature, was recorded during the various tests on Pyroformer.

Table 37 - Anticipated issues with the twin screw coupling to feed Pyroformer vapours to BFB gasifier

Cause	Effect	Action
Blockages in the connected pipework	Pressure build up, potential pipe rupture and gas leak from gaskets and Pyroformer	Install self-cleaning twin screws in pipework leading to gasifier to keep it clean
Gas leaks from the pipework joints	Explosive atmosphere leading to fire alarm and Emergency due to carbon monoxide gas release	Install high temperature graphite gaskets in the joints, do a leak test after connecting pipework
Reverse flow of gases from gasifier to Pyroformer due to higher pressures in gasifiers	Hazardous situation in Pyroformer which may lead to explosion in pyroformer due to oxygen presence	Install and interlink differential pressure measurements in gasifier and Pyroformer control system, also add a pressure controlled valve on the coupling to ensure valve closes when the differential pressure drops below certain minimum.
Twin screws not turning or broken, leading to blockage	Potential for gas escape from burst disc rupture	Install optical sensors on screw shafts to confirm rotation

Aston University

Illustration removed for copyright restrictions

Figure 45 – Dimensions of twin screw coupling part to fit between Pyroformer and gasifier (electric drive motor not shown) – taken from EBRI gasifier archive

Aston University

Illustration removed for copyright restrictions

Figure 46a - Isometric view of twin screw coupling showing extended screw ends - taken from EBRI gasifier archive

Aston University

Illustration removed for copyright restrictions

Figure 46b - Front view of twin screw coupling showing two holes for twin screw of diameter 61 mm - taken from EBRI gasifier archive

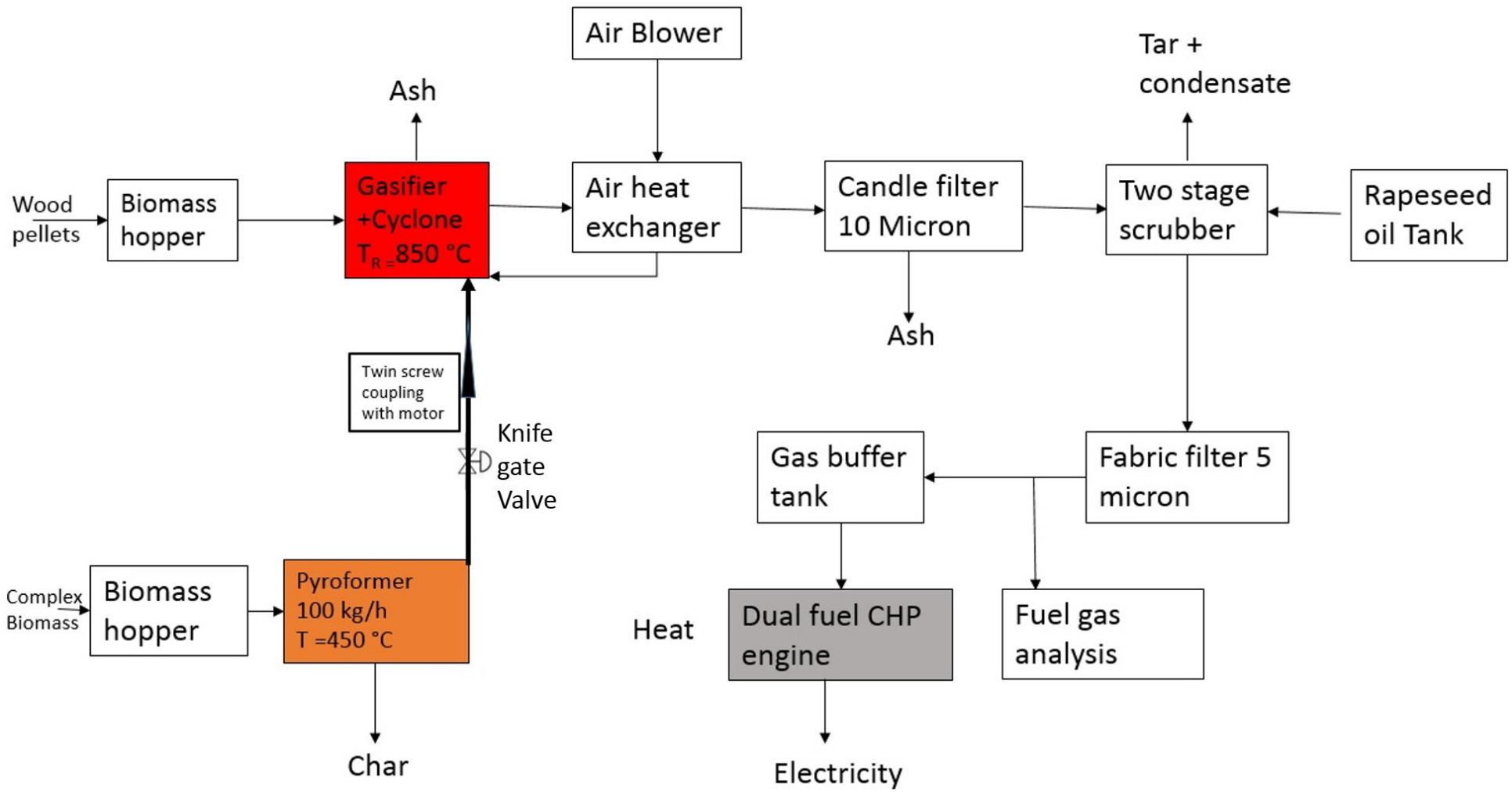

Figure 47 - Pyrogasification process flow diagram showing gasifier and Pyroformer

8.3 Operational principles of the Pyroformer and gasifier as a combined system

To safely operate both processes in integrated mode, it is essential to monitor and control a series of the pressures and temperatures in the Pyroformer and the gasifier. Pressure is important to predict the flow of gases i.e. from Pyroformer to gasifier or vice versa. The temperature and pressures can also be interlocked with the gasifier and the Pyroformer control system. It is to be understood that no hot tests of this twin-screw coupling are done between the Pyroformer and the gasifier. The information below is presented only to explain the working principles of both systems in integrated mode and no such real test was done so far. To maintain a high enough pressure in the Pyroformer so that pyrolysis vapour can flow towards the gasifier (with no reverse flow), an additional nitrogen gas purge was installed and made active during the heat-up phase of the Pyroformer. Once biomass is introduced to the gasifier and the Pyroformer then the evolution of pyrolysis vapour will maintain the gas pressure and flow from the Pyroformer to gasifier. A differential pressure of 20 mbar is maintained for normal operation and the knife gate valve is left open towards the twin screw line to transfer the pyrolysis vapours towards the gasifier. The differential pressure is measured by two separate pressure transducers, one in each system of the gasifier and Pyroformer. If the differential pressure drops to 5 mbar then the control system of gasifier sends a signal to the Pyroformer control system to close the knife gate valve to allow the pyrolysis vapours to rebuild pressure. Once the differential pressure is recovered to 20 mbar then knife gate valve is opened again. This control arrangement prevents any hazardous situation being developed due to reverse flow of gasifier gas (possibly air) to the Pyroformer leading to uncontrolled combustion and mechanical seal failures and gas leaks from the Pyroformer. During normal operation, the gasifier operates at 220 mbar and the Pyroformer operates at 240 mbar to maintain a positive flow of the pyrolysis gases to the gasifier. A nitrogen gas purge at 300 mbar is installed below the feeder valves of the Pyroformer and it can be opened or closed depending upon the need to maintain the slightly higher pressure (pyrolysis vapour flow to gasifier) within the Pyroformer compared to the gasifier.

8.3.1 General Preparations and working procedure

The working procedure involves basic health and safety compliance during the operation of the Pyroformer and gasifier in pyrogasification mode. The pyrogasification mode is defined as when the pyrolysis vapours are fed into the gasifier and both processes are working in tandem. At the beginning of the test, this includes general preparations to ensure sufficient resources are in place to conduct the test safely. The following procedures are followed:

- Ensure sufficiently well trained operational team of 5-6 people as the size of the plant dictates this many people as was highlighted in the Hazard and Operability Analysis reports.
- 2-way radio system should be available for communication between the operators on the plant floor and the operators in control room to control the Pyroformer and gasifier control systems.
- Turning on and monitoring all necessary ancillary systems such as compressed air for valves actuation, nitrogen gas system for purging, water cooling system for heat exchangers, chillers for water cooling system, gas detection system for health and safety, oil scrubbing system for gasifier, ash removing system for gasifier, gas flare system, char handling system for Pyroformer and any other relevant systems as described by the gasifier vendor in the gasifier operational manual
- Constant monitoring of the operational units by operators on the plant floor and by operators in the control room
- One operator to control the Pyroformer control system and one operator to control the gasifier control system, both of these to be situated in the control room
- Loading of biomass to be tested in the respective systems and topping up and fluids and checking of gauges etc. to ensure all equipment is functioning correctly

8.3.2 Heating up the gasifier to bring it to working temperature

In this step, the gasifier and Pyroformer are heated in parallel to ensure both systems are ready to feed the biomass at the same time to be operational in pyrogasification mode. Heating up of the gasifier is initiated with preheated air with 100 kW electrical heaters installed on the gasifier air supply from the blower

fan and combustion starts inside the gasifier after 450 °C temperature is reached in the preheated air with wood pellets feed. After this, due to wood pellets heat the gasifier in combustion mode and the electrical heat load is gradually reduced. The step by step process is carried out as below;

- Start electrical heating up the gasifier while running the air blower fan to the gasifier, monitor the gasifier control system for irregularities
- Switching on the twin interface screw motor to prevent solids intake in the pipe
- Switching on the N_2 purge of the twin interface screw to keep the screws cooled and cleaned of dolomite dust
- Wait for the gasifier to reach temperature of 450 °C
- Start feeding the wood pellets to the gasifier and initiate combustion process
- Start feeding the dolomite bed material in the gasifier and filling up to max level for desired pressure in the gasifier of 220 mbar
- Continue heating up the gasifier in combustion mode with wood pellets to optimum temperature 850 °C
- Hold the set temperature of gasifier in combustion mode and wait until the pyroformer has reached its working set-temperature 450 °C

8.3.3 Pyroformer heating up phase

In this mode the Pyroformer is heated to its desired set temperature (450 °C) while the hot gas temperature within the Pyroformer is always lower by between 50-100°C. This process is carried out in tandem with the gasifier heating process as described above. The process is executed in the following sequence

- Starting electrical heating of the pyroformer with 50 or 100 °C increments to pyrolysis temperature as per modified checklist similar to Appendix 2
- Start nitrogen purge to displace any organic vapours to ensure safe environment in the Pyroformer and maintain a slightly higher pressure compared to gasifier
- Continue electrical heating to the pyrolysis set temperature
- Hold the set temperature and wait until the gasifier has reached its set-temperature

8.3.4 General operation of Pyroformer-gasifier coupled mode (Pyrogasification mode)

This is the actual mode where pyrogasification takes place due to the Pyroformer and gasifier being integrated. During this mode as pyrolysis gases are fed into the gasifier, the gasifier control system makes the adjustments to the wood pellets feeding based on the pressure readings from pressure transducers installed on the gasifier. It is expected that the gasifier fluidised bed density will decrease due to the presence of extra gases per unit in the gasifier bed from the Pyroformer compared to normal operation of the gasifier alone. Only two parameters are measured in the gasifier to control the process. Firstly, the temperature in the gasifier is measured and maintained between 800-850°C so that ash melting point is not reached by a PID controller of the gasifier air blower. Secondly, the differential pressure in the gasifier is measured between two points i.e. the air pressure at the air inlet into distributor nozzles and the syngas pressure in the riser to be no greater than 20 mbar. If the air pressure becomes higher than 20 mbar this indicates high solids content or too much bed material and vice versa and to counter this effect of solids are added. To decide between which material (dolomite or wood pellets) is to be added, this is achieved by monitoring the syngas quality and quantity which is measured after final filtration stage where total gas flow volume is also measured by a gas flow meter and gas quality for CO, H_2 and CH_4 in gas analyser. If the gas quantity was reduced then more wood pellets are added and if the gas quality was deteriorated then more dolomite is added but only in small quantities to be within the temperature and pressure operational limits. Due to the extra pyrolysis gas coming from the Pyroformer the density of bed will decrease leading to a lower pressure drop which is compensated by wood pellets intake to maintain syngas quantity by the flow meter and by the pressure drop across the bed in the gasifier. In essence by using this integrated process the capacity of the produced syngas can be increased by up to one third of the gasifier design capacity. The operational and control sequence is continued from previous sections 8.6.2 and 8.6.3.

- Start feeding biomass pellets to the pyroformer with a desired feed rate lower than maximum design throughput of the Pyroformer
- At the point when feeding of pyrolysis gas is initiated to the gasifier, the feed of the gasifier plug screw will reduce proportionally to maintain certain

set pressure in the gasifier as energy will come from the pyroformer or syngas quantity will increase if the desired outcome is to enhance the syngas production volume. The temperature of the gasifier will stay at its set point due to the automation auto-pilot

- During operation actively monitor the pressure and temperature in the interface to ensure the positive flow of pyrolysis gases to the gasifier
- Monitor the fuel gas quality and flow on the control system
- Ensure constant monitoring of the plant by operators

8.3.5 Decoupling the Pyrogasification mode to end the test

When the desired objectives are achieved then both processes can be stopped. At this point operators can then choose to run both processes independently or shut them down. To continue running them independently the knife gate valve can be closed on the twin screw pyrolysis gas line and the other knife gate valve on the biodiesel quench line can be opened. If the objective here is to safely shut down both processes then the procedure below is followed.

- Stop the biomass feed to the Pyroformer but continue heating and nitrogen purging
- Allow the wood pellet feed rate of the gasifier plug screw to recover slowly due to automation auto-pilot to the same level as before the pyrogasification. Empty out the char from the pyroformer by activating empty char mode on Pyroformer
- Allow cool down of the pyroformer as described in the shutdown procedure of the pyroformer
- Constant monitoring of the plant by the operators

8.3.6 Shut down of both processes

The shutdown of both processes is completed in various stages to ensure plant safety and operability is not compromised. To shut down both processes the procedure is described below;

- After the char is taken out of the pyroformer stop feeding the wood pellets to the gasifier
- Allow the remaining wood pellets to burn out in the gasifier by stopping the feed of wood pellets and maintaining the air flow up to the point where the

temperature in the gasifier starts to drop down (all fuel consumed in the gasifier)

- After a waiting time of 5 minutes turn of the fluidized bed fan of the gasifier
- Shut down the gasifier as described in its normal shut down procedure by gradually turning off the ancillary systems one by one

8.3.7 End of test and complete shutdown of ancillary systems

The procedure below is followed after both processes are completely and safely shut down;

- Tour throughout the plant for inspection for any irregularities
- Inspect for any leaks, any local alarms and any equipment behaving abnormally
- Shutdown all ancillary equipment
- Remove any waste and arrange waste disposal.
- Tidy up the plant.
- Discuss and review the experiment with the team and record areas of improvement
- Acquire logged experimental data from control system for analysis

If for any reason some emergency situation is created then both processes can be safely shut down by means of their own emergency shutdown procedures. In all cases, failsafe pneumatic valves can be activated from the control system of both systems, even if the power is lost as they have uninterruptible power supply (UPS) for backup. In this case all electrical units are tripped and only the communication between valves, temperatures and pressures is available as well as the compressed air and nitrogen gas for purging. Because the motive force is applied by compressed air to the valves the valves can opened or closed and nitrogen gas can be purged if needed. If the gas pressure builds up because of the shutdown of the gas flaring system then the pressure relief valve is activated on the gasifier line and the bursting disc on Pyroformer may be activated. In both cases the escaping gases are released outside the building into a safe area as was approved by Hazard Operability (HazOp) Analysis.

8.4 Summary of the chapter

A very novel study to enable pyrogasification by integrating a Pyroformer and a BFB gasifier has been presented in this chapter. The benefits of pyrogasification

are: significantly lower tar content in the fuel gas and use of complex biomass feedstock flexibility. The process avoids making complex bio-oil requiring further upgrade downstream. In this chapter, results from the commissioning of a commercial scale bubbling fluidised bed gasifier have been presented. Though there were plans to do detailed scientific tests in the gasifier, due to resource limitations this was not possible and instead, the data from a BFB gasifier commissioning test only are presented here. During the test, the gasifier was running without major problems with automation. However, there were fluctuations in the syngas flow, gasification temperature and syngas composition. The syngas volume flow of 788 m^3/h, syngas total energy flow of 1.197 MW and a syngas composition containing CO (17.3 vol%), hydrogen (13.3 vol%), methane (4 vol%) and CO_2 17 vol% were recorded on average. The average gasification temperature was 818 °C. There was some correlation between gasification temperature and syngas flowrate, such that by increasing the temperature the carbon conversion efficiency was increased leading to increased gas flowrate.

It has been demonstrated that the pyrogasification treatment of complex biomass feedstocks can lead to benefits in improving the economics of gasification processes. The economics of the gasifier process can be improved by adding a pyrolysis process upstream, thus enabling a wide variety of complex feedstocks to be used in the pyrolysis step and then only taking the vapours and gaseous products into the gasifier. In this way problematic ash is retained in the pyrolysis step and most of the volatiles are used for fuel gas production which can then be used in the engines for electricity, heat and cooling production.

This means the gasifier which was designed for expensive (£200/ton) wood pellets of certain type can now be fed on a wide range of feedstocks (not conventionally used in gasifiers) such as dry digestates, chicken litter, sewage sludge and other complex industrial wastes entering first the Pyroformer. It is also possible that most (if not all) of the wood pellets taken into the gasifier can be replaced by pyrolysis gas and char (permitting char melting point above gasification temperature). This excess pyrolysis gas and char quantity can be supplied by more than one such Pyroformer or a bigger Pyroformer to match the scale of the gasifier. In both cases, the dolomite will still be required as catalytic material for fluidization and for gas cleaning. When the gasifier is combined in this way there are three important changes taking place. Firstly, there is low air demand for fluidisation

due to low bed density/pressure drop leading to lower nitrogen content in the syngas, which leads to an improvement in the calorific value. Secondly, a great portion of the heat demand for the gasifier is supplied from the hot pyrolysis gas thus lower air volume is needed to generate heat via exothermic reactions within the gasifier (this also links to first point). Thirdly, there will be a loss of the char bed catalytic effect due to the lower wood pellet intake to maintain the pressure drop across the gasifier bed, if Pyroformer char is not used in the gasifier. This leads to a lower char volume available per unit volume of air/syngas which is undesirable. There are three possibilities for tar cracking promoted by thermal cracking due to the high temperature in the gasifier, catalytic cracking by the dolomite and catalytic cracking by char. Hence, a compromise is to be made between tar cracking by char due to lowering of wood pellet feed rate and compensating it with pyrolysis gas and the Pyroformer char. Perhaps the loss of char activity could be compensated by the fact that pyrolysis gas is already gone through a volatile and tar cracking stage in the Pyroformer by char recirculation and now (with lower tar loading) it will be even easier for these gaseous vapours to be cracked further by dolomite and thermal cracking. The extent of these effects need to be further explored during combined pyrogasification hot tests.

The pyrogasification step as described above also provides the benefit of the avoidance of size reduction and/or pelletisation steps of the biomass preparation, as the screws of the Pyroformer can easily transport biomass materials of varying shapes and sizes thus providing feedstock diversity and easier handling of complex feedstocks. However, integration of both processes in this way needs to be fully proven through further experimentation. It is likely that there will be some minor teething issues such as pyrolysis gas flow management towards gasifier, fluidisation air pressure management in the gasifier and the wood pellet feed adjustments in the gasifier in first few tests. These will need resolving as is normal with any new technical design.

For pyrogasification to work in this integrated manner, it is absolutely essential that the twin-screw coupling works correctly without becoming blocked and to maintain a constant flow of pyrolysis gas from the Pyroformer to the gasifier. The success of the pyrogasification is very dependent on this twin-screw coupling and the operation steps as described above. The suggested design has been based on the available technology at EBRI for this research. Other designs would be

possible; for instance, it is also possible that, in downdraft or updraft gasifiers the twin-screw coupling may not be needed as there is no fluidization of the bed taking place, in which case a simple connecting pipe between both processes will be sufficient to enable the pyrogasification.

The emission reductions are possible by introducing a system change for currently naturally decaying woody biomass through pyrogasification and by displacing the energy production from fossil fuels and producing biochar for land application. Pyrogasification of naturally decaying waste wood provides an excellent route for carbon emissions reduction by using biochar from pyrolysis process for land application and fuel gas for substituting fossil fuels for energy production. Currently, pyrogasification is the only possible route which can provide the biochar and a fuel gas which can be used directly for bioenergy and carbon sequestration without further modifications in an engine as opposed to complex bio-oil from pyrolysis.

Chapter 9 – Conclusion and recommendations

In this chapter a detailed summary of the intermediate pyrolysis reactor (Pyroformer) based on experimental work is presented. This provides an overview of the objectives and the associated findings.

9.1 Conclusions

In this project, three different models of the intermediate pyrolysis reactor (Pyroformer) have been tested. Screw pyrolysis systems provide the added advantage of ease of material transportation of varying sizes and shapes within the reactor. The hypothesised potential benefits of tar cracking by char recycling with twin screw arrangement of the Pyroformer has been tested experimentally. Dry digestate, wood pellets (ENPlus A1 standard) and miscanthus have been used in the Pyroformer. Digestates are typically used for land spreading which causes management problems in terms of storage and odours. Land spreading, however, is only required at certain times of year while for the rest of the year the digestates have to be stored up for months in sealed digester vessels to prevent odours escaping. Using solid fractions from anaerobic digesters for pyrolysis provides an alternative way to manage digestates. This is achieved by mechanical separation of solids from the digestate and then further drying. The remaining liquid digestate can mostly be recycled back into the process or spread on the land. This also means digestate materials can now be processed through intermediate pyrolysis and more value can be added to this resource and storage risks eliminated. During pyrolysis these complex residues produce bio-oil, char and gases or the residues can be converted to a fuel gas through pyrogasification. Altogether the main objectives set out in Chapter 3 have been met in the following ways:

- The residence time of the biomass in the Pyroformer inner screw was calculated in Chapter 4 (section 4.2) by means of a cold model of the Pyroformer. A small difference of 10% between the theoretical and experimental residence times was discovered. It has been proven that residence time of more than 2 minutes was achievable in the Pyroformer by altering the rotational speed of the inner screw. Experimental residence times of 2, 3.5 and 6 minutes were achieved with an inner screw rpm of 7.1, 4 and 2.3 respectively. These were sufficient residence times to release

most of the volatiles from the biomass as be confirmed by thermogravimetric analysis.

- It was also discovered (Chapter 4, section 4.3) that the time taken to reach the steady state varies with the residence time as well as with the varying feeding rates.
- Char to biomass ratio has been calculated (shown in Table 17) for the first time for a twin screw counter rotating arrangement. The char to biomass ratios varied with the rpm of inner and outer screws as well as with the feed rates. It was discovered that higher feed rates lead to the lower char to biomass ratios and that this may affect the anticipated benefits of char recirculation for tar cracking.
- A variety of biomass feedstocks were tested In Chapter 5 in hot pyrolysis experiments and the results presented. It was discovered that lower feeding rates with increasing char to biomass ratio led to more gas product being formed whereas liquid yield was reduced. The optimum char to biomass ratio of 3.1 was discovered for the 5 kg/h feeding rate for green rye and corn derived digestate.
- The organic phase of the bio-oil from digestates exhibited a very low total acid number which is associated with the material composition. Nearly all digestate derived feedstocks led to a total acid number below 1. For wood and miscanthus pellets the total acid numbers were 17.0 and 5.33 mgKOH/g.
- Direct quenching of pyrolysis vapours with biodiesel was performed in a large scale Pyroformer of 100 kg/h and the resulting blend of bio-oil and biodiesel inherited similar properties to those of biodiesel with the exception of higher total acid number and viscosity.
- A blend of bio-oil and biodiesel was prepared by the in-situ blending technique involving direct quenching of pyrolysis vapours with biodiesel. The blend produced in this way contained 19.75 wt. % bio-oil from wood pellets and 11.28 wt. % bio-oil from miscanthus derived feedstocks, showing good fuel properties to be used in diesel engines.
- Biochars derived from miscanthus and wood pellets were analysed for application in soil amendment and were compared against voluntary standards from the International Biochar Initiative and British Biochar Foundation. The values for toxic metals were found to comply with these

standards. It was also shown that these biochars can be applied to agricultural land to achieve soil amendment benefits as is allowed by UK Environment Agency.

- Carbon emission reductions calculations in Chapter 6 were estimated based on the methodology developed by Gaunt et al [54] for wood pellet derived char for the 100 kg/h pyrogasification system. Emission reductions according to soil type for biochar application, and to the type of conventional energy source (without biochar production) against which the comparison was made, were thus found to be as follows. For biochar application in acidic soil, 685.24 and 870.78 tonnes per annum as compared to the use of natural gas and coal respectively. For application in alkaline soil, 711.48 and 897.02 tonnes per annum as compared to the use of natural gas and coal respectively.
- A design review of three critical components of Pyroformer process was carried out in Chapter 7. These three components included valves of the biomass feeding system, char collection and cooling system and biodiesel quenching system redesign to lower the high throughput of the biodiesel in the quenching process. A pair of knife gate valves for the feeding and char outlet assembly was recommended to overcome valve failure due to thermal issues. For char cooling and collection system, a water-cooled screw conveyor was recommended to ensure the continuous operation of the Pyroformer. A chiller based counter current heat exchanger was recommended to be used with the existing biodiesel quenching system to reduce the biodiesel consumption and to enhance the process economics and the bio-oil content in the resulting blend of bio-oil and biodiesel.
- In Chapter 8 the bubbling fluidised bed gasifier was used for a commissioning test and some data were presented. During the commissioning test of the gasifier, the syngas flowrate of 788 m^3/h, syngas total energy of 1.197 MW and a syngas composition containing CO (17.3 vol%), hydrogen (13.3 vol%), methane (4 vol%) and CO_2 17 vol% were recorded on average. The average gasification temperature was 818 °C. There was some correlation between gasification temperature and syngas flowrate as by increasing the temperature the carbon conversion efficiency was increased leading to increased gas flowrate.

- A detailed design of the twin screw coupling is presented with an electric drive motor to feed the pyrolysis vapours into a bubbling fluidised bed gasifier.
- In Chapter 8 a detailed operational and control philosophy for integrated Pyroformer and gasifier operation has been presented to ensure well-integrated, smooth and safe operation of both processes to enable operation in pyrogasification mode.

9.2 Recommendations

The cold flow experiments of Chapter 4 have provided understanding regarding the char to biomass ratios in intermediate pyrolysis. But more tests need to be conducted to validate fully the char to biomass ratio model developed from the experiments in the cold Pyroformer and apply it to hot Pyrolysis experiments. Validation tests in a hot pyroformer with duplicate and triplicate results are needed to conclusively understand the density differences between the hot and cold model.

The Pyroformer is based on a twin-screw counter rotating concept which has its limitations preventing the throughput being achieved without blockages at the feed inlet. More tests are needed for long durations, possibly extending to continuous operation for days if not weeks, to fully assess the design throughput of this system. Perhaps it will be better to use single screw rather than twin-screws system to counter the blockages in the system.

Some results for pyrolysis tests in Chapter 5 in a 20 kg/h Pyroformer gave scattered results in parametric studies, leading to ambiguous conclusions and hence it is recommended that further tests be carried out to establish more conclusive findings. It is recommended to repeat some of the tests at 3 and 5 kg/h and also do further tests at 10 kg/h to confirm conclusions about the impact of higher feeding rate and of char to biomass ratio at higher feeding rates on the pyrolysis products. Char analysis of the DCL and DAC materials should be further analysed for other mineral content to establish their suitability for application in agricultural soils. This will help to understand the char ash composition and detect further inorganic species (e.g. potassium and sodium) which may well have some catalytic effect in addition to char and potassium which tend to form a better organic phase in the bio-oil.

It was discovered that bio-oils from the digestate materials have very low total acid numbers compared to wood pellets derived bio-oil (Chapter 5). Hence it is recommended that digestate bio-oil be used as a quenching fluid to balance the total acid number of the bio-oil. It is also possible that digestate derived bio-oils can be blended post condensation with other bio-oils with high total acid numbers to reduce the total acid numbers of such highly acidic bio-oils. This could be more beneficial for fast pyrolysis bio-oils which are more acidic due to high oxygen content compared to intermediate pyrolysis oils.

In Chapter 6 quenching of pyrolysis vapours with biodiesel shows good potential but more needs to be understood about the chemical reactions between biodiesel and pyrolysis vapours at different blending conditions especially temperature. There could be some reforming reactions taking place leading to smaller fraction of aqueous phase, but this is not fully understood yet and deserves further exploration as minimum aqueous phase in bio-oil is highly desirable. Since the biodiesel content in the in-situ blended liquid is very high at >80 wt. %, it is recommended to use a heat exchanger with a separate chiller to lose heat outside the process and thus enhance the bio-oil ratio in the blend.

The literature shows that biochar exhibits some excellent properties for soil remediation, however biochar may contain some hazardous organic and inorganic components. Therefore, further characterization of biochar for nutrients and potential contaminants must be conducted in future. Field and pot trials of biochar produced from pyrolysis tests must be conducted on selected plant species and the anticipated benefits of biochar must be confirmed before applying the biochar on land at large scale. It is strongly recommended that detailed studies need to be conducted to include complete life cycle assessment (LCA) of the process. Also, there is some evidence of Polycyclic Aromatic Hydrocarbons (PAH), Polychlorinated Biphenyls (PCB) found in the biochar according to the literature. Each biochar source needs to be analysed to ensure no such carcinogens are deployed with.

The carbon emission reductions by the systems change for naturally decaying wood were estimated for bioenergy production and biochar application for carbon sequestration in land, were estimated in comparison ti conventional fossil fuel

energy supply. These estimations need to be validated by a complete lifecycle analysis of naturally decaying wood in bioenergy and biochar application.

In Chapter 8 the gasifier commissioning test was an attempt to highlight the experimental data about the syngas quantity, quality and operational parameters. However, further tests must be conducted on a prolonged and repeated basis to evaluate the apparent benefits of BFB gasifier technology and its coupling with the Pyroformer.

Pyrogasification is a novel concept and this thesis has presented an important first step to review the design for an integrated system which can work effectively. It is recommended that further tests be conducted on the integrated pyrogasification system. In particular, the possibility to obtain better turn down ratio of the gasifier merits further investigation, as wood pellet feed can be compensated by pyrolysis gas supply, such that inlet air velocity for effective fluidisation will also be low. Hence it may well be possible to have a better turn down ratio corresponding to reduced syngas output. Also, as mentioned there could be a beneficial effect on the syngas quality due to the two-stage pyrolysis and gasification process to reduce the tar content in the syngas. This anticipated benefit in syngas quality by tar conversion should also be fully tested as the Pyroformer and gasifier integrated system coupling is ready for the pyrogasification tests.

Benefits associated with pyrogasification can be huge if the pyrolysis step can be added to a gasifier system, as gasifier systems running on ENPlus wood are not currently economically viable. The benefits will include giving the gasifier flexibility to use cheap, more complex and abundantly available residues to be used via the upstream Pyroformer thus enhancing the gasifier process economics. However, until extensive tests are carried out in coupled Pyroformer and gasifier systems, the benefits and potential long-term technical problems are not fully quantifiable. It is therefore strongly recommended that further Pyrogasification tests be carried out on the EBRI plant at Aston University, as this is ready for operation.

List of References

1. Unknown. *Micro conveyor - Mechanical water cooled screw conveyor*. 2017 20/06/2017; Available from: http://velodynesystems.com/micro-conveyor.html.

2. Khandani, S., *Engineering design process: Education transfer plan.* Retrieved Feb, 2005. **6**: p. 2016.

3. Bridgwater, A.V., *Review of fast pyrolysis of biomass and product upgrading.* Biomass and bioenergy, 2012. **38**: p. 68-94.

4. Beaton, J., H. Peterson, and N. Bauer, *Some aspects of phosphate adsorption by charcoal.* Soil Science Society of America Journal, 1960. **24**(5): p. 340-346.

5. Steiner, C., *Biochar carbon sequestration.* University of Georgia, Biorefining and Carbon Cycling Program, Athens, GA, 2008. **30602**.

6. Goyal, H.B., D. Seal, and R.C. Saxena, *Bio-fuels from thermochemical conversion of renewable resources: A review.* Renewable & Sustainable Energy Reviews, 2008. **12**(2): p. 504-517.

7. Ni, M., et al, *An overview of hydrogen production from biomass.* Fuel processing technology, 2006. **87**(5): p. 461-472.

8. Topić, M. and H. Biedermann, *Planning of integrated/sustainable solid waste management (ISWM)-model of integrated solid waste management in Republika Srpska/B&H.* Serbian Journal of Management, 2015. **10**(2): p. 255-267.

9. Hoornweg, D. and P. Bhada-Tata, *What a waste: a global review of solid waste management.* 2012.

10. Morris, J.R., P.S. Phillips, and A.D. Read, *Developments: The UK Landfill Tax: Financial Implications for Local Authorities.* Public Money and Management, 2000. **20**(3): p. 51-54.

11. Astrup, T., C. Riber, and A.J. Pedersen, *Incinerator performance: effects of changes in waste input and furnace operation on air emissions and residues.* Waste Management & Research, 2011: p. 0734242X11419893.

12. Badeau, J.-P. and A. Levi, *Biomass gasification: chemistry, processes, and applications*. 2009: Nova Science Publishers.

13. Sawatdeenarunat, C., et al, *Anaerobic digestion of lignocellulosic biomass: Challenges and opportunities.* Bioresource technology, 2015. **178**: p. 178-186.

14. Erakhrumen, A.A., *Biomass gasification: documented information for adoption/adaptation and further improvements toward sustainable utilisation of renewable natural resources.* ISRN Renewable Energy, 2012. **2012**.

15. Hornung, A., A. Apfelbacher, and S. Sagi, *Intermediate pyrolysis: a sustainable biomass-to-energy concept-biothermal valorisation of biomass (BtVB) process.* Journal of scientific and industrial research, 2011. **70**(8).

16. Azeez, A.M., et al, *Fast pyrolysis of African and European lignocellulosic biomasses using Py-GC/MS and fluidized bed reactor.* Energy & Fuels, 2010. **24**(3): p. 2078-2085.

17. Faccini, C.S., et al, *Comprehensive 2D GC with TOF-MS detection: study of pyrolytic bio-oil of Kraft mill residues.* Journal of the Brazilian Chemical Society, 2013. **24**(7): p. 1085-1098.

18. Michailof, C., et al, *Quantitative and qualitative analysis of hemicellulose, cellulose and lignin bio-oils by comprehensive two-dimensional gas chromatography with time-of-flight mass spectrometry.* Journal of Chromatography A, 2014. **1369**: p. 147-160.

19. Oasmaa, A., E. Kuoppala, and Y. Solantausta, *Fast pyrolysis of forestry residue. 2. Physicochemical composition of product liquid.* Energy & fuels, 2003. **17**(2): p. 433-443.

20. Mahmood, A.S., et al, *The intermediate pyrolysis and catalytic steam reforming of Brewers spent grain.* Journal of analytical and applied pyrolysis, 2013. **103**: p. 328-342.

21. Moraes, M.S.A., et al, *Analysis of products from pyrolysis of Brazilian sugar cane straw.* Fuel Processing Technology, 2012. **101**: p. 35-43.

22. Moraes, M.S.A., et al, *Qualitative analysis of bio oils of agricultural residues obtained through pyrolysis using comprehensive two dimensional gas chromatography with time-of-flight mass spectrometric detector.* Journal of Analytical and Applied Pyrolysis, 2012. **98**: p. 51-64.

23. Duman, G., et al, *The slow and fast pyrolysis of cherry seed.* Bioresource Technology, 2011. **102**(2): p. 1869-1878.

24. Dayton, D., et al, *Release of inorganic constituents from leached biomass during thermal conversion.* Energy & Fuels, 1999. **13**(4): p. 860-870.

25. Bradbury, A.G., Y. Sakai, and F. Shafizadeh, *A kinetic model for pyrolysis of cellulose.* Journal of Applied Polymer Science, 1979. **23**(11): p. 3271-3280.

26. Saxena, R., D. Adhikari, and H. Goyal, *Biomass-based energy fuel through biochemical routes: a review.* Renewable and Sustainable Energy Reviews, 2009. **13**(1): p. 167-178.

27. Li, S., et al, *Fast pyrolysis of biomass in free-fall reactor for hydrogen-rich gas.* Fuel Processing Technology, 2004. **85**(8): p. 1201-1211.

28. Li, X., et al, *Biomass gasification in a circulating fluidized bed.* Biomass and bioenergy, 2004. **26**(2): p. 171-193.

29. Maher, K. and D. Bressler, *Pyrolysis of triglyceride materials for the production of renewable fuels and chemicals.* Bioresource technology, 2007. **98**(12): p. 2351-2368.

30. Bioenergy, I., *Bioenergy–a sustainable and reliable energy source.* International Energy Agency Bioenergy, Paris, France, 2009.

31. Hossain, A. and P. Davies, *Pyrolysis liquids and gases as alternative fuels in internal combustion engines–A review.* Renewable and sustainable energy reviews, 2013. **21**: p. 165-189.

32. Saidur, R., et al, *A review on biomass as a fuel for boilers.* Renewable and Sustainable Energy Reviews, 2011. **15**(5): p. 2262-2289.

33. Yaman, S., *Pyrolysis of biomass to produce fuels and chemical feedstocks.* Energy conversion and management, 2004. **45**(5): p. 651-671.

34. Diebold, J.P., *A review of the chemical and physical mechanisms of the storage stability of fast pyrolysis bio-oils*. 2000: Citeseer.

35. Llorente, M.F., et al, *Combustion in bubbling fluidised bed with bed material of limestone to reduce the biomass ash agglomeration and sintering.* Fuel, 2006. **85**(14): p. 2081-2092.

36. Wang, M., M. Wu, and H. Huo, *Life-cycle energy and greenhouse gas emission impacts of different corn ethanol plant types.* Environmental Research Letters, 2007. **2**(2): p. 024001.

37. Sharma, A., V. Pareek, and D. Zhang, *Biomass pyrolysis—A review of modelling, process parameters and catalytic studies.* Renewable and Sustainable Energy Reviews, 2015. **50**: p. 1081-1096.

38. Nhuchhen, D.R., P. Basu, and B. Acharya, *A comprehensive review on biomass torrefaction.* International Journal of Renewable Energy & Biofuels, 2014. **2014**: p. 1-56.

39. Balat, M., *Production of bioethanol from lignocellulosic materials via the biochemical pathway: a review.* Energy conversion and management, 2011. **52**(2): p. 858-875.

40. Schenk, P.M., et al, *Second generation biofuels: high-efficiency microalgae for biodiesel production.* Bioenergy research, 2008. **1**(1): p. 20-43.

41. Byrne, J., *Biofuels to Blame for Palm Oil Deforestation, Says Nestlé.* FoodNavigator. com, April, 2010. **19**.

42. Ullah, K., et al, *Assessing the lignocellulosic biomass resources potential in developing countries: A critical review.* Renewable and Sustainable Energy Reviews, 2015. **51**: p. 682-698.

43. Aramideh, S., et al, *Numerical simulation of biomass fast pyrolysis in an auger reactor.* Fuel, 2015. **156**: p. 234-242.

44. Openshaw, K., *A review of Jatropha curcas: an oil plant of unfulfilled promise.* Biomass and Bioenergy, 2000. **19**(1): p. 1-15.

45. Mohan, D., C.U. Pittman, and P.H. Steele, *Pyrolysis of wood/biomass for bio-oil: a critical review.* Energy & fuels, 2006. **20**(3): p. 848-889.

46. Bridgwater, A., P. Carson, and M. Coulson, *A comparison of fast and slow pyrolysis liquids from mallee.* International journal of global energy issues, 2007. **27**(2): p. 204-216.

47. Demirbaş, A., *Gaseous products from biomass by pyrolysis and gasification: effects of catalyst on hydrogen yield.* Energy Conversion and Management, 2002. **43**(7): p. 897-909.

48. Knoef, H. and J. Ahrenfeldt, *Handbook biomass gasification*. 2005: BTG biomass technology group The Netherlands.

49. Lam, S.S., et al, *Progress in waste oil to sustainable energy, with emphasis on pyrolysis techniques.* Renewable and Sustainable Energy Reviews, 2016. **53**: p. 741-753.

50. Center, B.E., *Biomassenergycentre. org. uk.* Retrieved on, 2012: p. 02-28.

51. Bridgwater, A.V., *Renewable fuels and chemicals by thermal processing of biomass.* Chemical Engineering Journal, 2003. **91**(2): p. 87-102.

52. Maschio, G., C. Koufopanos, and A. Lucchesi, *Pyrolysis, a promising route for biomass utilization.* Bioresource technology, 1992. **42**(3): p. 219-231.

53. Elliott, D., et al, *Developments in direct thermochemical liquefaction of biomass: 1983-1990.* Energy & Fuels, 1991. **5**(3): p. 399-410.

54. Veses, A., et al, *Production of upgraded bio-oils by biomass catalytic pyrolysis in an auger reactor using low cost materials.* Fuel, 2015. **141**: p. 17-22.

55. Zhang, Q., et al, *Review of biomass pyrolysis oil properties and upgrading research.* Energy conversion and management, 2007. **48**(1): p. 87-92.

56. Bridgwater, A., *Principles and practice of biomass fast pyrolysis processes for liquids.* Journal of analytical and applied pyrolysis, 1999. **51**(1): p. 3-22.

57. Tumiatti, V., *A Flexible Three-Stage Thermochemical Conversion Process.* 2015.

58. Bacq, A., et al, *NOTAR®-Novel two stage downdraft gasifier for production of clean syngas for industrial applications.*

59. Henriksen, U., et al, *The design, construction and operation of a 75kW two-stage gasifier.* Energy, 2006. **31**(10): p. 1542-1553.

60. Andreas Hornung, A.A., *GB2460156 - Thermal treatment of biomass* in *UK Patent Office*, L. Intellectual Property Office, Editor. 2009: United Kingdom.

61. Neumann, J., et al, *Production and characterization of a new quality pyrolysis oil, char and syngas from digestate–Introducing the thermo-catalytic reforming process.* Journal of Analytical and Applied Pyrolysis, 2015. **113**: p. 137-142.

62. Brandt, P., E. Larsen, and U. Henriksen, *High tar reduction in a two-stage gasifier.* Energy & Fuels, 2000. **14**(4): p. 816-819.

63. Wu, C. and P.T. Williams, *Hydrogen production by steam gasification of polypropylene with various nickel catalysts.* Applied Catalysis B: Environmental, 2009. **87**(3): p. 152-161.

64. Milhé, M., et al, *Autothermal and allothermal pyrolysis in a continuous fixed bed reactor.* Journal of Analytical and applied pyrolysis, 2013. **103**: p. 102-111.

65. Jahirul, M.I., et al, *Biofuels production through biomass pyrolysis—a technological review.* Energies, 2012. **5**(12): p. 4952-5001.

66. Haiping, Y., C. Hanping, and Y. Rong, *The influence of temperature on biomass pyrolysis in fixed bed.* ACTA ENERGIAE SOLARIS SINICA, 2007. **28**(10): p. 1152.

67. Mullen, C.A., et al, *Bio-oil and bio-char production from corn cobs and stover by fast pyrolysis.* Biomass and bioenergy, 2010. **34**(1): p. 67-74.

68. Oasmaa, A. and D. Meier, *Norms and standards for fast pyrolysis liquids: 1. Round robin test.* Journal of Analytical and Applied Pyrolysis, 2005. **73**(2): p. 323-334.

69. Oasmaa, A. and E. Kuoppala, *Fast pyrolysis of forestry residue. 3. Storage stability of liquid fuel.* Energy & Fuels, 2003. **17**(4): p. 1075-1084.

70. Domínguez, A., et al, *Production of bio-fuels by high temperature pyrolysis of sewage sludge using conventional and microwave heating.* Bioresource technology, 2006. **97**(10): p. 1185-1193.

71. Sharma, R.K., et al, *Characterization of chars from pyrolysis of lignin.* Fuel, 2004. **83**(11): p. 1469-1482.

72. Lehmann J and J. S., eds. *Biochar for environmental management: an introduction. in: Lehmann, J and Joseph, S. (Eds.), Biochar for Environmental Management Science and Technology*. 2009, Earthscan Publisher, UK and USA. 1-9.

73. Liang, B., et al, *Black carbon increases cation exchange capacity in soils.* Soil Science Society of America Journal, 2006. **70**(5): p. 1719-1730.

74. Bruun, E.W., et al, *Influence of fast pyrolysis temperature on biochar labile fraction and short-term carbon loss in a loamy soil.* Biomass and Bioenergy, 2011. **35**(3): p. 1182-1189.

75. Zhang, A., et al, *Change in net global warming potential of a rice–wheat cropping system with biochar soil amendment in a rice paddy from China.* Agriculture, ecosystems & environment, 2013. **173**: p. 37-45.

76. Zhai, L., et al, *Short-term effects of maize residue biochar on phosphorus availability in two soils with different phosphorus sorption capacities.* Biology and Fertility of Soils, 2015. **51**(1): p. 113-122.

77. Couhert, C., J.-M. Commandre, and S. Salvador, *Is it possible to predict gas yields of any biomass after rapid pyrolysis at high temperature from its composition in cellulose, hemicellulose and lignin?* Fuel, 2009. **88**(3): p. 408-417.

78. Dominguez, A., et al, *Conventional and microwave induced pyrolysis of coffee hulls for the production of a hydrogen rich fuel gas.* Journal of Analytical and Applied Pyrolysis, 2007. **79**(1): p. 128-135.

79. Bridgwater, A.V., G. Evans, and D. Teknik, *An assessment of thermochemical conversion systems for processing biomass and refuse*. 1993: Energy Technology Support Unit Harwell.

80. Vos, J. and M. Vis, *Making Charcoal Production in Sub Sahara Africa Sustainable.* NL Agency, The Netherlands, 2010.

81. Maschio, G., A. Lucchesi, and G. Stoppato, *Production of syngas from biomass.* Bioresource Technology, 1994. **48**(2): p. 119-126.

82. Tang, L. and H. Huang, *Plasma pyrolysis of biomass for production of syngas and carbon adsorbent.* Energy & fuels, 2005. **19**(3): p. 1174-1178.

83. Elliott, D.C., et al, *Catalytic hydroprocessing of biomass fast pyrolysis bio-oil to produce hydrocarbon products.* Environmental Progress & Sustainable Energy, 2009. **28**(3): p. 441-449.

84. Talmadge, M.S., et al, *A perspective on oxygenated species in the refinery integration of pyrolysis oil.* Green Chemistry, 2014. **16**(2): p. 407-453.

85. Yang, H., et al, *Characteristics of hemicellulose, cellulose and lignin pyrolysis.* Fuel, 2007. **86**(12): p. 1781-1788.

86. Antal, M.J. and M. Grønli, *The art, science, and technology of charcoal production.* Industrial & Engineering Chemistry Research, 2003. **42**(8): p. 1619-1640.

87. Nik-Azar, M., et al, *Mineral matter effects in rapid pyrolysis of beech wood.* Fuel Processing Technology, 1997. **51**(1): p. 7-17.

88. Akhtar, J. and N.S. Amin, *A review on operating parameters for optimum liquid oil yield in biomass pyrolysis.* Renewable and Sustainable Energy Reviews, 2012. **16**(7): p. 5101-5109.

89. Xiao, R. and W. Yang, *Influence of temperature on organic structure of biomass pyrolysis products.* Renewable energy, 2013. **50**: p. 136-141.

90. Difelice, R., et al, *Modeling of biomass devolatilization in a fluidized bed reactor.* The Canadian Journal of Chemical Engineering, 1999. **77**(2): p. 325-332.

91. Zeriouh, A. and L. Belkbir, *Thermal decomposition of a Moroccan wood under a nitrogen atmosphere.* Thermochimica acta, 1995. **258**: p. 243-248.

92. Wen, L.-H., et al, *Multicomponent kinetic model of biomass pyrolysis.* Zhejiang Daxue Xuebao(Gongxue Ban)/Journal of Zhejiang University(Engineering Science), 2005. **39**(2): p. 247-252.

93. Adrados, A., et al, *Upgrading of pyrolysis vapours from biomass carbonization.* Journal of Analytical and Applied Pyrolysis, 2013. **103**: p. 293-299.

94. Puy, N., et al, *Valorisation of forestry waste by pyrolysis in an auger reactor.* Waste management, 2011. **31**(6): p. 1339-1349.

95. Gilbert, P., et al, *Tar reduction in pyrolysis vapours from biomass over a hot char bed.* Bioresource technology, 2009. **100**(23): p. 6045-6051.

96. Bridgwater, A. and G. Peacocke, *Fast pyrolysis processes for biomass.* Renewable and sustainable energy reviews, 2000. **4**(1): p. 1-73.

97. Dufour, A., et al, *Synthesis gas production by biomass pyrolysis: effect of reactor temperature on product distribution.* international journal of hydrogen energy, 2009. **34**(4): p. 1726-1734.

98. Al-Rahbi, A.S., J.A. Onwudili, and P.T. Williams, *Thermal decomposition and gasification of biomass pyrolysis gases using a hot bed of waste derived pyrolysis char.* Bioresource Technology, 2016. **204**: p. 71-79.

99. El-Rub, Z.A., E. Bramer, and G. Brem, *Experimental comparison of biomass chars with other catalysts for tar reduction.* Fuel, 2008. **87**(10): p. 2243-2252.

100. Hosokai, S., et al, *Mechanism of decomposition of aromatics over charcoal and necessary condition for maintaining its activity.* Fuel, 2008. **87**(13): p. 2914-2922.

101. Shen, Y. and K. Yoshikawa, *Tar conversion and vapour upgrading via in situ catalysis using silica-based nickel nanoparticles embedded in rice husk char for biomass pyrolysis/gasification.* Industrial & Engineering Chemistry Research, 2014. **53**(27): p. 10929-10942.

102. Abdullah, H. and H. Wu, *Biochar as a fuel: 1. Properties and grindability of biochars produced from the pyrolysis of mallee wood under slow-heating conditions.* Energy & Fuels, 2009. **23**(8): p. 4174-4181.

103. Thangalazhy-Gopakumar, S., et al, *Physiochemical properties of bio-oil produced at various temperatures from pine wood using an auger reactor.* Bioresource technology, 2010. **101**(21): p. 8389-8395.

104. Ouadi, M., *Sustainable energy from paper industry wastes*. 2013, Aston University.

105. Sirijanusorn, S., K. Sriprateep, and A. Pattiya, *Pyrolysis of cassava rhizome in a counter-rotating twin screw reactor unit.* Bioresource technology, 2013. **139**: p. 343-348.

106. Roggero, C., et al, *Characterization of oils from Haloclean® pyrolysis of biomasses.* Energy Sources, Part A: Recovery, Utilization, and Environmental Effects, 2011. **33**(5): p. 467-476.

107. Hornung, A., et al, *Polypropylene as a reductive agent for dehalogenation of brominated organic compounds.* Journal of cleaner production, 2005. **13**(5): p. 525-530.

108. Hornung, U., et al, *Sequential pyrolysis and catalytic low temperature reforming of wheat straw.* Journal of Analytical and Applied pyrolysis, 2009. **85**(1): p. 145-150.

109. Lei, O. and R. Zhang, *Effects of biochars derived from different feedstocks and pyrolysis temperatures on soil physical and hydraulic properties.* Journal of Soils and Sediments, 2013. **13**(9): p. 1561-1572.

110. Yang, Y., et al, *Intermediate pyrolysis of biomass energy pellets for producing sustainable liquid, gaseous and solid fuels.* Bioresource technology, 2014. **169**: p. 794-799.

111. Ingram, L., et al, *Pyrolysis of wood and bark in an auger reactor: physical properties and chemical analysis of the produced bio-oils.* Energy & Fuels, 2007. **22**(1): p. 614-625.

112. Okoroigwe, E.C., et al, *Bio-oil yield potential of some tropical woody biomass.* Journal of Energy in Southern Africa, 2015. **26**(2): p. 33-41.

113. Yang, Y., et al, *Characterisation of waste derived intermediate pyrolysis oils for use as diesel engine fuels.* Fuel, 2013. **103**: p. 247-257.

114. Ouadi, M., et al, *The intermediate pyrolysis of de-inking sludge to produce a sustainable liquid fuel.* Journal of analytical and applied pyrolysis, 2013. **102**: p. 24-32.

115. Wongsiriamnuay, T., N. Kannang, and N. Tippayawong, *Effect of operating conditions on catalytic gasification of bamboo in a fluidized bed.* International Journal of Chemical Engineering, 2013. **2013**.

116. Gómez-Barea, A. and B. Leckner, *Modeling of biomass gasification in fluidized bed.* Progress in Energy and Combustion Science, 2010. **36**(4): p. 444-509.

117. Ciferno, J.P. and J.J. Marano, *Benchmarking biomass gasification technologies for fuels, chemicals and hydrogen production.* US Department of Energy. National Energy Technology Laboratory, 2002.

118. Rapagna, S. and A. Latif, *Steam gasification of almond shells in a fluidised bed reactor: the influence of temperature and particle size on product yield and distribution.* Biomass and Bioenergy, 1997. **12**(4): p. 281-288.

119. Mohammed, M., et al, *Air gasification of empty fruit bunch for hydrogen-rich gas production in a fluidized-bed reactor.* Energy iConversion and Management, 2011. **52**(2): p. 1555-1561.

120. Mahishi, M.R. and D. Goswami, *An experimental study of hydrogen production by gasification of biomass in the presence of a CO2 sorbent.* International Journal of Hydrogen Energy, 2007. **32**(14): p. 2803-2808.

121. Hanaoka, T., et al, *Hydrogen production from woody biomass by steam gasification using a CO2 sorbent.* Biomass and Bioenergy, 2005. **28**(1): p. 63-68.

122. Ahmad, A.A., et al, *Assessing the gasification performance of biomass: A review on biomass gasification process conditions, optimization and economic evaluation.* Renewable and Sustainable Energy Reviews, 2016. **53**: p. 1333-1347.

123. Doherty, W., A. Reynolds, and D. Kennedy, *The effect of air preheating in a biomass CFB gasifier using ASPEN Plus simulation.* Biomass and Bioenergy, 2009. **33**(9): p. 1158-1167.

124. Demirbas, A., *Biomass gasification for power generation in Turkey.* Energy Sources, Part A, 2006. **28**(5): p. 433-445.

125. André, R.N., et al, *Fluidised bed co-gasification of coal and olive oil industry wastes.* Fuel, 2005. **84**(12): p. 1635-1644.

126. Gañan, J., et al, *Energy production by means of gasification process of residuals sourced in Extremadura (Spain).* Renewable energy, 2005. **30**(11): p. 1759-1769.

127. McKendry, P., *Energy production from biomass (part 3): gasification technologies.* Bioresource technology, 2002. **83**(1): p. 55-63.

128. Rampling, T. and P. Gill, *Fundamental Research on the thermal treatment of wastes and biomass: thermal treatment characteristics of biomass*. Vol. 208. 1993: Harwell Laboratory, Energy Technology Support Unit.

129. Couto, N., et al, *Influence of the biomass gasification processes on the final composition of syngas.* Energy Procedia, 2013. **36**: p. 596-606.

130. Belgiorno, V., et al, *Energy from gasification of solid wastes.* Waste management, 2003. **23**(1): p. 1-15.

131. Milne, T.A., N. Abatzoglou, and R.J. Evans, *Biomass gasifier" tars": Their nature, formation, and conversion*. Vol. 570. 1998: National Renewable Energy Laboratory Golden, CO.

132. Fabry, F., et al, *Waste gasification by thermal plasma: a review.* Waste and Biomass Valorization, 2013. **4**(3): p. 421-439.

133. Yoon, S.J., et al, *Hydrogen and syngas production from glycerol through microwave plasma gasification.* international journal of hydrogen energy, 2013. **38**(34): p. 14559-14567.

134. Breeze, P., *Power generation technologies*. 2014: Newnes.

135. Maniatis, K. and A. Beenackers, *Tar protocols. IEA bioenergy gasification task.* Biomass and Bioenergy, 2000. **18**(1): p. 1-4.

136. Suzuki, T., H. Ohme, and Y. Watanabe, *Alkali metal catalyzed carbon dioxide gasification of carbon.* Energy & fuels, 1992. **6**(4): p. 343-351.

137. Devi, L., K.J. Ptasinski, and F.J. Janssen, *Pretreated olivine as tar removal catalyst for biomass gasifiers: investigation using naphthalene as model biomass tar.* Fuel Processing Technology, 2005. **86**(6): p. 707-730.

138. Brage, C., Q. Yu, and K. Sjöström, *Characteristics of evolution of tar from wood pyrolysis in a fixed-bed reactor.* Fuel, 1996. **75**(2): p. 213-219.

139. Hale, S.E., et al, *Quantifying the total and bioavailable polycyclic aromatic hydrocarbons and dioxins in biochars.* Environmental science & technology, 2012. **46**(5): p. 2830-2838.

140. Wiedner, K., et al, *Chemical evaluation of chars produced by thermochemical conversion (gasification, pyrolysis and hydrothermal carbonization) of agro-industrial biomass on a commercial scale.* Biomass and Bioenergy, 2013. **59**: p. 264-278.

141. Lu, Q., W.-Z. Li, and X.-F. Zhu, *Overview of fuel properties of biomass fast pyrolysis oils.* Energy Conversion and Management, 2009. **50**(5): p. 1376-1383.

142. Gassner, M. and F. Maréchal, *Thermodynamic comparison of the FICFB and Viking gasification concepts.* Energy, 2009. **34**(10): p. 1744-1753.

143. Malkow, T., *Novel and innovative pyrolysis and gasification technologies for energy efficient and environmentally sound MSW disposal.* Waste management, 2004. **24**(1): p. 53-79.

144. Ahrenfeldt, J., et al, *Biomass gasification cogeneration–A review of state of the art technology and near future perspectives.* Applied Thermal Engineering, 2013. **50**(2): p. 1407-1417.

145. Garcia-Perez, M., et al, *Production and fuel properties of pine chip bio-oil/biodiesel blends.* Energy & Fuels, 2007. **21**(4): p. 2363-2372.

146. Jin, W., K. Singh, and J. Zondlo, *Co-processing of pyrolysis vapours with bio-chars for ex-situ upgrading.* Renewable Energy, 2015. **83**: p. 638-645.

147. Mani, S., J.R. Kastner, and A. Juneja, *Catalytic decomposition of toluene using a biomass derived catalyst.* Fuel processing technology, 2013. **114**: p. 118-125.

148. Knudsen, J.N., P.A. Jensen, and K. Dam-Johansen, *Transformation and release to the gas phase of Cl, K, and S during combustion of annual biomass.* Energy & Fuels, 2004. **18**(5): p. 1385-1399.

149. Pan, W.-P. and G.N. Richards, *Influence of metal ions on volatile products of pyrolysis of wood.* Journal of Analytical and Applied Pyrolysis, 1989. **16**(2): p. 117-126.

150. Varhegyi, G., et al, *Simultaneous thermogravimetric-mass spectrometric studies of the thermal decomposition of biopolymers. 1. Avicel cellulose in the presence and absence of catalysts.* Energy & fuels, 1988. **2**(3): p. 267-272.

151. Williams, P.T. and P.A. Horne, *The role of metal salts in the pyrolysis of biomass.* Renewable Energy, 1994. **4**(1): p. 1-13.

152. Yang, Y., et al, *Characterisation of waste derived intermediate pyrolysis oils for use as diesel engine fuels.* Fuel, 2013. **103**: p. 247-257.

153. Jiang, X. and N. Ellis, *Upgrading bio-oil through emulsification with biodiesel: mixture production.* Energy & Fuels, 2009. **24**(2): p. 1358-1364.

154. Lehmann, J., J. Gaunt, and M. Rondon, *Bio-char sequestration in terrestrial ecosystems–a review.* Mitigation and adaptation strategies for global change, 2006. **11**(2): p. 395-419.

155. Gaunt, J.L. and J. Lehmann, *Energy balance and emissions associated with biochar sequestration and pyrolysis bioenergy production.* Environmental Science & Technology, 2008. **42**(11): p. 4152-4158.

156. Shackley, S., et al, *Biochar, reducing and removing CO2 while improving soils: A significant and sustainable response to climate change.* UK Biochar Research Centre, School of GeoSciences, University of Edinburgh, 2009.

157. Singh, B., B.P. Singh, and A.L. Cowie, *Characterisation and evaluation of biochars for their application as a soil amendment.* Soil Research, 2010. **48**(7): p. 516-525.

158. Gai, X., et al, *Effects of feedstock and pyrolysis temperature on biochar adsorption of ammonium and nitrate.* PloS one, 2014. **9**(12): p. e113888.

159. Robertson, S.J., et al, *Biochar enhances seedling growth and alters root symbioses and properties of sub-boreal forest soils.* Canadian Journal of Soil Science, 2012. **92**(2): p. 329-340.

160. Mukherjee, A. and A.R. Zimmerman, *Organic carbon and nutrient release from a range of laboratory-produced biochars and biochar–soil mixtures.* Geoderma, 2013. **193**: p. 122-130.

161. Ahmad, M., et al, *Effects of pyrolysis temperature on soybean stover- and peanut shell-derived biochar properties and TCE adsorption in water.* Bioresource technology, 2012. **118**: p. 536-544.

162. Keiluweit, M., et al, *Dynamic molecular structure of plant biomass-derived black carbon (biochar).* Environmental Science & Technology, 2010. **44**(4): p. 1247-1253.

163. Sohi, S., et al, *A review of biochar and its use and function in soil.* Advances in agronomy, 2010. **105**: p. 47-82.

164. Sun, K., et al, *Sorption of bisphenol A, 17α-ethinyl estradiol and phenanthrene on thermally and hydrothermally produced biochars.* Bioresource Technology, 2011. **102**(10): p. 5757-5763.

165. Novak[1], J.M., et al, *Characterization of designer biochar produced at different temperatures and their effects on a loamy sand.* 2009.

166. Chun, Y., et al, *Compositions and sorptive properties of crop residue-derived chars.* Environmental science & technology, 2004. **38**(17): p. 4649-4655.

167. Wu, W., et al, *Chemical characterization of rice straw-derived biochar for soil amendment.* Biomass and bioenergy, 2012. **47**: p. 268-276.

168. Ding, Y., et al, *Evaluation of biochar effects on nitrogen retention and leaching in multi-layered soil columns.* Water, Air, & Soil Pollution, 2010. **213**(1-4): p. 47-55.

169. Cantrell, K.B., et al, *Impact of pyrolysis temperature and manure source on physicochemical characteristics of biochar.* Bioresource technology, 2012. **107**: p. 419-428.

170. Cao, X. and W. Harris, *Properties of dairy-manure-derived biochar pertinent to its potential use in remediation.* Bioresource technology, 2010. **101**(14): p. 5222-5228.

171. Yuan, J.-H., R.-K. Xu, and H. Zhang, *The forms of alkalis in the biochar produced from crop residues at different temperatures.* Bioresource technology, 2011. **102**(3): p. 3488-3497.

172. Mimmo, T., et al, *Effect of pyrolysis temperature on miscanthus (Miscanthus× giganteus) biochar physical, chemical and functional properties.* Biomass and Bioenergy, 2014. **62**: p. 149-157.

173. Chen, B., D. Zhou, and L. Zhu, *Transitional adsorption and partition of nonpolar and polar aromatic contaminants by biochars of pine needles with different pyrolytic temperatures.* Environmental Science & Technology, 2008. **42**(14): p. 5137-5143.

174. Kalderis, D., et al, *Adsorption of polluting substances on activated carbons prepared from rice husk and sugarcane bagasse.* Chemical engineering journal, 2008. **144**(1): p. 42-50.

175. Augustenborg, C., et al, *Impact of biochar on soil N2O and CO2 emissions in the presence of earthworms.* J. Environ. Qual. in press, S. doi, 2011. **10**.

176. Glaser, B., et al, *The'Terra Preta'phenomenon: a model for sustainable agriculture in the humid tropics.* Naturwissenschaften, 2001. **88**(1): p. 37-41.

177. Forbes, M., R. Raison, and J. Skjemstad, *Formation, transformation and transport of black carbon (charcoal) in terrestrial and aquatic ecosystems.* Science of the total environment, 2006. **370**(1): p. 190-206.

178. Saldarriaga, J.G. and D.C. West, *Holocene fires in the northern Amazon basin.* Quaternary Research, 1986. **26**(3): p. 358-366.

179. Hammond, D.S., H.t. Steege, and K. Van Der Borg, *Upland soil charcoal in the wet tropical forests of central Guyana.* Biotropica, 2007. **39**(2): p. 153-160.

180. Titiz, B. and R.L. Sanford, *Soil Charcoal in Old-Growth Rain Forests from Sea Level to the Continental Divide.* Biotropica, 2007. **39**(6): p. 673-682.

181. Lehmann, J. and M. Rondon, *Bio-char soil management on highly weathered soils in the humid tropics.* Biological approaches to sustainable soil systems. CRC Press, Boca Raton, FL, 2006: p. 517-530.

182. Steiner, C., et al, *Long term effects of manure, charcoal and mineral fertilization on crop production and fertility on a highly weathered Central Amazonian upland soil.* Plant and soil, 2007. **291**(1-2): p. 275-290.

183. Major, J., et al, *Fate of soil-applied black carbon: downward migration, leaching and soil respiration.* Global Change Biology, 2010. **16**(4): p. 1366-1379.

184. Lehmann, J., et al, *Nutrient availability and leaching in an archaeological Anthrosol and a Ferralsol of the Central Amazon basin: fertilizer, manure and charcoal amendments.* Plant and soil, 2003. **249**(2): p. 343-357.

185. Steiner, C., et al, *Nitrogen retention and plant uptake on a highly weathered central Amazonian Ferralsol amended with compost and charcoal.* Journal of Plant Nutrition and Soil Science, 2008. **171**(6): p. 893-899.

186. Chan, K., et al, *Agronomic values of greenwaste biochar as a soil amendment.* Soil Research, 2008. **45**(8): p. 629-634.

187. Chan, K.Y. and Z. Xu, *Biochar: nutrient properties and their enhancement.* Biochar for environmental management: science and technology, 2009: p. 67-84.

188. Kimetu, J.M., et al, *Reversibility of soil productivity decline with organic matter of differing quality along a degradation gradient.* Ecosystems, 2008. **11**(5): p. 726-739.

189. DeLuca, T.H., et al, *Biochar effects on soil nutrient transformations.* Biochar for environmental management: Science, technology and implementation, 2015: p. 421-454.

190. Kolb, S.E., K.J. Fermanich, and M.E. Dornbush, *Effect of charcoal quantity on microbial biomass and activity in temperate soils.* Soil Science Society of America Journal, 2009. **73**(4): p. 1173-1181.

191. Thies, J.E. and M.C. Rillig, *Characteristics of biochar: biological properties.* Biochar for environmental management: Science and technology, 2009: p. 85-105.

192. Warnock, D.D., et al, *Mycorrhizal responses to biochar in soil–concepts and mechanisms.* Plant and soil, 2007. **300**(1-2): p. 9-20.

193. Steiner, C., et al, *Microbial response to charcoal amendments of highly weathered soils and Amazonian Dark Earths in Central Amazonia—preliminary results*, in *Amazonian Dark Earths: Explorations in space and time*. 2004, Springer. p. 195-212.

194. Lehmann, J., et al, *Biochar effects on soil biota–a review.* Soil Biology and Biochemistry, 2011. **43**(9): p. 1812-1836.

195. Rondon, M.A., et al, *Biological nitrogen fixation by common beans (Phaseolus vulgaris L.) increases with bio-char additions.* Biology and fertility of soils, 2007. **43**(6): p. 699-708.

196. Kammann, C.I., et al, *Influence of biochar on drought tolerance of Chenopodium quinoa Willd and on soil–plant relations.* Plant and Soil, 2011. **345**(1-2): p. 195-210.

197. Krull, E.S., et al, *Characteristics of biochar: organo-chemical properties.* Biochar for environmental management: Science and technology. Earthscan, London, 2009: p. 53-65.

198. Smernik, R.J., *Biochar and sorption of organic compounds.* Biochar for Environmental Management: Science and Technology, 2009: p. 289-300.

199. Buss, W., C. Kammann, and H.-W. Koyro, *Biochar Reduces Copper Toxicity in Willd. in a Sandy Soil.* Journal of environmental quality, 2012. **41**(4): p. 1157-1165.

200. Asai, H., et al, *Biochar amendment techniques for upland rice production in Northern Laos: 1. Soil physical properties, leaf SPAD and grain yield.* Field Crops Research, 2009. **111**(1): p. 81-84.

201. Laird, D.A., et al, *Impact of biochar amendments on the quality of a typical Midwestern agricultural soil.* Geoderma, 2010. **158**(3): p. 443-449.

202. Lehmann, J., et al *Slash-and-char-a feasible alternative for soil fertility management in the central Amazon*. in *Proceedings of the 17th World Congress of Soil Science*. 2002.

203. Mizuta, K., et al, *Removal of nitrate-nitrogen from drinking water using bamboo powder charcoal.* Bioresource technology, 2004. **95**(3): p. 255-257.

204. Radovic, L.R., C. Moreno-Castilla, and J. Rivera-Utrilla, *Carbon materials as adsorbents in aqueous solutions.* Chemistry and physics of carbon, 2001: p. 227-406.

205. Blackwell, P., G. Riethmuller, and M. Collins, *Biochar application to soil.* Biochar for environmental management: science and technology, 2009: p. 207-226.

206. Shackley, S., et al, *An assessment of the benefits and issues associated with the application of biochar to soil.* Department for Environment, Food and Rural Affairs, UK Government, London, 2010.

207. Schmidt, S.H.-P., *European Biochar Certificate–Guidelines for a Sustainable Production of Biochar.* European Biochar Foundation, 2013.

208. Definition, I.-S.P., *Product Testing Guidelines for Biochar That Is Used in Soil (aka IBI Biochar Standards) Version 2.1.* International Biochar Initiative (IB), 2015.

209. Shackley, S., et al, *Biochar Quality Mandate.* British Biochar Foundation (BRAF), UK (http://biocharbraf. files. wordpress. com/2013/06/bqm-document-v2. pdf [accessed on 9th June 2014]), 2013.

210. Agency, S.E.P., *Manufacture and use of Biochar from Waste.* 2012: p. 3.

211. Accardi-Dey, A. and P.M. Gschwend, *Assessing the combined roles of natural organic matter and black carbon as sorbents in sediments.* Environmental Science & Technology, 2002. **36**(1): p. 21-29.

212. Weintz, J., *Metering Technology - Rotary Valves.* 2017: p. 2.

213. Unknown, *Steel Ball Valves for High Temperatures.* p. 52.

214. Unknown. *Knife gate valve MV*. 2017 19/06/2017]; Available from: http://www.stafsjo.com/sites/default/files/ds-MV_EN.pdf.

215. Rechulski, M.K., et al, *Sulfur containing organic compounds in the raw producer gas of wood and grass gasification.* Fuel, 2014. **128**: p. 330-339.

216. Bergman, P.C., Boersma, A.R., Zwart, R.W.R. and Kiel, J.H.A., 2005. Torrefaction for biomass co-firing in existing coal-fired power stations. *Energy Centre of Netherlands, Report No. ECN-C-05-013*.

217. Fagbemi, L., Khezami, L. and Capart, R., 2001. Pyrolysis products from different biomasses: application to the thermal cracking of tar. *Applied energy*, *69*(4), pp.293-306.

218. Phuphuakrat T, Namioka T, Yoshikawa K. Tar removal from biomass gas in two-step function of decomposition and adsorption. Applied Energy 2009.

219. Chen Y, Luo Y, Wu W, Su Y. Experimental investigation on tar formation and destruction in a lab-scale two-stage reactor. Energy Fuels 2009; 23:4659–009

220. Onwudili, J.A., Lea-Langton, A.R., Ross, A.B. and Williams, P.T., 2013. Catalytic hydrothermal gasification of algae for hydrogen production: composition of reaction products and potential for nutrient recycling. *Bioresource technology*, *127*, pp.72-80.

221. Wang, T., Chang, J., Lv, P. and Zhu, J., 2005. Novel catalyst for cracking of biomass tar. *Energy & Fuels*, *19*(1), pp.22-27.

222. Narvaez, I., Orio, A., Aznar, M.P. and Corella, J., 1996. Biomass gasification with air in an atmospheric bubbling fluidized bed. Effect of six operational variables on the quality of the produced raw gas. *Industrial & Engineering Chemistry Research*, *35*(7), pp.2110-2120.

223. Li, X.T., Grace, J.R., Lim, C.J., Watkinson, A.P., Chen, H.P. and Kim, J.R., 2004. Biomass gasification in a circulating fluidized bed. *Biomass and bioenergy*, *26*(2), pp.171-193.

List of Publications

Conference papers

M. Saghir S. U. Siddiqui, A. Hornung, U. Wirtz; *Characterization of the products from Intermediate pyrolysis of Miscanthus and Wood pellets;* 21st European Biomass Conference and Exhibition, Bella Center - Copenhagen, Denmark, 03-07 June 2013.

M. Saghir, S. U. Siddiqui, U. Wirtz, A. Hornung; *Characterization and potential applications of char from Intermediate pyrolysis of different biomass feedstocks;* BCD2013 - International Conference on Biochars, Composts, and Digestates: Production, Characterization, Regulation, Marketing, Uses and Environmental Impact. (Cod. 88242), Bari, Italy http://www.biochar-international.org/sites/default/files/Bari_2013_final_program.pdf S.2.2.06

Book chapters

Muhammad Saghir, Mohammad Rehan, Abdul-Sattar Nizami, Recent Trends in Gasification-based Waste to Energy; Gasification (2018): Intech Open Access Publishers Prague, Czech Republic.

Muhammad Saghir, Fahd Rasul, Ashfaq Ahmad, Muhammad Arif, Ishaq Ahmad Mian, Kawsar Ali, Muhammad Farooq Qayyum, Qaiser Hussain, Muhammad Aon, Shahzad Latif, Ruben Sakrabani, Genxing Pan and Simon Shackley; 2017. Biochar for Agriculture in Pakistan. *Sustainable Agriculture Reviews*, *22*, p.57.

Poster presentations

S. Bonnett, S. Vink, K. Baker, M. Saghir & A. Hornung*; Impact of drying-rewetting events on the response of soil microbial functions to dairy fibre and Miscanthus biochars;* European Geosciences Union General Assembly 2014, Vienna, Austria 27 April – 02 May.

http://meetingorganizer.copernicus.org/EGU2014/posters/14866 B159 EGU2014-12269

Conference presentations

- British Biochar foundation 1st annual event Oxford 2013, United Kingdom
- British Biochar foundation 2nd annual event Oxford 2014, United Kingdom
- Pakistan Biochar initiative, Workshop: Biochar for climate friendly agriculture: shifting paradigms for higher precision and efficiency, 24-27 March 2014, University of Agriculture, Faisalabad, Pakistan
- Nutrition Policy to Practice in Pakistan: Exploring the Challenges and Research Opportunities, 08-11th March 2015, Islamabad, Pakistan
- Process systems engineering approaches for the provision of supplies and utilities for sustainable cities, 24-28 February 2016, Manila, Philippines
- Adapting a Rural-Urban Model: Empowering local communities to develop sustainable built environment, 30th November – 4th December 2016, Yogyakarta, Indonesia

Appendices

Appendix 1 - 3D Layout of Pyroformer 100 kg----------249

Appendix 2 - Harper Adams Pyroformer Daily Operations Checklist ----------250

Appendix 3 - Plant layout of BFB Gasifier and Pyroformer processes ----------252

Appendix 4 - Dimensions of the Gasifier ----------269

Appendix 5 - Characterization of the products from Intermediate pyrolysis of Miscanthus and Wood pellets – internal combustion engine application---------271

Appendix 6 - Characterisation and potential applications of char from Intermediate pyrolysis of different biomass feedstocks----------274

Page 249- 270 removed for copyright restrictions.

Characterization of the products from Intermediate pyrolysis of Miscanthus and Wood pellets – internal combustion engine application

M. Saghir[a,1], S. U. Siddiqui[a], U. Wirtz[c], A. Hornung[a, b]

[a]European Bioenergy Research Institute (EBRI), Aston University, Birmingham B4 7ET, UK

[b]Chair in Chemical Engineering and Applied Chemistry

[c]WSE Ltd. Niederlassung Deutschland, Rudolf-Schulten-St 52428 Juelich, Germany

1.0 Introduction

The demand for fossil fuels is constantly increasing and there has been extensive research continuing into this area to substitute them with various renewable energy alternates to reduce any further impact on the environment. Intermediate Pyrolysis is an advanced thermo-chemical technique which utilizes multiple waste biomass streams to economically generate sustainable heat and power thereby reducing world's reliance on fossil fuels, climate change and most importantly eliminating costly solid wastes disposal techniques such as landfill, landspread or incineration which are not so environmentally friendly.

2.0 Materials and Methods

Intermediate pyrolysis of two different biomass fuels (Pelletized Miscanthus and Wood, 6mm) was performed using a 100kg/hr pyrolysis reactor known as the Pyroformer recently developed by EBRI[2] which is the first Industrial scale plant of its kind in the UK. The process temperature was maintained at 400°C by means of external heaters for both the feedstocks with feedstock residence time estimated to be about 10 minutes which is realized by the internal conveyor screw of the Pyroformer, although the vapour residence time is only a few seconds. The evolved gases and vapours pass through a scrubbing system where a light spray of biodiesel is injected thereby condensing a fraction of vapours at first stage tank. The remaining fraction is then passed through an air cooled condenser where they are condensed to form most of the pyrolysis oil. The gases which escape the second stage condenser are then passed through an electrostatic precipitator where they are further condensed to a combination of oil and water fraction. Finally the rest permanent gases are either directed to an internal combustion (IC) dual fuel common rail CI engine for combustion or flared.

2.1 Feedstock Characterisation

Table 1: The Proximate and Ultimate analysis of the feedstocks is as shown below:

Feedstock	Unit	Wood pellets	Miscanthus
[a]*Ultimate analysis*			
Carbon	wt.%	46.2	41.34
Hydrogen	wt.%	5.96	5.27
Oxygen[b]	wt.%	47.55	52.47
Nitrogen	wt.%	<0.01	0.57
Sulphur	wt.%	0.28	0.35
[a]*Proximate analysis*			
Moisture	wt.%	8.71	10.44
Ash content	wt.%	0.46	2.98
Density @20°C	kg/m^3	688	640
Higher Heating Value (HHV)	MJ/kg	18.30	17.28

[a]Analysis based on pre-treated feedstock, dry basis, [b]Calculated by difference

It can be noted here that both the input materials have almost similar characteristic properties.

[1] Corresponding author: Tel: +44 (0)121 204 5027, email: m.saghir2@aston.ac.uk

[2] Hornung A et al. The thermal treatment of biomass, GB patent application number: GB 0808739.7, application submitted: May 15, 2009. World patent applied for (WO 2009/138757; Nov 19, 2009).

3.0 Results and discussion

3.1 Mass balance

As a general rule, for most of the feedstocks the product yield is evenly distributed (one-third of each product). From table 2, it can be observed that there is approximately 10% difference between the quantities of pyrolysis oil obtained from wood and miscanthus pellets which means wood pyrolysis vapours couldn't be condensed as efficiently as the miscanthus vapours. This can be due to the fact that wood pyrolysis vapour contains more permanent gases and lower molecular weight products compared to the miscanthus. The gas yield also increases due to the reforming mode of the Pyroformer, turning water and pyrolysis vapours into more gas phase products.

Table 2: The following table shows the Intermediate pyrolysis products' yield

Feedstock	Quantity (kg)	Feed rate (kg/h)	%Bio-oil	%Biochar	%Gases*
Wood pellets (6mm)	117	61.04	20.77	32.0	47.23
Miscanthus (6mm)	105	70.0	30.90	31.62	37.48

*Calculated by difference

3.2 Biochar Characterisation

Miscanthus and wood pellets biochar has the potential for carbon sequestration (if conditioned to C/O larger than 4) as well as soil conditioning or can be used as a co-combustion material in boilers and combustors since their heating value is as good as conventional coal. Moreover, experimental tests have been undertaken at Harper Adams University labs (UK) to study detailed effects of these biochars on the productivity of plants across a range of soils.

Table 3: Proximate and Ultimate analysis of Biochar

Biochar	Unit	Wood biochar	Miscanthus biochar
[a]*Ultimate analysis*			
Carbon	wt.%	71.58	62.2
Hydrogen	wt.%	4.62	4.37
Oxygen[b]	wt.%	23.04	32.35
Nitrogen	wt.%	0.54	0.8
Sulphur	wt.%	0.22	0.28
[a]*Proximate analysis*			
Moisture	wt.%	4.05	8.03
Ash content	wt.%	2.64	10.31
Density @20°C	kg/m^3	498	436
Higher Heating Value (HHV)	MJ/kg	28.78	24.64

[a]Analysis based on pre-treated feedstock, dry basis
[b]Calculated by difference

3.3 Bio-oil Characterization

The table 4 illustrate the Physio-chemical characteristics of wood and miscanthus pellets pyrolysis oil at all the three condensation stages. The higher heating values of these pyrolysis oils closely resemble to that of ASTM biodiesel which is an average of 38.5MJ/kg for wood pellets and 39.24MJ/kg for miscanthus with negligible amount of ash or solids content. Therefore, these oils could be readily used into an internal combustion (IC) engine by adopting minor fuel upgradation techniques.

Table 4: Elemental analysis and Characterisation of Intermediate Pyrolysis oils & ASTM standard for Biodiesel

Bio-oil	Unit	Wood pellets			Miscanthus			Biodiesel[c] ASTM
		Condensation Stage						
		1st	2nd	3rd	1st	2nd	3rd	
Compositional analysis								
Carbon	wt.%	76.14	76.21	76.09	76.33	76.09	70.6	77.04
Hydrogen	wt.%	12.46	12.04	11.55	11.83	11.92	11.01	11.73
Oxygen[a]	wt.%	11.38	11.73	12.34	11.80	11.97	18.37	11.21
Nitrogen	wt.%	<0.10	<0.10	<0.10	<0.10	<0.10	<0.10	<0.10
Sulphur	wt.%	<0.10	<0.10	<0.10	<0.10	<0.10	<0.10	<0.10
Higher Heating Value (HHV)	MJ/kg	39.58	39.30	38.92	39.39	39.38	35.70	40.11
Lower Heating Value (LHV)	MJ/kg	37.09	37.05	36.47	36.88	36.86	33.37	37.47
Ash content	wt.%	<0.01	<0.01	<0.01	<0.01	<0.01	2.08	<0.01
Density @20°C	kg/m^3	882	887	910	886	881	955	820
Total acid number	mg KOH/gm	27.85	18.05	NaN[b]	7.95	8.03	NaN	0.62
Kinematic Viscosity @40°C	cSt	21	19	-	21	21	-	6
Water Content	wt.%	0.23	0.59	-	0.31	0.42	-	0.12

[a]Calculated by difference, [b]No acid number detected
[c]Biodiesel obtained from a local supplier (Waste cooking oil)

However, the kinematic viscosity and the total acid number are significantly high with respect to the biodiesel. This can be overcome by blending it with proportionate amount of biodiesel which is found to be highly miscible with these pyrolysis oils or by emulsification to mitigate any related erosion/corrosion problems to the fuel injectors and additionally improve fuel atomisation during its combustion phase in the engine.
GC-MS of these pyrolysis oils showed that the chemical composition is mostly dominated by the presence of aromatics, long chain hydrocarbons apart from some phenols.

4.0 Conclusions and future work

Various experimental tests on the Pyroformer concluded that it has no negative environmental or food security impacts and its capability to process multiple waste streams such as sewage sludge, agricultural and cattle wastes indicates it's free from the requirement of special biocrops agricultural land or deforestation. This will help to achieve significant reduction in the fossil fuel usage in the UK and other countries and would also contribute towards the EU's target of achieving 20% of the energy from renewable sources by 2020.

All the three intermediate pyrolysis products are valuable sources of energy. It is observed that the pyrolysis oils obtained via this conversion process have high stability and energy density which can be easily stored and transported and already tested as a substitute to diesel in a slightly modified 150 kW NEK Compression ignition (CI) engine. The basic advantage of these oils is they are free from any tar as most of it retains in the biochar. This eliminates the need of using expensive filtration systems thereby making the process economically feasible.

The Syngas can also be used as a fuel in dual fuel CI engines and experimental investigation is continued to route this gas into multi-cylinder common rail NEK engine to fully utilize this pyrolysis output and there after the results of emission, combustion and performance of an IC engine operating on these Intermediate pyrolysis oil and gas fuel will be discussed in detail in future works.
In conclusion, further research is still under progress to effectively resolve some of the minor issues around the technology.

Characterisation and potential applications of char from Intermediate pyrolysis of different biomass feedstocks

M. Saghir [a,1], S. U. Siddiqui [a, c], U. Wirtz [c], A. Hornung [a, b]

[a]European Bioenergy Research Institute (EBRI), Aston University, Birmingham B4 7ET, UK

[b]Director of the Institute Branch Sulzbach-Rosenberg, Fraunhofer UMSICHT, Germany

[c]WSE Ltd. Niederlassung Deutschland, Rudolf-Schulten-Str 8 D-52428 Juelich, Germany

ABSTRACT

1.0 Introduction

This study aims to investigate the potential combustion and agricultural application of char derived from intermediate pyrolysis of four different biomass feedstocks namely wood, miscanthus, dairy fibre and compost material in pelletized form. These biomass feedstocks could be considered as the most promising sources for the sustainable production of biochar. The other pyrolysis products such as bio-oil and syngas are also considered a rich source of alternate renewable energy compared to the conventional fuels.

Intermediate Pyrolysis is an innovative thermo-chemical decomposition technique of biomass in the absence of oxygen in a specially designed industrial scale reactor known as the Pyroformer^{TM} recently developed by EBRI[2] at Aston University which is first of its kind in the UK. The reactor is capable to process multiple waste streams with a maximum biomass feed handling capacity as 100 kg/h.

2.0 Materials and Methods

The Pyroformer^{TM} is essentially an auger pyrolysis reactor with two counter-rotating co-axial screws which can process feedstocks in an inert atmosphere of nitrogen. The reactor is heated externally by means of electrical heating jackets and the feed is processed through the screw conveyor system whilst being heated to the specified pyrolysis temperature of around 400˚C. Some solid residue (char and ash) is re-circulated within the reactor, the remainder drops out at the downstream end of the reactor, and the pyrolysis vapours and gases exit through the Pyroformer^{TM} outlet. (Refer Figure: 2 in the Appendix for schematic of the entire process)

The recycling of char increases the char to feedstock ratio in the reaction zone which promotes catalytic cracking of the primary vapours to lower molecular weight hydrocarbon vapours and permanent gases. It also serves to recycle heat within the reactor and increase the heating rate experienced by the feedstock. This controlled thermal treatment and chemical reforming process produces a vapour stream that is free from particulates and tars and eliminates the need for expensive filtrations systems. At the end of the pyrolysis process, the system generates three different products: a combustible gas, a combustible bio-oil and a char solid.

[1] Corresponding author: Tel: +44 (0)121 204 5027, email: m.saghir2@aston.ac.uk

[2] Hornung A et al. The thermal treatment of biomass, GB patent application number: GB 0808739.7, application submitted: May 15, 2009. World patent applied for (WO 2009/138757; Nov 19, 2009).

High quality char outputs and low tar vapour streams can be much more effectively linked to this technology because of low vapour residence time of the order of few seconds which is also the main criteria to minimize the process energy requirements with another advantage being variable solids' residence time.

2.1 Feedstock characterization

Four different feedstocks were tested namely: Wood, Miscanthus, Dairy fibre and compost material. Wood and Miscanthus were tested to establish a standard relationship with reference to the other two materials. Wood and Miscanthus feedstock was obtained from a UK based local supplier in pelletized form (6 mm size) whereas the dairy fibre was obtained from a small cattle farm based at Harper Adams University (UK) and the compost material was from the household generated waste also referred to as 'brown-bag' waste which was obtained from Germany. Dairy fibre and compost material was initially in raw form which was pre-treated to form 8 mm sized pellets using a 200 kg/h die and roller electrical pelletiser. The characterisation of these feedstocks is discussed in detail below.

2.1.1 Inductively coupled plasma (ICP) metals analysis

Metals and a range of non-metals, such as phosphorus, for the feedstocks were analysed using Varian Vista MPX ICP-OES system. (Analysis based on dry, ash-free basis)

Table 1: Elemental analysis of Biomass feedstocks (expressed in parts per million, ppm unless indicated in wt. %)

Feedstock / Element	Wood pellets	Miscanthus	Dairy fibre	Compost
Al	46	70	0.6%	1.03%
As	<1	3	3	5
B	<1	<1	30	53
Ba	7	9	78	343
Ca	0.08%	0.5%	6.5%	5.75%
Cd	<1	<1	<1	1
Ce	<1	<1	6	8
Co	<1	<1	1	10
Cr	1	1	15	74
Cu	32	<1	107	150
Fe	91	99	0.22%	1.89%
Hg	1	1	<1	1
Li	<1	1	5	8
Mg	0.012%	0.042%	0.75%	0.5%
Mn	70	27	154	560
Mo	<1	<1	3	3
Na	17	87	0.21%	0.3%
Nb	<1	<1	40	29
Ni	1	1	7	24
Pb	<1	<1	34	86
Pd	<1	<1	<1	17
Sc	<1	<1	<1	1
Si	0.016%	0.21%	2.08%	3.96%
Sn	1	2	2	8
Sr	4	8	130	133
Ti	5	4	204	152
V	<1	1	4	16

Y	<1	<1	1	4
Yb	<1	<1	<1	<1
Zn	12	13	319	417
Zr	<1	<1	13	11

2.1.2 Proximate and Ultimate analysis

The Ultimate analysis was determined using combustion analysis on a Flash EA 1112 Series CHNS analyzer. Oxygen was calculated by difference. The density was measured following the ASTM D-285 methods with slight modifications. All moisture contents of the feedstocks were determined using a moisture analyser (Sartorius MA35) with a programmed temperature of 105°C. The gross heating value in (MJ/Kg) of the dried feedstocks were determined using a Parr 6100 bomb calorimeter whereas the LHV was theoretically calculated using a standard empirical formula. The results are as shown in the table below:

Feedstock	Unit	Wood pellets	Miscanthus	Dairy fibre	Compost
[a]*Ultimate analysis*					
Carbon	wt.%	46.2	41.34	25.02	30.03
Hydrogen	wt.%	5.96	5.27	3.18	4.19
Oxygen[b]	wt.%	46.69	51.81	62.82	55.83
Nitrogen	wt.%	<0.01	0.57	1.62	1.83
Sulphur	wt.%	0.28	0.35	0.36	0.88
Phosphorous	wt.%	0.004	0.045	0.25	0.12
Potassium	wt.%	0.3	0.23	0.98	0.42
C/O ratio		0.99	0.81	0.40	0.54
[a]*Proximate analysis*					
Moisture	wt.%	8.71	10.44	10.84	6.38
Ash content	wt.%	0.46	2.98	24.61	35.46
Density @20°C	kg/m^3	688	640	633	672
Higher Heating Value (HHV)	MJ/kg	18.34	17.28	11.34	11.52
Lower Heating Value (LHV)	MJ/kg	17.08	16.16	10.67	10.63

[a]Analysis based on pre-treated feedstock, dry basis,
[b]Calculated by difference

The moisture content of the feedstocks was in the range of 6-10 wt. % which is optimum for the process with a gross heating value (MJ/kg) ranging in between 10-17 MJ/kg, highest being for wood pellets and lowest for the compost material.

3.0 Results & discussion

3.1 Mass balance

The maximum feed rate that was practically tested during the test runs was restricted to 70 kg/h which was for miscanthus pellets. The results indicate that the char yield remained almost one-third of the initial feedstock quantity whereas the bio-oil and syngas was in the range of 20-35% and 35-50% respectively depending upon the feedstock. The bio-oil and syngas were also analysed for use as a fuel in a dual fuel internal combustion (IC) compression ignition (CI) engine which have already been discussed in previous works.

Table 2: Mass yields (wt. %) of pyrolysis products from different biomass feedstocks

Feedstock	**Quantity** (kg)	**Feed rate** (kg/h)	**Bio-oil** wt. %	**Biochar** wt. %	**Syngas*** wt. %
Wood pellets (6 mm)	117	61.0	20.77	32.0	47.23
Miscanthus (6 mm)	105	70.0	30.90	31.62	37.48
Dairy fibre (8 mm)	65	25.0	33.73	30.2	36.07
Compost (8 mm)	290	66.5	19.74	32.55	47.72

*Gas yield was calculated by difference

3.2 Bio-oil Characterization

The table 3 illustrates the Physico-chemical characteristics of all the four tested feedstocks. The higher heating values of these pyrolysis oils closely resemble to that of ASTM biodiesel which is in the range 38-40 MJ/kg with negligible amount of ash or solids content. Therefore, these oils could be readily used into an internal combustion (IC) engine by adopting minor fuel upgradation techniques.

Table 3: Elemental analysis and Characterisation of Intermediate Pyrolysis oils & ASTM standard for Biodiesel

Bio-oil	**Unit**	**Wood pellets**	**Miscanthus**	**Dairy Fibre**	**Compost material**	**Biodiesel[b] ASTM**
Compositional analysis						
Carbon	wt.%	76.34	74.34	76.82	76.70	77.04
Hydrogen	wt.%	11.13	11.59	11.23	11.87	11.73
Oxygen[a]	wt.%	12.33	13.87	11.75	10.98	11.21
Nitrogen	wt.%	<0.10	<0.10	<0.10	0.34	<0.10
Sulphur	wt.%	<0.10	<0.10	<0.10	<0.10	<0.10
Higher Heating Value (HHV)	MJ/kg	38.50	38.16	38.84	39.63	40.11
Lower Heating Value (LHV)	MJ/kg	36.14	37.01	36.46	37.11	37.47
Ash content	wt.%	<0.01	0.70	<0.01	<0.01	<0.01
Density @20°C	kg/m^3	886	885	910	895	820
Total acid number	mg KOH/gm	17.06	5.33	3.51	4.42	0.62
Kinematic Viscosity @40°C	cSt	14.0	21.0	22.0	9.66	6.0
Water Content	wt.%	0.52	0.36	0.28	1.1	0.12

[a]Calculated by difference
[b]Biodiesel obtained from a local supplier (Waste cooking oil)

However, the kinematic viscosity is slightly high with respect to the biodiesel. This can be overcome by blending it with proportionate amount of biodiesel which is found to be highly miscible with these pyrolysis oils or by emulsification to mitigate any related erosion/corrosion problems to the fuel injectors and additionally improve fuel atomisation during its combustion phase in the engine. A complimentary post processing technology to the Pyroformer™ namely Bio-activated fuel (BAF) technology is currently being tested to improve these bio-oils' quality and this is most likely to be discussed in future works.

3.3 Biochar Characterisation

Biomass char is a solid co-product of the pyrolysis process and is a renewable source of energy with heating value as good as conventional coal and when this char is utilised for special agricultural purposes it is referred to as biochar.

The biochar is a carbon rich product and its production from waste streams is a good way to minimise the demand for fertilisers and could also be used as a potential solid biofuel during the combustion process in boilers, combustors, gasifiers etc. or for co-firing in power stations to generate electricity.

Biochar is also an attractive means for sequestering carbon to mitigate global climate change and as a potentially valuable input for agricultural fields to enhance soil fertility, crop productivity and could be produced in large volumes per batch.

Table 4: The proximate and ultimate analysis of different chars is presented in the table below:

Biochar	Unit	Wood	Miscanthus	Dairy	Compost
[a]*Ultimate analysis*					
Carbon	wt.%	71.58	62.20	26.29	26.90
Hydrogen	wt.%	4.62	4.37	2.06	2.27
Oxygen[b]	wt.%	22.23	31.45	44.46	48.86
Nitrogen	wt.%	0.54	0.8	1.61	1.58
Sulphur	wt.%	0.22	0.28	0.77	0.72
Phosphorous	wt.%	0.1	0.13	0.4	0.39
Potassium	wt.%	0.61	0.77	1.77	0.61
C/O ratio		3.35	2.07	0.59	0.55
[a]*Proximate analysis*					
Moisture	wt.%	4.05	8.03	2.50	1.94
Ash content	wt.%	2.64	10.31	56.29	55.3
Density @20°C	kg/m^3	498	436	794	821
Higher Heating Value (HHV)	MJ/kg	28.78	24.64	10.81	10.37
Lower Heating Value (LHV)	MJ/kg	27.03	23.71	10.99	10.51

[a]Analysis based on pre-treated feedstock, dry basis,
[b]Calculated by difference

The carbon content of the carbonised residue increased with regard to wood and miscanthus feed but remained almost similar for dairy and compost biomass feed along with deoxygenation of the feedstocks as a result of loss of functional groups during the pyrolysis process. The gross heating values (MJ/kg) of the chars were high for wood and miscanthus which was due to the an increase in the carbon content and decrease in the oxygen and ash content with respect to the initial biomass material but this slightly decreased for dairy and compost feedstocks because of an increase in the ash content.

Figure: 1 below shows a sample of miscanthus char after pyrolysis

Figure 1: Miscanthus Biochar

Table 5: Inductively coupled plasma (ICP) metals analysis (expressed in parts per million, ppm unless indicated in wt. %)

Biochar / Element	Wood	Miscanthus	Dairy	Compost
Al	0.018%	0.023%	1.18%	1.13%
As	<1	<1	3	2
B	413	12	43	68
Ba	94	26	151	487
Ca	0.94%	1.45%	16.64%	7.67%
Cd	<1	<1	1	1
Ce	<1	1	11	13
Co	<1	<1	4	13
Cr	2	3	30	103
Cu	182	4	140	211
Fe	0.04%	0.78%	0.56%	2.34%
Hg	<1	<1	1	<1
Li	1	2	5	8
Mg	0.25%	0.17%	1.15%	0.80%
Mn	<1	0.012%	0.03%	0.15%
Mo	1	<1	3	5
Na	0.045%	0.016%	0.36%	0.40%
Nb	<1	<1	55	37
Ni	41	2	13	33
Pb	3	1	62	116
Pd	<1	<1	<1	4
Sc	<1	<1	1	1
Si	0.33%	0.82%	2.28%	5.39%
Sn	3	1	6	12
Sr	28	21	263	176
Ti	8	11	310	213
V	1	1	8	21
Y	<1	<1	3	6
Yb	<1	<1	<1	1
Zn	62	317	312	447
Zr	<1	<1	23	15

3.4 NPK rating

NPK rating is a term commonly used to label a fertilizer based on the presence of relative content of the chemical elements such as Nitrogen (N), Phosphorous (P) and Potassium (K) which basically promotes plants' growth and productivity.

A balanced fertiliser is when all the three chemical nutrients NPK are included in equal proportion and reflected so in the ratio. This type of fertiliser is mostly preferred for all round general use. The table below shows approximate NPK values for the gained chars:

Biochar	N	P	K	N:P:K
Wood	0.54	0.1	0.61	5:1:6
Miscanthus	0.8	0.13	0.77	6:1:6
Dairy	1.61	0.4	1.77	4:1:4
Compost	1.58	0.39	0.61	4:1:2

4.0 Conclusions & future work

The main advantage of using these biochars as a fertilizer is that they are produced from renewable resources. These biochars could potentially be used as special purpose fertilizers which can be intended to meet most plants' requirements.

The biochars contained moderate amounts of the essential plant nutrient, P, as well as substantial amounts of plant-available macronutrients, K, Ca and Mg along with reasonable amounts of Fe. (Refer Table: 4)

The biochars also contained trace amounts of plant micronutrients, Mn, Zn, Cu, Co and Mo. The plant-available toxic elements such as As, Cr, Pb and Cd are also present in trace amounts but are below the authorized limits for organic soil amendments which is a positive indication.

Additionally, these biochars when returned to agricultural land will increase the soil's carbon content permanently and would establish a carbon sink for atmospheric CO_2 and hence is proposed as a soil amendment in environments with low carbon sequestration capacity and previously depleted soils.

Therefore, it can be concluded that these biochars are a good source of beneficial plant macro and micronutrients and contains negligible levels of toxic elements. Unfortunately, these biochars could not be considered as a balanced fertilizer on its own, as it contains relatively low levels of water soluble nutrients. However, this can be overcome by making blends which can be formulated to obtain balanced amount of required ingredient.

Another interesting criteria to consider when using these chars as fertiliser is the presence of Polycyclic aromatic hydrocarbons (PAH's). In particular, the presence of PAHs on biochar could be of concern when chars with high levels of PAHs are used in human food production

which could potentially result into food contamination. However, further research is still in progress on this aspect of biochar which will be discussed in future works.

Moreover, agricultural field trials have currently been undertaken at Harper Adams University (UK) to study detailed effects of these biochars on the productivity of plants across a range of soils. This study will lead to a novel determination method of the char quality and the establishment of standards thereby will be helpful in reaching a definitive conclusion.

Additionally, the future work will also be focussed on developing a business case for national scale-up sustainable biochar production, standardisation and utilization along with an application project which would be prepared based on available carbon finance opportunities in the region.

5.0 Appendix

Figure 2: Schematic Diagram of the Pyrolysis System for Production of Pyrolysis products

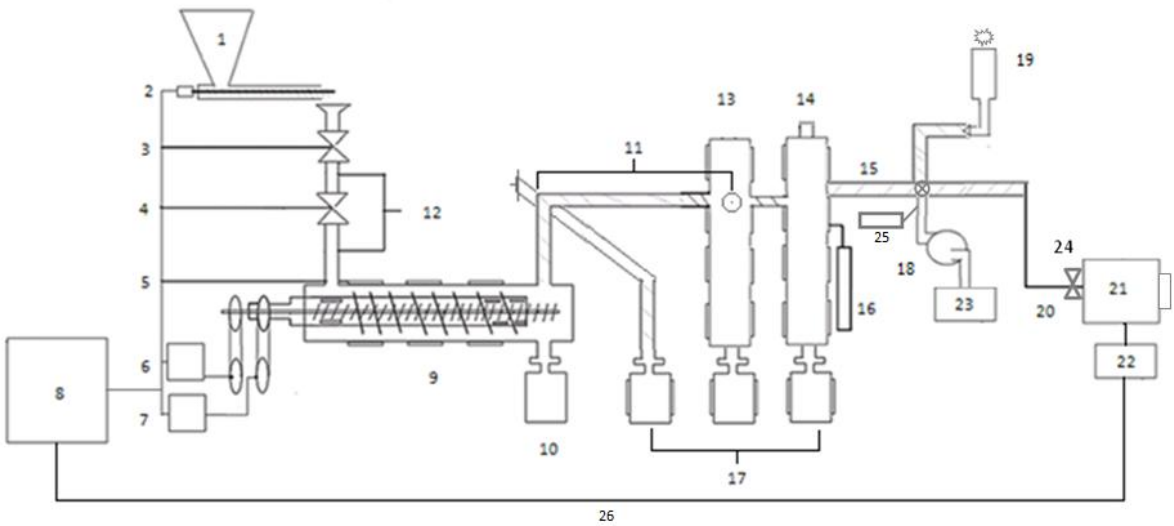

1-Feed Hopper, 2 -Auger, 3&4-Pneumatic Ball Values, 5-Electric Heating Bands, 6&7-Electric Motors, 8-Main Control Board, 9-Pyrolysis Reactor, 10-Char Collection Vessel, 11-Wet Scrubber, 12-N2 Purge Line, 13-Air cooled condenser, 14-Electrostatic Precipitator ESP, 15-Syngas line 16-ESP Control Board, 17-Pyrolysis Oil Collection Tanks, 18-Gas Suction Pump, 19-Flare, 20-Gas Line to Engine, 21-Dual Fuel Engine, 22-Electrical Generator, 23-Gas Calorimeter, 24-Electronic valve, 25-Oxygen sensor, 26-Electrical connection